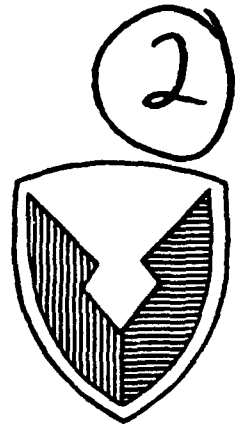


AD-A254 930



AD No. _____

DPG No. DPG-CR-92-902



US ARMY
MATERIEL COMMAND

METEOROLOGICAL INFLUENCES ON SMOKE/OBSCURANT
EFFECTIVENESS PHASE I I

Volume II

by

Steven R. Hanna, David G. Strimaitis
Joseph C. Chang and Sharon M. McCarthy

Sigma Research Corporation
234 Littleton Road, Suite 2E
Westford, Massachusetts 01886

Contract DAAD09-89-C-0039

DTIC
ELECTE
AUG 05 1992
S A D

November 1991

Prepared for

METEOROLOGY DIVISION
MATERIEL TEST DIRECTORATE
U.S. ARMY DUGWAY PROVING GROUND
DUGWAY, UTAH 84022-5000

92-21104



425447

Approved for Public Release; Distribution Unlimited

92 8 03 105

Disposition Instructions

Destroy this report when no longer needed. Do not return to the originator.

Disclaimer Statement

The views, opinions, and/or findings in this report are those of the authors and should not be construed as an official Department of the Army position, unless so designed by other official documentation.

Trade Names Statement

The use of trade names in this report does not constitute an official endorsement or approval of the use of such commercial hardware or software. This report may not be cited for purpose of advertisement.

DTIC QUALITY INSPECTED 5

Accession For	
NTIS CRA&I	<input checked="" type="checkbox"/>
DTIC TAB	<input type="checkbox"/>
Unannounced	<input type="checkbox"/>
Justification	
By	
Distribution /	
Availability Codes	
Dist	Avail and/or Special
A-1	

TABLE OF CONTENTS

Appendix A:	Representativeness of Wind Measurements on a Mesoscale Grid with Station Separations of 312 m to 10000 m
Appendix B1:	Uncertainty Associated with Emission Rate Estimation
Appendix B2:	Analysis of Fog-Oil Smoke Emissions
Appendix C:	Uncertainties in Source Emission Rate Estimates using Dispersion Models
Appendix D:	Display of Relations among Data using Box Plots
Appendix E:	User's Guide for the Sigplot Plotting Package
Appendix F1:	Listings of the Dugway Data Archives - Historical Datasets
Appendix F2:	Listings of the Dugway Data Archives - Smoke/Obscurant Datasets

APPENDIX A

REPRESENTATIVENESS OF WIND MEASUREMENTS ON A
MESOSCALE GRID WITH STATION SEPARATIONS OF 312m TO 10000m

To Appear in Boundary Layer Meteorology

Appendix A

Table of Contents

Abstract	A-1
1. Objective	A-2
2. Previous Studies of Mesoscale Wind Variability	A-2
Empirical Studies of St. Louis Data	A-3
Theoretical Analysis of Spatial Structure	A-4
3. Proposed Formula	A-6
4. Field Experiment at Hereford, Colorado	A-8
5. Analysis of Hereford Data	A-11
5.1 Single Station Variances as a Function of Averaging Time	A-11
5.2 Statistics of Pairs of Observing Stations	A-14
6. Recommended Empirical Formula for Variances	A-19
7. Test of General Equation with Independent Data	A-20
Acknowledgement	A-23
References	A-23

Appendix A

List of Tables

Table	Page
A-1 Steady-State Periods from the Herford Dataset Selected for Analysis.	A-12
A-2 Ratios of Variances $\sigma^2(T_a)/\sigma^2(1 \text{ min})$ for Averaging Times, T_a , of 10 and 60 min., for Wind Speed and Wind Direction at the Herford Site. Results are Given for Each Run. The Median of the Ratios for the Thirteen Stations is Given. The Scatter of the Ratios for the Thirteen Stations about any Median has a Standard Deviation of about 0.05 to 0.10. Medians over all Dates are Given at the Bottom.	A-15
A-3 Observations and Model Predictions for Dugway Proving Ground Wind Data, with Tower Separation of 500m, for All Levels Combined, and Wind Speed and Direction Combined. Medians are Listed for the Observed Values. Model Parameters are given in the Footnotes.	A-22

Appendix A

Table of Figures

Figure	Page
A-1 Schematic diagram of wind station locations at the Hereford site. Terrain sloped slightly downward from west to east with an average slope of 1%. North is towards the tip of the figure and there is 10 km spacing between stations 1 and 7 or stations 7 and 13.	A-10
A-2 Time series of five-minute averaged wind speed (u) and wind direction (θ) for Station 3 for 31 March 1990 at the Hereford site. Thick lines indicate steady-state periods selected for analysis.	A-13
A-3 Spatial correlation coefficient, R , as a function of station separation for E-W and N-S legs of Hereford monitoring network. Wind speed (u) correlations are on the left, and wind direction (θ) correlations are on the right. Medians over all eleven runs are shown for averaging times of 1 min. (Long Dashes), 10 min. (Short Dashes), and 60 min. (Solid Line). The standard deviation of the scatter of the 11 points about each line is about 0.2.	A-17
A-4 Spatial correlation coefficients, R , for various spatial separations, Δx , and averaging times, T_a (1 min; * 10 min; + 60 min) from Hereford site. Plotted are the medians over eleven runs, E-W and N-S legs, and wind speed and wind direction observations. Typical scatter of all the data about each line is about 0.2 at a correlation of 0.5. Empirical curves from Equation (A-17) are drawn (dotted, $T_a = 1$ min.; dashed, $T_a = 10$ min.; solid, $T_a = 60$ min.).	A-18

Appendix A

Representativeness of Wind Measurements on a Mesoscale Grid with Station Separations of 312m to 10000m

by

Steven R. Hanna and Joseph C. Chang

Sigma Research Corp., 234 Littleton Road, Suite 2E, Westford, MA 01886

Abstract

A field experiment was carried out in which wind speed and direction were measured over flat terrain at a height of 10 m using 13 identical instruments spaced logarithmically along two perpendicular 10 km lines. Station separations ranged from 312 m to 1000 m. One-minute data from 11 sampling periods of duration 6 to 10 hours were studied.

The statistics showed little dependence on whether the line of instruments was oriented along the wind or across the wind, or whether wind speeds or wind directions were being analyzed. The integral time scale derived from the variation of the single station variances with averaging time was found to equal several minutes. The correlation coefficients between two stations separated by distance Δx were found to vary exponentially with Δx , with an integral distance scale on the order of 1 km. At a station separation of 10 km, the correlation coefficient equals 0.24, 0.37, and 0.47 for averaging times of 1, 10, and 60 minutes respectively. These correlation coefficients correspond to root-mean-square differences in wind speed at the two stations of about 1.2, 1.1, and 1.0 m/s respectively.

Empirical equations based on dimensional analysis are suggested for fitting these observations. It is found that the observations are best fit if two independent integral time scales are used - a boundary-layer time scale about 300s that best applies to small averaging times or small separations and a mesoscale time scale of about 1800s that applies to larger averaging times or large separations.

1. Objectives

In order to solve most atmospheric transport and dispersion problems, it is necessary to assume that the wind measurements at one site represent the wind flow at a nearby site. The separation between these two sites can range from 10 m to 100 km. This assumption is sometimes quite good, but situations often occur where wind direction observations differ by 180° between two towers in the same mesoscale network. There are a few limited studies of wind variability over mesoscale distances (e.g. Perry et al. (1978), Lockhart and Irwin (1980), Hanna (1982), and Panofsky and Dutton (1984)), but there is much more theoretical and observational work needed.

This study is part of a comprehensive research program in which the contributions of meteorological uncertainties to errors in air quality modeling and source emission estimation are being investigated. A cooperative two week field experiment was conducted in which 13 wind instruments were set up along an "L-shaped" pattern with maximum station separation of 10 km. Variances and spatial correlations of wind speeds and directions are calculated, with the objective being the development of simplified empirical/theoretical formulas. The accuracy of these simplified formulas is calculated and suggestions made for using these formulas in more generalized mesoscale settings. Finally, the formulas were tested with independent data from a wind study at Dugway Proving Ground.

2. Previous Studies of Mesoscale Wind Variability

The literature contains two types of studies of mesoscale wind variability. Both employ near-surface wind observations made by two or more wind monitors with separations of 10 m to 100 km. In the first type of study, the variances for a variety of wind monitor separations are calculated and presented, and a very simple empirical formula is suggested (e.g., Lockhart and Irwin (1980) and Hanna (1982)). In the second type of study, theoretical formulas based on spectral analyses are applied to the problem (e.g., Pielke and Panofsky (1970), Perry et al. (1978) and Panofsky and Dutton (1984)). Reviews of these two types of studies are given below.

Empirical Studies of St. Louis Data. During the St. Louis Regional Air Pollution Study (RAPS), hourly-averaged wind observations were recorded for one year from a network of twenty-five wind monitors. The separation of the wind monitors ranged from 3 km to 80 km. Lockhart and Irwin (1980) and Hanna (1982) report calculations of the standard deviation, σ , of the difference in wind speed, u , and wind direction, θ , for concurrent measurements between each pair of stations. For example, the following procedure is used to calculate $\sigma(u_a - u_b)$ for any pair of stations, a and b , over the entire sampling period:

$$\sigma^2(u_a - u_b) = \frac{\sum_{i=1}^N (u'_a - u'_b)^2}{N} \quad (A-1)$$

where the primes indicate deviations from the average speed at each station and N is the total number of time periods being analyzed. As the separation distance between the stations decreases, this standard deviation should asymptotically approach the standard deviation due to instrument errors for two co-located wind monitors. Lockhart and Irwin (1980) suggested the regression formulas:

$$\sigma(\theta_a - \theta_b) = 15 + 5.7 \ln x \quad (A-2)$$

$$\sigma(u_a - u_b) = 0.47 + 0.24 \ln x \quad (A-3)$$

where x is in km, θ is in degrees, and u is in m/s. The median value of $\sigma(\theta_a - \theta_b)$ is about 33° and $\sigma(u_a - u_b)$ is about 1.2 m/s, at a median separation distance of about 20 km. The standard deviations of the points scattered about equations (A-2) and (A-3) are 0.16 m/s and 4° , respectively.

Hanna (1982) reported an analysis by Nappo of the same set of RAPS wind data, emphasizing the dependence of the standard deviations of the wind differences upon wind speed. Nappo defined the spatial standard deviations, $\sigma_{\Delta u}$ and $\sigma_{\Delta \theta}$ using the set of concurrent measurements at the 25 monitoring stations. For example, the following procedure is used to calculate $\sigma_{\Delta u}^2$ for any given hour:

$$\sigma_{\Delta u}^2 = \frac{\sum_{i=1}^{24} \sum_{n=i+1}^{25} (u'_i - u'_n)^2}{24!} \quad (A-4)$$

where the prime indicates a deviation from the overall average speed for the 25 stations. The magnitude of the spatial standard deviation, $\sigma_{\Delta u}$ is expected to be somewhat larger than that calculated from equation (A-2), since the differences in the means among the stations are included in equation (A-4). It was found that the differences in wind speed and direction among the stations increase by a factor of three or four as wind speed decreases from 5.0 m/s to about 1.5 m/s. At higher wind speeds (~10 m/s), asymptotic limits of about 5° for σ_{θ} and about 0.15 for σ_u/u are evident. The following empirical formulas fit these data:

$$\sigma_{\Delta \theta} = (5^\circ)^2 + (60^\circ/u)^2 \quad (A-5)$$

$$(\sigma_{\Delta u}/u)^2 = (0.15)^2 + (0.6/u)^2 \quad (A-6)$$

where u is in m/s and σ_{θ} is in degrees.

Theoretical Analyses of Spatial Structure

Panofsky and Dutton (1984, Chapter 9) discuss the technical issues related to the differences in wind velocities measured at two points. They look at the problem from the point of view of the spectrum of sizes of turbulent eddies. They make a distinction between vertical separations, Δz , lateral (cross-wind) separations, Δy , and longitudinal (along-wind) separations, Δx , between the locations of the measurements. Because turbulent eddies tend to maintain their identities as they travel with the wind, at a given separation the along-wind correlations in wind velocities between the measurement stations should be larger than the vertical or cross-wind correlations.

These authors also point out that most of the correlation between wind velocities at two points is due to larger turbulent eddies, with dimensions approximately equal to or larger than the separation between the points. By the same argument, the wind fluctuations in small eddies at one point are uncorrelated with the wind fluctuations in the same size of eddies at a distant point.

Because of the fact that the larger eddies move with the wind flow and slowly change with time, the maximum correlation between two time series of wind velocities at two points separated by an along-wind distance, Δx , may occur at a time lag of about $\Delta x/\bar{u}$, where \bar{u} is the mean wind speed. This is the approximate time required for an air parcel to travel from the first point to the second point.

The issues raised in the previous three paragraphs have led Panofsky and Dutton (1984) and others to the hypothesis that the spatial correlations are functions of the eddy size, the wind speed, and the separation between the wind observation points. They use a mathematical expression known as the coherence, which "is a measure of the square of the correlation between the Fourier component of two time series with their phases adjusted to obtain maximum correlation." The coherence is a function of eddy frequency, n , and is given by:

$$\text{coh}(n) = \frac{[\text{Co}^2(n) + Q^2(n)]}{S_1(n) S_2(n)} \quad (\text{A-7})$$

where $S_1(n)$ and $S_2(n)$ are estimates of the spectral density of the two time series at points 1 and 2, $\text{Co}(n)$ is the cospectrum, and $Q(n)$ the quadrature spectrum. The frequency, n , can have units of cycles per second or radians per second. The cospectrum refers to the correlation due to in-phase fluctuations and the quadrature spectrum refers to the correlation due to fluctuations that are 90° out of phase. The coherence ranges from zero, for no correlation, to one for perfect correlation. In order to calculate $\text{coh}(n)$ for two long time series, specialized computer software for carrying out time series analysis is needed.

Pielke and Panofsky (1970) generalized an empirical expression for the coherence, $\text{coh}(n)$, based on a suggestion by Davenport (1961):

$$\text{coh}(n) = \exp(-a_i n \Delta x_i / u) \quad (\text{A-8})$$

where the subscript i refers to the direction component and the dimensionless "constant", a_i , is called the "decay parameter." Observations show that " a_i " is typically in the range from 1 to 10. The dimensionless variable, $n \Delta x_i / u$, is often referred to as the reduced frequency. It is found that the "constant," a_i , is in fact a function of station separation, Δx . Other investigators have found a_i to be a function of the ambient stability, the turbulence intensity, and the integral time or distance scale of the turbulence. For example, Perry et al (1978) propose the following formula for horizontal station separations, Δx :

$$a = (65\sigma_w/u) + (6.3\sigma_v \Delta x / u L_y) \quad (\text{A-9})$$

where σ_w and σ_v are the standard deviations of turbulent velocity fluctuations in the vertical and cross-wind directions, and L_y is the lateral integral distance scale of the lateral turbulence.

3. Proposed Formula

The relation between wind speed, u , or wind direction, θ , observed at two stations at positions 1 and 2 can be expressed in terms of a variance or a correlation. The relationship between the two quantities can be derived by beginning with the identity:

$$\sigma_{\Delta u}^2 = \overline{(u_2' - u_1')^2} = \overline{u_2'^2} + \overline{u_1'^2} - 2 \overline{u_1' u_2'} \quad (\text{A-10})$$

where the primes refer to fluctuations (i.e., the means have been already subtracted) and the overbar refers to a time average. If the two variances $\overline{u_2'^2}$ and $\overline{u_1'^2}$ are equal, then equation (A-10) can be written in the form:

$$\sigma_{\Delta u}^2 / 2\sigma_u^2 = 1 - R_{12} \quad (A-11)$$

where $\sigma_u^2 = \overline{u'^2}$ and the correlation coefficient $R_{12} = \overline{u_1' u_2'} / \sigma_u^2$. Thus if the correlation equals 1, 0, or -1, the ratio $\sigma_{\Delta u}^2 / 2\sigma_u^2$ will equal 0, 1, or 2, respectively. For two stations that are separated by such a large distance that the correlation equals zero, then Equation (A-11) states that $\sigma_{\Delta u}^2 = 2\sigma_u^2$.

After investigating the semi-theoretical formulas (A-8) and (A-9), it was decided that there was so much adjustment of "constants" taking place that it was best to begin with a simpler formula based on dimensional analysis. This simpler formula does not explicitly include the frequency, n , but does account for frequency effects through the implicit assumption that wind speed autocorrelograms are exponential (i.e., $R = \exp(-\Delta t / T_I)$, implying that a so-called Markov energy spectrum is valid) and are completely determined once an integral time scale, T_I , or space scale, Λ_I , is specified. The following dimensionless relationship can then be postulated:

$$\sigma_{\Delta u}^2 / 2\sigma_u^2 = f(\Delta x, T_I, \Lambda_I, T_a) \quad (A-12)$$

where f is a universal dimensionless function, and variables and parameters are defined in the following way:

$$\sigma_{\Delta u}^2 = \overline{(u_2' - u_1')^2}, \quad \text{where } u_1' \text{ and } u_2' \text{ are wind speed fluctuations at positions 1 and 2.}$$

$$\sigma_u^2 = (\sigma_{u_1}^2 + \sigma_{u_2}^2) / 2 \quad \text{is the average turbulent energy at positions 1 and 2.}$$

Δx is the horizontal separation between positions 1 and 2.

T_I is the integral time scale of the time series of wind speed fluctuations measured at position 1 or position 2.

Λ_I is the integral space scale of the correlogram of wind fluctuation differences $(u_i' - u_1')$ measured between positions 1 and i for several positions.

T_a is the averaging time.

The averaging time, T_a , is very important because it is typically of the same order of magnitude as the integral time scale (i.e., within the range from 1 min to 1 hr). As T_a approaches zero, the ratio $\sigma_{\Delta u}^2 / 2\sigma_u^2$ reaches a maximum at any given station separation, since there are poor correlations between wind fluctuations in smaller eddies at two positions.

Exponential shapes are proposed for all correlation functions:

$$R(\Delta x / \Lambda_I) = \exp(-\Delta x / \Lambda_I) \quad (A-13a)$$

$$R(\Delta t / T_I) = \exp(-\Delta t / T_I) \quad (A-13b)$$

The following approximation to Taylor's equation is used to account for the effects of averaging time on variances:

$$\sigma^2(T_a) / \sigma^2(0) = (1 + T_a / 2T_I)^{-1} \quad (A-14)$$

For a given separation, Δx , the spatial correlation $R(\Delta x / \Lambda_I)$ is also going to depend on averaging time, T_a , since the effects of the fluctuations due to small eddies will drop to zero at large averaging times. Consequently, $R(\Delta x / \Lambda_I)$ should approach unity as T_a increases, and the second term in the following empirical formula is proposed to account for this effect:

$$\begin{aligned} R(T_a, \Delta x) &= [\overline{u_2' u_1'} / \sigma_{u_1} \sigma_{u_2}] (T_a, \Delta x) \\ &= \exp(-\Delta x / \Lambda_I) + (1 - \exp(-\Delta x / \Lambda_I)) g(T_a u / \Lambda_I) \end{aligned} \quad (A-15)$$

where the dimensionless function $g(T_a u / \Lambda_I)$ approaches zero as T_a approaches zero and approaches unity as T_a becomes very large.

4. Field Experiment at Hereford, Colorado

The research programs summarized in Section 2 all took advantage of wind observations made at two or more locations. However, none of these wind observations satisfied all of the following desired characteristics of a study

in which differences in wind observations are being calculated.

- Flat terrain with few obstructions.
- All wind instruments alike, with relatively fast response and adequate calibration procedures.
- Five or more wind stations along a line with spacings ranging from a few hundred meters to 10000 meters.
- Two perpendicular lines of wind stations.
- Several days or more of one-minute averaged wind observations.

A field experiment was designed to satisfy these characteristics, using instruments and technicians from the National Center for Atmospheric Research (NCAR). Thirteen identical wind stations from NCAR's Portable Automated Mesonetwork (PAM) were set up in flat, open farmland (mostly covered by short, winter-weathered grass) near Hereford, Colorado, and operated for the two week period between 30 March 1990 and 14 April 1990. The instruments were installed, maintained and calibrated by experienced NCAR technicians. The anemometers were located at an elevation of 10 m above the ground. A schematic diagrams of the relative instrument locations is given in Figure A-1. The slope of the terrain is less than about 1% over the entire network. It is seen that logarithmic spacings (312.5m, 625m, 1250m, 2500m, 5000m, 10000m) are used for the instruments along each leg of the "L"-shaped network. The perpendicular axes were used in order to determine if there was a significant difference between the along-wind and cross-wind statistics.

The resulting "Hereford" dataset contained values of N-S and E-W components of the wind velocity at one minute resolution. First, these wind components were converted to wind speed, u , and wind direction, θ , for each minute. Because the threshold of these instruments was about 0.5m/s, periods with reported wind speeds less than 0.5m/s were flagged and not used in the analysis. 5-minute averages of u and θ were made and the resulting time series for each station plotted for the entire 16 day duration of the study (see Figure A-2 for an example of the time series plots for 31 March 1990 Station 6). Visual inspection of the 15 days of time series in the figure revealed that, most of the time, the wind speed and direction are quite variable and unsteady in time. For example, during the afternoon on 1 April and 10 April, the wind speed went through a cycle in which it increased from

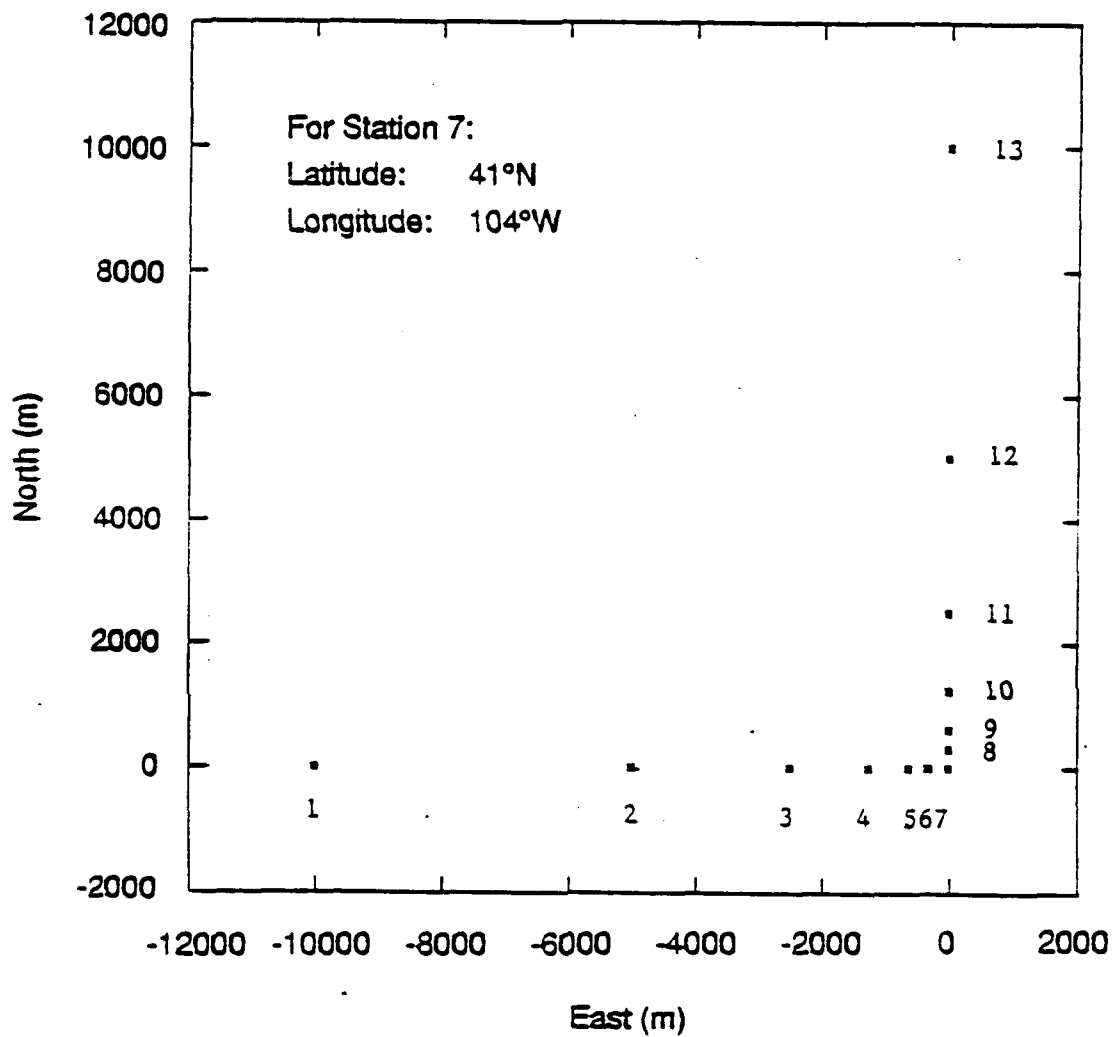


Figure A-1. Schematic diagram of wind station locations at the Hereford site. Terrain sloped slightly downward from west to east with an average slope of 1%. North is towards the top of the figure and there is 10 km spacing between stations 1 and 7 or stations 7 and 13.

nearly zero to about 10 m/s and decreases back down to zero again. This large half-sine-wave would totally dominate any statistical analysis of these wind data.

Because it became clear that any time series analysis of the 16 days would be overly influenced by diurnal changes and synoptic effects, it was decided to confine the analysis to time periods on the order of 6 to 10 hours, when the wind speed and direction appeared to be relatively steady. The eleven steady-state periods that were chosen are listed in Table A-1. Two of these periods are indicated by thick lines in Figure A-2. Median values of wind speed, u , wind direction, θ , standard deviation of wind speed, σ_u , and standard deviation of wind direction, σ_θ , are also listed on the table. These eleven periods are seen to cover a wide range of wind speeds (2.5 to 10.5 m/s), wind directions (170° to 330°) and times of the day.

5. Analysis of Hereford Data

This section presents the results of the analysis of the Hereford data and the next section presents some empirical formulas that fit this dataset. As a first step, variances and time and space correlations were calculated for averaging times of 1, 10, and 60 minutes. A linear trend (estimated from the data from all 13 stations) was removed from the data from each run. Because steady-state periods have been selected and linear trends have been removed, much of the influence of larger mesoscale and regional eddies has been removed there statistics. As will be shown, mesoscale eddies with time scales less than the sampling time are still strongly reflected in the statistics.

5.1 Single Station Variances as a Function of Averaging Time

The variances in the wind speed and wind direction time series were calculated for each of the eleven "steady-state" runs, for each of the thirteen stations, for averaging times of 1, 10, and 60 min. The data are presented in a Table A-2, in the form of ratios of the variance for 10 or 60 minute time periods to the variance for the one minute time period. The medians over the thirteen stations are listed. The overall medians at the

Table A-1

Steady-State Periods from the Hereford Dataset Selected for Analysis.

Meteorological Parameters Represent Medians over 13 Stations

Date/Run	Time	Wind Speed $u(\text{m/s})$	Wind Direction $\theta(^{\circ})$	$\sigma_u(\text{m/s})$	$\sigma_{\theta}(^{\circ})$
0330	00-10	2.5	130	0.7	17
0330	14-24	3.0	215	0.8	17
0331	00-08	3.5	200	0.45	10
0331	16-24	7.5	325	1.2	13
0404	06-12	5.5	90	1.2	13
0404	12-20	7.5	135	1.2	10
0406	18-24	4.0	215	0.9	14
0409	14-24	10.5	10	1.3	8
0411	06-16	3.0	170	0.9	13
0412	00-08	5.5	140	1.1	11
0413	14-20	7.5	330	1.1	10

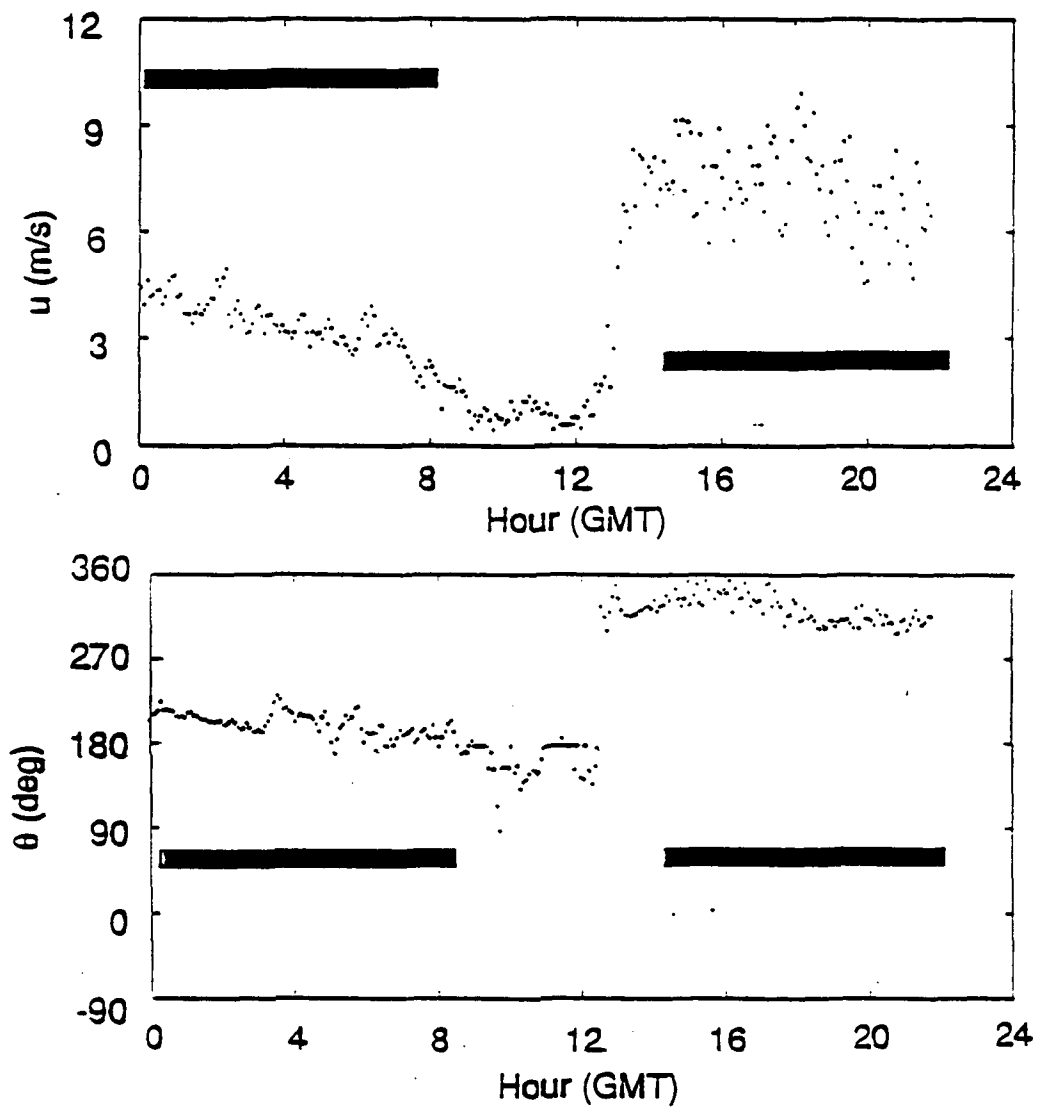


Figure A-2. Time series of five-minute averaged wind speed (u) and wind direction (θ) for Station 3 for 31 March 1990 at the Hereford site. Thick lines indicate steady-state periods selected for analysis.

bottom of the table suggest that there is little difference between the statistics for wind speed and wind direction, with medians of the variance ratios of about 0.68 for $\sigma^2(10 \text{ min})/\sigma^2(1 \text{ min})$ and about 0.39 for $\sigma^2(60 \text{ min})/\sigma^2(1 \text{ min})$. The run-to-run variability in the median variance ratios is about ± 0.20 , with no dependence on wind speed, wind direction, σ_u , σ_θ , or time of day. For a given day, the station-to-station variability in the variance ratios is typically about ± 0.05 to 0.10.

Table A-2 suggests that observed median values of $\sigma^2(10 \text{ min})/\sigma^2(1 \text{ min})$ and $\sigma^2(60 \text{ min})/\sigma^2(1 \text{ min})$ are 0.68 and 0.37, respectively. Solving Equation (14) for the integral time scale T_I , we obtain $T_I \approx 9 \text{ min}$ for $T_a = 10 \text{ min}$ and $T_I \approx 15 \text{ min}$ for $T_a = 60 \text{ min}$. This trend is duplicated in all types of calculations in this analysis, i.e., the derived time and distance integral scales increase as the averaging time, T_a , or station separation, Δx , increase. Persistent mesoscale eddies are associated with turbulence at time scales of several hours and distance scales of several tens of kilometers. Superimposed on these "baseline mesoscale eddies" are the smaller turbulent eddies normally thought to be associated with the atmospheric boundary layer. Consequently it is assumed that the turbulent velocity field is described by two time scales, one (T_{I1}) associated with boundary layer turbulence, and another (T_{I2}) associated with mesoscale eddies. These two time scales are assumed to contribute equally to $\sigma^2(T_a)$, leading to the following modification to Equation (A-14):

$$\frac{\sigma^2(T_a)}{\sigma^2(0)} = \frac{0.5}{1 + T_a/2T_{I1}} + \frac{0.5}{1 + T_a/2T_{I2}} \quad (\text{A-16})$$

The Hereford dataset is best-fit by $T_{I1} \approx 300\text{s}$ and $T_{I2} \approx 1800\text{s}$, which yield $\sigma^2(10)/\sigma^2(1) = 0.71$ (slightly above the median observation of 0.68) and $\sigma^2(60)/\sigma^2(1) = 0.35$ (slightly below the median observation of 0.37).

5.2 Statistics for Pairs of Observing Stations

The spatial statistics to be presented are all keyed to wind station (7) at the corner of the "L" of the network shown in Figure A-1. The results in this section are given for the spatial correlation coefficient,

Table A-2

Ratios of Variances $\sigma_u^2(T_a)/\sigma_u^2(1 \text{ min})$ for Averaging Times, T_a , of 10 and 60 min., for Wind Speed and Wind Direction at the Hereford Site. Results are Given for Each of Eleven Runs. The Median of the Ratios for the Thirteen Stations is Given. The Scatter of the Ratios for the Thirteen Stations about any Median has a Standard Deviation of about 0.05 to 0.10. Medians over all Dates are Given at the Bottom.

Run Date/Time	$\sigma_u^2(T_a)/\sigma_u^2(1 \text{ min})$		$\sigma_\theta^2(T_a)/\sigma_\theta^2(1 \text{ min})$	
	Wind Speed		Wind Direction	
	10 Minute	60 Minute	10 Minute	60 Minute
0330/00-10	.88	.61	.93	.58
0330/14-24	.71	.58	.69	.50
0331/00-08	.74	.39	.77	.36
0331/16-24	.41	.21	.64	.25
0404/06-12	.55	.19	.81	.50
0404/12-20	.51	.37	.42	.17
0406/18-24	.31	.13	.40	.10
0409/14-24	.68	.58	.63	.34
0411/06-16	.81	.51	.76	.38
0412/00-08	.80	.56	.92	.52
0413/14-20	.38	.15	.50	.20
Overall Median	0.68	0.39	0.69	0.36

$R(\Delta x, T_a) = \overline{u_1' u_7'} / \sigma_{u_1} \sigma_{u_7}$, which are functions of the separation, Δx , of stations 1 and 7, the averaging time, T_a and the integral scale of the turbulence. Averaging times of 1, 10 and 60 min are used. Results are presented separately for the E-W and N-S legs of the "L". Rather than showing the correlation for all eleven time periods or runs, we present the median of the 11 periods. These correlations, are plotted in Figure A-3. There does not appear to be a strong dependence on E-W or N-S leg, or on whether wind speed or wind direction is being plotted.

As expected, the calculated correlations are lowest for the shorter averaging times and the largest station separations, due to the fact that the dominant turbulent eddies are characterized by space scales of a few hundred meters and time scales on the order of a few minutes.

At the 10 km separation distance, the correlations average about 0.5. Because of the relation between spatial correlation, R_{12} , spatial variance, $\sigma_{\Delta u}^2$, and variance, σ_u^2 , indicated by Equation (A-11), it follows that, at 10 km separation, $\sigma_{\Delta u}^2 = \sigma_u^2$. Knowing that $\sigma_u^2(T_a = 1 \text{ min}) \approx 1.2 \text{ m}^2/\text{s}^2$, and using the median values of $\sigma_u^2(T_a)/\sigma_u^2(1 \text{ min})$ in Table A-2, it can be concluded that $\sigma_{\Delta u}^2 \sim 1.1 \text{ m}^2/\text{s}^2$ for $T_a = 1 \text{ min}$, $\sigma_{\Delta u}^2 \sim 0.8 \text{ m}^2/\text{s}^2$ for $T_a = 10 \text{ min}$, and $\sigma_{\Delta u}^2 \sim 0.4 \text{ m}^2/\text{s}^2$ for $T_a = 60 \text{ min}$ at the 10 km separation distance. This value of $\sigma_{\Delta u} \sim 0.7 \text{ m/s}$ for one-hour averages is close to that found with the St. Louis RAPS data, as discussed in Section 2.

At small averaging times, T_a , Equation (A-15) suggests that the correlation coefficient for wind speed fluctuations at two points separated by a distance, Δx , should be an exponential function of Δx . Therefore, if $\ln R$ is plotted against Δx , a straight line should be seen. Observations of R from this wind network are plotted in Figure A-4, for the six Δx values (312.5, 625, 1250, 2500, 5000, and 10000 m) and three averaging times (1, 10, and 60 min) of interest. Because the correlations in Figure A-3 did not indicate much dependence on E-W or N-S direction, and were similar for wind speed and wind direction, all runs, legs, and variables are combined in this table and figure.

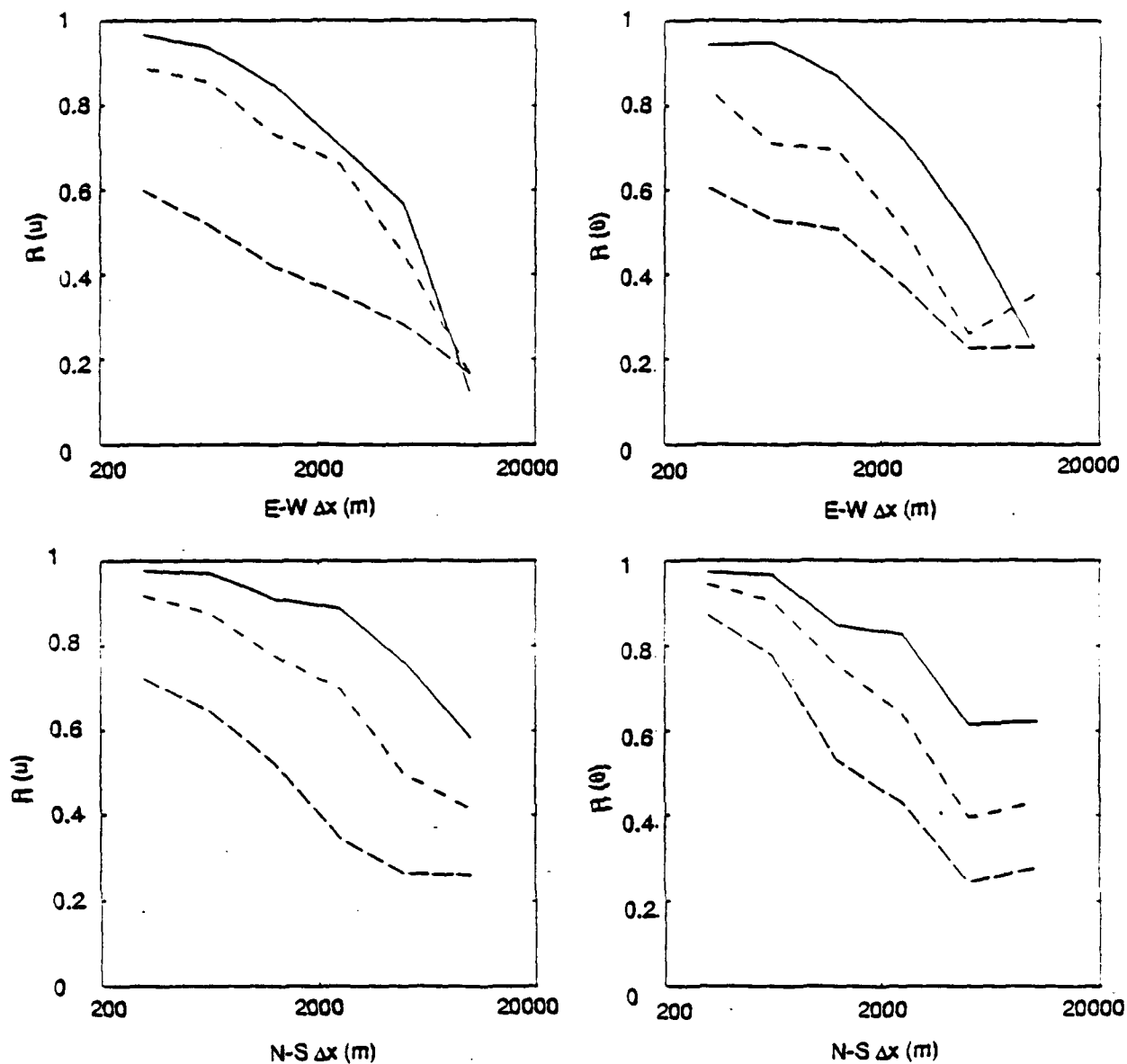


Figure A-3. Spatial correlation coefficient, R , as a function of station separation for E-W and N-S legs of Hereford monitoring network. Wind speed (u) correlations are on the left, and wind direction (θ) correlations are on the right. Medians over all eleven runs are shown for averaging times of 1 min. (Long Dashes), 10 min. (Short Dashes), and 60 Min. (Solid Line). The standard deviation of the scatter of the 11 points about each line is about 0.2.

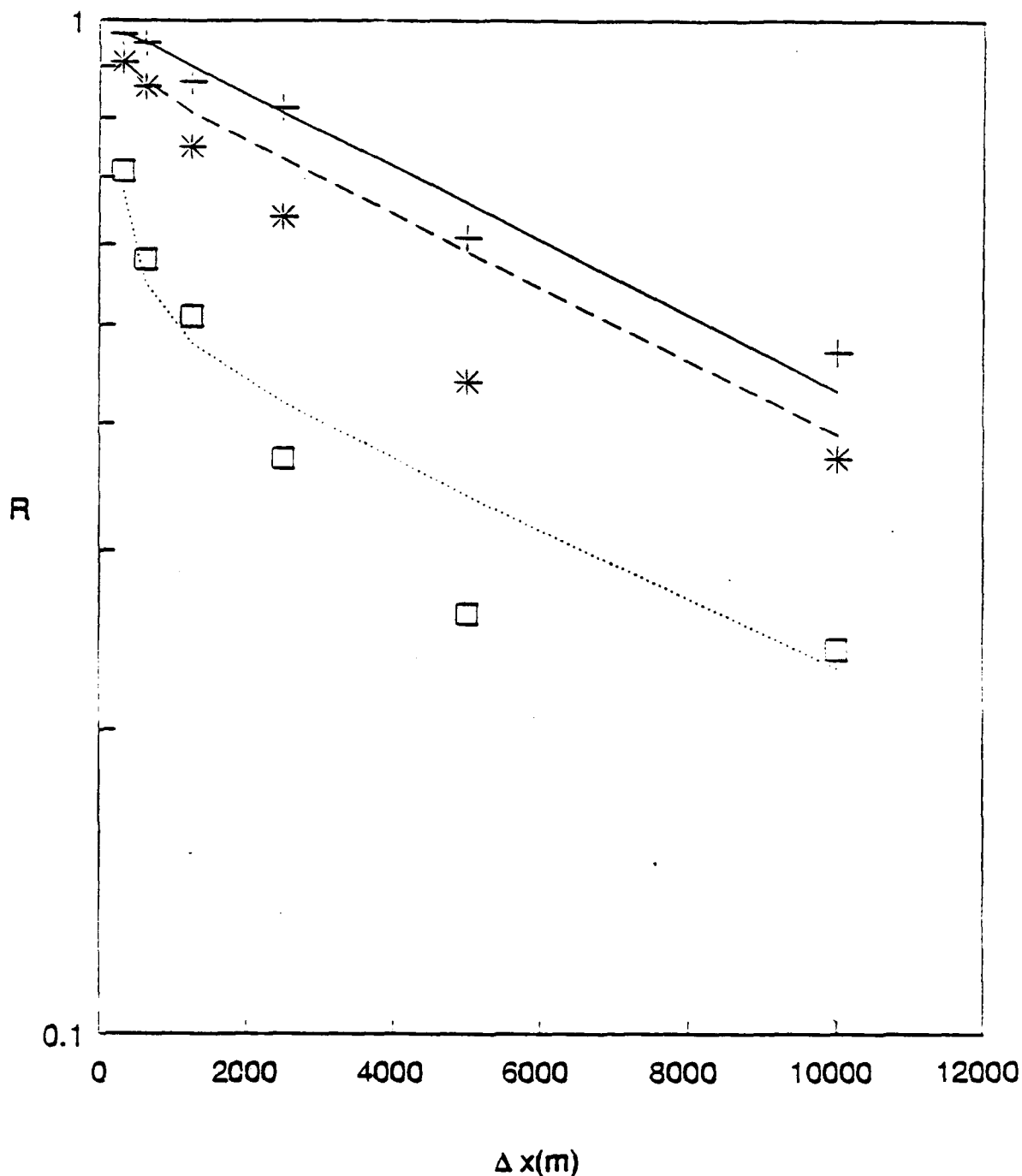


Figure A-4. Spatial correlation coefficients, R , for various spatial separations, Δx , and averaging times, T_a (\square 1 min; $*$ 10 min; $+$ 60 min), from Hereford site. Plotted are the medians over eleven runs. E-W and N-S legs, and wind speed and wind direction observations. Typical scatter of all the data about each line is about 0.2 at a correlation of 0.5. Empirical curves from Equation (A-17) are drawn (dotted, $T_a = 1$ min.; dashed, $T_a = 10$ min.; solid, $T_a = 60$ min.).

The points in the figure follow a straight line only for the largest averaging time (60 min). For the smallest averaging time (1 min), there is a much more rapid drop-off in correlation at small separation distances. This behavior can be explained by the same two-scale phenomenon discussed under Section 5.1 in the analysis of the effects of averaging time; i.e., the results are influenced by a smaller eddy scale, Λ_1 , representative of boundary layer processes, and a larger eddy scale, Λ_2 , representative of mesoscale fluctuations. However, the effects of the smaller scales tend to disappear at large averaging times, T_a , when the condition $T_a > \Lambda_1/u$ is satisfied. Thus, equation (A-15) appears to be satisfied, with the limits:

$$R(\Delta x, T_a \rightarrow 60 \text{ min}) = e^{-\Delta x/\Lambda_2}$$

$$R(\Delta x, T_a \rightarrow 1 \text{ min}) = 0.5e^{-\Delta x/\Lambda_1} + 0.5e^{-\Delta x/\Lambda_2}$$

The following empirical equation fits these data and has the proper asymptotic behavior:

$$R(\Delta x, T_a) = e^{-\Delta x/\Lambda_2} - 0.5 \left(e^{-\Delta x/\Lambda_2} - e^{-\Delta x/\Lambda_1} \right) / \left(1 + (T_a u / a \Lambda_1)^2 \right) \quad (\text{A-17})$$

where $\Lambda_1 = 300 \text{ m}$, $\Lambda_2 = 12000 \text{ m}$, and $a = 5$ when $u \approx 5 \text{ m/s}$. The predicted curves are drawn on Figure A-4. The value of $a = 5$ is consistent with "Pasquill's Beta" = 4, which is the known proportionality factor between Lagrangian and Eulerian scales. Because the actual eddy diameters are equal to about five times the integral scales Λ , the smaller eddy diameters would be about 1500 m and the larger eddy diameters would be about 60 km. Of course the confidence limits on the data (\pm about 0.2) are so broad that a much wider range of scales, Λ_1 and Λ_2 , is possible. Furthermore, these results are limited to this particular site and time of year, and to the ranges of Δx , T_a , and meteorological conditions that we have considered. The sampling time (a maximum of 10 hours) also imposes a maximum limit on integral scales.

6. Recommended Empirical Formula for Variances

Our analysis of the Hereford data has suggested that the variances and correlations for wind speed and wind direction are similar. In addition, we

have found that, despite the theoretical prediction that along-wind correlations will be larger than cross-wind correlations, there is no clear dependency of the correlations on wind direction (or any other meteorological variable). This apparent lack of dependency may be due to the fact that this effect is overwhelmed by the natural variability in the observations.

The similarity relations in Equation (A-8) have been shown to be valid, resulting in Equation (A-16) for the effects of averaging time and Equation (A-17) for the effects of station separation. These equations can be combined into the following general equation:

$$\frac{\sigma_{\Delta u}^2(\Delta x, T_a)}{2\sigma_u^2(T_a = 0)} = \left[\frac{0.5}{1 + T_a/2T_{I1}} + \frac{0.5}{1 + T_a/2T_{I2}} \right] \cdot \left[1 - e^{-\Delta x/\Lambda_2} + 0.5 \frac{(e^{-\Delta x/\Lambda_2} - e^{-\Delta x/\Lambda_1})}{(1 + (T_a u/a\Lambda_1)^2)} \right] \quad (A-18)$$

where $T_{I1} \sim 300$ s $T_{I2} \sim 1800$ s
 $\Lambda_1 \sim 300$ m $\Lambda_2 \sim 1200$ m
 a (Lagrangian-Eulerian scale) ~ 5

This equation should be tested with independent data from a different site. Slightly different values of the time and distance scales may be appropriate at a different site. For any given time and place, the confidence limits on the results would be expected to be in the same range (about 20% to 30%) has been found here.

7. Test of General Equation with Independent Data

A set of independent wind data from the so-called XM21 field study at Dugway Proving Ground, Utah, were provided by C. Biltoft. Data were available from two towers, separated by 500m, on a relatively flat test range. Instruments were located at heights of 2, 4, 8, 16, and 32m, and measurements were made at a frequency of one per second. Because the towers were constructed of scaffolding, it was necessary to disregard periods when the

wind blew through one of the towers. Two periods of valid data were analyzed--from 1110 to 1651 on 11 April 1989, and from 0937 to 2059 on 2 May 1989. Both periods were marked by wind speeds of about 3.5 m/s and relatively strong turbulence intensities ($\sigma_u/\bar{u} \sim 0.3$ and $\sigma_\theta \sim 30^\circ$).

Because the integral scales of the horizontal components of turbulence are not strongly dependent on height, the results from all five levels are combined in our analysis. This assumption will cause a slight error, since the various ratios $\sigma^2(T_a)/\sigma^2(1\text{sec})$ and correlations are observed to increase by about 10% to 20% between heights of 2m and 32m. In addition, the wind speed and direction results appear similar and are combined in our analysis. The combined data results (two variables, two days, five levels) are presented in Table A-3.

The predictions of $\sigma^2(T_a)/\sigma^2(1\text{sec})$ in the table have been made using Equation (A-16), with the same time scales derived from the NCAR wind network ($T_1 = 300\text{s}$ and $T_2 = 1800\text{s}$). There is a $\pm 10\%$ agreement between the predictions and the observed medians, and the predictions are within the \pm standard deviation error bounds of the observations. It can be concluded that the variances $\sigma^2(T_a)$ show similar behavior at the two sites, and that Equation (A-16) can adequately simulate this behavior.

Equation (A-17) (for spatial correlations) does not transfer as well to the new site. Its predictions are shown under column (2), assuming the parameters ($\Lambda_1 = 300\text{m}$, $\Lambda_2 = 12000\text{m}$, and $a = 5$) derived from the NCAR wind network. Clearly the predictions of $R_{\Delta u}(T_a)$ are too low by about 10 to 30%. If the Λ_1 , Λ_2 , and "a" parameters are "tuned" with these new data, the predictions under column (3) are all within $\pm 4\%$ of the observations. However, the smaller of the length scales, Λ_1 , has to be increased from 300m to 1000m, and the Lagrangian-Eulerian parameter "a" has to be reduced from 5 to 0.2. It appears that the weakest part of Equation (A-17) is the correction term, $(1 + (uT_a/a\Lambda_1)^2)^{-1}$, for averaging time, T_a . This term is intended to cause an increase in the spatial correlation as averaging time increases. However, the functional form for this correction term is not obvious and more thought is clearly needed.

Table A-3

Observations and Model Predictions for Dugway Proving Ground Wind Data,
with Tower Separation of 500m, for All Levels Combined,
and Wind Speed and Direction Combined. Medians are Listed for the
Observed Values. Model Parameters are given in the
Footnotes.

Averaging Time T_a	$\frac{\sigma^2(T_a)}{\sigma^2(1\text{sec})}$	$\frac{\sigma^2(T_a)}{\sigma^2(1\text{sec})}$	$R_{\Delta u}(T_a)$	$R_{\Delta u}(T_a)$	
	Observed	Predicted	Observed	Predicted	
		(1)		(2)	(3)
1 sec			0.78	0.57	0.77
60 sec	0.87	0.95	0.83	0.58	0.86
600 sec	0.68	0.65	0.94	0.83	0.95

- Footnotes: (1) Equation (A-16) is used, with the same values for the parameters as derived from the NCAR data ($T_1 = 300\text{s}$ and $T_2 = 1800\text{s}$)
- (2) Equation (A-17) is used, with the same values for the parameters as derived from the NCAR data ($\Lambda_1 = 300\text{m}$, $\Lambda_2 = 12000\text{m}$, and $a = 5$)
- (3) Equation (A-17) is used, with $\Lambda_1 = 1000\text{m}$, $\Lambda_2 = 12000\text{m}$, and $a = 0.2$.

Acknowledgements:

This research would not have been possible without the assistance of scientists and technicians from the National Center for Atmospheric Research who were responsible for all aspects of the Hereford field study. In particular, the authors thank Dr. Thomas Horst, who managed the study.

The authors appreciate the assistance of Christopher Biltoft, and James Bowers of the U.S. Army Dugway Proving Ground. This research was co-sponsored by the U.S. Army (James Bowers, Project Monitor) and the U.S. Air Force (Captain Michael Moss, Project Monitor.)

References:

- Davenport, A.G., :1961, "The Spectrum of Horizontal Gustiness near the Ground in High Winds," *Quart. J. Roy. Meteorol. Soc.* 87, 194-211.
- Hanna, S.R. :1982, "Applications in Air Pollution Modeling," Ch. 7 in *Atmospheric Turbulence and Air Pollution Modelling*. (Eds: F.T.M. Nieuwstadt and H. van Dop), 275-310.
- Lockhart, T.J. and Irwin J.S., :1980, "Methods for Calculating the Representativeness of Data," *Proceedings, DOE Symposium on Intermediate Range Atmospheric Transport Processes and Technology Assessment*, CONF801064, NTIS, 169-176.
- Panofsky, H.A. and Dutton J.A., :1984, "*Atmospheric Turbulence*," John Wiley and Sons, New York, Chapter 9.
- Perry, S.G., Norman J.M., Panofsky H.A. and Martsolf J.D., :1978, "Horizontal Coherence Decay near Large Mesoscale Variations in Topography," *J. Atmos. Sci.* 35, 1884-1889.
- Pielke, R.A. and Panofsky H.A., :1970, "Turbulence Characteristics along Several Towers," *Bound. Lay. Meteorol.* 1, 115-130.

Intentionally Blank

APPENDIX B-1

UNCERTAINTY ASSOCIATED WITH EMISSION RATE ESTIMATION

Appendix B-1

Table of Contents

Uncertainty Associated with Emission Rate Estimation

	Page
1. Introduction	B-1
2. Measurement of Smoke Munition Emissions	B-2
2.1 Wind Tunnel Experiments	B-2
2.2 Field Experiments	B-4
3. The Emission Rate Expression	B-6
3.1 Input Parameters	B-6
3.2 Approach to Estimating Uncertainty in the Emission Rate	B-10
3.3 Uncertainty Analysis Results	B-16
4. Conclusions and Recommendations	B-19
References	B-21

Definition of Terms

A, B, C, D	coefficients which are determined by fitting the observed wind tunnel experiments to a curve
COV_{xy}	covariance of xy
CV_x^2	squared coefficient of variation of x, $\frac{\sigma_x^2}{\bar{x}^2}$
CV_y^2	squared coefficient of variation of y, $\frac{\sigma_y^2}{\bar{y}^2}$
h	relative humidity
M_o	initial mass
M_x	mass of zinc or phosphorus aerosolized, as measured in the wind tunnel experiments
MYF	munition yield factor, the ratio $\frac{M_x}{M_o}$
Q_t	mass emission rate
q	$\frac{Q_t}{M_o}$
\bar{x}	mean of x
\bar{y}	mean of y
YF	yield factor, theoretical adjustment to mass of aerosol based on the ability of the active ingredient to absorb water vapor
ΔM	mass lost during burn, initial mass less final mass, as measured by the load cell
σ_{xy}^2	variance of the product xy
σ_x^2	variance of x
σ_y^2	variance of y

UNCERTAINTY ASSOCIATED WITH EMISSION RATE ESTIMATION

1. Introduction

To estimate the uncertainty of an entire model it is necessary to evaluate the uncertainty of its components. The input data for atmospheric dispersion models consists of emission rate data and meteorological data. In this discussion we address the issue of uncertainty associated with the estimation of emission rates of aerosols from smoke munitions. Emission rates are generally expressed in terms of weight per unit time; in this case they are expressed as grams of active ingredient, (e.g., phosphorus) per second.

The issue of estimating the emission rate of obscurant munitions is complex, aside from the issue of estimating the associated uncertainty. There are several reasons for this. First, the critical property which provides the obscurant effect is not directly emitted by the munition; it results from an interaction of the active ingredient, e.g., red phosphorus, and moisture in the ambient atmosphere to form a dense smoke cloud. Second, munitions contain other materials which burn simultaneously but do not contribute directly to the obscurant effect; thus measuring total weight loss over burn time only indirectly measures the amount of active ingredient which has been released. Third, to experimentally determine the amount of active ingredient released, the mass of the active ingredient in the entire smoke cloud must be determined and this measurement can only be carried out in a wind tunnel. Thus, data from the wind tunnel experiments are extrapolated to the field setting. These issues affect emission rate estimation as well as contribute to the associated uncertainty.

This discussion covers the following topics: how emissions are measured in both wind tunnel and field experiments, the model used for estimating emission rates, a technique for estimating uncertainty (using existing data as an example), and conclusions and recommendations for the collection of additional data which would enhance the uncertainty analysis. Several reports were reviewed for this analysis, but the information on the method of measuring and modeling emission rates is based on two reports: *Basic*

Smoke Characterization Test (DPG-FR-77-311) (DPG, 1978) and *Methodology Investigation Final Report Validation of a Transport and Dispersion Model for Smoke* (DPG-FR-702) (Carter et al., 1979). These reports contain data on three different types of smoke obscurant munitions: white phosphorus, red phosphorus, and zinc oxide-hexachloroethane-aluminum. Because only limited amounts of appropriate data are available for the uncertainty analysis, the conclusions drawn from this analysis must be considered tentative.

2. Measurement of Smoke Munition Emissions

2.1 Wind Tunnel Experiments

The most detailed measurement of emission rates of submunitions were conducted in wind tunnel experiments. Although field measurements have been collected, these data are not adequate for developing a model. Thus, the model used to predict emission rates is based on the wind tunnel experiments. The experiments and the data described in this section are summarized from DPG (1978).

The wind tunnel experiments were conducted at the Dugway wind tunnel. In the experiments, single submunitions (e.g., an individual component which contains the smoke producing compound) of zinc and white phosphorus were burned. In actual field use of smoke munitions, multiple submunitions are loaded into a canister and burn simultaneously. For red phosphorus, three submunitions (wedges) were burned simultaneously. The wind tunnel tests were conducted at a wind speed of 2 m/s and the ambient temperature, relative humidity, (%RH), and barometric pressures were recorded. Pre-weighed submunitions were placed on a load cell in the center line of the tunnel and fired remotely. The load cell recorded the elapsed time and weight loss of the submunition as it burned. The end of the tunnel had a barrier that contained a grid of holes through which the air in the tunnel passed. The air passed into sampling lines and through collection devices, impingers. (See Figure B-1.) The impingers were then analyzed for zinc or phosphorus, the appropriate active ingredient. The concentrations in all impingers were summed to determine the total amount of active ingredient which had been aerosolized during the burn. Data collected on each test included: weight loss with burn time, total zinc or phosphorus, tunnel wind speed, temperature, and relative humidity.

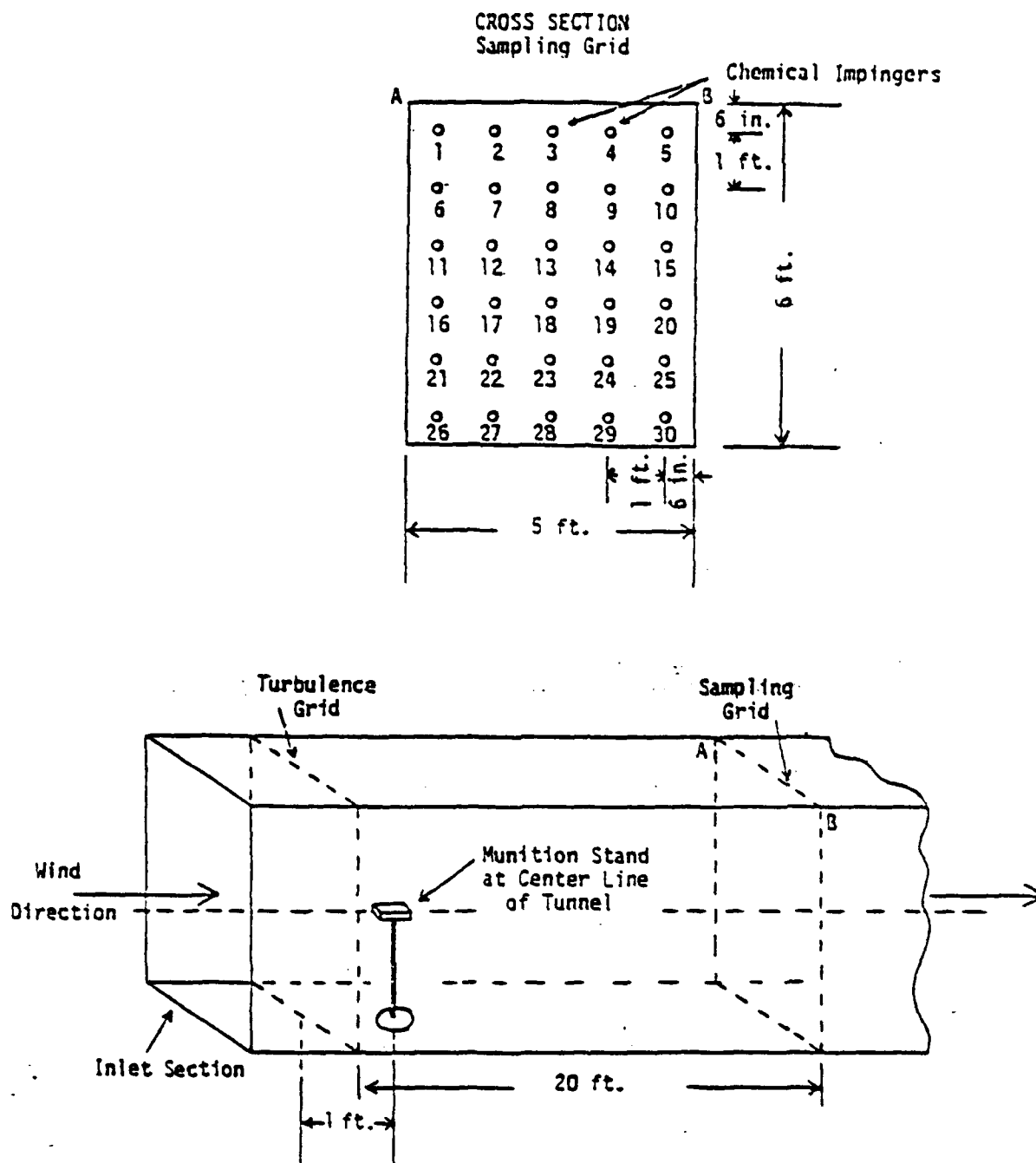


Figure B-1. Diagram of Wind Tunnel.

Source: DPG, 1978

Transmittance, which is routinely measured in the field, cannot be measured in the wind tunnel because the concentrations are too high. The types of submunitions tested (as reported in DPG (1978)) were:

- 155mm HC M1 Canister (zinc)
- 155mm HC M2 Canister (zinc)
- 105mm HC M1 Canister (zinc)
- 6 inch WP Wick (white phosphorus)
- 2.75 inch Rocket WP Wick (white phosphorus)
- 81mm Navy RP Wedge (red phosphorus)
- 155mm Navy RP Wedge (red phosphorus)
- 81mm German RP Wedge (red phosphorus).

For each type of submunition, two burns were conducted.

2.2 Field Experiments

The field experiments were conducted at the Horizontal Grid, Dugway Proving Ground, Utah. The experiments described in this section are summarized from DPG (1978). The data were collected by means of photography, aerosol sampling with aerosol photometers, particle size analyzers, and impingers. Samplers were located 1.22 meters above the ground. Motion pictures recorded the size and shape of the smoke cloud; aerosol photometers recorded total particle concentration; particle size analyzers recorded size distributions; and impingers measured zinc or phosphorus concentrations. The mass of zinc or phosphorus from these impingers cannot be summed to calculate total zinc or phosphorus aerosolized as was done in the wind tunnel experiments because the total smoke cloud is not collected by the impingers.

Figure B-2 (DPG, 1978) shows the layout of the instruments for these experiments. The sampling line was always oriented perpendicular ($\pm 45^\circ$) to the prevailing wind direction. The impingers were located halfway between the aerosol photometers. As in the wind tunnel experiments, the munitions were placed in a load cell so that data on weight loss with burn time were recorded. The types of submunitions tested were the same as those used in the wind tunnel experiments. For each type of submunition, two burns were conducted.

The meteorological data recorded in these experiments included: wind speed and direction, temperature, and relative humidity.

3. The Emission Rate Expression

The critical parameter to be derived from these experiments is the amount of smoke generated per second of burn time. In its simplest form, this would be calculated by dividing the mass lost by the burn time to derive a value in units of grams per second. However, the amount of smoke generated is more than a function of the mass burned; it is also a function of the interaction of the zinc or phosphorus with water vapor to create the smoke. Zinc and phosphorus are hygroscopic, absorbing upwards of four times their mass in water vapor. Thus, the actual emission rate of interest is total amount of hydrated smoke generated per second. To add one further complexity to the equation, the burn rate of the munitions is not constant with time. There is an initial growth period, followed by a plateau of relatively constant rate of emissions, followed by a rapid decline. In field tests, there are data which indicate munitions can burn unevenly; this is characterized as "flashing" toward the end of the burn time by the observers.

The following discussion covers two topics. The first topic presents the parameters in the emission rate expression and the second discusses the uncertainty associated with those parameters and presents a technique for computing the uncertainty in the overall emission rate value.

3.1 Input Parameters

The emission rate of hydrated smoke is a function of the initial mass of the munition, the fraction of this mass which is the aerosolized zinc or phosphorus, the increase in mass of the aerosol due to hydration, and burn time. The expression which was developed from the wind tunnel experiments to estimate the emission rate is as follows (DPG, 1978):

$$Q_s = M_o MYF YF(A/t_b + 2Bt/t_b^2 + 3Ct^2/t_b^3 + 4Dt^3/t_b^4) \quad (B-1)$$

where: Q_t = mass emission rate

M_o = initial mass

MYF = munition yield factor

YF = yield factor

A,B,C,D = coefficients which are determined by fitting the
observed data in the wind tunnel experiments to a curve.
They are constrained to sum to unity.

The munition yield factor, MYF, is the ratio of the mass of zinc or phosphorus burned, M_x , to the initial mass of the munition, M_o . M_x is determined from the wind tunnel experiments and is calculated by summing the mass of zinc or phosphorus collected by all the impingers. These wind tunnel values of M_x are used to predict the emission rate, Q_t , for field experiments, as M_x cannot be measured in the field setting.

The yield factor takes into account the hygroscopic growth of the aerosolized zinc or phosphorus and is a function of ambient relative humidity. For the three different types of smoke munitions, yield factors are based on theoretical calculations or experimental data. The conceptual definition of the yield factor is:

$$YF = \frac{\text{mass of smoke (including aerosol)}}{\text{mass of starting material}}$$

In the case of phosphorus, the final material is primarily hydrated orthophosphoric acid, ($H_3PO_4 + nH_2O$). According to DPG (1977), it is assumed that the hydration of the droplets of H_3PO_4 proceeds until their aqueous vapor pressure equals the partial pressure of H_2O in the atmosphere. The mass of hydrated H_3PO_4 is then constant (assuming no other environmental changes occur) and the yield factor can be expressed as:

$$YF = \frac{\text{mass } H_3PO_4 + nH_2O}{\text{mass P}}$$

DPG (1977) contains the following example of how a yield factor is calculated. Yield factors for phosphorus can be readily computed from tables correlating aqueous vapor pressures with the composition of various mixtures

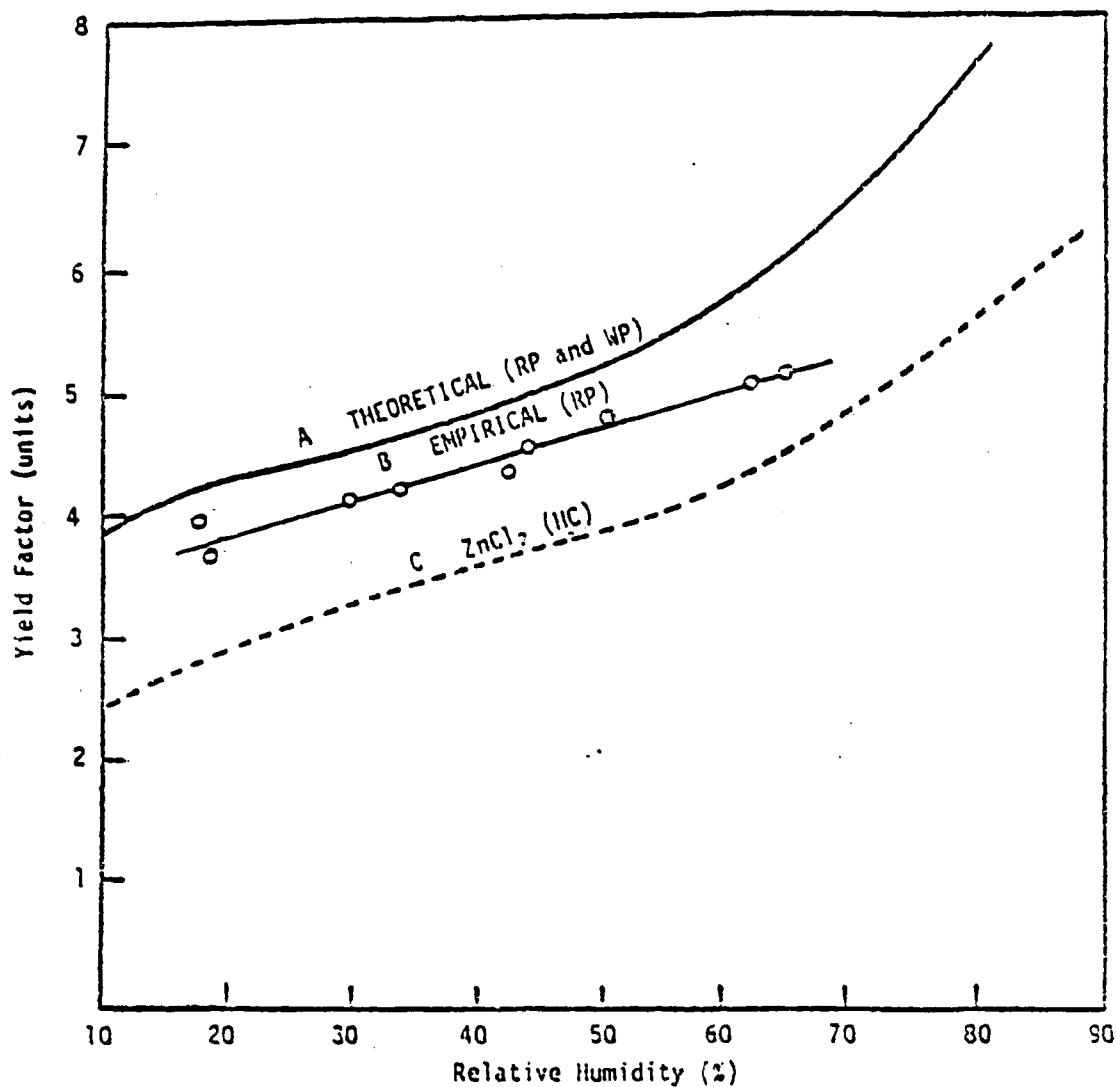
of H_3PO_4 , when the concentration of H_3PO_4 in the solution is expressed as weight %, (i.e., $\text{mass}(\text{H}_3\text{PO}_4) \times 100 / \text{mass}(\text{H}_3\text{PO}_4 + n\text{H}_2\text{O})$). For a specified aqueous vapor pressure, the ratio of the molecular weight of H_3PO_4 to the atomic weight of P is 3.16:

$$\text{YF} = \frac{100 \times 3.16}{\text{H}_3\text{PO}_4(\text{wt } \%)} = \frac{316}{\text{H}_3\text{PO}_4(\text{wt } \%)}$$

Taking, as an example, the burning of 1 gram of P in the air at 25°C and containing moisture at a partial pressure of 22.39 mmHg, the oxidation to phosphoric oxide and hydrolysis of phosphoric oxide will result in $1 \times 98/31$ gram or 3.16 gram H_3PO_4 . H_3PO_4 will then hydrate until the aqueous vapor pressure of the diluted H_3PO_4 ($\text{H}_3\text{PO}_4 + n\text{H}_2\text{O}$) equals the ambient vapor pressure. At 22.39 mmHg and 25°C , the equilibrium composition of the mixture is found to be 20.07 weight % H_3PO_4 . The YF is then $316/20.07 = 15.7$, (i.e., under these conditions, the mass of smoke is 15.7 gram for every gram of P burned). An additional correction will be necessary if the munition efficiency is not 100%.

DPG (1978) notes that the theoretical curve for phosphorus assumes that orthophosphoric acid is produced immediately during combustion. If this assumption does not hold, the yield factor may overestimate the effective dosage. DPG (1977) also presents a derivation which proves that YF's are insensitive to temperature up to 100°C .

Figure B-3 (DPG, 1978) presents yield factor curves based on theoretical calculations for P as well as empirical data for red phosphorus and theoretical calculations for zinc oxide-hexachloroethane-aluminum (HC). It can be seen from these figures that the slope of the lines for all three materials, white phosphorus, red phosphorus, and the zinc based munition, is relatively shallow over the range of relative humidity from approximately 20% to 65%. For example, over the range of 20% to 65% RH, the yield factor for red phosphorus increases by a factor of 1.4. However, the theoretical curves rise sharply at humidities greater than 65%. Between humidity levels of 65% to 80% red and white phosphorus increase by a factor of approximately 1.3 and hydrated zinc chloride by a factor of 1.7. For field tests conducted on one day, the relative humidity would not be expected to vary over this wide a range, so that



Curve A: Yield factors for the conversion of P to hydrated H_3PO_4 (ref. 8).
 Curve B: Yield factors empirically determined for RP.
 Curve C: Yield factors for the conversion of Zn to hydrated $ZnCl_2$ (ref. 5).

Figure B-3. Yield factors as a function of relative humidity for various smoke producing agents. Source: DPG, 1978.

the yield factor between burns should not vary substantially. For example, an increase from 40% to 50% RH only produces a difference in the yield factor of 1.04 for red phosphorus. During the field experiments, which took place on several different days, the relative humidity varied from 40% to 80%, but within a given day the RH only varied by 2%-4%.

3.2 Approach to Estimating Uncertainty in the Emission Rate

A direct method for determining uncertainty values would be to compare modeled emission rates with actual emission rates; however, emission rate measurements from the field experiments are not available. In the absence of actual data, uncertainty values can be modeled based on estimated uncertainty values for the input parameters and on the uncertainty inherent in the emissions rate model. To estimate uncertainty values for the variables, there should be sufficient data available to calculate the probability density functions (i.e., measures of variability) of the input variables. To model the uncertainty in the emission rate model, an assumption must be made regarding the independence or dependence of the variables in the model, as there are different approaches for each case.

The following discussion presents both a qualitative and quantitative assessment of the emission rate uncertainty of the various smoke munitions. The qualitative assessment highlights the sources of uncertainty of the input parameters to the emission rate model and the limitations imposed by the amount of data (for each type of munition) available for the analysis. The quantitative assessment presents a model for estimating the emission rate uncertainty and an example application for several munitions.

Two factors limit the uncertainty analysis of the smoke munitions data. First, too few experiments were conducted for each type of munition to determine robust probability density functions for the various parameters. For both wind tunnel and field experiments only two burns were conducted for each type of submunition, thus means or variances will not be stable or robust. Confidence intervals are large when $n = 2$. Therefore the quantitative uncertainty analysis presented subsequently is neither a precise nor an accurate measure of uncertainty, but the method is valid with sufficient data.

Second, the data from the wind tunnel experiment are suspect. For five of the nine munitions tested in the wind tunnel, the mass of aerosolized active ingredient, M_x , as measured by the bubblers exceeded the mass burned, ΔM , as measured by the load cell on which the munition was placed. This clearly violates the law of conservation of mass. There are two plausible hypotheses for these results. First, the design of the wind tunnel is suspect. It has been observed that there may have been insufficient downwind distance from the load cell to establish laminar flow at the sampling point (Carter, (1991), personal communication). Second, the wind speed was measured at only one location and the assumption of constant velocity may not be correct (Bowers, (1991), personal communication). Either or both of these situations could have led to an overestimation of air velocity at the point of sampling. Although this condition most likely existed for all tests, it was not evident in the data from the three types of zinc oxide-hexachloroethane-aluminum (HC) smoke munitions (155mm M1 and M2 and the 105mm canisters) and one red phosphorus (RP) munition (81mm Navy wedge). (This observation is based on data reported in DPG, 1978.) The reason for the differences between munitions is not readily evident, and it is not possible to ascertain given the age of the data. The error associated with the inaccuracy of the bubbler data will affect all field experiment data because of the fundamental assumption in the emission rate model. Namely, the MYF relationship (the ratio of the mass of active ingredient aerosolized, M_x , to the initial mass of the munition, M_0), as measured in the wind tunnel experiments, is assumed to apply to the field experiments. As the wind tunnel tests overestimated the MYF, the emission rate, Q_t , would also be overestimated.

A simple analysis was performed to (1) determine if there was a consistent bias in the data which could be used to adjust the mass aerosolized, M_x , and the MYF for those munitions where M_x was greater than the mass burned, ΔM , and (2) evaluate the within munition variability for M_x and ΔM . The computation performed was:

$$\text{bias} = 1 - M_x / \Delta M$$

where a negative value indicates the mass of Zn or P aerosolized is greater than the mass burned and a positive value indicates this relationship is reversed.

The data were taken from DPG (1978) and the results are shown in Table B-1. The first five entries in the table are for the munitions where M_x , the mass of Zn or P aerosolized, exceeds ΔM mass burned; the next four entries are for munitions where M_x is less than ΔM . For one munition, the 155mm RP Navy Wedge, in one test result M_x was less than ΔM and for the second test M_x was greater than ΔM . The reason for this anomaly within a munition type is not clearly evident. It can be observed from this table that for munitions where the mass of Zn or P is less than the mass burned, the within munition variability is relatively small, less than 20%. However, for the munitions where the mass of Zn or P is greater than the mass burned, the within variability was much larger, ranging from approximately 45%-88%. Because the within munition variability is so large for those cases when M_x is greater than ΔM , it is not appropriate to adjust M_x or MYF for these munitions.

Three conclusions can be made based on this analysis. First, those munitions for which the mass of Zn or P aerosolized exceeds the mass burned will be dropped from further analysis because the data violate the law of conservation of mass and the large within munition variability precludes adjusting the original data. Second, the results indicate that there may be another source of error affecting the data in addition to the wind tunnel design. One would anticipate that the design error would affect all munitions equally, however, this is clearly not the case. There could appear to be other sources of variation related to the type of munition (e.g., mass aerosolized is less than mass burned is for all of the zinc canister munitions). Or there may have been some other source of experimental error associated with the operation of the wind tunnel or in the analyses of the bubblers. These additional sources of error cannot be evaluated further due to the age of the data. Third, if one assumes that the affect of the wind tunnel design on the munitions is constant across all experiments, then it must be concluded that M_x , the mass of Zn or P aerosolized, is overestimated for all munitions even if M_x is less than ΔM , the mass burned. It follows then that the MYF, which is the ratio of mass aerosolized to mass burned, is overestimated for all munitions.

To estimate the uncertainty in the emission rate model the issue of independence or dependence of the variables must be considered. The

Table B-1
Evaluating Wind Tunnel Bias

		Initial Mass (M _o)	Mass burned (ΔM)	Mass ¹ Aerosolized (M _x)	Bias ²
2.75" WP Wedge	A9	217	125	150	-.20
	A10	203	116	129	-.11
6" WP Wick	A5	102	59	64	-.09
	A6	101	51	77	-.51
3" WP Wick	A7	63	40	45	-.13
	A8	52	36	Void	
155mm RP Navy Wedge	A15	114	78	72	+.08
	A16	117	69	79	-.15
81mm RP German Wedge	A11	30	15	24	-.60
	A14	35	14	15	-.07
155mm HC M1 Canister	A1	3450	2330	425	+.82
	A2	3572	2412	382	+.84
155mm HC M2 Canister	A12	2055	1162	369	+.68
	A13	1987	1182	391	+.67
105mm HC Canister	A3	1178	646	154	+.76
	A4	1177	633	234	+.63
81mm Navy RP Wedge	A17	117	73	64	+.12
	A18	116	68	61	+.10

¹ Zn or P

² Bias = $1 - \frac{M_x}{\Delta M}$

assumption of independence allows one to use a relatively simple expression to calculate overall model uncertainty as the covariance terms can be neglected. However, if this assumption is incorrect and the variables are dependent, the estimated uncertainty will be unrealistically low.

In the case where the variables can be assumed to be independent, Goodman (1960) presents the expression:

$$\sigma_{xy}^2 = \bar{x}^2 \sigma_y^2 + \bar{y}^2 \sigma_x^2 = (\bar{xy})^2 [CV_x^2 + CV_y^2] \quad (B-2)$$

where σ_{xy}^2 = variance of the product xy

\bar{x} = mean of x

σ_x^2 = variance of $X = \frac{\sum (x - \bar{x})^2}{n - 1}$

\bar{y} = mean of Y

σ_y^2 = variance of Y

CV_x^2 = squared coefficient of variation of x , $\frac{\sigma_x^2}{\bar{x}^2}$

CV_y^2 = squared coefficient of variation of y , $\frac{\sigma_y^2}{\bar{y}^2}$

The variables in the emission rate model (see equation B-1) are not independent, both the munition yield fraction, MYF, and the yield fraction, YF, depend on the type of active ingredient. The variance of the product of two or more variables, which are not independent, is given as (Goodman, 1960):

$$\sigma_{xy}^2 = \bar{x}^2 \sigma_y^2 + \bar{y}^2 \sigma_x^2 + 2\bar{x} \bar{y} (COV_{xy})$$

where the variables are defined as above and COV_{xy} , the covariance of xy , is expressed as:

$$COV_{xy} = \sigma_x \sigma_y = \frac{1}{N} \sum_{i=1}^N (x_i - \bar{x})(y_i - \bar{y}) = \frac{1}{N} \sum_{i=1}^N (x_i y_i) - \bar{x} \bar{y} \quad (B-3)$$

To apply Equation (B-2) to the model for Q_t , the emission rate, integrating over the total burn time, it is written as:

$$Q = \int_0^{t_b} dt Q_t = M_o \cdot MYF \cdot YF \quad (B-4)$$

Let $E = MYF$ and $Y = YF$. Assuming the uncertainty associated with the initial mass, M_o , is small (i.e., the load cell is accurate), Q_t can be divided by M_o and expressed as q

$$q = \frac{Q_t}{M_o} = E \cdot Y \quad (B-5)$$

The variance of $q(\sigma_q^2)$ is

$$\sigma_q^2 = \bar{Y}^2 \sigma_E^2 + \bar{E}^2 \sigma_Y^2 + 2\bar{E} \bar{Y} \text{COV}_{EY} \quad (B-6)$$

where COV_{EY} is the covariance of the munition yield fraction, now expressed as E , with the yield factor, now expressed as Y . Since the yield factor is a function of the relative humidity ($Y = Y(h)$ where h is fractional relative humidity), this value can be incorporated into the expression for σ_q^2 as follows:

$$\sigma_q^2 = \bar{Y}^2 \sigma_E^2 + \bar{E}^2 Y'^2 \sigma_h^2 + 2\bar{E} \bar{Y} Y' \text{COV}_{Eh} \quad (B-7)$$

The fractional relative humidity, h , is = 0 at zero humidity and 1 at 100% humidity and Y' is defined as:

$$Y' = \left. \frac{\Delta y}{\Delta h} \right|_{h = \bar{h}} \quad (B-8)$$

As there are only two values for each munition, Y' is simply the slope of the straight line between the two points. The term COV_{Eh} is the covariance of the munition yield fraction (E) with relative humidity (h).

3.3 Results of Uncertainty Analysis

Table B-2 presents a sample set of data taken from DPG (1978) and used to calculate the variance of the quantity Q_t/M_o , expressed as σ_q^2 . The munitions included in this analysis were only those where the mass of Zn or P aerosolized, M_x , was less than mass burned, ΔM , as discussed previously. An example of how the variance of Q_t/M_o (or σ_q^2) is calculated is given below for the zinc munition 155mm HC M1 canister.

Step 1. Calculate the covariance of the munition yield fraction (E) and relative humidity (h) for trials B1R1 and B2R1. The values for E and h are given in Table B-2. Equation B-3 is the definitional formula for covariance; the computation formula is:

$$\text{COV}_{E,h} = \frac{N(\sum E \cdot h) - (\sum E)(\sum h)}{N^2}$$

$$\begin{aligned}\text{COV}_{E,h} &= \frac{2([0.12 \times 0.76] + [0.11 \times 0.72]) - ([0.12 + 0.11][0.76 + 0.72])}{2^2} \\ &= \frac{0.3408 - 0.3404}{4} \\ &= 1 \times 10^{-4}\end{aligned}$$

Step 2. Calculate Y' according to Equation B-8 where y , the yield factors (YF), are 5.2 and 5.0, and h , the fractional relative humidity, is 0.76 and 0.72.

$$\begin{aligned}Y' &= \frac{\Delta y}{\Delta h} \\ &= \frac{5.2 - 5.0}{0.76 - 0.72} \\ &= 5\end{aligned}$$

Table B-2^a

Variance of the Ratio of the Emission Rate to the Initial
Mass, (Q_t/M_o) for Selected Munitions

Munition	Trial	Munition ^b Yield Fraction	Relative Humidity	Yield ^c Factor	Variance of $\frac{Q_t}{M_o}$
155mm HC M1 Canister	B1R1	.12	76	5.2	2.15×10^{-3}
	B2R1	.11	72	5.0	
155mm HC M2 Canister	B3R1	.18	75	5.2	5.41×10^{-3}
	B4R1	.20	75	5.2	
105mm HC Canister	B15	.13	73	5.1	4.68×10^{-2}
	B16	.19	73	5.1	
81mm Navy RP Wedge	B11	.55	70	6.6	0.160
	B12	.52	80	7.8	

- Data taken from Tables III and IV in DPG (1978) for the field experiments conducted at the horizontal grid.
- MYF values are from the wind tunnel data for the particular munitions.
- Estimated values from Figure B-3 for $ZnCl_2$ (Curve C) and for the theoretical curve for white phosphorus and red phosphorus (Curve A).

Step 3. Calculate σ_q^2 according to Equation B-7. The variance of E, the munition yield fraction, is

$$\sigma_E^2 = 2 \times 10^{-4}. \text{ Equation B-7 is as follows:}$$

$$\sigma_q^2 = \bar{Y}^2 \sigma_E^2 + \bar{E}^2 Y'^2 \sigma_h^2 + 2\bar{E} \bar{Y} Y' \text{COV}_{Eh}$$

and by making the following substitutions:

$$\begin{aligned} \sigma_q^2 &= (5.1)^2 (5 \times 10^{-5}) + (0.115)^2 (5)^2 (8 \times 10^{-4}) + 2(0.115)(5.1) \\ &\quad (5)(1 \times 10^{-4}) \\ &= 2.15 \times 10^{-3} \end{aligned}$$

Interpretation of the variance estimates is limited by the potential error in the munition yield fraction (MYF) values and the limited amount of data ($n = 2$) for each type of munition. However, some summary comments can be made about these data and this approach to calculating variance. The variance of the 81mm Navy red phosphorus wedge is larger than the three zinc based munitions (zinc oxide-hexachloroethane-aluminum). The cause of this difference could be due to the type of munition. For example, the red phosphorus MYF is larger than the MYF for zinc munitions. Further, for phosphorus munitions the relative humidity on the two days of red phosphorus tests differed by 10% whereas for two of the zinc munition tests it was constant. If there is no variation in relative humidity the variance of q is the product of the mean of the yield factor and the variance of the MYF (see Equation B-7).

Bevington (1969) defines the standard deviation, σ , as the estimated error or uncertainty of a parameter. When a parameter, e.g., x , is a function of two or more other variables ($x = ab$) the standard deviations of a and b , when combined, give the uncertainty of x . To put the standard deviation values for each munition in perspective, Table B-3 presents the mean emission rates integrated over time, the standard deviation, σ , (as calculated according to Equation B-7), and the standard deviation expressed as a percentage of the mean. This table shows that the emission rates of the two 155mm HC (zinc) canisters (M1 and M2) have the least uncertainty and the 105mm HC (zinc) wedge has the greatest uncertainty. The uncertainty of the 81mm Navy RP wedge is only slightly greater than the 155mm HC canisters.

Table B-3

Comparison of the Mean and Standard Deviation
of the Ratio of the Emission Rate to the Initial Mass $\left(\frac{Q_t}{M_o}\right)$

Munition	Mean $\frac{Q_t}{M_o}$	Standard Deviation of $\frac{Q_t}{M_o}$	Standard Deviation as a % of the mean
155mm HC M1 Canister	0.587	0.046	7.8
155mm HC M2 Canister	0.962	0.074	7.7
105mm HC Canister	0.817	0.216	26.6
81mm Navy RP Wedge	3.844	0.40	10.4

- Q_t is integrated over the burn time, thus the quantity $\frac{Q_t}{M_o}$ is actually $\frac{Q_t}{M_b} \cdot t_b$.

An approach to evaluating emission test results from future experiments would be to compute the 95% confidence interval ($95\% \text{ CI} = \bar{x} \pm 1.96\sigma$) of the quantity $\frac{Q_t}{M_o}$ for each munition. If a subsequent experiment produced a $\frac{Q_t}{M_o}$ value outside of the confidence interval, then it could be concluded that the munition was significantly different from the original sample of munitions. Ideally, a larger dataset than that currently available would be necessary to assure that the standard deviations were stable.

An interesting comparison can be made between these results and the findings presented in *Methodology Investigation Final Report, Validation of Transport and Dispersion Model for Smoke* (DPG, 1979). In DPG, (1979), modeled concentrations along the line of sight (CL) were compared to field measurements as well as comparisons between measured and modeled concentration line integrated dosage (CLID). DPG (1979) reports that the CLID were consistently underpredicted for the zinc based munitions (HC) by a factor of 1.4-1.5 and overpredicted by a factor of 2 for the red and white phosphorus munitions. A comparison of these air dispersion modeling results to standard deviations of the source term (presented in Table B-3) shows a similar relationship among munitions. The zinc based munitions exhibited less variability than the red phosphorus munition. One hypothesis which could partially explain the discrepancies in the modeled versus measured comparisons in DPG (1979) is uncertainty in source terms. The red phosphorus has the largest uncertainty (as measured by the standard deviation) and it also shows the greatest difference between measured and modeled values. The large uncertainty in the red phosphorus source term may account for a portion of the uncertainty in the modeled red phosphorus concentrations.

4. Conclusions and Recommendations

The smoke munitions data from DPG (1978) have been reviewed and a method for estimating uncertainty, as expressed as the standard deviation, in the emission rates has been presented. Available data for the present analysis is limited, but the approach to variance estimation is applicable to larger data sets. The quality of the smoke munitions data is suspect due to design problems with the wind tunnel. The number of tests conducted on each munition, $n = 2$, means the variance computations are not stable. The uncertainty

analysis of the source terms indicated that the 105mm HC munition has the largest uncertainty, being slightly more than 3 times the uncertainty of the 155mm HC munitions and 2.6 times the 81mm Navy RP wedge. For the two 155mm HC canisters, the relative humidity was constant for the M2 test runs and varied for the M1 test runs. However, when uncertainty is expressed by the standard deviation as a percent of the mean, the two munitions have almost the same uncertainty.

Two recommendations can be made based on the preceding analysis. First, the munition yield factor should be determined in an accurate and precise manner. This variable is critical, as it is applied to all the field test data. Second, to assess meaningfully the uncertainty in the emission rate values, more than two sets of data must be available for the results to be more stable, and thus reliable.

To use this technique of computing variance to evaluate munition variability, the following plan is suggested. Assuming the wind tunnel design issue has been resolved and accurate MYF's determined, field data from numerous test burns should be collected. This should be done at the horizontal grid, but without simultaneous aerosol and meteorological monitoring. This is because to compute uncertainty for the emission rate value, the only parameters needed are initial weight, M_0 , munition yield fraction, and yield factor (as computed based on relative humidity); thus only M_0 and %RH would need to be recorded. Numerous burns for each type of munition should be conducted, e.g., $N = 30$. Tests should be conducted under as wide a range of humidities as possible. Such a database could then be used to compute robust variance and 95% confidence intervals. Subsequent test results would be compared to this confidence interval to determine if the emission rate is statistically different. Further, with sufficient data to compute stable variances, these values could be incorporated into an expression with meteorological variances to compute overall model uncertainty.

References

- Bevington, P.R., 1969: *Data Reduction and Error Analysis for the Physical Sciences*, McGraw-Hill Book Co., NY.
- Carter, F.L., R.K. Dumbauld and J.E. Rafferty, 1979: Methodology Investigation, Final Report, Validation of Transport and Dispersion Model for Smoke, TECOM Project No. 7-CO-PB8-DPI-004, U.S. Army Dugway Proving Ground, Dugway, UT.
- DPG, 1977: Methodology Investigation for Testing Effectiveness of Smoke/Aerosol Munitions Pilot Study, Final Report, TECOM Project No. CO-RD6-DPI-005, U.S. Army Dugway Proving Ground, Dugway, UT.
- DPG, 1978: Basic Smoke Characterization Test, Final Report, TECOM Project No. 7-CO-RD7-DPI-001, U.S. Army Dugway Proving Ground, Dugway, UT.
- Goodman, L.A., 1960: On the exact variance of products, *J. of the American Statistical Assoc.*, 55, 708-713.

APPENDIX B-2

ANALYSIS OF FOG-OIL SMOKE EMISSIONS

Appendix B-2

Table of Contents

Analysis of Fog-Oil Smoke Emissions

	Page
1. Introduction	B-25
2. Method	B-25
3. Results	B-35
4. Conclusions	B-36

Appendix B-2
Analysis of Fog-Oil Smoke Emissions

1. Introduction

This analysis focuses on the fog-oil smoke generator emission rates as tested at the Dugway Proving Ground in March and April, 1985 (Liljegren et al., 1988). Liljegren et al. (1988) reported the details of how the experiment was conducted. Only the method of computing the emission rate will be addressed here. The objectives of this analysis are threefold: (1) to assess the variability in the emission rate from the fog-oil smoke generator, (2) to compare two methods of computing the emission rate, and (3) to evaluate the influence of averaging time on emission rate variability.

2. Method

The fog-oil smoke emission data were taken from Liljegren et al. (1988). The configuration of the smoke test provided for the "instantaneous" measurement of the emission rate based on the weight loss of the oil drum and the exit velocity of the generator. Due to mechanical difficulties, the weight loss values are actually 1-minute averages, as opposed to "instantaneous" values. Plots of these data (and exit temperature) versus time for seven experiments were reported in Figures 3.2 through 3.8 in Liljegren et al. (1988). (For reference, copies of those figures are included, with the original figure numbers.) These data were digitized and the means, \bar{x} , and standard deviations, σ , were computed for each experiment. These values and the coefficient of variation (σ/\bar{x}) for each test are presented in Table B-1. Some experiments were screened to remove values which were approximately zero at the end of the test. Otherwise, the data reflect the actual emissions for the duration of the experiment.

Liljegren et al. (1988) computed a time integrated emission rate based on the total mass of oil burned divided by the duration of operation of the smoke generator. These values, taken from Table 3.1, are shown in Table B-2.

To evaluate the influence of averaging time on the variability in the emission rate, the emission rates were re-calculated based on averaging times up to 510 seconds. To do this the data were processed through a program which

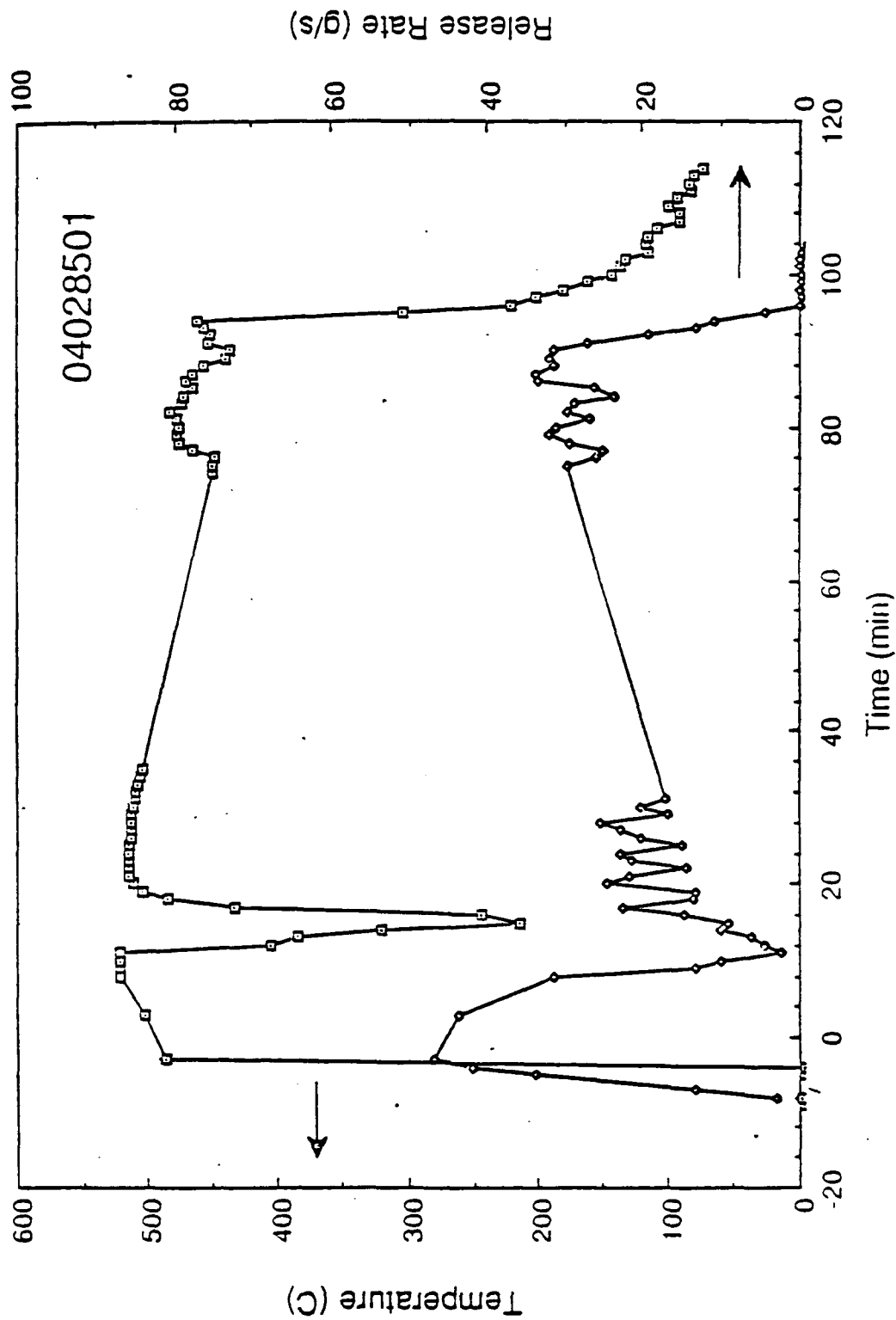


Figure 3.2. Exit Temperature ($^{\circ}\text{C}$) and Release Rate (g/s) as a function of time for test 10003 (2 April 85).
Missing data due to equipment failure (tape jam) "Taken from Liljegren et al., (1988)".

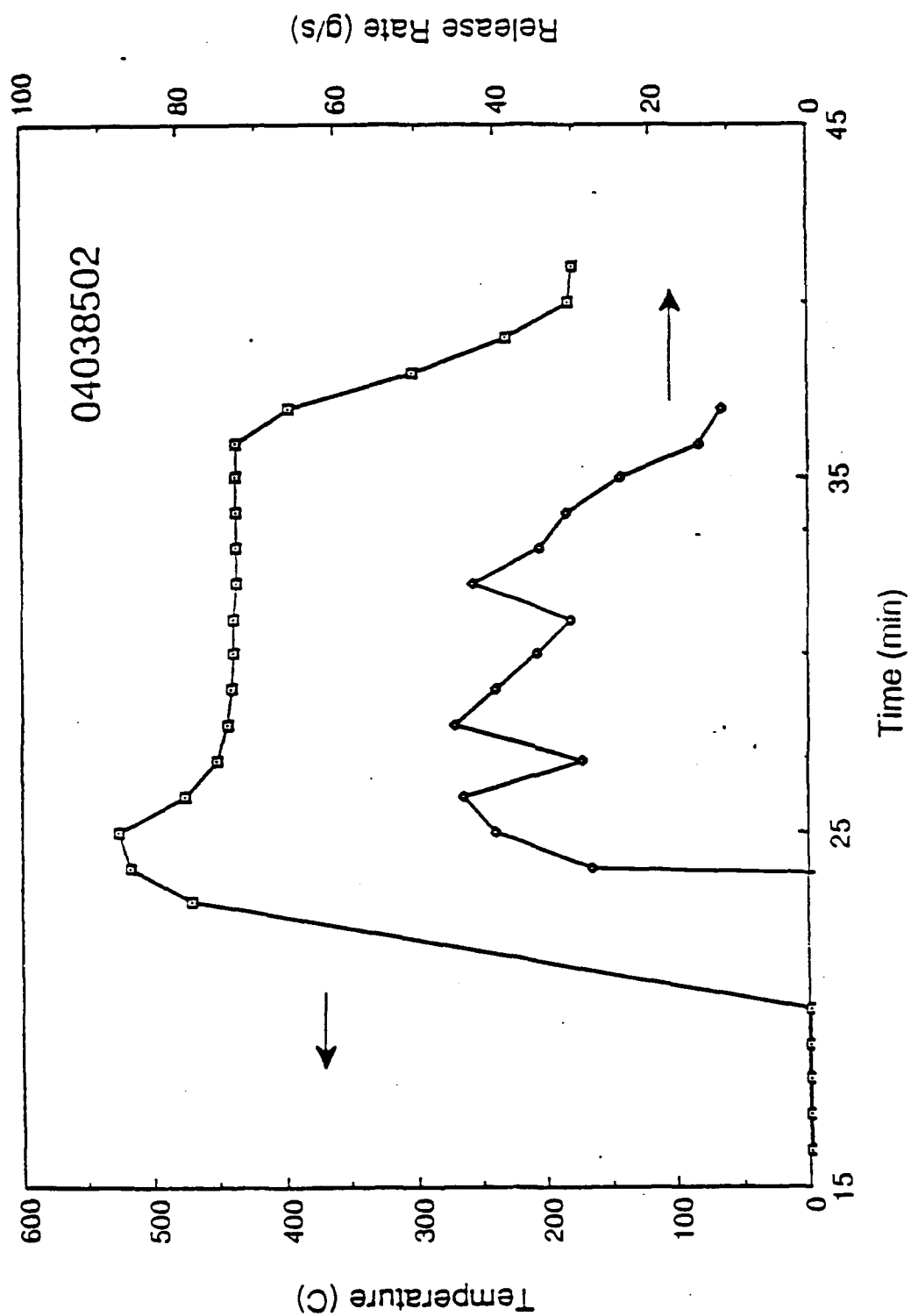


Figure 3.3. Exit Temperature (°C) and Release Rate (g/s) as a function of time for test T0004 (3 April 1985).
 "Taken from Liljegren et al., (1988)".

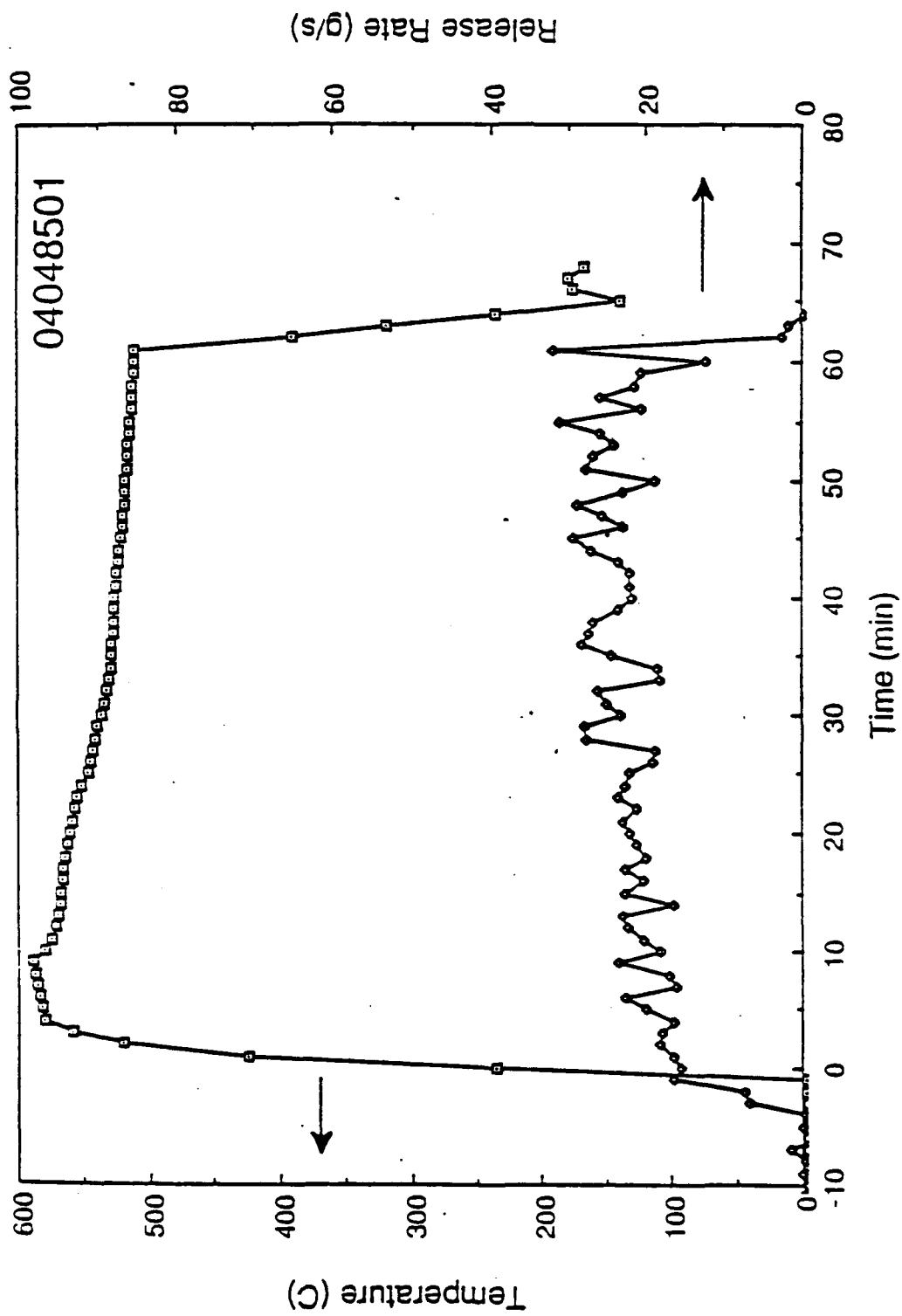


Figure 3.4. Exit Temperature (°C) and Release Rate (g/s) as a function of time for test T0005 (4 April 1985).
 "Taken from Liljegren et al., (1988)".

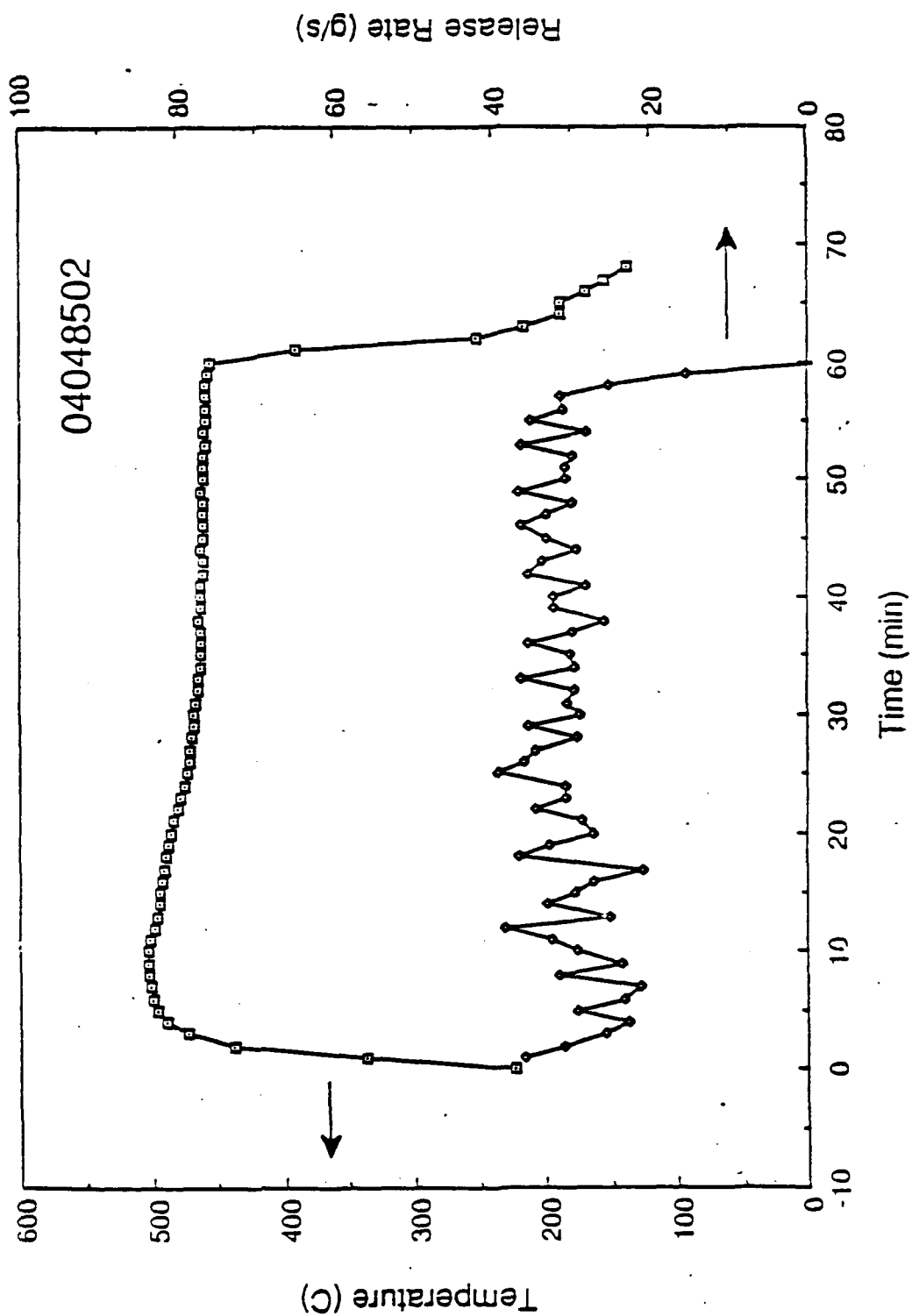


Figure 3.5. Exit Temperature ($^{\circ}\text{C}$) and Release Rate (g/s) as a function of time for test T0006 (4 April 1985).
 "Taken from Lillegren et al., (1988)".

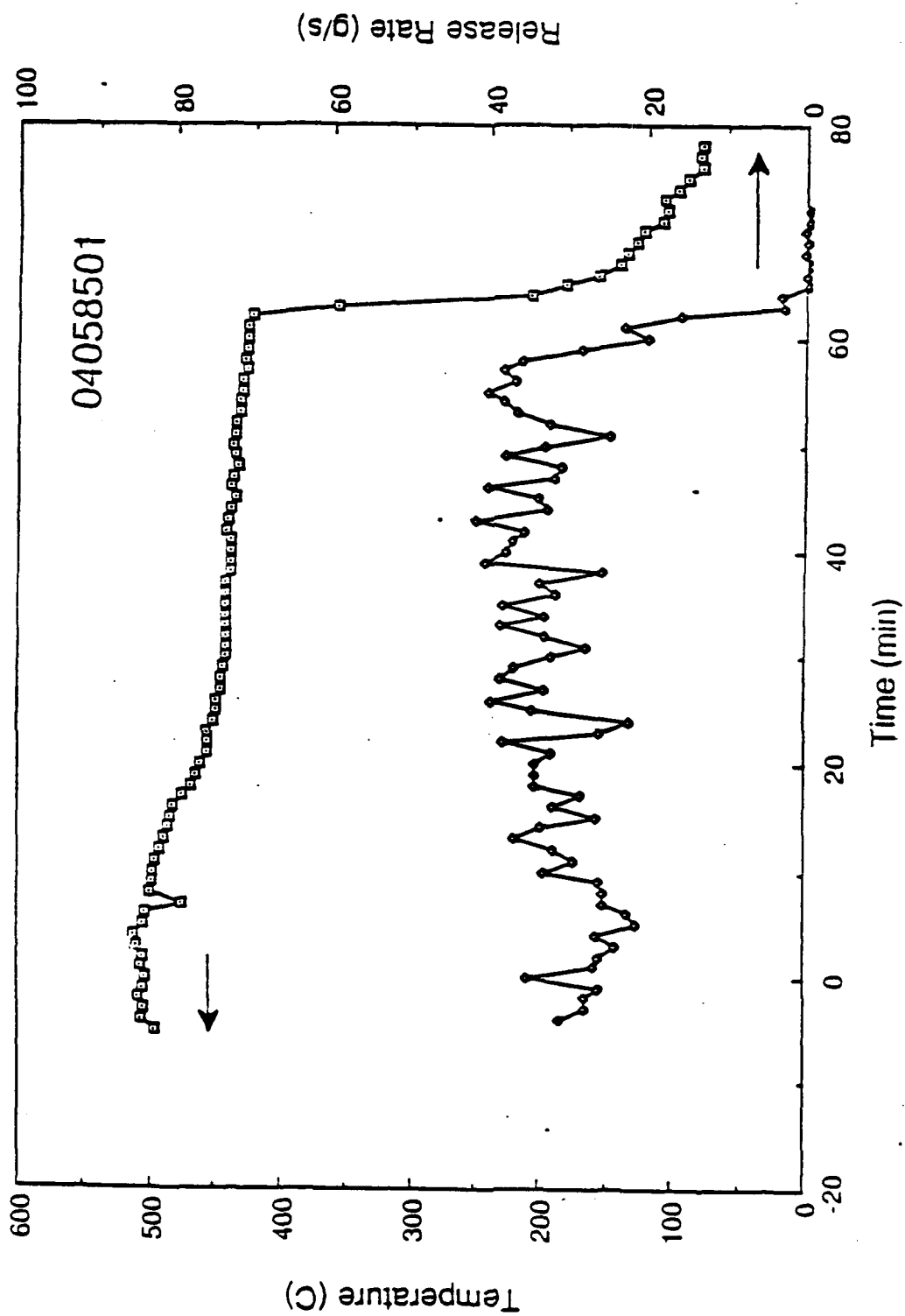


Figure 3.6. Exit Temperature (°C) and Release Rate (g/s) as a function of time for test T0007 (5 April 1985).
"Taken from Liljegren et al., (1988)".

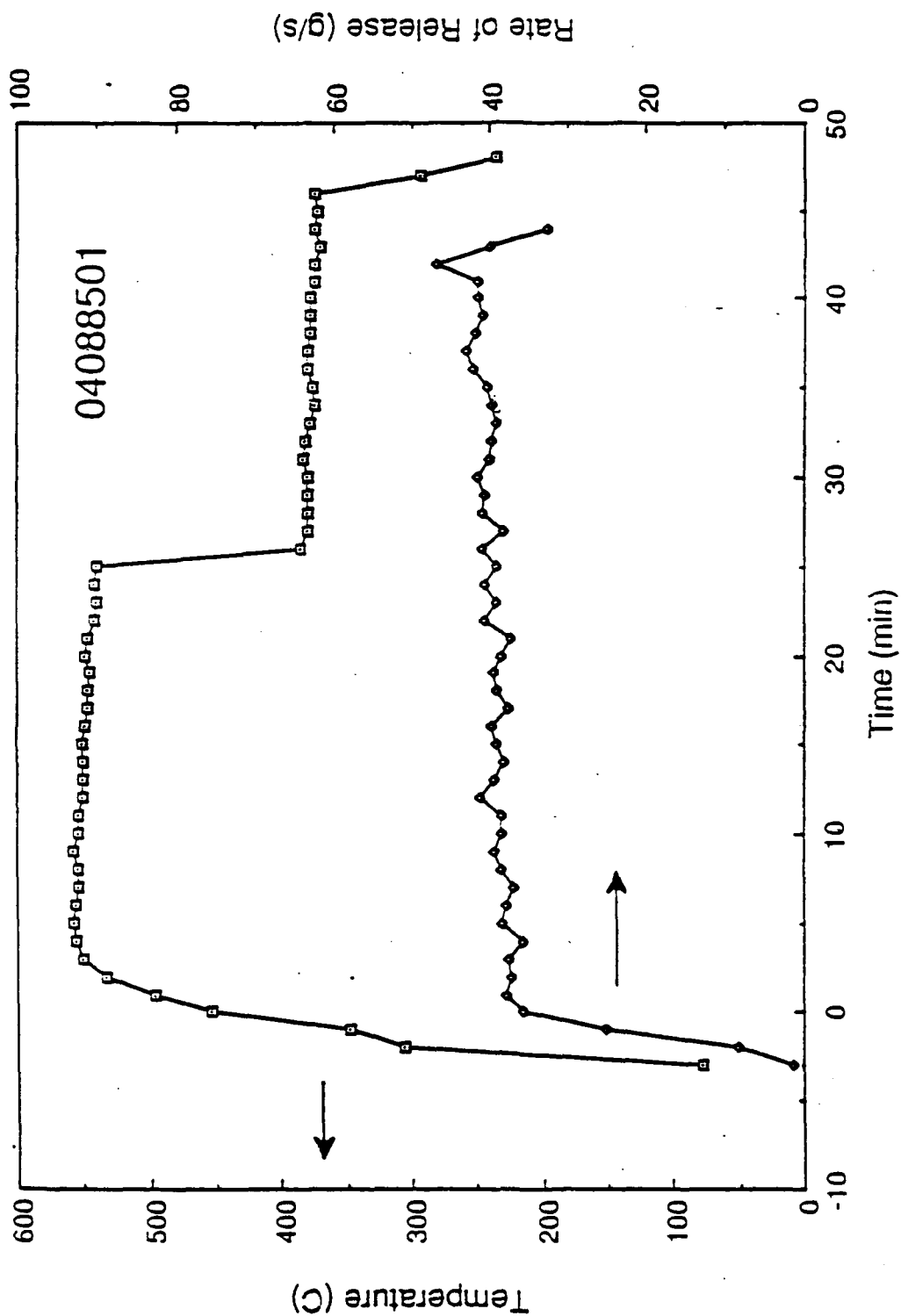


Figure 3.7. Exit Temperature (°C) and Release Rate (g/s) as a function of time for test T0008 (8 April 1985).
 "Taken from Liljegren et al., (1988)".

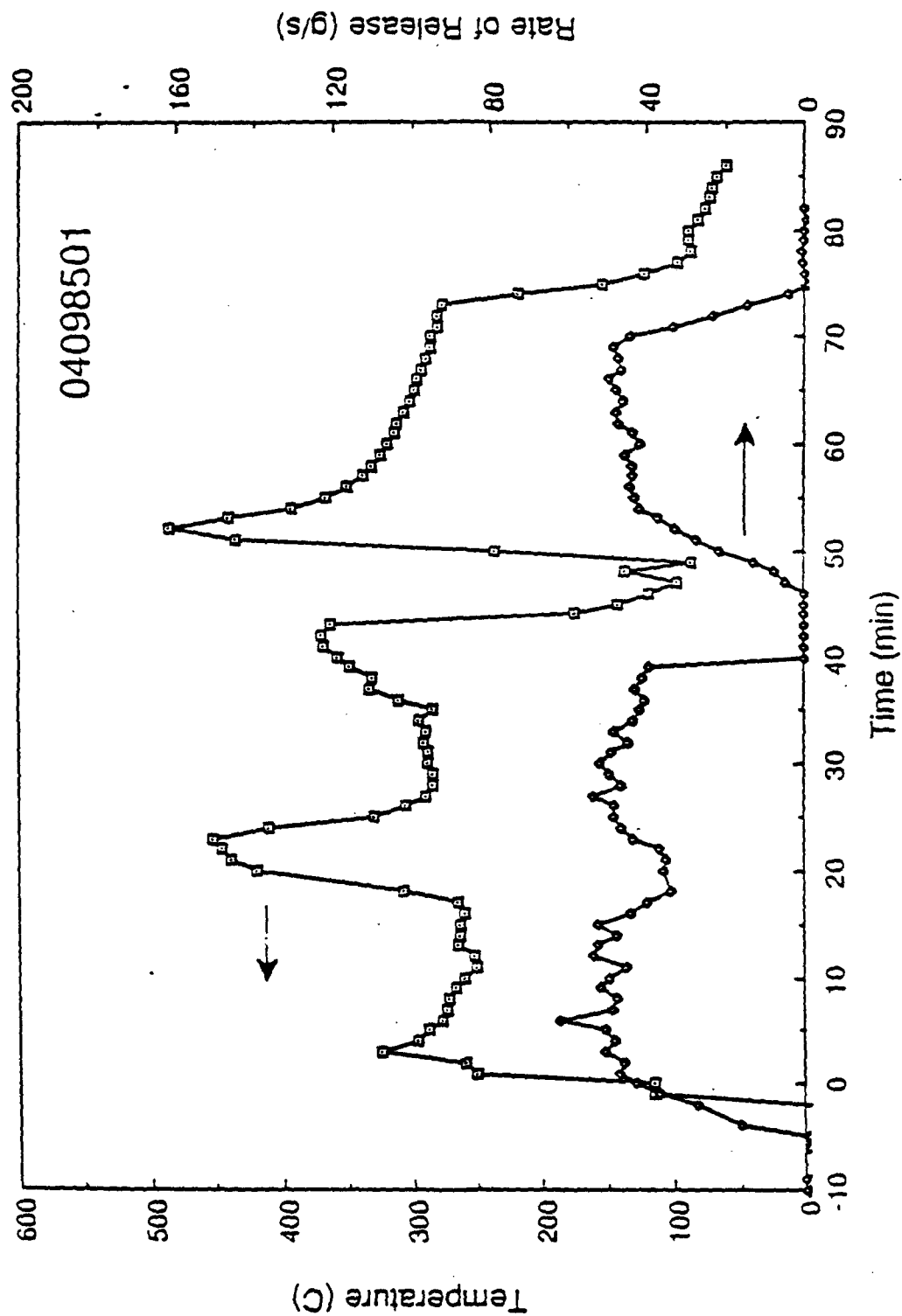


Figure 3.8. Exit Temperature (°C) and Release Rate (g/s) as a function of time for test T0009 (9 April 1985).
 "Taken from Liljegren et al., (1988)".

Table B-1

Variation in Instantaneous (i.e., one-minute averaged)
Fog-Oil Smoke Emission Rates

Figure No.	Test No.	Average Instantaneous Emission Rate (g/s)	Standard Deviation	Coefficient of Variation
3.2	T0003	21.7	10.9	0.5
3.3	T0004	33.8	8.9	0.3
3.4	T0005	21.5	5.9	0.3
3.5	T0006	31.1	4.2	0.1
3.6	T0007	30.9	7.5	0.2
3.7	T0008	37.9	7.5	0.2
3.8	T0009	37.9	16.8	0.4

Table B-2

Comparison of Integrated and Averaged Instantaneous Methods
of Calculating Emission Rates

Figure No.	Test No.	Integrated Emission Rate (g/s)	Average Instantaneous Emission Rate (g/s)	Percent Difference
3.2	T0003	24.3	21.7	-12
3.3	T0004	22.5	33.8	+33
3.4	T0005	22.4	21.5	-4
3.5	T0006	28.7	31.1	+8
3.6	T0007	30.7	30.9	-0.1
3.7	T0008	36.3	37.9	+6
3.8	T0009	43.2	37.9	-12

* Taken from Liljegren et al., (1988), Table 3.1

interpolated the emission rate at 30 second intervals from the existing data which are at approximately one minute intervals. From this processed data, means and standard deviations were computed by grouping the data at 30 sec, 60 sec, 90 sec, etc. increments up to 510 seconds (8.5 minutes). To evaluate how the variability changed with averaging time, the following equation was used

$$R' = \left(\frac{\sigma_{i \text{ sec}}}{\sigma_{30 \text{ sec}}} \right) \quad (\text{B-1})$$

where $\sigma_{i \text{ sec}}$ is the standard deviation for the i-th averaging time (i = 60 sec, 90 sec, 120 sec, 510 sec) and $\sigma_{30 \text{ sec}}$ is the standard deviation from the 30 second averaging time.

3. Results

The first objective of this analysis is to evaluate the variance in the fog-oil generator emissions. Table B-1 shows that the variation in the emission rate, expressed as the standard deviation, can be large. The coefficient of variation (CV) normalizes the standard deviation by the mean. Test T0006 has the smallest CV - 0.1. Tests T0003 and T0009 have the largest CV's, 0.5 and 0.4 respectively. During these tests the smoke generator malfunctioned and the emissions were particularly erratic (see Figures 3.2 and 3.8).

The second objective of this analysis is to compare the methods for calculating the average emission rate. Table B-2 shows a comparison of the two methods of computing the mean emission rate. Liljegren et al. (1988) calculated the time integrated average by dividing the mass of oil burned by the duration of operation of the smoke generator. Our approach averaged the "instantaneous" 1 minute emission rates, as digitized from plots. The percent difference between the two methods ranges from -12% to +33%. The largest difference in the computed emission rates is for experiment T0004. A review of Figure 3.3 and the digitizing indicates that there were no errors in that step and that the mean rate of 33.8 g/sec accurately reflects the data in the plot. It is hypothesized that there may be an error in the field data relating to oil burned or duration of operation of the smoke generator, which may have caused Liljegren et al. to compute a lower emission rate. (In addition, Liljegren et al. note that the data for this experiment were divided into two groups based on a shift in wind direction. It is not clear

how this was done or if this would affect the emission rate calculation. The smallest difference was for T0007, an experiment when the smoke generator functioned in a very consistent mode (see Figure 3.6). There does not appear to be a bias in the Liljegren et al. method, with their approach producing a higher mean rate four times and a lower rate three times. The r^2 for the two methods of computing the emission rate is 0.56. This means the time integrated method of computing emissions can only account for 56% of the variance in the method based on averaging the "instantaneous" values.

The third objective of this analysis is to evaluate how the variability in the emission rate changes with averaging time. The data from five experiments, T0005 (Figure 3.4) through T0009 (Figure 3.8), were analyzed using equation (B-1). Two experiments, T0003 and T0004 (Figures 3.2 and 3.3, respectively), were excluded from this analysis due to insufficient data. Table B-3 presents the squared standard deviation ratios by averaging time for the five experiments as well as the median ratio for each averaging interval. These data are plotted in Figure B-1, with the solid line representing the median value and the minimum and maximums represented by the boxes.

A theoretical curve is also plotted in Figure B-1, representing the equation:

$$\frac{\sigma^2(T_a)}{\sigma^2(30s)} = \frac{1 + 30_s/2T_I}{1 + T_a/2T_I} \quad (B-2)$$

where T_I is the integral time scale of the physical process. This equation is based on work by G.I. Taylor in the 1920's and is further discussed in Section VIII of the main text. This theory assumes that the time scales of the fluctuations cover a wide range of values, and the time series data in the figures verify that this is the case. An integral scale, T_I , of 150 seconds provides the best fit to the data in Table B-1.

4. Conclusions

This analysis shows that the variation in the one-minute averaged emission rate from the fog-oil smoke generator can vary from 10% to 50% of the mean rate, based on the coefficient of variation. From the comparison of the two methods of computing the emission rate, it appears that when the smoke

Table B-3

Variations in Emission Rate with Averaging Time

Averaging Times (s)	Squared Standard Deviation Ratios [*]					Median Ratio
	T0005	T0006	T0007	T0008	T0009	
30.	1.000	1.000	1.000	1.000	1.000	1.000
60.	0.879	0.848	0.934	0.922	0.950	0.9220
90.	0.858	0.746	0.837	0.806	0.932	0.8370
120.	0.738	0.605	0.745	0.774	0.872	0.7450
150.	0.639	0.465	0.695	0.823	0.823	0.6950
180.	0.649	0.473	0.696	0.697	0.818	0.6960
210.	0.609	0.415	0.574	0.716	0.804	0.6090
240.	0.652	0.388	0.537	0.551	0.752	0.5510
270.	0.627	0.460	0.574	0.560	0.747	0.5740
300.	0.554	0.356	0.534	0.524	0.636	0.5340
330.	0.544	0.319	0.506	0.483	0.666	0.5060
360.	0.523	0.267	0.518	0.670	0.742	0.5230
390.	0.529	0.300	0.484	0.426	0.498	0.4840
420.	0.557	0.334	0.537	0.680	0.391	0.5370
450.	0.481	0.303	0.484	0.411	0.384	0.4110
480.	0.510	0.278	0.436	0.469	0.573	0.4690
510.	0.492	0.318	0.444	0.700	0.650	0.4920

$$R' = \left(\frac{\sigma_{1 \text{ sec}}}{\sigma_{30 \text{ sec}}} \right)^2$$

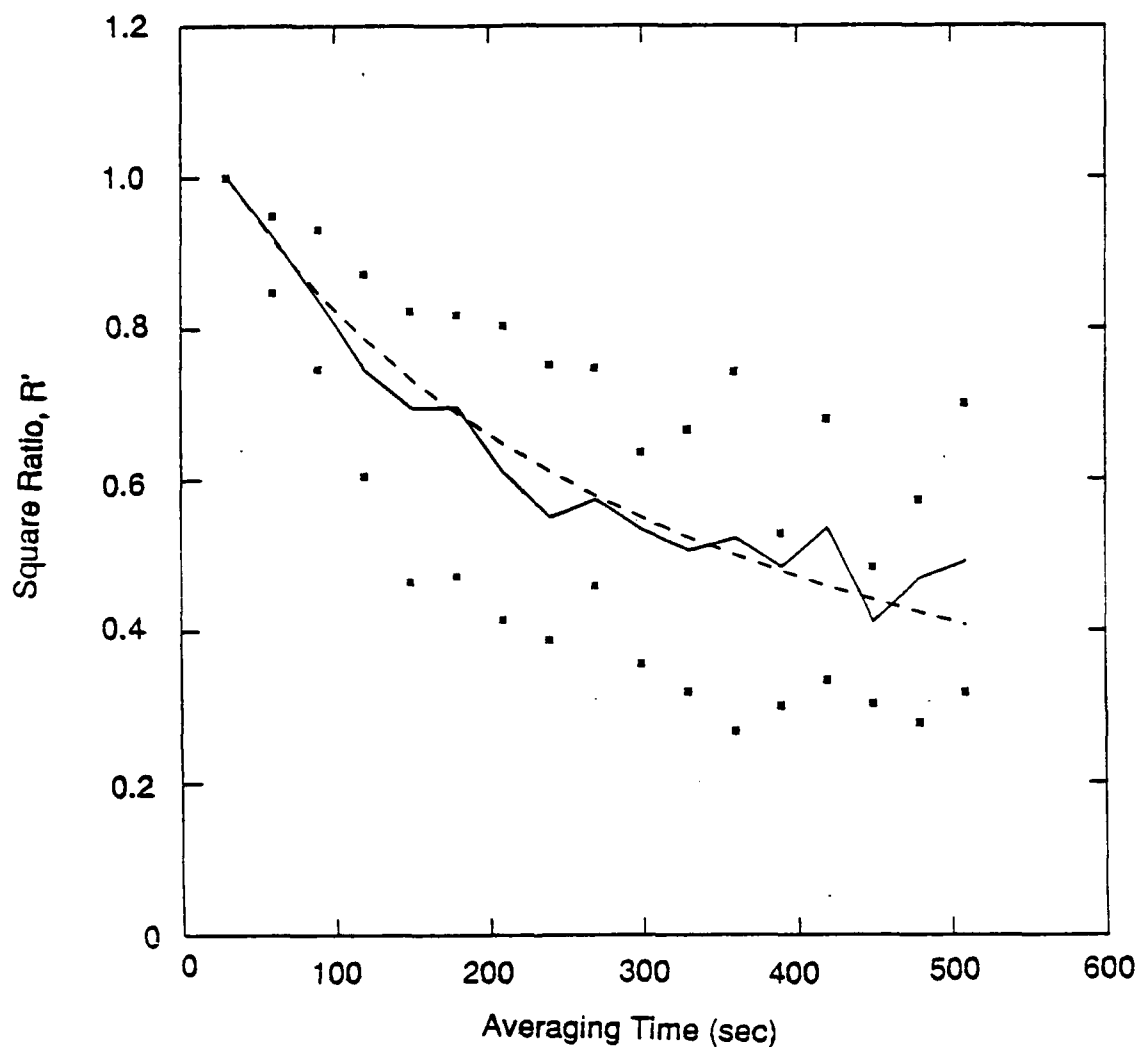


Figure B-1. Variation of emission rate fluctuation variance with averaging time. The solid line represents the median of the five experiments and the stars represent the range at that averaging time. The dashed line represents the theoretical curve given by Equation (B-2).

generator is operating in a consistent manner, both computational methods produce the same result (e.g., T0007, Figure 3.6). However, when the smoke generator malfunctions (e.g., T0003 and T0009, Figures 3.2 and 3.8, respectively), emissions can be highly variable, and the method of Liljegren et al. will over-estimate emissions relative to our method of averaging "instantaneous" emissions. An analysis of the emission rate variability with different averaging time showed that a time interval of 150 seconds best represented the experimental data.

5. References

Liljegren, J.C., W.E. Dunn, G.E. DeVaul, A.J. Policastro, Field Study of Fog-Oil Smokes, Supported by U.S. Army Medical Research and Development Command, Fort Detrick, MD, January, 1988.

Intentionally Blank

APPENDIX C

UNCERTAINTIES IN SOURCE EMISSION RATE ESTIMATES
USING DISPERSION MODELS

Reprint from Atmospheric Environment, 24A 2971-2980 (1990)

UNCERTAINTIES IN SOURCE EMISSION RATE ESTIMATES USING DISPERSION MODELS

STEVEN R. HANNA, JOSEPH S. CHANG and DAVID G. STRIMAITIS
Sigma Research Corp., 234 Littleton Rd., Suite 2E, Westford, MA 01886, U.S.A.

(First received 7 April 1990 and in final form 5 June 1990)

Abstract—The source emission rates during the Prairie Grass dispersion experiments were carefully observed and were adjusted by the experimentalists so that they were about twice as high during unstable conditions as during stable conditions. The question was asked whether observed concentrations and meteorological conditions could be used in dispersion models in order to predict source emission rates and verify this factor of two difference. Three types of simple dispersion models were applied to this problem, with the result that for the model based on Monin-Obukhov similarity theory, the uncertainties in predictions of source emission rates for individual runs were at best about ± 10 –20% when observed cross-wind integrated concentrations from the 50 m arc were used. Consequently this model could discern the factor of two difference in average source emission rates for the two sets of field trials which consisted of about 20 runs each. However, some models, such as the Gaussian plume model, exhibit uncertainties of about $\pm 70\%$ to a factor of two in predictions for individual runs, and hence could not discern the difference in average source emission rates when concentration observations at downwind distances of 100–300 m are used. It is found that the use of observed cross-wind integrated concentrations produces more accurate conclusions than the use of observed point concentrations, for the uncertainties in predictions of source emission rates are about a factor of two larger when the observed point concentrations are used.

Key word index: Dispersion models, uncertainties in models, source emission estimates.

OBJECTIVE AND METHODS

As source emission rates for air pollutants are seldom well-known, air pollution control decisions must often be made based on observations of air pollution concentrations on monitoring networks. Observed concentrations can be combined with meteorological observations (e.g. wind speed and direction, stability, and mixing depth) and used in so-called hybrid source-receptor models in order to estimate source emission rates (Watson, 1989). These models are based on the concept that atmospheric transport and dispersion models are a mathematical link between observed concentrations and predicted source emission rates.

The specific objective of this research, funded by the U.S. Army, is to develop methods for estimating whether there is a significant difference in the source emission rate of similar types of sources from one experiment to another. For example, a typical source might be a fog oil generator (used for smoke obscuration purposes), and the question may be whether the source characteristics of the fog oil generator have significantly changed between 1980 and 1990. It is assumed that the source emission rate is not directly measured, but that several field trials are carried out at the same site in 1980 and in 1990. In each field trial, cross-wind integrated concentrations are observed at a distance 100 m downwind of the source, and wind velocities, turbulence, and vertical temperature gradients are observed on a tower near the source. The source position and orientation is not varied. Some

data of this type exist, and the procedures will eventually be tested with these data; however, first we have chosen to apply the source emission rate estimation methods to a simpler data set.

The Prairie Grass dispersion experiments produced a high-quality database (Barad, 1958) that has been used extensively in the development and testing of dispersion models. The experiments were simple, with near-ground-level continuous point sources, and extensive concentration and meteorological observations were made over the flat, homogeneous terrain. Source emission rates were also reported, and were deliberately varied so that they were twice as high during the day as during the night. Because of the care with which the Prairie Grass experiments were conducted, this database serves as an excellent test bed for study of the uncertainty in source emission rate estimation procedures. If the procedures cannot discern the known factor of two difference in average source emission rates in this highly controlled set of experiments, it would be of little use at more complicated sites, where the terrain may be more complex and the observations are likely to contain more errors.

Three representative dispersion models are used to relate observed concentrations and meteorological conditions to source emission rates. The three models include a statistical regression model, a Monin-Obukhov similarity model, and a Gaussian plume model. The Student-*t* test is used to determine whether the models can discern a factor of two difference, at the 95% confidence level, between average night and day

source emission rates. Another output of this procedure is an estimate of the typical error or uncertainty in the source emission rate estimate.

DESCRIPTION OF PRAIRIE GRASS DATABASE

Barad (1958) discusses the Prairie Grass database in great detail. SO_2 tracer gas was released over periods of about 10 min from a point source located at an elevation of 0.45 m. Ten minute averaged tracer concentrations were obtained from measurements observed at an elevation of 1.5 m along arcs at distances of 50, 100, 200, 400 and 800 m from the source. Supporting meteorological observations were made from a nearby tower, located in a flat area, representative of the site, where the average surface roughness, z_0 , was determined to be 0.6 cm. Data from 44 experiments were used in our analysis, covering a wide range of meteorological conditions. The data are approximately equally divided into unstable and stable periods.

The Prairie Grass data are listed in Table 1, based on information in the report by Barad (1958) and in papers by van Ulden (1978), Nieuwstadt (1980), and Briggs (1982). The 2 m wind speed, u , the 2 m standard deviation of wind direction fluctuations σ_d , and the 16 m to 2 m temperature difference, DT , were given in Barad's (1958) report, and the friction velocity, u_* , and the Monin-Obukhov length, L , were estimated by van Ulden (1978). The mixing depth and convective scaling velocity, w_* , were calculated for most unstable experiments by Nieuwstadt (1980). The stability class, SC , is estimated using observations of surface roughness, z_0 , Monin-Obukhov length, L , and Golder's (1972) nomogram. Briggs (1982) carefully reviewed all of the data and suggested that certain arcs for some experiments be removed from the data set because of problems with those particular data. At each downwind distance, the table lists observations of C/Q , C^*/Q , and σ_y , where C is the maximum concentration on that arc, C^* is the cross-wind integrated concentration and σ_y is the standard deviation of the lateral concentration distribution. The C^* and σ_y data were given by Nieuwstadt (1980) for most of the unstable periods. The standard deviation of vertical wind direction fluctuations, σ_z , has been estimated using boundary layer similarity theory.

DISPERSION MODELS

Data from the Prairie Grass experiments (Barad, 1958) were used extensively by Pasquill (1961) and others in the development and testing of a Gaussian diffusion model now known as the Pasquill-Gifford-Turner model (Gifford, 1962, 1968, 1976; Turner, 1967), which is the basis for most decisions regarding air pollution control in the U.S. The data were also part of the database used by Nou (1963) in the

development of the empirical OB-DG model, which is the basis of the U.S. Air Force procedures for calculating toxic gas impacts. Because the early data analyses did not make use of Monin-Obukhov similarity modeling or convective scaling concepts, there was a flurry of activity with reanalyses of the Prairie Grass data from this new point of view in the late 1970s (e.g. van Ulden, 1978; Horst, 1979; Nieuwstadt, 1980; Venkatram, 1981; Briggs, 1982). In several of these papers, the new scaling parameters (e.g. the mixing depth, h , the friction velocity, u_* , and the Monin-Obukhov length, L) were derived by reanalyzing the original field data.

The variety of dispersion models in the references listed above can be grouped into three classes.

- Class 1. Empirical or statistical regression models (e.g. Nou, 1963).
- Class 2. Similarity models (e.g. Briggs, 1982).
- Class 3. Gaussian plume models (e.g. Gifford, 1976).

Because Nou's (1963) empirical or statistical regression formula was based on several other databases besides the Prairie Grass database, and he did not suggest a formula for the cross-wind integrated concentration, we decided not to use his formula directly, but instead we applied a multivariate linear regression procedure to the data in Table 1 in order to derive the following best-fit power-law formulas:

$$C/Q = 0.000137x^{-1.31}(DT + 10^\circ\text{F})^{4.72} \quad (1)$$

$$C^*/Q = 0.00666x^{-1.03}(DT + 10^\circ\text{F})^{2.34} \quad (2)$$

where C/Q and C^*/Q are in units of s m^{-3} and s m^{-2} , respectively, x is in units of m and DT is in units of $^\circ\text{F}$. This is the same statistical procedure applied by Nou (1963), and the units for all variables are consistent with those that he used. Nou (1963) also used the 10°F additive factor, which is necessary to prevent negative values of the temperature term. These formulas explain 91 and 84%, respectively, of the variance in the C/Q and C^*/Q observations, where most of the variance is explained by the x term. Note that these formulas are not based at all on physical insights, but are based on least-square fits of linear relationships to the data.

The group of similarity models proposed by van Ulden (1978), Horst (1979), Nieuwstadt (1980), Venkatram (1981) and Briggs (1982) is based on applications of Monin-Obukhov similarity theory and convective scaling similarity theory. According to Monin-Obukhov similarity theory, the following functional relations can be postulated for dispersion from continuous ground-level point sources in the surface boundary layer (Briggs, 1982):

$$Cu_*x^2/Q = f_1(x/L) \quad (3)$$

$$C^*u_*x/Q = f_2(x/L) \quad (4)$$

where f_1 and f_2 are non-dimensional universal functions. The friction velocity, u_* , and the Monin-

Table 1. Prairie Grass database for 44 experiments, including observations of wind speed, u , and standard deviation, σ_u , at 2 m, temperature difference $DT = T(16\text{ m}) - T(2\text{ m})$, and mixing depth, h . Derived values of friction velocity, u_* , convective scaling velocity, w_* , Monin-Obukhov length, L , and stability class, SC, are listed. Observations on five monitoring areas ($x = 50, 100, 200, 400$ and 800 m) of peak normalized concentration, C/Q , cross wind integrated concentration, C/Q , and lateral standard deviation, σ_y , are also given. If a blank appears, then that piece of data is unavailable

Exp	u (m/s)	σ_u (deg)	DT (C)	h (m)	Q (g/s)	w_* (m/s)	L (m)	SC	$x = 50\text{ m}$					$x = 100\text{ m}$					$x = 200\text{ m}$					$x = 400\text{ m}$				
									u_*	C/Q	σ_y	C/Q	σ_y	C/Q	σ_y	C/Q	σ_y	C/Q	σ_y	C/Q	σ_y	C/Q	σ_y	C/Q	σ_y	C/Q	σ_y	C/Q
1	6.2	23.6	-1.6	1335	89.9	0.31	2.27	-9.6	6.6	B	6.2	2.41E-03	4.43E-02	6.2	2.41E-03	2.63E-02	12.0	4.78E-03	1.11E-02	22.0	7.41E-03	6.45E-03	39.0	6.13E-03	2.80E-03	71.0	6.13E-03	2.80E-03
2	4.9	10.2	-1.2	1500	91.1	0.31	1.07	-10.0	3.3	C	4.33E-03	5.60E-02	6.6	1.17E-03	2.63E-02	12.0	2.61E-04	1.21E-02	21.0	4.13E-03	4.20E-03	41.0	3.37E-04	1.34E-03	66.0	3.37E-04	1.34E-03	
3	6.9	10.2	-1.6	626	92.0	0.46	1.70	-31.0	3.3	C	2.02E-03	4.02E-02	9.0	5.73E-04	2.39E-02	18.0	1.42E-04	1.09E-02	33.0	2.92E-03	6.46E-03	63.0	5.26E-04	1.41E-03	116.0	5.26E-04	1.41E-03	
4	4.6	16.6	-2.0	1050	92.1	0.32	2.01	-11.0	6.1	B	1.63E-03	6.09E-02	12.3	4.40E-04	1.93E-02	20.0	1.14E-04	7.71E-03	35.0	2.70E-03	2.17E-03	61.0	1.72E-04	3.30E-04	97.0	1.72E-04	3.30E-04	
5	1.3	3.2	1.9		61.1	0.09			3.4	F																		
6	3.4	12.0	-1.1	66	95.5	0.23	0.70	-7.6	6.3	A	4.07E-03	7.43E-02	6.6	1.00E-03	3.56E-02	16.0	2.16E-04	1.41E-02	26.0	4.73E-03	3.67E-03	45.0	5.43E-04	1.15E-03	92.0	5.43E-04	1.15E-03	
7	16	3.2	10.3	-1.0	1235	93.0	0.26	2.03	-5.2	7.0	A	1.04E-03	3.38E-02	13.7	3.53E-04	1.93E-02	26.0	6.42E-03	3.46E-03	49.0	6.37E-04	1.00E-03	72.0	3.11E-03	1.40E-04	116.0	1.40E-04	1.00E-03
8	17	3.3	5.6	0.5	36.5	0.21			6.0	A	1.04E-02	1.03E-01																
9	16	3.3	5.3	1.6	37.6	0.20			33.0	B	1.03E-02	1.00E-01																
10	19	5.0	11.6	-1.3	765	101.0	0.30	1.30	-20.0	5.4	C	1.39E-03	4.42E-02	6.7	5.01E-04	2.19E-02	16.0	1.20E-04	6.43E-03	32.0	1.40E-03	2.45E-03	55.0	3.21E-04	3.70E-04	65.0	3.21E-04	3.70E-04
11	20	0.6	0.3	-2.3	613	101.2	0.50	1.92	-62.0	5.3	D	1.53E-03	3.34E-02	3.9	4.00E-04	1.70E-02	14.0	1.40E-04	6.40E-03	27.0	2.97E-03	3.36E-03	49.0	7.04E-04	1.24E-03	90.0	7.04E-04	1.24E-03
12	21	6.1	6.6	0.3	30.9	0.30			122.0	6.3	D	5.29E-03	5.00E-02															
13	22	6.4	5.6	0.3	60.4	0.46			204.0	6.9	D	4.58E-03	4.70E-02															
14	23	5.9	7.3	0.2	40.9	0.30			193.0	6.5	D	4.09E-03	4.70E-02															
15	24	6.2	7.1	0.2	61.2	0.36			240.0	4.2	D	3.60E-03	4.70E-02															
16	25	2.0	24.0	-0.7	763	101.4	0.20	1.35	-6.2	6.9	A	2.16E-02	7.38E-02	16.2	3.60E-04	2.66E-02	36.0	5.39E-03	7.40E-03	72.0	1.33E-03	2.96E-03	134.0	2.13E-04	6.20E-04	214.0	2.13E-04	6.20E-04
17	26	2.6	6.4	1.0		61.7	0.16		34.0	6.2	A	1.64E-02	1.34E-01															
18	29	3.5	0.0	0.9		61.5	0.23		36.0	4.5	D	5.47E-03	5.90E-02															
19	32	2.2	3.6	6.3		61.6	0.13		-51.0	6.1	F																	
20	33	0.5	10.5	-1.0		91.7	0.16		-76.0	5.0	D	1.92E-03	3.00E-02															
21	34	9.0	7.3	-1.1		97.4	0.46																					
22	36	1.9	3.0	1.0		60.0	0.10		7.0	3.6	F	1.99E-02	1.93E-01															
23	37	4.6	7.0	0.4		60.3	0.20		95.0	4.3	D	5.50E-03	6.10E-02															
24	38	4.1	5.0	0.2		65.4	0.20		95.0	6.7	D	7.77E-03	7.00E-02															
25	41	0.0	5.0	1.4		39.9	0.23		35.0	6.0	E	1.49E-02	7.50E-02															
26	42	5.0	6.6	0.4		56.4	0.37		120.0	4.4	D	4.70E-03	5.20E-02															
27	43	5.0	12.2	-1.4	603	90.6	0.33	1.66	-16.0	5.9	C	2.30E-03	5.07E-02	10.3	5.31E-04	2.61E-02	21.0	1.49E-04	1.10E-02	40.0	2.32E-03	3.75E-03	69.0	6.76E-04	1.22E-03	200.0	6.76E-04	1.22E-03
28	44	5.7	12.7	-1.5	1644	100.7	0.40	2.20	-25.0	5.7	C	1.73E-03	4.67E-02	11.0	4.53E-04	2.28E-02	22.0	1.38E-04	1.00E-02	43.0	2.63E-03	4.27E-03	73.0	3.31E-04	1.39E-03	126.0	3.31E-04	1.39E-03
29	45	6.1	6.9	-0.4		100.0	0.30		-97.0	4.7	D	3.20E-03	5.20E-02															
30	46	5.2	7.7	0.4		99.7	0.30		114.0	6.5	D	5.20E-03	6.30E-02															
31	48	0.0	6.1	-1.2		104.1	0.31		-63.0	4.0	D	2.04E-03	4.00E-02															
32	49	6.3	11.9	-1.0	636	102.0	0.45	1.73	-20.0	5.7	C	1.99E-03	4.42E-02	8.9	6.23E-04	2.33E-02	17.0	1.72E-04	1.14E-02	35.0	3.03E-03	4.41E-03	62.0	4.41E-03	1.47E-03	110.0	4.41E-03	1.47E-03
33	50	6.6	10.9	-1.3	631	102.0	0.45	1.91	-26.0	5.6	C	2.17E-03	4.09E-02	8.2	6.37E-04	2.24E-02	15.0	1.64E-04	8.55E-03	28.0	3.13E-03	3.79E-03	55.0	3.37E-04	1.07E-03	115.0	3.37E-04	1.07E-03
34	51	6.1	10.0	-1.4	2136	102.4	0.45	2.30	-40.0	5.7	D	2.50E-03	4.50E-02	9.6	6.59E-04	2.34E-02	18.0	1.93E-04	9.77E-03	32.0	2.64E-03	3.71E-03	60.0	3.46E-04	6.20E-04	77.0	3.46E-04	6.20E-04
35	52	2.5	3.9	3.9		45.2	0.17		10.0	6.7	F	2.02E-02	1.54E-01															
36	53	4.0	5.9	0.9		43.4	0.24		40.0	4.1	D	5.33E-03	8.10E-02															
37	55	5.4	5.0	0.4		45.3	0.37		124.0	6.7	D	4.59E-03	5.30E-02															
38	56	4.3	6.1	0.6		45.9	0.20		76.0	6.6	D	6.61E-03	7.10E-02															
39	57	6.7	0.0	-0.6		101.5	0.46		-194.0	4.9	D	2.33E-03	4.20E-02															
40	58	1.9	4.1	5.9		60.5	0.11		6.4	6.0	F																	
41	59	2.6	5.2	3.0		40.2	0.16		11.0	3.7	F	1.74E-02	1.40E-01															
42	60	4.9	5.9	0.7		30.5	0.20		56.0	3.9	D	7.43E-03	6.20E-02															
43	61	0.0	11.0	-1.4	513	102.1	0.31	1.65	-30.0	5.0	D	1.73E-03	3.43E-02	10.4	5.02E-04	2.04E-02	19.0	1.49E-04	1.12E-02	35.0	3.71E-03	3.19E-03	63.0	6.46E-04	1.36E-03	109.0	6.46E-04	1.36E-03
44	62	5.2	0.0	-1.0		102.1	0.34		-30.0	5.2	C																	

Obukhov length, L , are the fundamental scaling velocity and scaling length in the surface boundary layer, according to Monin-Obukhov similarity theory. The Prairie Grass data are plotted in Fig. 1 in the dimensionless forms suggested by Equations (2) and (3), illustrating that the data are ordered quite well by these similarity relations.

Because the data in the four parts of Fig. 1 appear to approach a constant as x/L approaches zero, the following functional relation is proposed:

$$f(x/L) = a(1 + bx/L)^f. \quad (5)$$

A least-squares algorithm was applied to each figure, with the following results:

$$f_1(x/L) = 3.37(1 - 0.019x/L)^{-1.36} \quad x/L < 0 \quad (6)$$

$$f_1(x/L) = 3.01(1 - 2.20x/L)^{0.57} \quad x/L > 0 \quad (7)$$

$$f_2(x/L) = 1.06(1 - 0.021x/L)^{-1.74} \quad x/L < 0 \quad (8)$$

$$f_2(x/L) = 1.07(1 + 0.10x/L)^{0.68} \quad x/L > 0. \quad (9)$$

These curves are drawn on the figures and appear to

provide a good fit at all values of x/L . However, they have been derived with no requirements that certain physically-based asymptotic functional relationships be satisfied. For example, Briggs (1982) points out that $f_2(x/L)$ should be proportional to $(-x/L)^{1/2}$ in the limit of free convection ($-x/L \rightarrow \infty$). Consequently, Briggs' (1982) suggests a third term in Equation (5), which he claims to better account for "convective sweep-out" of the plume at large $|x/L|$. The similarity model is represented by Equations (6)–(9) in our analysis rather than the equations proposed in any of the above references because the other equations are based on a slightly different subset of the Prairie Grass database.

The Gaussian plume models comprise the third class of models in our analysis. The Gaussian model is based on the formulas (Gifford, 1976)

$$C/Q = (\pi u \sigma_y \sigma_z)^{-1} \exp(-(z_s - z_r)^2 / 2\sigma_z^2) \quad (10)$$

$$C^*/Q = (2/\pi)^{1/2} (u \sigma_z)^{-1} \exp(-(z_s - z_r)^2 / 2\sigma_z^2). \quad (11)$$

The source height, z_s , and receptor height, z_r , equal

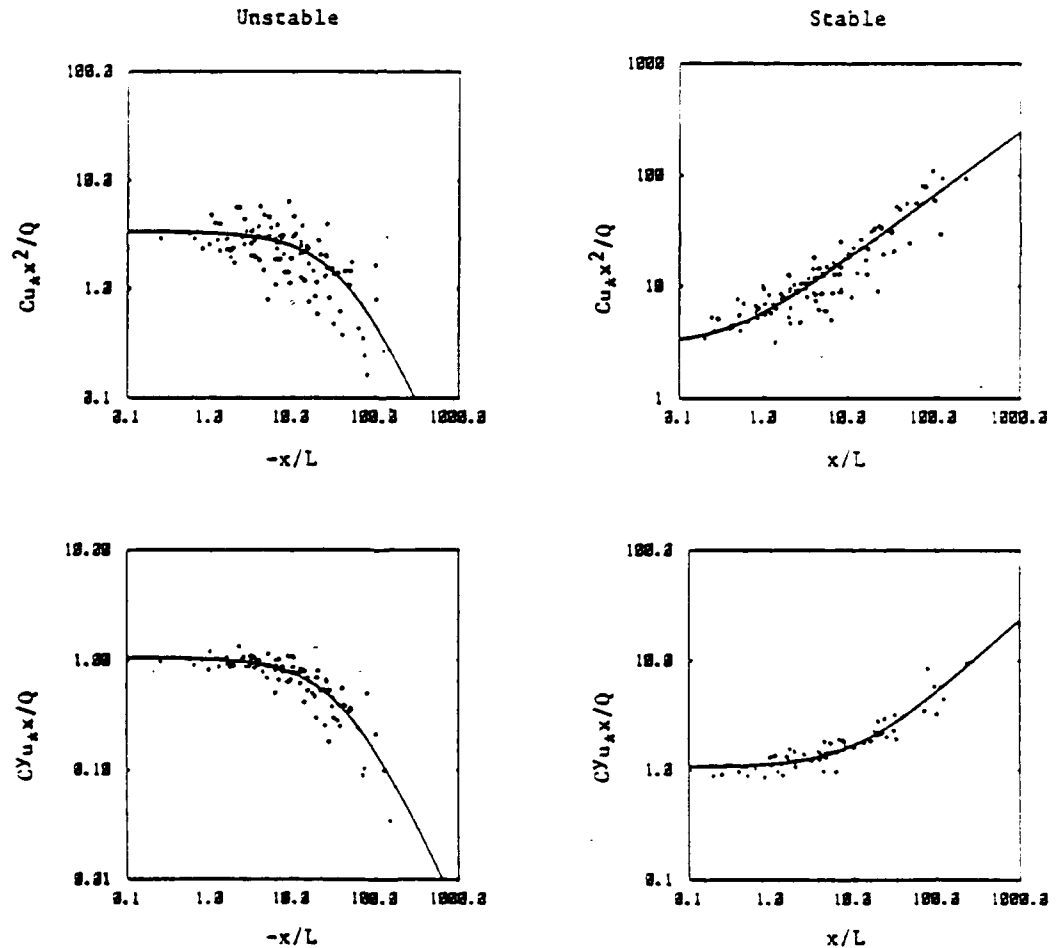


Fig. 1. Prairie Grass data plotted in the dimensionless form suggested by Equations (3) and (4). Best-fit lines of the form $a(1 + bx/L)^f$ are drawn on each figure (see Equations (6)–(9)).

0.45 m and 1.5 m, respectively, in the Prairie Grass experiments. The wind speed, u , is assumed to be that measured at a height of 2 m (see Table 1). The values for lateral and vertical dispersion coefficients, σ_y and σ_z , that are substituted into Equations (10) and (11) are based on suggestions by Briggs (1973), who used the Prairie Grass experiments, along with many other field experiments, in their derivation. These σ_y and σ_z formulas are given in Table 2. The required stability class is found in Table 1 for each Prairie Grass test.

Note that the empirical and similarity classes of dispersion models have been best-fit to the exact same data (Table 1) that will be used for further testing. The Gaussian plume model has not been subjected to these same best-fit procedures, but has been based on data from many experiments. Because of these differences in databases used to derive the models, it is expected that the Gaussian plume model will have the least success in any comparisons with field data from the Prairie Grass database.

The dispersion models in Equations (3) and (4) and (6)–(10) are inverted in order to predict source emission rates:

$$Q_p = C_o(C'/Q)_p \quad (12)$$

$$Q_p = C'_o(C'/Q)_p \quad (13)$$

where subscripts o and p represent observed and predicted variables, respectively. Because of the characteristics of the multiple linear regression or least-squares statistical procedures, an equation that produces a best-fit for C/Q or C'/Q may not necessarily produce a best-fit for Q . These statistical procedures attempt to minimize the mean-square error and to force the mean of the observed variable to equal the mean of the predicted variable. We should therefore not be surprised if an equation which produces zero mean bias in C/Q is discovered to produce a mean bias of 20–30% or more in Q .

STATISTICAL PROCEDURES

A primary objective of this research is the development of methods for estimating whether there is a significant difference in the source emission rate of similar types of sources from one experiment to another, as determined by observations of meteorological conditions and of point concentrations or

cross-wind integrated concentrations. Dispersion models, such as the three presented above, can be used to remove the effects on the concentration observations of variations in meteorological parameters and down-wind position of the concentration monitor.

A listing of the observed source emissions, Q , during the Prairie Grass experiment is given in Table 1, and the data are plotted in Fig. 2 as a function of the stability parameter $1/L$ (the point for run 46 has been excluded, since it was an evening transition period when Q was still high although $1/L$ had just become positive). During the Prairie Grass experiment the night-time emissions, Q , of tracer gas were controlled so that Q averaged 45.2 g s^{-1} with a range from about 38 to 58 g s^{-1} and a standard deviation of 5.91 g s^{-1} , and the daytime emissions were controlled so that Q averaged 98.25 g s^{-1} with a range from about 90 to 105 g s^{-1} and a standard deviation of 4.48 g s^{-1} . The experimentalists deliberately maintained this factor of 2 difference in day-night Q s so that the magnitude of concentrations at the monitors would not vary much from day to night. With 19 stable (night) runs and 20 unstable (day) runs, the Student- t parameter (Panofsky and Brier, 1968, p. 63) can be calculated in order to determine if the daytime \bar{Q} is significantly different from the night-time \bar{Q} :

$$t = (\bar{Q}_d - \bar{Q}_n) / \left(\frac{N_d \sigma_d^2 + N_n \sigma_n^2}{N_d + N_n - 2} \left(\frac{1}{N_d} + \frac{1}{N_n} \right) \right)^{1/2} \quad (14)$$

where subscripts d and n indicate day and night. If $|t|$ is less than 2.04, then the difference $(\bar{Q}_d - \bar{Q}_n)$ is not significantly different from zero, at the 95% confidence level. In fact, using the observed \bar{Q} and σ_Q

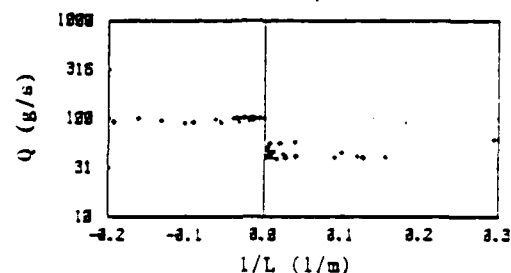


Fig. 2. Observed tracer gas source emission rates, Q , as a function of inverse Monin-Obukhov length, $1/L$, for the Prairie Grass data (run 46 excluded).

Table 2. Formulas recommended by Briggs (1973) for σ_y and σ_z for rural conditions

Stability class	σ_y (m)	σ_z (m)
A	$0.22x(1 - 0.0001x)^{-1/2}$	$0.20x$
B	$0.16x(1 - 0.0001x)^{-1/2}$	$0.12x$
C	$0.11x(1 - 0.0001x)^{-1/2}$	$0.08x(1 - 0.0002x)^{-1/2}$
D	$0.08x(1 - 0.0001x)^{-1/2}$	$0.06x(1 - 0.0015x)^{-1/2}$
E	$0.06x(1 - 0.0001x)^{-1/2}$	$0.03x(1 + 0.0003x)^{-1}$
F	$0.04x(1 - 0.0001x)^{-1/2}$	$0.016x(1 - 0.0003x)^{-1}$

figures quoted above, the calculated Student-*t* parameter is 30.86 for the difference between the mean night-time and daytime emission rates, which implies that the difference is significant at far greater than the 95% confidence level.

Because there is such a clear difference in the observed day and night tracer gas source emission rates, Q , at the Prairie Grass site, it is interesting to ask whether the dispersion models would be able to predict this significant difference in the mean emission rates, based on observed concentrations and meteorological variables. The three types of models described earlier were used to prepare predictions of source emission rate, Q_p (one set of predictions using C_p and another set using C_p^*). This calculation of Q_p was made individually using data from each of five monitoring arcs (50, 100, 200, 400 and 800 m) for C_p , and each of three monitoring arcs (50, 200 and 800 m) for C_p^* . For each set of predictions, values of night-time and daytime \bar{Q}_p and σ_{Qp} were calculated. Then Equation (14) was used to calculate the Student-*t* parameter. If the resulting *t* value exceeds 2.04, it is concluded that the model successfully simulated the difference in source emission rates. If *t* is less than 2.04, then it is concluded that the model has failed to simulate the difference.

Besides investigating the day-night difference in mean source emission rate predictions, it is also of interest to investigate the ability of the models to predict emission rates for all Prairie Grass runs taken as a group. For this purpose, the following performance measures are calculated (where an overbar represents an average over all the database).

$$\text{Relative bias: } (\bar{Q}_p - \bar{Q}_o) / \bar{Q}_o$$

$$\text{Correlation: } r = (Q_p - \bar{Q}_p)(Q_o - \bar{Q}_o) / \sigma_{Qp} \sigma_{Qo}$$

Fractions of predictions, Q_p , within a factor of two of observations, Q_o .

$$\text{Normalized mean square error: } (\bar{Q}_p - \bar{Q}_o)^2 / \bar{Q}_o \bar{Q}_o$$

These performance measures are tabulated for each model and for C_p and C_p^* on each monitoring arc. In addition, the individual residuals ($Q_p - Q_o$) are plotted as a function of downwind distance for each model.

RESULTS AND CONCLUSIONS

Predictions of average daytime and night-time source emission rates

The procedures for estimating the daytime and night-time average source emission rates reviewed above were applied to the Prairie Grass database, with the results given in Tables 3 and 4, for C_p and C_p^* , respectively. By comparing the numbers in the two tables, it is evident that use of the observed cross-wind integrated concentration, C_p^* , produced better results than use of the observed point concentration, C_p . The standard deviations, σ_{Qp} , of the predicted source emission rates are about 50% larger during the night, and a factor of 2 or 3 larger during the day, for C_p than for C_p^* . Consequently the calculated Student-*t* parameters are about twice as large for C_p^* than for C_p , implying that there is more confidence in the conclusions for C_p^* . We expected that there would be a difference, because

Table 3. Predictions of source emission rate, Q_p (g s^{-1}), for night-time and daytime Prairie Grass runs, using observed maximum concentrations, C_p , on monitoring arcs at distances of 50, 100, 200, 400 and 800 m. Three different models are used to calculate $Q_p = C_p(C/Q)_p$. The average, \bar{Q}_p , and standard deviation, σ_{Qp} , for night-time and daytime conditions is listed. Student-*t* is calculated using Equation (14)

Model	Monitoring distance (m)	Student <i>t</i>	Night (<i>N</i> = 19)		Day (<i>N</i> = 20)	
			\bar{Q}_p (g s^{-1})	σ_{Qp} (g s^{-1})	\bar{Q}_p (g s^{-1})	σ_{Qp} (g s^{-1})
Observed Q		30.86	45.2	5.9	98.2	4.5
Regression	50	7.40	30.1	12.0	144.6	64.7
	100	5.47	43.8	19.4	139.1	71.6
	200	4.27	52.0	23.0	128.3	72.5
	400	2.20	61.2	27.3	93.4	56.2
	800	-1.19	84.2	51.6	64.5	48.9
Similarity	50	5.68	39.9	14.1	70.8	18.5
	100	4.62	49.2	16.2	84.0	37.1
	200	5.51	48.7	16.2	101.1	37.1
	400	5.52	45.8	15.6	105.4	43.2
	800	4.30	46.3	14.6	116.2	60.1
Gaussian	50	2.40	55.2	45.5	115.5	96.9
	100	1.07	76.3	94.9	109.2	92.2
	200	0.05	98.1	150.9	100.2	70.1
	400	-0.88	118.8	196.3	76.8	62.7
	800	-1.67	150.1	264.1	48.0	30.1

Table 4. Predictions of source emission rate, Q_p (g s^{-1}), for night-time and daytime Prairie Grass runs, using observed cross-wind integrated concentrations, C_p^* , on monitoring arcs at distances of 50, 200 and 300 m. Three different models are used to calculate $Q_p = C_p^* (C^* Q)_p$. The average, \bar{Q}_p , and standard deviation, σ_{Q_p} , for night-time and daytime conditions listed. Student- t is calculated using Equation (14)

Model	Monitoring distance (m)	Student t	Night ($N = 19$)		Day ($N = 20$)	
			\bar{Q}_p (g s^{-1})	σ_{Q_p} (g s^{-1})	\bar{Q}_p (g s^{-1})	σ_{Q_p} (g s^{-1})
Observed Q		27.27	45.2	5.9	97.8	4.7
Regression	50	17.19	29.7	9.8	140.1	24.8
	200	7.43	46.9	16.9	124.8	40.1
	300	-0.58	69.4	34.3	62.1	36.4
Similarity	50	16.24	39.7	8.3	89.6	9.0
	200	9.54	49.0	9.0	100.1	20.3
	300	4.38	45.2	13.8	99.6	50.2
Gaussian	50	6.18	61.7	30.9	161.0	58.4
	200	2.83	65.5	60.3	116.6	34.9
	300	-0.99	85.5	145.1	46.9	20.3

σ_p is another complicating factor included in C_p that would act to increase the uncertainty, but did not expect that the difference would be this large.

The ability of the models to arrive at the proper answer (i.e. that the daytime \bar{Q} is significantly larger than the night-time \bar{Q} , with at least 95% confidence) can be seen by identifying cases where $t \geq 2.04$ in Tables 3 and 4. It is seen that most models are able to reproduce this conclusion at most arc distances. However, false conclusions ($t < 2.04$) are reached for the following arcs and models.

- C_p : 100 m arc: Gaussian
 200 m arc: Gaussian
 400 m arc: Gaussian
 800 m arc: Regression and Gaussian.
 C_p^* : 800 m arc: Regression and Gaussian.

It is seen that the use of C_p and C_p^* from the closest arc (50 m) leads to the correct conclusion for all three models, with a value for Student- t ranging from 2.4 to 7.4 for C_p and 5.2 to 17.2 for C_p^* . The regression and similarity models are seen to be better able to simulate the difference in observed Q (i.e. they yield a higher t) than the Gaussian model. However, the number of false conclusions increases as downwind distance increases. At the 800 m arc in both tables, only the similarity model yields the proper conclusion. Figs 3 and 4 contain extreme examples of plots of predicted source emission rates, Q_p , as a function of $1/L$, in the same format as the observations in Fig. 2. The similarity model predictions in Fig. 3, using observations of C_p^* on the 50 m arc, produce patterns similar to the observed data, but with slightly more scatter. However, the Gaussian plume model predictions in Fig. 4, using observations of C_p on the 800 m arc, obviously miss the overall trend of the observations of Q_p , as well as containing much more scatter.

The failure of the regression model and the Gaussian model to estimate \bar{Q} using C_p and C_p^* observations

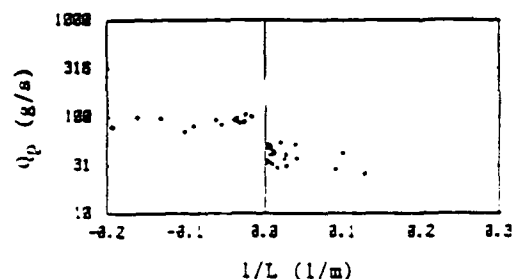


Fig. 3. Tracer gas source emission rates, Q_p , predicted by the similarity model as a function of inverse Monin-Obukhov length, $1/L$, for the Prairie Grass data (run 46 excluded). Observed cross-wind integrated concentrations on the 50 m arc are used.

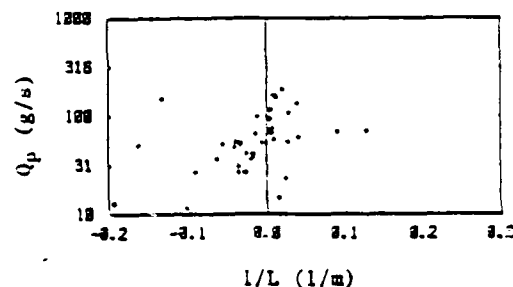


Fig. 4. Gas source emissions rate predicted by the Gaussian plume model, Q_p , as a function of inverse Monin-Obukhov length, $1/L$, for the Prairie Grass data (run 46 excluded). Observed concentrations on the 800 m arc are used.

at the largest distances may be seen by investigating the variation of the ratio C_p/C_p^* with distance for the three models for stable and unstable conditions (Figs 5 and 6). The C_p/C_p^* values for the similarity model have very little trend with distance and are always centered

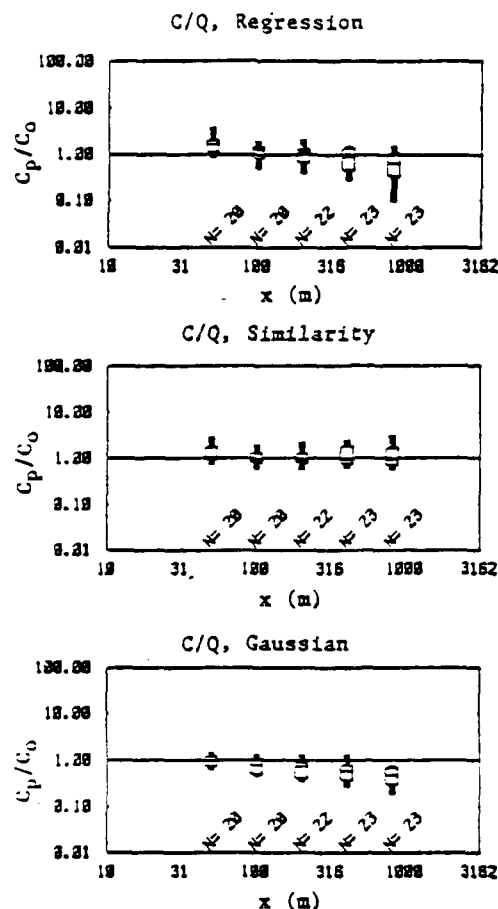


Fig. 5. Ratios of predicted to observed concentrations (C/Q) for the Prairie Grass dataset, as a function of downwind distance, for three models (regression, similarity, and Gaussian) for stable conditions. N is the number of data points at each distance. The midline of each box plot is the median, and the other lines represent \pm one and two standard deviations.

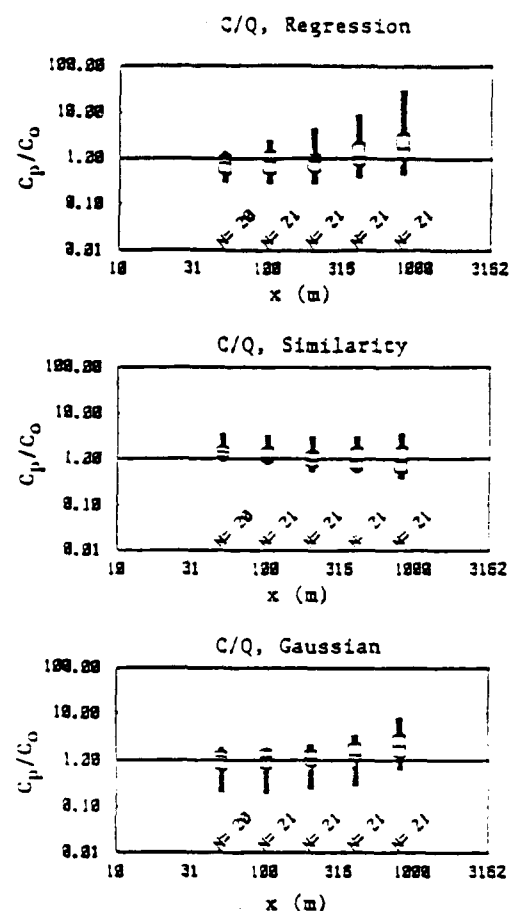


Fig. 6. Ratios of predicted to observed concentrations (C/Q) for the Prairie Grass dataset, as a function of downwind distance, for three models (regression, similarity, and Gaussian) for unstable conditions. N is the number of data points at each distance. The midline of each box plot is the median, and the other lines represent \pm one and two standard deviations.

on 1.0. In contrast, at large distances, the regression and Gaussian models tend to underpredict ($C_p/C_o < 1$) during stable conditions (Fig. 3) and overpredict ($C_p/C_o > 1$) during unstable conditions. It is important to note that a model which overpredicts the concentration, C , will underpredict the source emission rate, Q . Consequently, at large distances, the regression and Gaussian models can be expected to overpredict the source emission rate, Q , during stable conditions, and underpredict it during unstable conditions. But since the observed stable \bar{Q} is about 45 gs^{-1} and the unstable \bar{Q} is about 98 gs^{-1} , the \bar{Q} s predicted by these two models will tend to be either nearly the same, or their relative magnitudes may even be switched. This problem is seen to occur for the Gaussian model on the 800 m arc, using the C_o data, where the following discrepancy is found in Table 3 and can be seen in Figs 2 and 4

Thus the Gaussian model leads to the opposite conclusion regarding daytime and night-time \bar{Q} differences if the 800 m C_o data are used. Note that if the experimentalists had controlled the emissions in the opposite way, such that the night-time Q exceeded the daytime Q , then these trends in the errors in the regression and Gaussian models would have led to a correct conclusion regarding the differences in Q .

	Night	Day
Observed \bar{Q}_o	45.2	98.2
Gaussian predicted \bar{Q}_o	150.1	48.0

Consider the best-performing model in Table 6, where C_o^* data from the 50 m arc are used in the similarity model to predict the average source emission rate, \bar{Q} (see Fig. 3). The calculated Student- t value

Table 5. Evaluations of predictions of source emission rate, Q_o (g s^{-1}), for all Prairie Grass runs, using observed maximum point concentrations, C_o , on monitoring arcs at distances of 50, 200 and 800 m. Three different models are used to calculate $Q_o = C_o(C/Q)_o$.

Distance to C_o observation	Model	\bar{Q}_o (g s^{-1})	$\frac{\bar{Q}_o - Q_o}{Q_o}$	Correlation r	Fraction within factor of 2	$\frac{Q_o - Q_o^2}{\bar{Q}_o \bar{Q}_o}$
	Observed	72.4				
50 m	Regression	88.8	0.23	0.77	0.82	0.53
	Similarity	55.7	-0.23	0.74	0.90	0.15
	Gaussian	86.1	0.19	0.36	0.80	0.97
200 m	Regression	91.2	0.26	0.59	0.85	0.51
	Similarity	75.6	0.04	0.71	0.92	0.14
	Gaussian	99.2	0.37	0.02	0.74	2.08
800 m	Regression	74.1	0.02	-0.15	0.54	0.70
	Similarity	82.1	0.13	0.65	0.90	0.34
	Gaussian	97.6	0.35	-0.25	0.49	5.75

Table 6. Evaluation of predictions of source emission rate, Q_o (g s^{-1}), for all Prairie Grass runs, using observed cross-wind integrated concentrations, C_o^* , on monitoring arcs at distances of 50, 200 and 800 m. Three different models are used to calculate $Q_o = C_o^*(C^*/Q)_o$.

Distance to C_o observation	Model	\bar{Q}_o (g s^{-1})	$\frac{\bar{Q}_o - Q_o}{Q_o}$	Correlation r	Fraction within factor of 2	$\frac{Q_o - Q_o^2}{\bar{Q}_o \bar{Q}_o}$
	Observed	68.4				
50 m	Regression	78.4	0.14	0.94	0.91	0.23
	Similarity	61.7	-0.10	0.98	1.00	0.02
	Gaussian	106.0	0.55	0.74	0.88	0.55
200 m	Regression	81.2	0.19	0.80	0.94	0.21
	Similarity	71.6	0.05	0.89	1.00	0.04
	Gaussian	88.1	0.29	0.46	0.88	0.48
800 m	Regression	66.1	-0.03	-0.07	0.74	0.46
	Similarity	69.2	0.01	0.60	0.88	0.26
	Gaussian	68.4	0.00	-0.15	0.65	2.98

in this case is 16.2. Since $\bar{Q}_o(\text{day}) - \bar{Q}_o(\text{night}) \cong 53 \text{ g s}^{-1}$, it is concluded that a significant difference in \bar{Q} values could be discerned by this model if $\Delta\bar{Q}_o = \bar{Q}_o(\text{day}) - \bar{Q}_o(\text{night})$ drops as low as $53 \times (2.04/16.2) = 6.7 \text{ g s}^{-1}$; that is, if $\Delta\bar{Q}_o$ is about 15% of \bar{Q}_o . Therefore, in these best of research-grade experiments, where there are about 20 daytime and 20 night-time tests, and where a dispersion model is fit to these same data, a day-night difference in \bar{Q} of less than 15% of the mean would not be estimated to be significant by this procedure.

Predictions of source emission rates for all cases

Putting aside the question of differences in daytime and night-time averages in \bar{Q} , it is possible to use the complete database to estimate the overall ability of the models to estimate the 39 individual source emission rates. The relative bias, the correlation, the fraction of predictions within a factor of two of observations, and the normalized mean square error for the three models are listed in Table 5 and 6, for maximum point concentrations and cross-wind integrated concentra-

tions, respectively. These performance measures are calculated using data from the 50 m, 200 m and 800 m arcs.

In most cases, the similarity model shows the most accuracy and the Gaussian model shows the least accuracy. Also, the use of observed cross-wind integrated concentrations, C_o^* , leads to better results than the use of observed point maximum concentrations. The deterioration of model performance as distance increases can also be seen. Focusing on Table 6, for cross-wind integrated concentrations, it is seen that the most accurate model, the similarity model, produces a mean relative bias with a magnitude of 0.10 or less on all three distance arcs. The correlation drops from 0.98 to 0.60 as distance increases from 50 to 800 m, and the fraction within a factor of two drops from 1.00 to 0.88 over the same distance. The normalized mean-square-error increases from 0.02 to 0.26 over those distances, implying that the root-mean-square-error (rmse) increases from about 15% to 50% of the mean. In contrast, the Gaussian model yields a

much larger rmse that increases from about 70% to 300% of the mean.

The factor of 5 or 6 difference in rmse between the similarity and Gaussian models implies that the similarity model can discern differences in source emission rates that are a factor of 5 or 6 less than the minimum differences in source emission rates discerned by the Gaussian model. By comparing these numbers between Tables 5 and 6, it is seen that the relative rmse using C_0 observations are about 50% to 100% larger than the relative rmse using C_0^* observations. Consequently the use of C_0^* data permits one to discern differences in source emission rate that are 50% to 100% smaller than the minimum differences in source emission rates discerned by C_0 data.

IMPLICATIONS FOR FUTURE RESEARCH

The uncertainties in estimating source emission rates were first investigated using the Prairie Grass database, since the source conditions were simplified (a single continuous non-buoyant point source near the ground), the source emission rate was closely monitored, the site was flat and uniform, comprehensive meteorological data were taken, and observations of ground-level concentrations were taken at many points along monitoring arcs at five downwind distances. This experiment represents the optimum database of its type, and has been used in numerous research programs on atmospheric turbulence and dispersion. For this reason, the uncertainties in any analysis procedure should be *minimized* at this site. Conversely, if these procedures were to be applied to other experiments at other sites, where conditions are not so steady, smooth, or carefully-observed, the uncertainties would be expected to be larger.

In the future, we will test these procedures using less ideal observations from other field experiments. These will include U.S. Army field tests of fog oil generators, which are used for smoke obscuration purposes. The plumes from fog oil generators are more complicated than those in the Prairie Grass experiments, since the fog oil plumes are characterized by significant momentum and buoyancy fluxes. Furthermore, the supporting meteorological data are not as complete as at Prairie Grass. Future tests will also include experimental data obtained for plumes from tall power plant stacks, where plume rise and mixing depth are complicating factors. From each set of experiments, the relative uncertainty of the procedures for estimating source emission rate will be assessed. It is expected that the uncertainty will increase as source conditions become more complex or as input data are less complete.

This study has demonstrated that models that do well (in a least squares sense) in estimating point concentrations do not necessarily do well when they are 'turned around' to estimate source emission rate. The reason for this difference is the strong variation

with distance of the plume centerline concentration. Consequently it is possible that a model which has zero mean bias in its concentration estimates, will have a 50% mean bias in its source emission rate estimates. For the same reason, if a variable is first made non-dimensional and the model is 'tuned' with the data (e.g. the similarity model described above), the predictions of the non-dimensional variable (e.g. Cu_0x^2/Q) may have zero bias, while the predictions of the concentration, C , may have significant bias. For optimum results, any tuning or regression analysis should be done with the variable that is of ultimate interest.

Acknowledgements—This research was sponsored by the U.S. Army. The authors appreciate the assistance of Mr James Bowers, Mr Christopher Biltott and Mr James Rafferty of Dugway Proving Ground.

REFERENCES

- Barad M. L. (ed.) (1958) Project Prairie Grass. A field program in diffusion. *Geophys. Res. Paper No. 59*, Vols. I and II, AFRCF-TR-58-235, Air Force Cambridge Research Center, Bedford, MA.
- Briggs G. A. (1973) Diffusion estimation for small emissions. ATDL Cont. File No. 79, ATDL, Oak Ridge, TN.
- Briggs G. A. (1982) Similarity forms for ground source surface layer diffusion. *Boundary-Layer Met.* 23, 489-502.
- Draxler R. R. (1984) Diffusion and transport experiments. Chapter 9 In *Atmospheric Science and Power Production*, Chapter 9 (edited by D. Randerson), pp. 367-422. DOE/TIC-27601, USDOE.
- Gifford F. A. (1961) Use of routine meteorological observations for estimating atmospheric dispersion. *Nucl. Saf.* 2, 47-57.
- Gifford F. A. (1968) An outline of theories of diffusion in the lower layers of the atmosphere. In *Meteorology and Atomic Energy—1968* (edited by D. H. Slade), pp. 66-116. USAEC Report TID-24190, NTIS, 66-116.
- Gifford F. A. (1976) Turbulent diffusion typing schemes. A review. *Nucl. Saf.* 17, 68-86.
- Golder D. (1972) Relations among stability parameters in the surface layer. *Boundary-Layer Met.* 3, 47-58.
- Horst T. W. (1979) Lagrangian similarity modeling of vertical diffusion from a ground-level source. *J. appl. Met.* 18, 733-740.
- Nieuwstadt F. T. M. (1980) Application of mixed-layer similarity to the observed dispersion from a ground-level source. *J. appl. Met.* 19, 157-162.
- Nou J. V. (1963) The Ocean Breeze and Dry Guich diffusion programs. AFRL, Hanscom AFB, MA.
- Pasquill F. (1961) The estimation of dispersion of windborne material. *Met. Mag.* 90, 33-49.
- Turner D. B. (1967) Workbook of atmospheric dispersion estimates. Public Health Service, Pub. No. 999-AP-26, Robert A. Taft Sanitary Engineering Center, Cincinnati, OH.
- van Ulden A. P. (1973) Simple estimates for vertical diffusion from sources near the ground. *Atmospheric Environment* 12, 2125-2129.
- Venkatram A. (1981) A semi-empirical method to compute concentrations associated with surface releases in the stable boundary layer. *Atmospheric Environment* 15.
- Watson J. G. (ed.) (1989) Receptor models in air resources management. *Transactions of an International Specialty Conference*. Air and Waste Management Association, Pittsburgh, PA.

APPENDIX D

DISPLAY OF RELATIONS AMONG DATA USING BOX PLOTS

APPENDIX D

DISPLAY OF RELATIONS AMONG DATA USING BOX PLOTS

One way of displaying large numbers of data is through the use of box plots, where the cumulative distribution function (cdf) of the dependent variables within a group of data is represented by a set of significant percentile values. For example, the 2th, 16th, 50th, 84th, and 98th percentiles are used in our analyses. These five significant points in the cdf are plotted by the SIGPLOT program using a "box" pattern as seen in the examples below. Variations of one type of data with another can be seen by breaking up the first type of data into groups defined by ranges of the second type of data.

The SIGPLOT plotting package (see Appendix E) is used to generate the box plots. The ANADISTR program, described below, is used to generate the special input file required by SIGPLOT from a file containing multiple columns of data, representing concurrent values of variables such as observations of concentrations, wind speed, or stability. In the ANADISTR program, the user defines certain ranges of the primary variables in the input file to be used for grouping the dependent variables and plotting them by means of box plots. The ANADISTR program requires one input file and generates one output file. The output file then serves as the input file to the SIGPLOT plotting package. There are no default names associated with these files, and the user is prompted for the file names during the execution of the program. The ANADISTR program is written in FORTRAN 77.

The input data file of the ANADISTR program could contain multiple columns of dependent variables (such as concurrent values of concentration observation) and other primary variables such as wind speed and stability. The ranges of the primary variables are also defined in the input file, to be used for grouping the data prior to generating the box plots. Table D-1 describes the format of the input file. Figure D-1 shows an example of an input file. Note that the ANADISTR program makes no corrections or substitutions for missing data; it is the responsibility of the user to provide valid data at each position.

The output file of the ANADISTR program contains distributions (the 2th, 16th, 50th, 84th, and 98th percentiles of the cdf) of the first variable as a function of the second variable. The information stored in this output file can then be plotted using the SIGPLOT plotting package (see Figure D-2 for an example).

During the execution of the ANADISTR program, the following questions will be asked:

- Name of the input file:

The user must specify the name of the input data file here. There is no default answer.

- Name of the output file:

The user must specify the name of the output file. There is no default answer.

- An input file typically contains several columns of dependent and independent data. The ANADISTR program handles one such column or the ratio of any two columns of dependent data, specified by the user, at a time. This is accomplished by asking the user to select any two columns between 0 and MM, (see Table D-2). The distribution of the ratio of the numbers in these columns will be analyzed. Note that column "0" is simply all 1's, and is not part of the input data file. Therefore, if the user wants to investigate the distribution of the dependent data in column 2, then two integers, 2 and 0 should be entered. If the user wants to investigate the distribution of the ratio of the dependent data in column 2 to the data in column 1, then 2 and 1 should be entered.

- Implement a lower threshold for the dependent variable? (y/n):

The user has the option of specifying a lower threshold for the one dependent variable or the ratio of the two dependent variables chosen above. This is sometimes necessary if the logarithmic scale is to be used and there are zero or minute values in the data whose distribution is to be analyzed. The default (i.e., hitting the RETURN key) answer is "y".

TABLE D-1. FORMAT OF THE MANDATORY INPUT DATA FILE OF THE ANADISTR PROGRAM.
THE FOLLOWING KEY LETTERS ARE USED IN THE FORMAT COLUMN - FF: FREE
FORMAT, C: CHARACTER, I: INTEGER, AND R: REAL.

LINE NO.	FORMAT	DESCRIPTION
1	FF/I	There are four integer constants in this line, representing the total number of observations (NN, < 501), the total number of dependent variable (MM, < 16), the total number of blocks (KK), and the total number of primary variables (NVAR, < 11). Note that KK is not used by ANADISTR since the blocking of data is performed internally according to the defined ranges of the primary variables. The limits on NN, MM, and NVAR are assigned in the program using the PARAMETER statements, and can be easily changed.
2	FF/I	There are KK integer constants in this line, representing the number of pieces in each block. The sum of all these integers should equal NN. Note that the information in this line is currently not used by the ANADISTR program.
3	FF/I	There are MM character constants in this line; each one can be at most eight characters long, containing the name of each of the dependent variables. All character constants must be enclosed in apostrophes.
4	FF/I	There should be KK character constants in this line. Each one can be at most 20 characters long, containing the name of each of the blocks. All character constants must be enclosed in apostrophes. Note that the information in this line is not used by the ANADISTR program.

LINE NO. FORMAT

DESCRIPTION

Next NN lines:

FF/R

There are MM+NVAR real numbers in each line, with the first MM numbers representing the dependent variables, and the following NVAR numbers representing of the primary variables.

Next NVAR lines:

FF/

I,C,R

Each line describes the way each of the NVAR primary variables is to be blocked. The first parameter is an integer (IXR, < 21), representing the number of ranges for the primary variable. The second parameter is a character constant, at most 40 characters long, enclosed in apostrophes, representing the name of the primary variable. The next IXR+1 real numbers, in numerical ascending order, define the boundaries of the ranges. For example, the following line:

4 'u (m/s)' 0. 2. 5. 10. 20.

means that wind speeds should be divided into four groups where the distribution of the dependent variables within each group is to be calculated. The first group is for those data when wind speeds are between 0. and 2. m/s, the second group is for wind speeds between 2. and 5. m/s, etc.

The limits on IXR are assigned in the program using the PARAMETER statement, and can be easily changed. Note that the sequence of the NVAR lines must be consistent with that of the last NVAR columns described in the previous section. As an example, if the MM+1th column in the previous section contains information for wind speeds, then the first line in this section should also contain grouping information for wind speeds.

```

79      4      2      4
39 40
'DEPVAR-A' 'DEPVAR-B' 'DEPVAR-C' 'DEPVAR-D'
'SUBSET1' 'SUBSET2'
616.0 708.7 594.7 516.5 11 3.0 800. 2
604.1 689.2 585.9 496.7 12 3.4 1000. 2
868.0 674.8 580.3 516.8 13 3.5 1100. 2
498.6 668.8 652.1 548.3 14 3.8 1200. 2
393.1 560.2 704.7 581.9 15 4.7 1300. 2
409.0 740.9 570.1 621.4 16 5.2 1000. 3
640.2 249.6 510.1 553.5 17 5.4 1100. 3
265.3 259.6 463.4 446.0 18 4.9 1100. 4
192.7 91.6 131.0 485.0 19 4.2 1100. 5
1149.1 1217.5 1116.1 520.6 10 2.6 1600. 2
972.8 1275.8 1175.1 536.9 11 3.2 1900. 2
1137.5 1225.7 1081.7 617.4 12 3.8 1600. 2
669.5 1052.8 905.1 637.3 13 4.5 1600. 2
595.5 862.0 862.0 664.1 14 5.0 1500. 2
741.2 589.5 767.0 665.3 15 5.1 1500. 2
612.6 602.4 728.2 672.4 16 5.0 1500. 3
312.0 398.9 637.3 659.5 17 5.2 1500. 3
400.2 340.2 412.3 586.0 18 5.1 1500. 4
264.7 612.1 774.2 705.9 16 5.7 1400. 3
290.0 428.4 757.3 708.8 17 5.1 1800. 3
459.5 355.0 512.3 602.4 18 5.1 2000. 4
444.0 216.0 441.4 681.1 19 4.4 2000. 5
175.1 216.6 456.1 825.4 20 4.6 2000. 5
102.3 126.1 255.6 522.9 21 4.9 2000. 6
128.8 16.5 0.5 834.9 22 4.6 0. 6
200.2 301.9 208.9 728.0 23 5.4 0. 6
358.3 481.8 354.0 742.4 24 5.4 0. 6
611.1 1010.2 987.1 679.0 14 4.4 1500. 2
499.3 752.5 921.6 725.7 15 5.0 1500. 2
537.8 724.0 826.8 675.9 16 4.7 1500. 3
220.0 523.3 908.2 640.8 17 3.9 1800. 3
479.2 357.5 788.6 544.7 18 4.2 2000. 4
133.2 195.3 383.1 738.5 19 3.1 1800. 5
98.2 167.3 213.5 1064.9 20 3.2 1500. 6
92.5 104.6 142.2 741.2 21 3.1 1200. 6
21.0 127.4 176.3 805.2 22 3.3 1200. 6
353.0 307.8 167.1 576.9 20 3.8 2000. 5
358.0 280.9 188.4 225.3 21 2.3 2000. 4
233.3 355.3 234.9 719.1 22 2.4 2000. 5
198.3 12.7 184.0 745.2 23 3.6 2000. 6
507.2 0.0 126.3 564.9 24 3.5 2000. 6
313.7 0.0 0.0 667.1 1 4.2 0. 5
165.1 0.0 0.0 703.9 2 3.6 0. 5
295.6 329.9 454.6 695.3 4 5.2 0. 6
527.7 308.0 295.9 775.0 5 4.7 0. 6
454.1 301.0 1.0 995.6 6 2.9 0. 6
240.3 417.5 361.1 933.8 7 3.4 0. 6
590.8 579.3 144.2 666.5 8 3.1 1500. 5
638.3 756.6 608.9 400.1 9 3.4 1500. 4
949.8 1004.2 805.4 528.9 10 3.4 1500. 3
886.8 855.6 706.2 517.4 11 3.0 1300. 2
635.5 761.0 670.9 596.6 12 4.5 1200. 2
359.3 412.6 232.5 937.6 1 2.3 1200. 6
484.7 360.7 226.8 979.0 2 2.5 1200. 6
529.7 332.0 202.5 980.0 3 2.4 1200. 6
585.8 291.4 186.1 1100.1 4 2.1 1200. 6
367.7 368.0 260.2 1005.6 5 2.1 1200. 6
324.7 270.9 72.7 1058.6 6 2.0 1200. 6
489.0 274.6 208.5 942.2 7 2.6 1200. 6
570.8 337.1 218.0 646.5 8 2.8 1200. 5
419.7 254.4 206.1 344.0 9 4.3 1200. 4
532.8 414.2 197.9 477.3 9 4.8 1800. 3
425.2 365.7 198.7 469.5 10 7.1 1700. 4
467.5 411.5 228.5 455.3 11 7.5 2000. 4
362.2 306.4 147.6 405.2 12 5.1 2000. 4
429.2 287.4 139.2 450.6 13 5.4 2000. 4
446.0 338.1 169.5 461.2 14 5.7 2000. 4
192.9 253.8 145.6 460.7 15 5.8 2400. 4
630.3 322.5 257.2 460.5 16 7.3 2700. 4
364.9 326.7 251.1 510.6 17 7.8 3000. 4
111.4 196.4 248.5 0.0 23 1.9 250. 4
89.8 146.5 254.9 0.0 24 1.9 250. 4
82.5 248.0 160.9 0.0 1 2.9 250. 4
296.5 253.2 193.2 0.0 2 2.8 250. 4
215.4 299.7 165.0 0.0 3 2.9 250. 4
454.5 274.2 154.0 0.0 4 3.5 250. 4
384.7 324.6 163.2 0.0 5 3.5 250. 4
253.2 488.3 175.6 0.0 6 3.5 250. 4
289.5 304.1 193.1 0.0 7 3.1 250. 4
6 'hour of day' -0.01, 4., 8., 12., 16., 20., 24.01
10 'u (m/s)' 0.5, 1.5, 2.5, 3.5, 4.5, 5.5, 6.5, 7.5, 8.5, 9.5, 10.5
6 'h (m)' -0.01, 200., 600., 1000., 1500., 2000., 3000.1
3 'pg class' 0.5 3.5 4.5 6.5

```

Figure D-1. An example of the input data file for the ANADISTR program.

DEMONSTRATION OF THE RESULTS GENERATED BY THE ANADISTR PROGRAM.

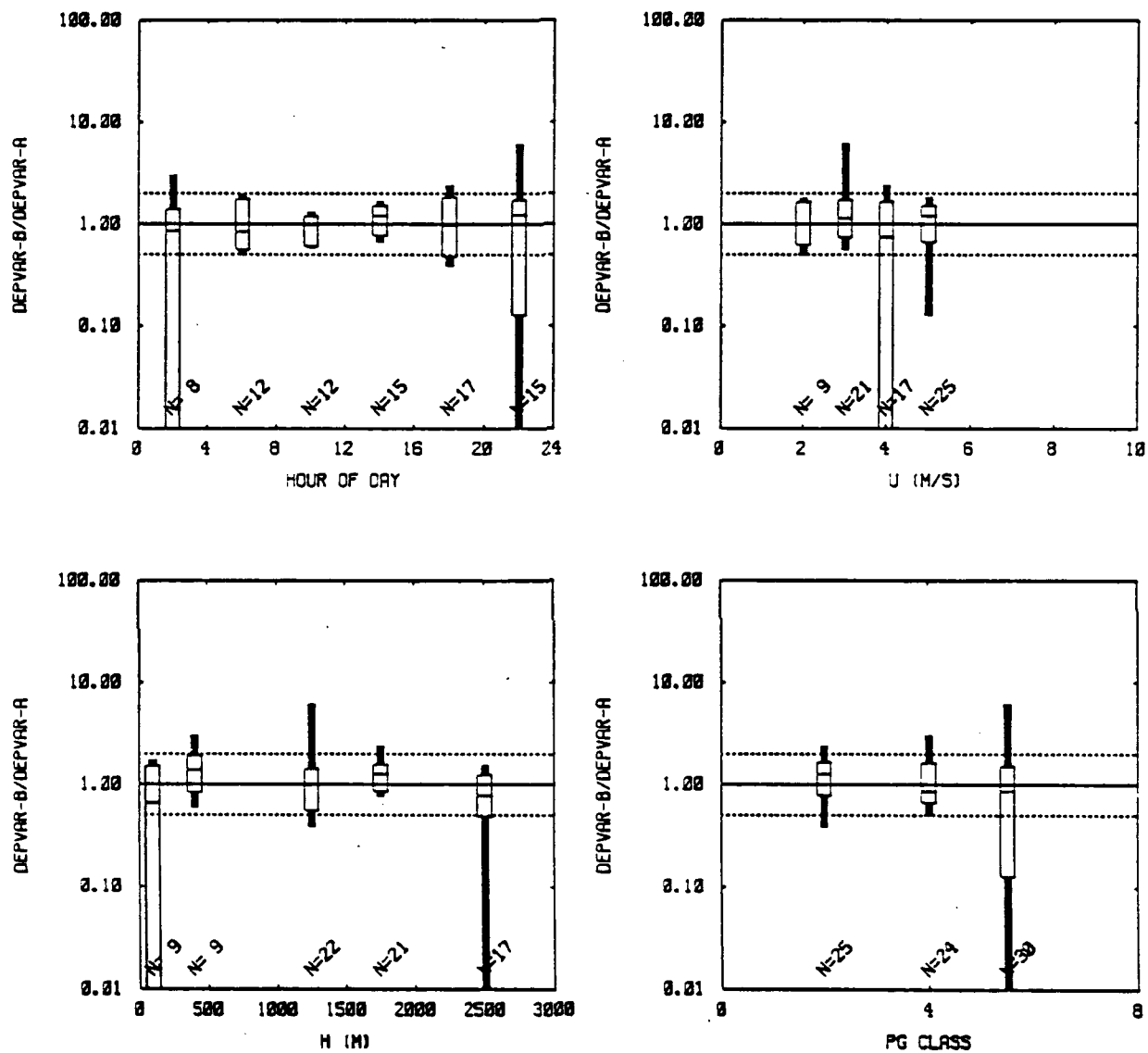


Figure D-2. An example of the results generated by the ANADISTR program and plotted using SIGPLOT. Significant points on each box represent the 2nd, 16th, 50th, 84th, and 98th percentiles. The dashed lines represent the factor of two lines.

The next question will be asked only if the user answers "y" to the above question.

- Enter the lower threshold (e.g. 0.01):

There is no default answer, but 0.01 has proven to be a good choice for the ratio of two dependent variables in our tests.

- Implement an upper threshold for the dependent variable? (y/n):

This is sometimes necessary if the logarithmic scale is to be used and there are very large values in the data whose distribution is to be analyzed. The default (i.e., hitting the RETURN key) answer is "y".

The following question will be asked only if the user answers "y" to the above question.

- Enter the upper threshold of the ratio (e.g. 100.):

There is no default answer, but 100 has proven to be a good choice for the ratio of two dependent variables in our tests.

Intentionally Blank

APPENDIX E

USER'S GUIDE FOR THE SIGPLOT PLOTTING PACKAGE

APPENDIX E

A. USER'S GUIDE FOR THE SIGPLOT PLOTTING PACKAGE

The SIGPLOT plotting package developed at Sigma Research Corporation is a versatile tool for producing different kinds of two-dimensional plots, such as scatter plots, graphs, box plots (sometimes called residual or whisker plots), or error bar plots. The user can specify many parameters including the number of frames per page, the aspect ratio of the frame, and the mapping of the coordinates. The graphics library routines used by SIGPLOT, together with the screen and printer drivers (described later) were originally developed by Dr. Arlindo daSilva of the University of Wisconsin at Milwaukee.

SIGPLOT requires two input files: 1) the template file that contains the control parameters which influence the appearance of the plots, and 2) the input data file that contains the data to be plotted. Tables E-1 and E-2 describe the formats of the template file and the input data file, respectively. Examples of the template file are shown in Figures E-1 and E-2. Examples of the input data file are shown in Figures E-3 and E-4.

SIGPLOT creates a Tektronix picture file that can be viewed directly on any kind of the PC graphics environments (e.g., Hercules, CGA, EGA, and VGA) using the screen driver, TEKPC. Hard copy output can also be generated from the Tektronix picture file with a printer driver. There are three printer drives, TEKEPS, TEKELQ, and PS, that are currently available. The first two drivers are used to drive an EPSON-compatible dot matrix printer, with TEKEPS for low resolution and TEKELQ for high resolution. The PS program is used to drive a PostScript printer, such as Apple LaserWriter, NEC LC-890, or TI MicroLaser PS35. It is recommended that the user have access to a PostScript printer to obtain the best results in the shortest time.

SIGPLOT requires about 200KB of memory. The other screen and printer drivers require less than 100KB of memory, except for TEKELQ, where 450KB of memory is required due to the high resolution and the use of the bitmap approach in the driver program. The SIGPLOT plotting package and the graphics library routines were written in FORTRAN. The screen and printer drivers were written in C.

TABLE E-1. THE FORMAT OF THE TEMPLATE FILE OF SIGPLOT. THE FOLLOWING KEY LETTERS ARE USED IN THE FORMAT COLUMN - FF: FREE FORMAT, C: CHARACTER, I: INTEGER, AND R: REAL.

The global control parameters are specified in the first section of the template file, lines 1 through 16.

LINE NO.	FORMAT	DESCRIPTION
1-3		Reserved for comments
4	FF/C	Name of the input data file, currently not used
5	FF/C	Name of the output Tektronix picture file, currently not used
6	FF/I	Flag for the frame aspect ratio, 1-5, 1: x:y = 1:1 2: x:y = 1:2 3: x:y = 2:1 4: x:y = 1:3 5: x:y = 3:1
7	FF/I	Number of frames per page, 1-4
8-9	A80	Title for the page (no title will be drawn if "0" appears as the first character of the line)
10	FF/C	Flag (PAXIS) for the axis along which the first column, representing the independent variable, of the data in the input data file (see Table E-2) will be plotted (x or y). PAXIS must = x if IPATTN (described below) = 4, and PAXIS must = y if IPATTN = 6
11	FF/I	Flag for mapping, 1-4, 1: linear in x, linear in y 2: linear in x, logarithmic in y 3: logarithmic in x, linear in y 4: logarithmic in x, logarithmic in y

TABLE E-1. THE FORMAT OF THE TEMPLATE FILE OF SIGPLOT. THE FOLLOWING KEY LETTERS ARE USED IN THE FORMAT COLUMN - FF: FREE FORMAT, C: CHARACTER, I: INTEGER, AND R: REAL. Continued.

LINE NO.	FORMAT	DESCRIPTION
12	FF/I	Flag (IPATTN) for plot pattern, 1-6, 1: scatter plot 2: line graph 3: scatter plot except line graph for the last variable 4: box plot 5: error bar plot 6: same as 5 but with extra labelling
13	FF/I	Flag for background, 0 or 2, 0: no background 2: gridded background
14	FF/C	Flag for system time, y or n, if y: system time will be printed out on the upper right corner of each page
15	SA1	Five point patterns for the scatter plot
16	FF/I	Flag (IEXTRA) for the plotting of extra lines, 1: $x=0$ will be plotted 2: $y=0$ will be plotted 3: $x=0$ and $y=0$ will be plotted 4: $x=1$ will be plotted 5: $y=1$ will be plotted 6: $x=1$ and $y=1$ will be plotted 7: diagonal line will be plotted 8: $y=0.5$ and $y=2$ (factor of two) will be plotted 9: $x=-0.667$, 0 , and 0.667 , and $y=4x^2/(4-x^2)$. (see text) will be plotted. else: no extra lines will be plotted. Note that IEXTRA = 9 is effective only if IPATTN = 6

TABLE E-1. THE FORMAT OF THE TEMPLATE FILE OF SIGPLOT. THE FOLLOWING KEY LETTERS ARE USED IN THE FORMAT COLUMN - FF: FREE FORMAT, C: CHARACTER, I: INTEGER, AND R: REAL. Continued.

The next section of the template file (lines 17 through 29) contains the parameters that are applicable to a frame. This section can be repeated if there are multiple frames to be plotted in a print job. However, the user can prepare just one such section if the same information is to be used repeatedly by all frames.

LINE NO.	FORMAT	DESCRIPTION
17-19		Reserved for comments
20	FF/R	Constants, a and b, for the linear transformation of the independent variable, where $x_{\text{new}} = a \cdot x_{\text{old}} + b,$ a=1 and b=0 means no transformation is needed
21	FF/R	Constants, a and b, for the linear transformation of the first dependent variable, where $y_{1,\text{new}} = a \cdot y_{1,\text{old}} + b,$ a=1 and b=0 means no transformation is needed
22	FF/R	Same as above, but for the second dependent variable
23	FF/R	Same as above, but for the third dependent variable
24	FF/R	Same as above, but for the fourth dependent variable

TABLE E-1. THE FORMAT OF THE TEMPLATE FILE OF SIGPLOT. THE FOLLOWING KEY LETTERS ARE USED IN THE FORMAT COLUMN - FF: FREE FORMAT, C: CHARACTER, I: INTEGER, AND R: REAL. Concluded.

LINE NO.	FORMAT	DESCRIPTION
25	FF/R	Same as above, but for the fifth dependent variable. Note that lines 22 through 25 cannot be omitted even if only one group of data were to be plotted
26	FF/R	xmin, xmax, and dx of the x-axis
27	FF/R	ymin, ymax, and dy of the y-axis
28	FF/C	Format specifier for the numerical labels of the x-axis. If "!" appears as the first character of the line, the appropriate format will be determined internally by the program; otherwise, the user should supply a simple FORTRAN I-, F-, or E-format specifier, enclosed in parentheses, e.g., (I5), (F6.3), and (E8.1) are accepted, but (3I5), (I5,f6.3), (1P,E8.1), and (G9.1) are not accepted
29	FF/C	Format specifier for the numerical labels of the y-axis

TABLE E-2. THE FORMAT OF THE INPUT DATA FILE OF SIGPLOT. THE FOLLOWING KEY LETTERS ARE USED IN THE FORMAT COLUMN - FF: FREE FORMAT, C: CHARACTER, I: INTEGER, AND R: REAL.

LINE NO.	FORMAT	DESCRIPTION
1	A40	Title for the frame (no title will be drawn if "0" appears as the first character of the line)
2	A40	Label for the x-axis (no label will be drawn if "0" appears as the first character of the line)
3	A40	Label for the y-axis (no label will be drawn if "0" appears as the first character of the line)
4	FF/I	Two integers specifying the number of points (NPTS) and the number of groups of data (MANY) to be plotted. MANY cannot be > 5 for IPATTN = 1, 2, 3, and 5, and MANY must be = 1 for IPATTN = 4 and 6. NPTS cannot be > 700 for IPATTN = 1, 2, and 3. NPTS cannot be > 50 for IPATTN = 4, 5, and 6 (see text).

Next NPTS lines:

For IPATTN = 1, 2, and 3,

FF/R There are 1+MANY real numbers in each line. The first number represents the independent variable, which can be plotted either along the x- or the y-axis depending the value of PAXIS (see Table E-1). The next MANY numbers represent the dependent variables. For example, if three curves (MANY=3), $f_1(x)$, $f_2(x)$, and $f_3(x)$ were to be plotted, then each line here should contain four real numbers, x_i , $f_{1,i}$, $f_{2,i}$, and $f_{3,i}$, where $i=1, \text{NPTS}$. If PAXIS = "x", the x will be plotted along the abscissa, and f_1 , f_2 , and f_3 will be plotted along the ordinate; vice versa PAXIS = "y".

TABLE E-2. THE FORMAT OF THE INPUT DATA FILE OF SIGPLOT. THE FOLLOWING KEY LETTERS ARE USED IN THE FORMAT COLUMN - FF: FREE FORMAT, C: CHARACTER, I: INTEGER, AND R: REAL. Continued.

LINE NO.	FORMAT	DESCRIPTION
----------	--------	-------------

For IPATTN = 4,

FF/R,I	There are six real numbers and one integer in each line. The first real number represents the independent variable. The next five real numbers represent the values of the dependent variable at the 2th, 16th, 50th, 84th, and 98th percentiles, respectively. Note that the value of the independent variable listed here frequently represents a range of the independent variable; for example, a wind speed of 7 m/s actually represents wind speeds in the range of 6 to 8 m/s. The integer represents the number of data points based on which the distribution of the dependent variable is derived. No box will be plotted if the number of data points is less than five since not enough information is available to define a distribution.
--------	--

For IPATTN = 5,

FF/R	There are 1+3*MANY real numbers in each line. The first number represents the independent variable. The remaining numbers for the dependent variables are in MANY groups of three numbers. The three numbers, which must be in order, represent the distribution of a dependent variable. This distribution can be 1) $\mu - \sigma$, μ , and $\mu + \sigma$, where μ is the mean, and σ is the standard deviation, or 2) lower c.l., nominal value, and upper c.l., where c.l. is the confidence limit.
------	---

TABLE E-2. THE FORMAT OF THE INPUT DATA FILE OF SIGPLOT. THE FOLLOWING KEY LETTERS ARE USED IN THE FORMAT COLUMN - FF: FREE FORMAT, C: CHARACTER, I: INTEGER, AND R: REAL. Concluded

LINE NO.	FORMAT	DESCRIPTION
----------	--------	-------------

For IPATTN = 6,

FF/R,C	There are four real numbers and one character constant (no more than 17 characters long) in each line. The definition of the first four real numbers is identical to that when IPATTN = 5, except now MANY must = 1. The character constant, enclosed in apostrophes, is used to label each data point.
--------	---

The above 4+NPTS lines provide enough information to plot a frame. Additional data, similar in structure, can be appended here if the plotting of more than one frames in a print job is desired.

```

!-----
!      Main switches for plotting.
!-----0-----0-----0-----0-----
urrs.1   Name of input data file.
tekl.pic Name of output tektronix file.
1        Aspect ratio (integer, 1 - 5).
1        Number of plots per page (integer, 1 - 4).
demo of ipattn=2
0
x        Which axis serves as independent variable (x or y).
1        Flag indicating log or linear mapping (1 - 4).
2        Pattern.
0        Background specification.
y        Print out system time on the upper right hand corner (y or n).
.+o$     Patterns of scatter plots (5a1)
0        Extra line, 1:x=0,2:y=0,3:x,y=0,4:x=1,5:y=1,6:x,y=1,7:diag,8:y=fac. 2.,9:fb-nmse, else:nothing.
!-----
!      Parameters for plot 1.
!-----
1. 0.    ascale, bscale for the independent variable axis.
1. 0.    ascale, bscale for curve 1.
1. 0.    ascale, bscale for curve 2.
1. 0.    ascale, bscale for curve 3.
1. 0.    ascale, bscale for curve 4.
1. 0.    ascale, bscale for curve 5.
-6.28319 6.28319 3.141595 xmin, xmax, and dx for the x axis.
-1.2 1.2 0.3 ymin, ymax, and dy for the y axis.
(f5.2)    format for x label
(f4.1)    format for y label

```

Figure E-1. An example of the template file of SIGPLOT. Refer to Figure E-6 for the results.

```

!-----
!      Main switches for plotting.
!-----0-----0-----0-----
urrs.1   Name of input data file.
tekl.pic Name of output tektronix file.
1        Aspect ratio (integer, 1 - 5).
1        Number of plots per page (integer, 1 - 4).
demo of ipattn=5
0
x        Which axis serves as independent variable (x or y).
3        Flag indicating log or linear mapping (1 - 4).
5        Pattern.
0        Background specification. (0 or 2)
n        Print out system time on the upper right hand corner (y or n).
-o.##$   Patterns of scatter plots (5al)
0        Extra line,1:x=0,2:y=0,3:x,y=0,4:x=1,5:y=1,6:x,y=1,7:diag,8:y=fac. 2.,9:fb-nmse, else:nothing.
!-----
!      Parameters for plot 1.
!-----
1. 0.    ascale, bscale for the independent variable axis.
1. 0.    ascale, bscale for curve 1.
1. 0.    ascale, bscale for curve 2.
1. 0.    ascale, bscale for curve 3.
1. 0.    ascale, bscale for curve 4.
1. 0.    ascale, bscale for curve 5.
200. 20000. 10. xmin, xmax, and dx for the x axis.
-1.5 1.5 0.5 ymin, ymax, and dy for the y axis.
(15)
(f4.1)

```

Figure E-2. An example of the template file of SIGPLOT. Refer to Figure E-9 for the results.

0
x
y

```

50 5
-6.03186 0.248690 -0.368124 -0.844328 -0.998027 -0.770514
-5.78053 0.481754 -0.125333 -0.684547 -0.982287 -0.904827
-5.52920 0.684547 0.125333 -0.481753 -0.904827 -0.982287
-5.27788 0.844328 0.368125 -0.248690 -0.770513 -0.998027
-5.02655 0.951057 0.587786 0.397359E-06 -0.587785 -0.951056
-4.77522 0.998027 0.770513 0.248690 -0.368125 -0.844328
-4.52389 0.982287 0.904827 0.481754 -0.125333 -0.684547
-4.27257 0.904827 0.982287 0.684547 0.125333 -0.481753
-4.02124 0.770513 0.998027 0.844328 0.368125 -0.248690
-3.76991 0.587785 0.951056 0.951057 0.587785 0.254308E-06
-3.51858 0.368125 0.844328 0.998027 0.770513 0.248690
-3.26726 0.125333 0.684547 0.982287 0.904827 0.481754
-3.01593 -0.125333 0.481753 0.904827 0.982287 0.684547
-2.76460 -0.368125 0.248690 0.770513 0.998027 0.844328
-2.51327 -0.587785 0.397391E-07 0.587785 0.951056 0.951057
-2.26195 -0.770513 -0.248690 0.368124 0.844328 0.998027
-2.01062 -0.904827 -0.481754 0.125333 0.684547 0.982287
-1.75929 -0.982287 -0.684547 -0.125334 0.481753 0.904827
-1.50796 -0.998027 -0.844328 -0.368124 0.248690 0.770513
-1.25664 -0.951057 -0.951057 -0.587785 -0.556284E-07 0.587785
-1.00531 -0.844328 -0.998027 -0.770513 -0.248690 0.368124
-0.753983 -0.684547 -0.982287 -0.904827 -0.481753 0.125333
-0.502655 -0.481754 -0.904827 -0.982287 -0.684547 -0.125333
-0.251328 -0.248690 -0.770513 -0.998027 -0.844328 -0.368125
0.000000 0.000000 -0.587785 -0.951056 -0.951057 -0.587785
0.251328 0.248690 -0.368124 -0.844328 -0.998027 -0.770513
0.502655 0.481753 -0.125333 -0.684547 -0.982287 -0.904827
0.753982 0.684547 0.125333 -0.481754 -0.904827 -0.982287
1.00531 0.844328 0.368125 -0.248690 -0.770513 -0.998027
1.25664 0.951056 0.587785 -0.381470E-06 -0.587786 -0.951057
1.50796 0.998027 0.770513 0.248690 -0.368125 -0.844328
1.75929 0.982287 0.904827 0.481754 -0.125333 -0.684547
2.01062 0.904827 0.982287 0.684547 0.125333 -0.481754
2.26195 0.770513 0.998027 0.844328 0.368125 -0.248690
2.51327 0.587785 0.951056 0.951057 0.587785 0.190735E-06
2.76460 0.368124 0.844328 0.998027 0.770513 0.248690
3.01593 0.125334 0.684548 0.982287 0.904827 0.481753
3.26726 -0.125333 0.481754 0.904827 0.982287 0.684547
3.51858 -0.368124 0.248690 0.770514 0.998027 0.844328
3.76991 -0.587785 0.341731E-06 0.587785 0.951057 0.951056
4.02124 -0.770513 -0.248690 0.368125 0.844328 0.998027
4.27257 -0.904827 -0.481754 0.125333 0.684547 0.982287
4.52389 -0.982287 -0.684547 -0.125333 0.481754 0.904827
4.77522 -0.998027 -0.844327 -0.368124 0.248691 0.770514
5.02655 -0.951057 -0.951056 -0.587785 0.723200E-06 0.587786
5.27787 -0.844328 -0.998027 -0.770513 -0.248689 0.368125
5.52920 -0.684548 -0.982287 -0.904827 -0.481753 0.125334
5.78053 -0.481754 -0.904827 -0.982287 -0.684547 -0.125333
6.03186 -0.248690 -0.770513 -0.998027 -0.844328 -0.368124
6.28319 -0.301992E-06 -0.587785 -0.951057 -0.951056 -0.587785

```

Figure E-3. An example of the input data file of SIGPLOT. Refer to Figure E-6 for the results.

```

all periods
n-s distance (m)
var(dws) / median 1-min var(ws) / 2
6 3
312.5 -0.029 0.002 0.034 -0.027 0.043 0.112 0.166 0.275 0.383
625.0 -0.009 0.005 0.019 0.011 0.048 0.085 0.209 0.361 0.513
1250.0 -0.035 0.012 0.059 -0.007 0.070 0.148 0.330 0.480 0.630
2500.0 -0.155 0.015 0.185 -0.126 0.100 0.325 0.359 0.565 0.771
5000.0 -0.033 0.170 0.373 0.013 0.323 0.633 0.440 0.751 1.062
10000.0 -0.417 0.061 0.539 -0.137 0.369 0.876 0.406 0.873 1.339

```

Figure E-4. An example of the input data file of SIGPLOT. Refer to Figure E-9 for the results.

As one can see from Table E-1, SIGPLOT is capable of creating the following kinds of plots:

- IPATTN = 1: scatter plot (e.g., Fig. E-5)
- IPATTN = 2: line graph (e.g., Fig. E-6)
- IPATTN = 3: scatter plot except line graph for the last variable (e.g., Fig. E-7)
- IPATTN = 4: box plot (e.g., Fig. E-8)
- IPATTN = 5: error bar plot (e.g., Fig. E-9)
- IPATTN = 6: same as IPATTN = 5 but with extra labelling (e.g., Fig. E-10)

The usage of each option is described below.

For IPATTN = 1, groups of data are represented by different dot patterns that are defined in the template file (see Table E-1). At most, five groups of data (MANY = 5) can be plotted, with a maximum of 700 points for each group.

IPATTN = 2 is similar to IPATTN = 1 except that points are now connected. The following line patterns are used to represent different curves: solid, short-dashed, long-dashed, dot-dashed, and dotted. At most, five curves (MANY = 5) can be plotted, with a maximum of 700 points for each group. No user customization of the line patterns is allowed. It is important that the data points in the input file are sorted according to the independent variable.

IPATTN = 3, a combination of IPATTN = 1 and 2, is useful when the user wants to see how well a theoretical curve fits the observed data. Although the order of the data points does not matter for a scatter plot, in this case it is important that the data points in the input file are sorted according to the independent variable. At most, five groups of data (MANY = 5) can be plotted, with a maximum of 700 points for each group.

The IPATTN = 4 option is an alternative to the scatter plot when the number of data points is large. In preparing the input data file for SIGPLOT,

the user first defines certain ranges of the independent variable to be used for grouping the dependent variable. The distribution of the dependent variables within each group is then determined and represented by five significant points in the cumulative distribution function (cdf). These five values could be the 2th, 16th, 50th, 84th, and 98th percentiles of the cdf, or the mean and mean \pm one and two standard deviations. SIGPLOT then uses a box pattern to represent the distribution of the dependent variable within each grouping or range of the independent variable. Only one set of data (i.e., MANY = 1, even though five points are needed to define a box) is accepted for this option, with a maximum of 50 boxes.

IPATTN = 5 is similar to IPATTN = 4 except that three values (vs. five) are needed to define an error bar (vs. a box). These three values can be the mean and mean \pm one standard deviation of a dependent variable, or the nominal value of a dependent variable and its 95% confidence limits. At most, five groups (MANY = 5) of data can be plotted, with a maximum of 50 error bars for each group. The following error bar patterns are used: filled square, empty square, filled triangle, empty triangle, and cross.

IPATTN = 6 is similar to IPATTN = 5 except that the user can label each data point. Because of the additional information to be plotted, only one group of data (MANY = 1) is accepted, with a maximum of 50 error bars. This option is designed primarily to plot the FB (fractional bias), together with its confidence limits, against the NMSE (normalized mean square error), where

$$FB = \frac{(\bar{C}_o - \bar{C}_p)}{(0.5(\bar{C}_o + \bar{C}_p))} \quad (E-1)$$

$$NMSE = \frac{(\bar{C}_o - \bar{C}_p)^2}{\bar{C}_o \bar{C}_p} \quad (E-2)$$

If IEXTRA = 9 (see Table E-1), SIGPLOT will plot the additional $x = -0.667$, 0 , and 0.667 lines, representing the factor of two and zero FB lines, together with the $y = 4x^2/(4-x^2)$ line, representing the "minimum" NMSE (due only to the mean bias) as a function of FB.

The information concerning the usage of the driver programs, TEKPC, TEKELQ, TEKEPS, and PS, can be obtained by simply executing the programs without providing any arguments, and will not be repeated here.

Finally, an example is given below of the procedures followed to use the graphics package.

- Step 1: The user prepares the template file (DEMO.INQ) and the input data file (DEMO.DAT) according to the formats described in Tables E-1 and E-2. The user can create his own template file by editing the sample template file. The input data file is usually generated by some other programs.
- Step 2: After the execution of SIGPLOT, a Tektronix picture file (DEMO.PIC) is generated.
- Step 3: The user can view the results on screen by typing:
TEKPC DEMO.PIC
if a Hercules graphics card is installed, or
TEKPC DEMO.PIC 16
if an EGA (with a resolution of 640x350 pixels) graphics card is installed.
- Step 4: A high resolution hard copy output can be generated on an EPSON-compatible dot matrix printer by typing:
TEKELQ DEMO.PIC.
- Step 5: Or if the user has access to a PostScript printer, a PostScript file (DEMO.PS) will be created by typing:
PS DEMO.PIC,
and this file can be printed out by typing:
PRINT DEMO.PS

DEMO OF IPATTN=1

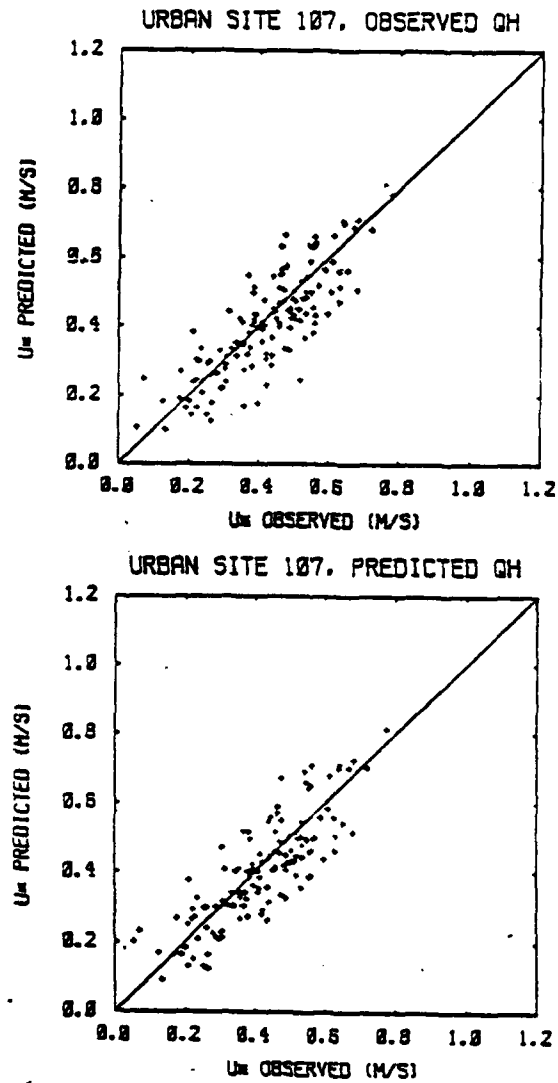


Figure E-5. A sample scatter plot (IPATTN = 1) generated by SIGPLOT.

DEMO OF IPATTN=2

03/25/91

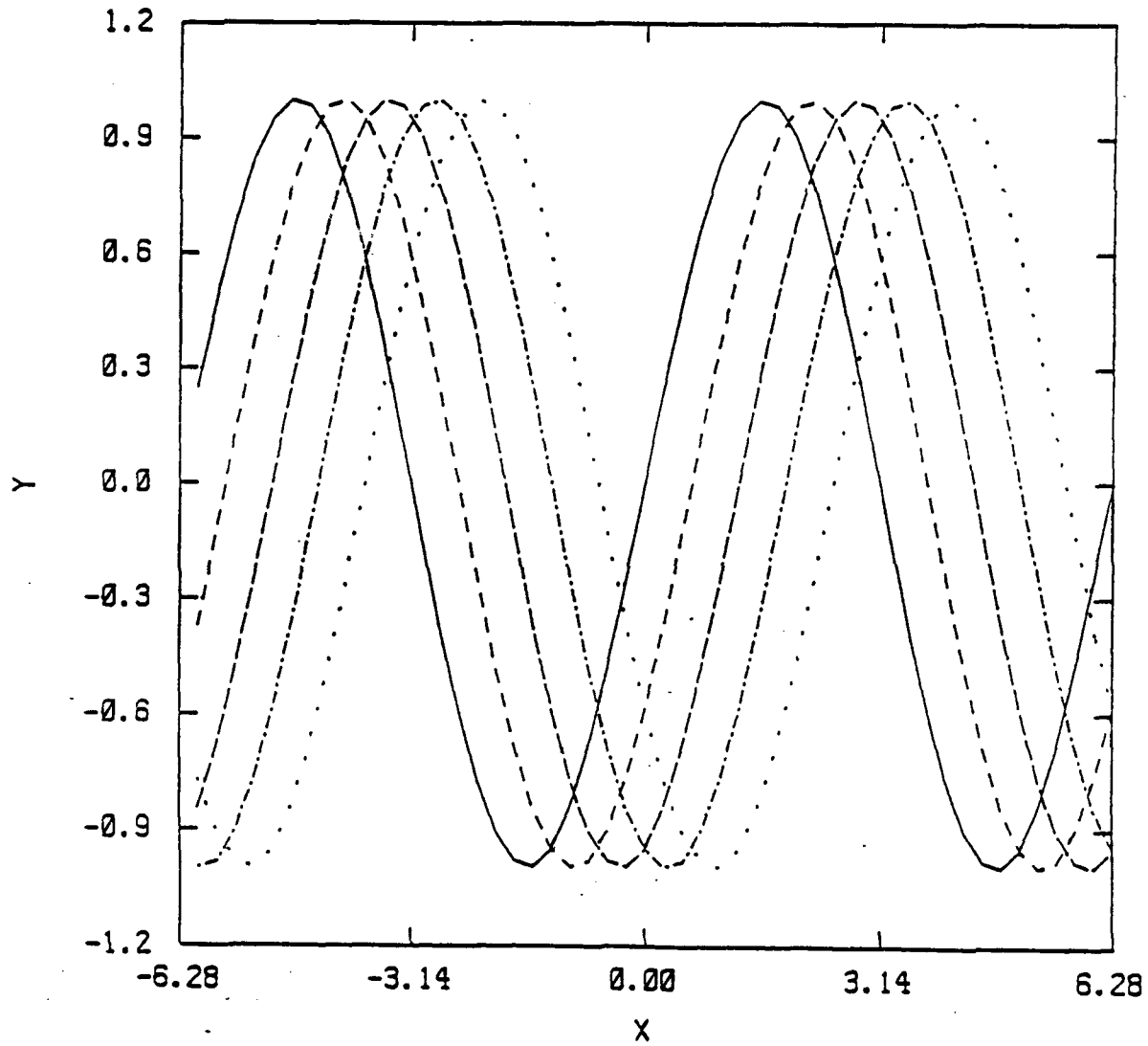


Figure E-6. A sample line graph (IPATTN = 2) generated by SIGPLOT. Refer to Figures E-1 and E-3 for the template and data files used for this figure.

DEMO OF IPATTN=3

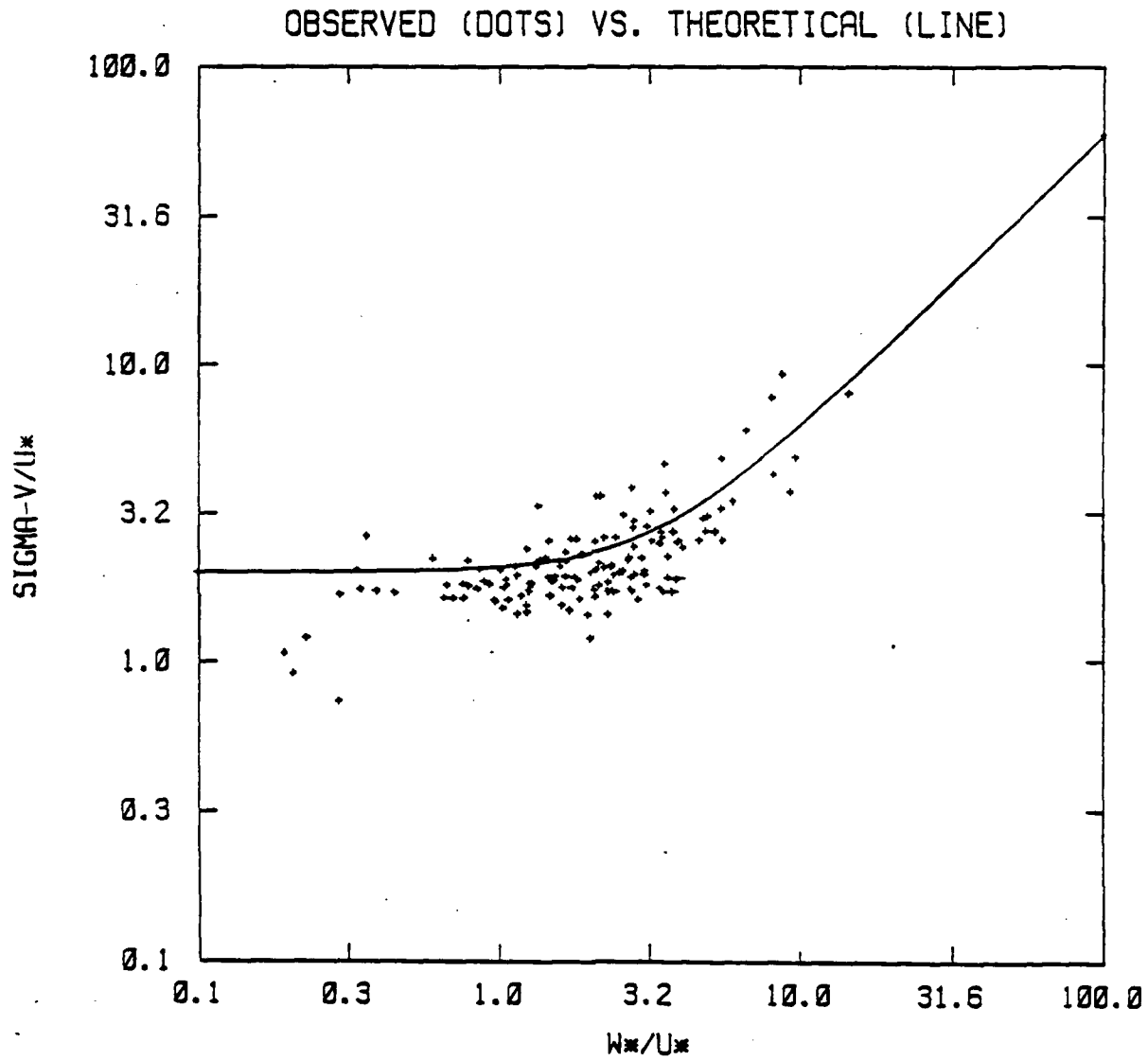


Figure E-7. A sample scatter plot and line graph (IPATTN = 3) generated by SIGPLOT.

DEMO OF IPATTN=4

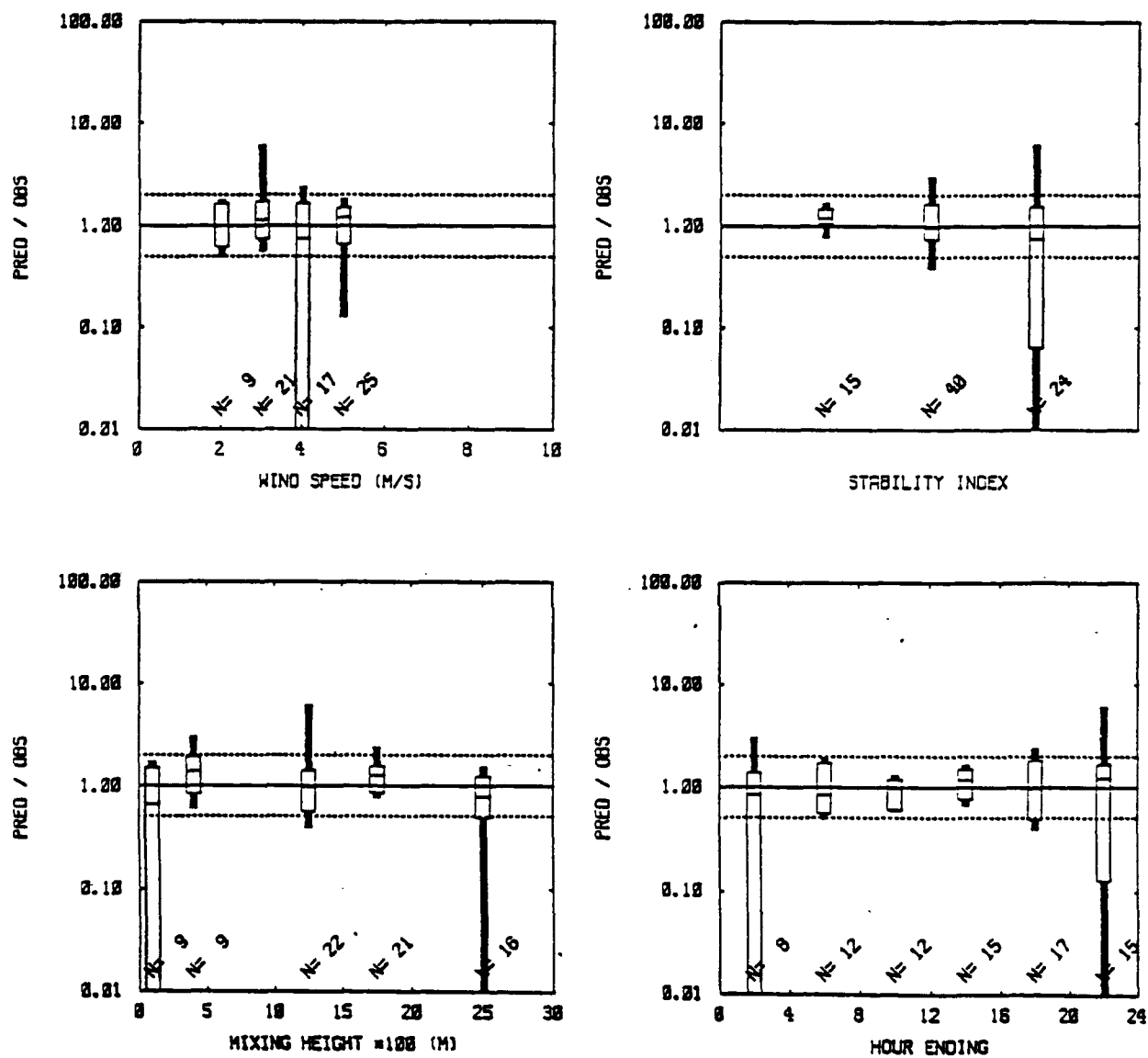


Figure E-8. A sample box plot (IPATTN = 4) generated by SIGPLOT.

DEMO OF IPATTN=5

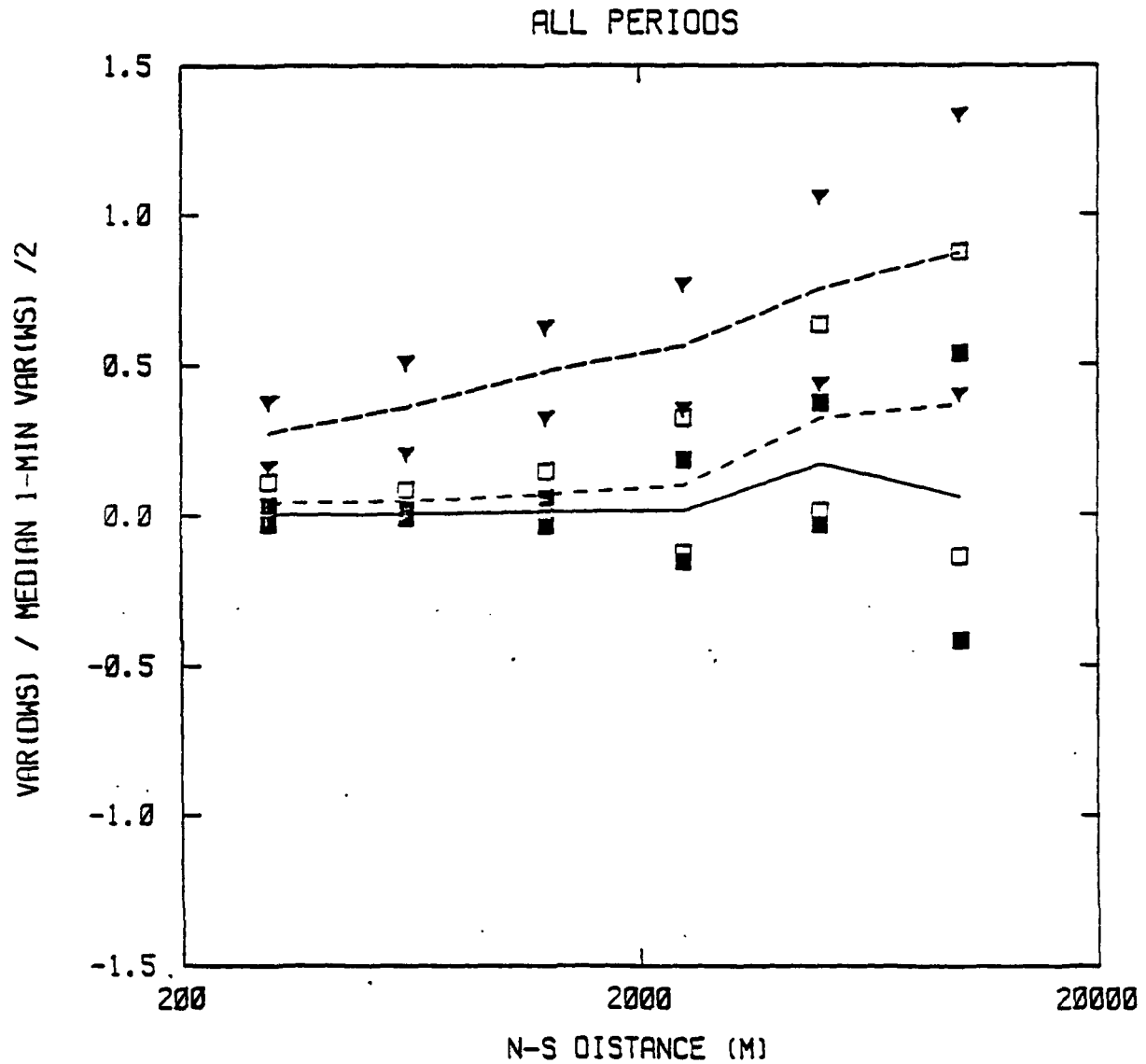


Figure E-9. A sample error bar plot (IPATTN = 5) generated by SIGPLOT. Refer to Figures E-2 and E-4 for the template and data files used for this figure.

DEMO OF IPATTN=6

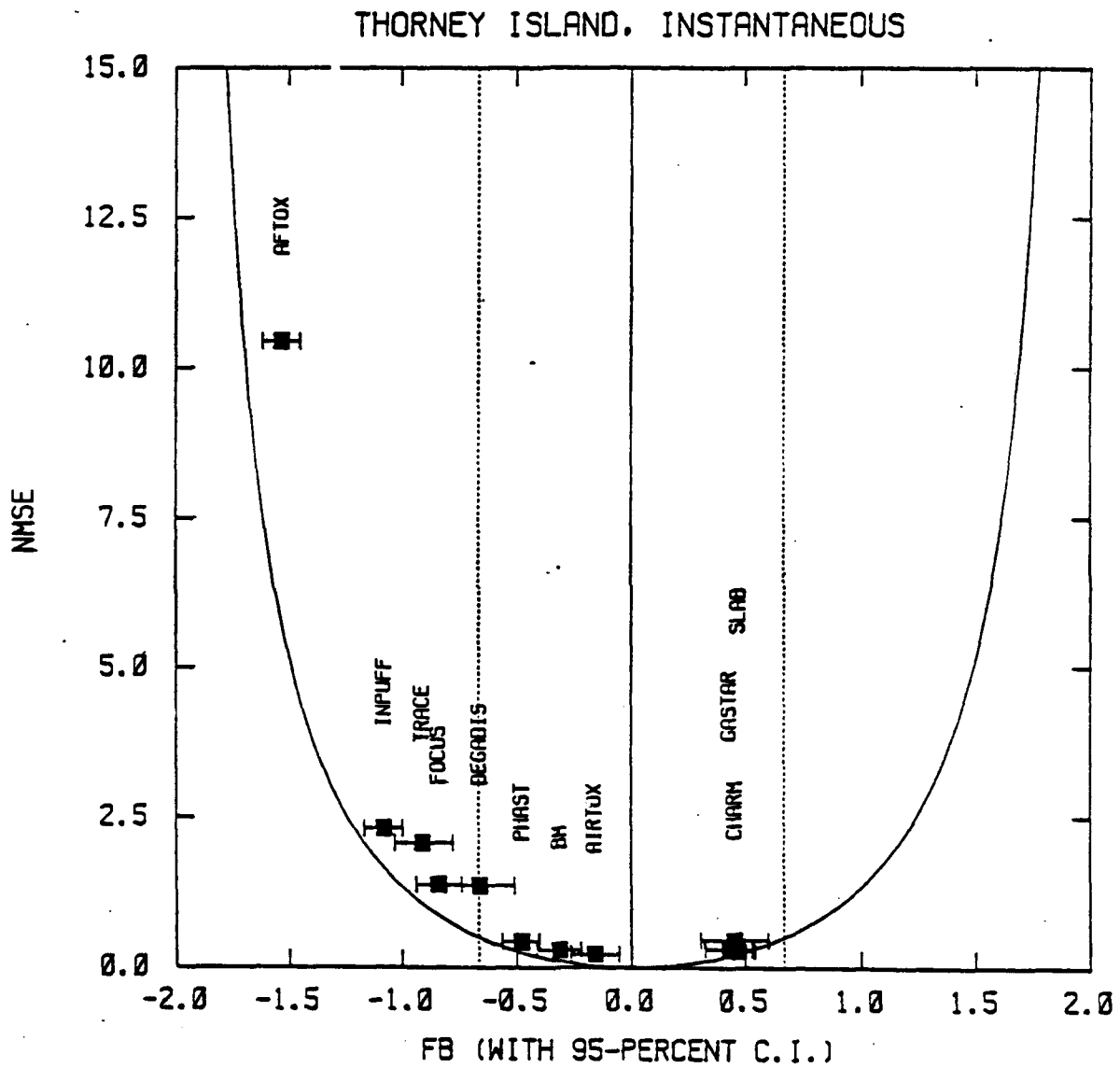


Figure E-10. A sample error bar plot with labelling (IPATTN = 6) generated by SIGPLOT.

.. Intentionally Blank

APPENDIX F-1

LISTINGS OF THE DUGWAY DATA ARCHIVES - HISTORICAL DATASETS

Dry Gulch, Course B

12 : number of trials included in DDA

13 : time zone designation

34.50 : latitude (deg)

120.50 : longitude (deg)

34b25 : longitude (deg)

34b26 : longitude (deg)

34b27 : longitude (deg)

34b28 : longitude (deg)

34b29 : longitude (deg)

34b30 : longitude (deg)

34b31 : longitude (deg)

34b32 : longitude (deg)

34b33 : longitude (deg)

34b34 : longitude (deg)

34b35 : longitude (deg)

34b36 : longitude (deg)

34b37 : longitude (deg)

34b38 : longitude (deg)

34b39 : longitude (deg)

34b40 : longitude (deg)

34b41 : longitude (deg)

34b42 : longitude (deg)

34b43 : longitude (deg)

34b44 : longitude (deg)

34b45 : longitude (deg)

34b46 : longitude (deg)

34b47 : longitude (deg)

34b48 : longitude (deg)

34b49 : longitude (deg)

34b50 : longitude (deg)

34b51 : longitude (deg)

34b52 : longitude (deg)

34b53 : longitude (deg)

34b54 : longitude (deg)

34b55 : longitude (deg)

34b56 : longitude (deg)

34b57 : longitude (deg)

34b58 : longitude (deg)

34b59 : longitude (deg)

34b60 : longitude (deg)

34b61 : longitude (deg)

34b62 : longitude (deg)

34b63 : longitude (deg)

34b64 : longitude (deg)

34b65 : longitude (deg)

34b66 : longitude (deg)

34b67 : longitude (deg)

34b68 : longitude (deg)

34b69 : longitude (deg)

34b70 : longitude (deg)

34b71 : longitude (deg)

34b72 : longitude (deg)

34b73 : longitude (deg)

34b74 : longitude (deg)

34b75 : longitude (deg)

34b76 : longitude (deg)

34b77 : longitude (deg)

34b78 : longitude (deg)

34b79 : longitude (deg)

34b80 : longitude (deg)

34b81 : longitude (deg)

34b82 : longitude (deg)

34b83 : longitude (deg)

34b84 : longitude (deg)

34b85 : longitude (deg)

34b86 : longitude (deg)

34b87 : longitude (deg)

34b88 : longitude (deg)

34b89 : longitude (deg)

34b90 : longitude (deg)

34b91 : longitude (deg)

34b92 : longitude (deg)

34b93 : longitude (deg)

34b94 : longitude (deg)

34b95 : longitude (deg)

34b96 : longitude (deg)

34b97 : longitude (deg)

34b98 : longitude (deg)

34b99 : longitude (deg)

34b100 : longitude (deg)

Dry Gulch, Course 8

12 : number of trials included in ODA

8 : time zone designation

34.20 : latitude (deg)

120.50 : longitude (deg)

dab37 : dab38

dab39

dab40

dab41

dab42

dab43

dab44

dab45

dab46

dab47

dab48

dab49

dab50

dab51

dab52

dab53

dab54

dab55

dab56

dab57

dab58

dab59

dab60

dab61

dab62

dab63

dab64

dab65

dab66

dab67

dab68

dab69

dab70

dab71

dab72

dab73

dab74

dab75

dab76

dab77

dab78

dab79

dab80

dab81

dab82

dab83

dab84

dab85

dab86

dab87

dab88

dab89

dab90

dab91

dab92

dab93

dab94

dab95

dab96

dab97

dab98

dab99

dab100

dab101

dab102

dab103

dab104

dab105

dab106

dab107

dab108

dab109

dab110

dab111

dab112

dab113

dab114

dab115

Dry Gulch, Course B

Dry Gulch, Course B

dqb49	dqb50	dqb51	dqb52	dqb53	dqb54	dqb55
120.30 : longitude (deg)	6	6	6	6	6	6
trial ID	6	6	6	6	6	6
month	22	25	25	28	28	6
day	1962	1962	1962	1962	1962	1962
year	20	20	20	20	20	15
hour	35	15	25	32	32	15
minute	1	1	1	1	1	50
no. of sources	0.0	0.0	0.0	0.0	0.0	1
x-coord. of source (m)	0.0	0.0	0.0	0.0	0.0	0
y-coord. of source (m)	0.0	0.0	0.0	0.0	0.0	0
source elevation (m)	2.50	2.50	2.50	2.50	2.50	1.578
emission rate (g/s)	1.489	1.350	1.217	1.072	1.072	1800.0
emission duration (s)	1800.0	1800.0	1800.0	1800.0	1800.0	-99.9
total mass emitted (kg)	-99.9	-99.9	-99.9	-99.9	-99.9	0.000
sign0 at the source (m)	0.000	0.000	0.000	0.000	0.000	0.000
sign0 at the source (m)	0.000	0.000	0.000	0.000	0.000	0.000
sign0 at the source (m)	0.000	0.000	0.000	0.000	0.000	0.000
ambient pressure (atm)	-99.9	-99.9	-99.9	-99.9	-99.9	-99.9
relative humidity (%)	-99.9	-99.9	-99.9	-99.9	-99.9	-99.9
temperature at level #1 (K)	285.15	285.15	285.15	285.15	285.15	285.15
measuring height for temperature #1 (m)	1.40	1.40	1.40	1.40	1.40	1.40
temperature at level #2 (K)	284.75	284.75	284.75	284.75	284.75	284.75
measuring height for temperature #2 (m)	16.50	16.50	16.50	16.50	16.50	16.50
wind speed (m/s) at a tower	0.30	0.30	0.30	0.30	0.30	3.30
measuring height for wind data (m)	3.70	3.70	3.70	3.70	3.70	3.30
domain-averaged wind speed (m/s)	0.30	0.30	0.30	0.30	0.30	33.0
domain-averaged wind direction (deg)	346.0	342.0	335.0	338.0	338.0	-99.90
domain-averaged sigma-u (m/s)	-99.90	-99.90	-99.90	-99.90	-99.90	16.00
domain-averaged sigma-theta (deg)	13.20	11.10	16.30	13.30	10.30	-99.90
domain-averaged sigma-phi (deg)	-99.90	-99.90	-99.90	-99.90	-99.90	3.70
measuring ht for domain-avg wind speed (m)	3.70	3.70	3.70	3.70	3.70	2820.0
averaging time for domain-avg data (s)	1800.0	1800.0	2820.0	2820.0	2820.0	-99.900
wind speed power law exponent	-99.900	-99.900	-99.900	-99.900	-99.900	0.2000
surface roughness (m)	0.2000	0.2000	0.2000	0.2000	0.2000	-99.900
friction velocity (m)	-99.900	-99.900	-99.900	-99.900	-99.900	-99.9000
Inverse Monin-Obukhov length (1/m)	-99.9000	-99.9000	-99.9000	-99.9000	-99.9000	0.30
albedo	0.30	0.30	0.30	0.30	0.30	0.20
moisture availability	0.20	0.20	0.20	0.20	0.20	5.00
Bowen ratio	5.00	5.00	5.00	5.00	5.00	-99.9
mixing height (m)	-99.9	-99.9	-99.9	-99.9	-99.9	37.5
cloud cover (%)	0.0	0.0	0.0	100.0	100.0	-99.9
P-G stability class	-99	-99	-99	-99	-99	2820.0
averaging time for concentration (s)	2820.0	2820.0	2820.0	2820.0	2820.0	4.57
suggested receptor height (m)	4.57	4.57	4.57	4.57	4.57	2
no. of distances downwind	2	2	2	2	2	2301.0
distances downwind (m)	2301.0	2301.0	2301.0	2301.0	2301.0	1.430E-02
concentration (mg/m**3)	3.390E-04	4.430E-03	4.430E-03	4.430E-03	4.430E-03	-9.90E-01
cross-wind integrated conc. (mg/m**2)	-9.90E-01	-9.90E-01	-9.90E-01	-9.90E-01	-9.90E-01	-99.90
sigma-y (m)	-99.90	-99.90	-99.90	-99.90	-99.90	5665.0
distances downwind (m)	5665.0	5665.0	5665.0	5665.0	5665.0	7.220E-04
concentration (mg/m**3)	2.170E-03	2.060E-04	7.010E-04	6.970E-04	7.000E-05	-99.90E-01
cross-wind integrated conc. (mg/m**2)	-9.90E-01	-9.90E-01	-9.90E-01	-9.90E-01	-9.90E-01	-99.90
sigma-y (m)	-99.90	-99.90	-99.90	-99.90	-99.90	0
no. of lines-of-sight	0	0	0	0	0	0

Dry Gulch, Course D
12 : number of trials included in DOA
8 : time zone designation
34.50 : latitude (deg)
120.50 : longitude (deg)

dgd1	dgd2	dgd3	dgd4	dgd5	dgd6	dgd7	dgd8	dgd9	dgd10	dgd11	dgd12	trial ID
6	6	6	6	6	6	6	6	6	6	6	6	7 : month
14	15	20	22	24	27	27	29	29	5	6	7	7 : day
1961	1961	1961	1961	1961	1961	1961	1961	1961	1961	1961	1961	1961 : year
10	19	19	19	19	14	19	16	25	9	7	8	8 : hour
45	5	5	5	5	50	28	17	25	45	42	8	8 : minute
1	1	1	1	1	1	1	1	1	1	1	1	1 : no. of sources
0.0	0.0	0.0	0.0	0.0	0.0	0.0	0.0	0.0	0.0	0.0	0.0	0.0 : y-coord. of source (m)
0.0	0.0	0.0	0.0	0.0	0.0	0.0	0.0	0.0	0.0	0.0	0.0	0.0 : y-coord. of source (m)
2.50	2.50	2.50	2.50	2.50	2.50	2.50	2.50	2.50	2.50	2.50	2.50	2.50 : source elevation (m)
1.400	1.400	1.400	1.400	1.400	1.400	1.400	1.400	1.400	1.400	1.400	1.400	1.400 : emission rate (g/s)
1800.0	1800.0	1800.0	1800.0	1800.0	1800.0	1800.0	1800.0	1800.0	1800.0	1800.0	1800.0	1800.0 : total mass emitted (kg)
-99.9	-99.9	-99.9	-99.9	-99.9	-99.9	-99.9	-99.9	-99.9	-99.9	-99.9	-99.9	0.000 : sign0 at the source (m)
0.000	0.000	0.000	0.000	0.000	0.000	0.000	0.000	0.000	0.000	0.000	0.000	0.000 : sign0 at the source (m)
0.000	0.000	0.000	0.000	0.000	0.000	0.000	0.000	0.000	0.000	0.000	0.000	0.000 : sign0 at the source (m)
0.000	0.000	0.000	0.000	0.000	0.000	0.000	0.000	0.000	0.000	0.000	0.000	0.000 : sign0 at the source (m)
-99.9	-99.9	-99.9	-99.9	-99.9	-99.9	-99.9	-99.9	-99.9	-99.9	-99.9	-99.9	0.000 : ambient pressure (atm)
-99.9	-99.9	-99.9	-99.9	-99.9	-99.9	-99.9	-99.9	-99.9	-99.9	-99.9	-99.9	0.000 : relative humidity (%)
293.15	293.15	293.15	293.15	293.15	293.15	293.15	293.15	293.15	293.15	293.15	293.15	293.15 : temperature at level #1 (K)
1.80	1.80	1.80	1.80	1.80	1.80	1.80	1.80	1.80	1.80	1.80	1.80	1.80 : measuring height for temperature #1 (m)
293.25	293.25	293.25	293.25	293.25	293.25	293.25	293.25	293.25	293.25	293.25	293.25	293.25 : temperature at level #2 (K)
16.50	16.50	16.50	16.50	16.50	16.50	16.50	16.50	16.50	16.50	16.50	16.50	16.50 : measuring height for temperature #2 (m)
2.40	2.40	2.40	2.40	2.40	2.40	2.40	2.40	2.40	2.40	2.40	2.40	2.40 : wind speed (m/s) at a tower
3.70	3.70	3.70	3.70	3.70	3.70	3.70	3.70	3.70	3.70	3.70	3.70	3.70 : measuring height for wind data (m)
2.90	2.90	2.90	2.90	2.90	2.90	2.90	2.90	2.90	2.90	2.90	2.90	2.90 : domain-averaged wind speed (m/s)
287.0	287.0	287.0	287.0	287.0	287.0	287.0	287.0	287.0	287.0	287.0	287.0	287.0 : domain-averaged wind direction (deg)
-99.90	-99.90	-99.90	-99.90	-99.90	-99.90	-99.90	-99.90	-99.90	-99.90	-99.90	-99.90	20.40 : domain-averaged sigma-u (m/s)
13.40	13.40	13.40	13.40	13.40	13.40	13.40	13.40	13.40	13.40	13.40	13.40	20.40 : domain-averaged sigma-theta (deg)
-99.90	-99.90	-99.90	-99.90	-99.90	-99.90	-99.90	-99.90	-99.90	-99.90	-99.90	-99.90	-99.90 : domain-averaged sigma-phi (deg)
3.70	3.70	3.70	3.70	3.70	3.70	3.70	3.70	3.70	3.70	3.70	3.70	3.70 : measuring ht for domain-avg wind speed (m)
2820.0	2820.0	2820.0	2820.0	2820.0	2820.0	2820.0	2820.0	2820.0	2820.0	2820.0	2820.0	1800.0 : averaging time for domain-avg wind speed (s)
-99.900	-99.900	-99.900	-99.900	-99.900	-99.900	-99.900	-99.900	-99.900	-99.900	-99.900	-99.900	-99.900 : wind speed power law exponent
0.5000	0.5000	0.5000	0.5000	0.5000	0.5000	0.5000	0.5000	0.5000	0.5000	0.5000	0.5000	0.5000 : surface roughness (m)
-99.900	-99.900	-99.900	-99.900	-99.900	-99.900	-99.900	-99.900	-99.900	-99.900	-99.900	-99.900	-99.900 : friction velocity (m)
-99.9000	-99.9000	-99.9000	-99.9000	-99.9000	-99.9000	-99.9000	-99.9000	-99.9000	-99.9000	-99.9000	-99.9000	-99.9000 : inverse Monin-Obukhov length (1/m)
0.30	0.30	0.30	0.30	0.30	0.30	0.30	0.30	0.30	0.30	0.30	0.30	0.30 : albedo
0.20	0.20	0.20	0.20	0.20	0.20	0.20	0.20	0.20	0.20	0.20	0.20	0.20 : moisture availability
5.00	5.00	5.00	5.00	5.00	5.00	5.00	5.00	5.00	5.00	5.00	5.00	5.00 : Bowen ratio
-99.9	-99.9	-99.9	-99.9	-99.9	-99.9	-99.9	-99.9	-99.9	-99.9	-99.9	-99.9	-99.9 : mixing height (m)
0.0	0.0	0.0	0.0	0.0	0.0	0.0	0.0	0.0	0.0	0.0	0.0	0.0 : cloud cover (%)
-99	-99	-99	-99	-99	-99	-99	-99	-99	-99	-99	-99	-99 : P-G stability class
1800.0	1800.0	1800.0	1800.0	1800.0	1800.0	1800.0	1800.0	1800.0	1800.0	1800.0	1800.0	1800.0 : averaging time for concentration (s)
4.57	4.57	4.57	4.57	4.57	4.57	4.57	4.57	4.57	4.57	4.57	4.57	4.57 : suggested receptor height (m)
853.0	853.0	853.0	853.0	853.0	853.0	853.0	853.0	853.0	853.0	853.0	853.0	853.0 : no. of distances downwind (m)
1.340E-02	2.720E-02	1.020E-02	4.800E-03	4.740E-03	1.820E-03	7.610E-03	4.670E-03	3.580E-02	2.730E-03	5.210E-03	1.260E-02	1.260E-02 : concentration (mg/m**3)
-9.990E+01	-9.990E+01	-9.990E+01	-9.990E+01	-9.990E+01	-9.990E+01	-9.990E+01	-9.990E+01	-9.990E+01	-9.990E+01	-9.990E+01	-9.990E+01	-9.990E+01 : cross-wind integrated conc. (mg/m**2)
-99.90	-99.90	-99.90	-99.90	-99.90	-99.90	-99.90	-99.90	-99.90	-99.90	-99.90	-99.90	-99.90 : sigma-y (m)
1500.0	1500.0	1500.0	1500.0	1500.0	1500.0	1500.0	1500.0	1500.0	1500.0	1500.0	1500.0	1500.0 : distances downwind (m)
8.360E-03	1.270E-02	3.380E-03	9.770E-04	1.340E-03	5.630E-04	2.750E-03	1.570E-03	1.450E-02	6.120E-04	1.780E-03	4.780E-03	4.780E-03 : concentration (mg/m**3)
-9.990E+01	-9.990E+01	-9.990E+01	-9.990E+01	-9.990E+01	-9.990E+01	-9.990E+01	-9.990E+01	-9.990E+01	-9.990E+01	-9.990E+01	-9.990E+01	-9.990E+01 : cross-wind integrated conc. (mg/m**2)
-99.90	-99.90	-99.90	-99.90	-99.90	-99.90	-99.90	-99.90	-99.90	-99.90	-99.90	-99.90	-99.90 : sigma-y (m)
4715.0	4715.0	4715.0	4715.0	4715.0	4715.0	4715.0	4715.0	4715.0	4715.0	4715.0	4715.0	4715.0 : distances downwind (m)
5.080E-04	3.200E-04	4.760E-04	5.300E-04	1.350E-03	2.290E-04	3.510E-04	2.020E-04	1.220E-03	9.940E-05	5.390E-05	3.010E-04	3.010E-04 : concentration (mg/m**3)
-9.990E+01	-9.990E+01	-9.990E+01	-9.990E+01	-9.990E+01	-9.990E+01	-9.990E+01	-9.990E+01	-9.990E+01	-9.990E+01	-9.990E+01	-9.990E+01	-9.990E+01 : cross-wind integrated conc. (mg/m**2)
-99.90	-99.90	-99.90	-99.90	-99.90	-99.90	-99.90	-99.90	-99.90	-99.90	-99.90	-99.90	-99.90 : sigma-y (m)
0	0	0	0	0	0	0	0	0	0	0	0	0 : no. of lines-of-sight

Dry catch, Course D

12 : number of trials included in DOA

11 : time zone designation

10 : latitude (deg)

9 : longitude (deg)

8 : day

7 : month

6 : year

5 : hour

4 : minute

3 : no. of sources

2 : x-coord. of source (m)

1 : y-coord. of source (m)

0 : source elevation (m)

-1 : emission rate (g/s)

-2 : emission duration (s)

-3 : total mass emitted (kg)

-4 : signal at the source (m)

-5 : signal at the source (m)

-6 : signal at the source (m)

-7 : ambient pressure (atm)

-8 : relative humidity (%)

-9 : temperature at level #1 (K)

-10 : measuring height for temperature #1 (m)

-11 : temperature at level #2 (K)

-12 : measuring height for temperature #2 (m)

-13 : wind speed (m/s) at a tower

-14 : measuring height for wind data (m)

-15 : domain-averaged wind speed (m/s)

-16 : domain-averaged wind direction (deg)

-17 : domain-averaged sigma-u (m/s)

-18 : domain-averaged sigma-theta (deg)

-19 : measuring ht for domain-avg wind speed (m)

-20 : averaging time for domain-avg data (s)

-21 : wind speed power law exponent

-22 : surface roughness (m)

-23 : friction velocity (m)

-24 : inverse Monin-Obukhov length (1/m)

-25 : albedo

-26 : moisture availability

-27 : Bowen ratio

-28 : mixing height (m)

-29 : cloud cover (%)

-30 : p-g stability class

-31 : averaging time for concentration (s)

-32 : suggested receptor height (m)

-33 : no. of distances downwind

-34 : distances downwind (m)

-35 : concentration (mg/m**3)

-36 : cross-wind integrated conc. (mg/m**2)

-37 : sigma-y (m)

-38 : distances downwind (m)

-39 : concentration (mg/m**3)

-40 : cross-wind integrated conc. (mg/m**2)

-41 : sigma-y (m)

-42 : distances downwind (m)

-43 : concentration (mg/m**3)

-44 : cross-wind integrated conc. (mg/m**2)

-45 : sigma-y (m)

-46 : no. of lines-of-sight

34.50	12	11	10	9	8	7	6	5	4	3	2	1	0	-1	-2	-3	-4	-5	-6	-7	-8	-9	-10	-11	-12	-13	-14	-15	-16	-17	-18	-19	-20	-21	-22	-23	-24	-25	-26	-27	-28	-29	-30	-31	-32	-33	-34	-35	-36	-37	-38	-39	-40	-41	-42	-43	-44	-45	-46
170.50	12	11	10	9	8	7	6	5	4	3	2	1	0	-1	-2	-3	-4	-5	-6	-7	-8	-9	-10	-11	-12	-13	-14	-15	-16	-17	-18	-19	-20	-21	-22	-23	-24	-25	-26	-27	-28	-29	-30	-31	-32	-33	-34	-35	-36	-37	-38	-39	-40	-41	-42	-43	-44	-45	-46
170.50	12	11	10	9	8	7	6	5	4	3	2	1	0	-1	-2	-3	-4	-5	-6	-7	-8	-9	-10	-11	-12	-13	-14	-15	-16	-17	-18	-19	-20	-21	-22	-23	-24	-25	-26	-27	-28	-29	-30	-31	-32	-33	-34	-35	-36	-37	-38	-39	-40	-41	-42	-43	-44	-45	-46
170.50	12	11	10	9	8	7	6	5	4	3	2	1	0	-1	-2	-3	-4	-5	-6	-7	-8	-9	-10	-11	-12	-13	-14	-15	-16	-17	-18	-19	-20	-21	-22	-23	-24	-25	-26	-27	-28	-29	-30	-31	-32	-33	-34	-35	-36	-37	-38	-39	-40	-41	-42	-43	-44	-45	-46
170.50	12	11	10	9	8	7	6	5	4	3	2	1	0	-1	-2	-3	-4	-5	-6	-7	-8	-9	-10	-11	-12	-13	-14	-15	-16	-17	-18	-19	-20	-21	-22	-23	-24	-25	-26	-27	-28	-29	-30	-31	-32	-33	-34	-35	-36	-37	-38	-39	-40	-41	-42	-43	-44	-45	-46
170.50	12	11	10	9	8	7	6	5	4	3	2	1	0	-1	-2	-3	-4	-5	-6	-7	-8	-9	-10	-11	-12	-13	-14	-15	-16	-17	-18	-19	-20	-21	-22	-23	-24	-25	-26	-27	-28	-29	-30	-31	-32	-33	-34	-35	-36	-37	-38	-39	-40	-41	-42	-43	-44	-45	-46
170.50	12	11	10	9	8	7	6	5	4	3	2	1	0	-1	-2	-3	-4	-5	-6	-7	-8	-9	-10	-11	-12	-13	-14	-15	-16	-17	-18	-19	-20	-21	-22	-23	-24	-25	-26	-27	-28	-29	-30	-31	-32	-33	-34	-35	-36	-37	-38	-39	-40	-41	-42	-43	-44	-45	-46
170.50	12	11	10	9	8	7	6	5	4	3	2	1	0	-1	-2	-3	-4	-5	-6	-7	-8	-9	-10	-11	-12	-13	-14	-15	-16	-17	-18	-19	-20	-21	-22	-23	-24	-25	-26	-27	-28	-29	-30	-31	-32	-33	-34	-35	-36	-37	-38	-39	-40	-41	-42	-43	-44	-45	-46
170.50	12	11	10	9	8	7	6	5	4	3	2	1	0	-1	-2	-3	-4	-5	-6	-7	-8	-9	-10	-11	-12	-13	-14	-15	-16	-17	-18	-19	-20	-21	-22	-23	-24	-25	-26	-27	-28	-29	-30	-31	-32	-33	-34	-35	-36	-37	-38	-39	-40	-41	-42	-43	-44	-45	-46
170.50	12	11	10	9	8	7	6	5	4	3	2	1	0	-1	-2	-3	-4	-5	-6	-7	-8	-9	-10	-11	-12	-13	-14	-15	-16	-17	-18	-19	-20	-21	-22	-23	-24	-25	-26	-27	-28	-29	-30	-31	-32	-33	-34	-35	-36	-37	-38	-39	-40	-41	-42	-43	-44	-45	-46
170.50	12	11	10	9	8	7	6	5	4	3	2	1	0	-1	-2	-3	-4	-5	-6	-7	-8	-9	-10	-11	-12	-13	-14	-15	-16	-17	-18	-19	-20	-21	-22	-23	-24	-25	-26	-27	-28	-29	-30	-31	-32	-33	-34	-35	-36	-37	-38	-39	-40	-41	-42	-43	-44	-45	-46
170.50	12	11	10	9	8	7	6	5	4	3	2	1	0	-1	-2	-3	-4	-5	-6	-7	-8	-9	-10	-11	-12	-13	-14	-15	-16	-17	-18	-19	-20	-21	-22	-23	-24	-25	-26	-27	-28	-29	-30	-31	-32	-33	-34	-35	-36	-37	-38	-39	-40	-41	-42	-43	-44	-45	-46
170.50	12	11	10	9	8	7	6	5	4	3	2	1	0	-1	-2	-3	-4	-5	-6	-7	-8	-9	-10	-11	-12	-13	-14	-15	-16	-17	-18	-19	-20	-21	-22	-23	-24	-25	-26	-27	-28	-29	-30	-31	-32	-33	-34	-35	-36	-37	-38	-39	-40	-41	-42	-43	-44	-45	-46
170.50	12	11	10	9	8	7	6	5	4	3	2	1	0	-1	-2	-3	-4	-5	-6	-7	-8	-9	-10	-11	-12	-13	-14	-15	-16	-17	-18	-19	-20	-21	-22	-23	-24	-25	-26	-27	-28	-29	-30	-31	-32	-33	-34	-35	-36	-37	-38	-39	-40	-41	-42	-43	-44	-45	-46
170.50	12	11	10	9	8	7	6	5	4	3	2	1	0	-1	-2	-3	-4	-5	-6	-7	-8	-9	-10	-11	-12	-13	-14	-15	-16	-17	-18	-19	-20	-21	-22	-23	-24	-25	-26	-27	-28	-29	-30	-31	-32	-33	-34	-35	-36	-37	-38	-39	-40	-41	-42	-43	-44	-45	-46
170.50	12	11	10	9	8	7	6	5	4	3	2	1	0	-1	-2	-3	-4	-5	-6	-7	-8	-9	-10	-11	-12	-13	-14	-15	-16	-17	-18	-19	-20	-21	-22	-23	-24	-25	-26	-27	-28	-29	-30	-31	-32	-33	-34	-35	-36	-37	-38	-39	-40	-41	-42	-43	-44	-45	-46
170.50	12	11	10	9	8	7	6	5	4	3	2	1	0	-1	-2	-3	-4	-5	-6	-7	-8	-9	-10	-11	-12	-13	-14	-15	-16	-17	-18	-19	-20	-21	-22	-23	-24	-25	-26	-27	-28	-29	-30	-31	-32	-33	-34	-35	-36	-37	-38	-39	-40	-41	-42	-43	-44	-45	-46
170.50	12	11	10	9	8	7	6	5	4	3	2	1	0	-1	-2	-3	-4	-5	-6	-7	-8	-9	-10	-11	-12	-13	-14	-15	-16	-17	-18	-19	-20	-21	-22	-23	-24	-25	-26	-27	-28	-29	-30	-31	-32	-33	-34	-35	-36	-37	-38	-39	-40	-41	-42	-43	-44	-45	-46
170.50	12	11	10	9	8	7	6	5	4	3	2	1	0	-1	-2	-3	-4	-5	-6	-7	-8	-9	-10	-11	-12	-13	-14	-15	-16	-17	-18	-19	-20	-21	-22	-23	-24	-25	-26	-27	-28	-29	-30	-31	-32	-33	-34	-35	-36	-37	-38	-39	-40	-41	-42	-43	-44	-45	-46
170.50	12	11	10	9	8	7	6	5	4	3	2	1	0	-1	-2	-3	-4	-5	-6	-7	-8	-9	-10	-11	-12	-13	-14	-15	-16	-17	-18	-19	-20	-21	-22	-23	-24	-25	-26	-27	-28	-29	-30	-31	-32	-33	-34	-35	-36	-37	-38	-39	-40	-41	-42	-43	-44	-45	-46
170.50	12	11	10	9	8	7	6	5	4	3	2	1	0	-1	-2	-3	-4	-5	-6	-7	-8	-9	-10	-11	-12	-13	-14	-15	-16	-17	-18	-19	-20	-21	-22	-23	-24	-25	-26	-27	-28	-29	-30	-31	-32	-33	-34	-35	-36	-37	-38	-39	-40	-41	-42	-43	-44	-45	-46
170.50	12	11	10	9	8	7	6	5	4	3	2	1	0	-1	-2	-3	-4	-5	-6	-7	-8	-9	-10	-11	-12	-13	-14	-15	-16	-17	-18	-19	-20	-21	-22	-23	-24	-25	-26	-27	-28	-29	-30	-31	-32	-33	-34	-35	-36	-37	-38	-39	-40	-41	-42	-43	-44	-45	-46
170.50	12	11	10	9	8	7	6	5	4	3	2	1	0	-1	-2	-3	-4	-5	-6	-7	-8	-9	-10	-11	-12	-13	-14	-15	-16	-17	-18	-19	-20	-21	-22	-23	-24	-25	-26	-27	-28	-29	-30	-31	-32	-33	-34	-35	-36	-37	-38	-39	-40	-41	-42	-43	-44	-45	-46
170.50	12	11	10	9	8	7	6	5	4	3	2	1	0	-1	-2	-3	-4	-5	-6	-7	-8	-9	-10	-11	-12	-13	-14	-15	-1																														

Dry Gulch, Course D

12 : number of trials included in DDA

8 : time zone designation

34.50 : latitude (deg)

120.50 : longitude (deg)

deg31 : deg38

deg39 : deg40

deg41 : deg42

deg43 : deg44

deg45 : deg46

deg47 : deg48

deg49 : deg50

deg51 : deg52

deg53 : deg54

deg55 : deg56

deg57 : deg58

deg59 : deg60

deg61 : deg62

deg63 : deg64

deg65 : deg66

deg67 : deg68

deg69 : deg70

deg71 : deg72

deg73 : deg74

deg75 : deg76

deg77 : deg78

deg79 : deg80

deg81 : deg82

deg83 : deg84

deg85 : deg86

deg87 : deg88

deg89 : deg90

deg91 : deg92

deg93 : deg94

deg95 : deg96

deg97 : deg98

deg99 : deg100

deg101 : deg102

deg103 : deg104

deg105 : deg106

deg107 : deg108

deg109 : deg110

deg111 : deg112

deg113 : deg114

deg115 : deg116

deg117 : deg118

deg119 : deg120

deg121 : deg122

deg123 : deg124

deg125 : deg126

deg127 : deg128

deg129 : deg130

deg131 : deg132

deg133 : deg134

deg135 : deg136

deg137 : deg138

deg139 : deg140

deg141 : deg142

deg143 : deg144

deg145 : deg146

deg147 : deg148

deg149 : deg150

deg151 : deg152

deg153 : deg154

deg155 : deg156

deg157 : deg158

deg159 : deg160

deg161 : deg162

deg163 : deg164

deg165 : deg166

deg167 : deg168

deg169 : deg170

deg171 : deg172

deg173 : deg174

deg175 : deg176

deg177 : deg178

deg179 : deg180

deg181 : deg182

deg183 : deg184

deg185 : deg186

deg187 : deg188

deg189 : deg190

deg191 : deg192

deg193 : deg194

deg195 : deg196

deg197 : deg198

deg199 : deg200

deg201 : deg202

deg203 : deg204

deg205 : deg206

deg207 : deg208

deg209 : deg210

deg211 : deg212

deg213 : deg214

deg215 : deg216

deg217 : deg218

deg219 : deg220

deg221 : deg222

deg223 : deg224

deg225 : deg226

deg227 : deg228

deg229 : deg230

deg231 : deg232

deg233 : deg234

deg235 : deg236

deg237 : deg238

deg239 : deg240

deg241 : deg242

deg243 : deg244

deg245 : deg246

deg247 : deg248

deg249 : deg250

Dry Gulch, Course D

1 : number of trials included in DOA
 2 : time zone designation
 34.50 : latitude (deg)
 120.50 : longitude (deg)
 dgd49 : trial ID
 6 : month
 26 : day
 1962 : year
 17 : hour
 45 : minute
 1 : no. of sources
 0.0 : x-coord. of source (m)
 0.0 : y-coord. of source (m)
 2.50 : source elevation (m)
 1.130 : emission rate (g/s)
 1800.0 : emission duration (s)
 -99.9 : total mass emitted (kg)
 0.000 : signal at the source (m)
 0.000 : signal at the source (m)
 -99.9 : ambient pressure (atm)
 -99.9 : relative humidity (%)
 281.15 : temperature at level #1 (K)
 1.80 : measuring height for temperature #1 (m)
 281.95 : temperature at level #2 (K)
 16.50 : measuring height for temperature #2 (m)
 16.50 : wind speed (m/s) at a tower
 3.20 : measuring height for wind data (m)
 3.20 : domain-averaged wind speed (m/s)
 317.0 : domain-averaged wind direction (deg)
 -99.90 : domain-averaged sigma-u (m/s)
 17.70 : domain-averaged sigma-theta (deg)
 -99.90 : domain-averaged sigma-phi (deg)
 1.70 : measuring ht for domain-avg wind speed (m)
 2820.0 : averaging time for domain-avg data (s)
 -99.900 : wind speed power law exponent
 0.5000 : surface roughness (m)
 -99.900 : friction velocity (m)
 -99.9000 : inverse Monin-Obukhov length (1/m)
 0.30 : albedo
 0.20 : moisture availability
 5.00 : Bowen ratio
 -99.9 : mixing height (m)
 0.0 : cloud cover (%)
 -99 : P-G stability class
 2820.0 : averaging time for concentration (s)
 4.57 : suggested receptor height (m)
 3 : no. of distances downwind
 853.0 : distance downwind (m)
 3.520E-03 : concentration (mg/m**3)
 -9.990E+01 : cross-wind integrated conc. (mg/m**2)
 -99.90 : sigma-y (m)
 1500.0 : distance downwind (m)
 3.850E-04 : concentration (mg/m**3)
 -9.990E+01 : cross-wind integrated conc. (mg/m**2)
 -99.90 : sigma-y (m)
 4715.0 : distance downwind (m)
 1.030E-04 : concentration (mg/m**3)
 -9.990E+01 : cross-wind integrated conc. (mg/m**2)
 -99.90 : sigma-y (m)
 0 : no. of lines-of-sight

Ocean Breeze

12 : number of trials included in DDA

5 : time zone designation

28.40 : latitude (deg)

80.70 : longitude (deg)

ob28 : ob30

ob31

ob32

ob33

ob34

ob35

ob36

ob37

ob38

ob39

ob40

trial ID

1 : month

26 : day

1962 : year

16 : hour

22 : minute

1 : no. of sources

0.0 : x-coord. of source (m)

0.0 : y-coord. of source (m)

2.50 : source elevation (m)

1.600 : emission rate (g/s)

1800.0 : emission duration (s)

-99.9 : total mass emitted (kg)

0.000 : sigd0 at the source (m)

0.000 : sigy0 at the source (m)

-99.9 : ambient pressure (atm)

-99.9 : relative humidity (%)

292.65 : temperature at level #1 (K)

1.80 : measuring height for temperature #1 (m)

292.15 : temperature at level #2 (K)

16.50 : measuring height for temperature #2 (m)

2.00 : wind speed (m/s) at a tower

3.70 : measuring height for wind data (m)

2.0 : domain-averaged wind speed (m/s)

142.0 : domain-averaged wind direction (deg)

-99.90 : domain-averaged sigma-u (m/s)

12.40 : domain-averaged sigma-theta (deg)

-99.90 : domain-averaged sigma-phi (deg)

3.70 : measuring ht for domain-avg wind speed (m)

2820.0 : averaging time for domain-avg wind speed (s)

-99.9000 : surface roughness (m)

0.1000 : friction velocity (m)

-99.9000 : inverse Monin-Obukhov length (1/m)

0.18 : albedo

0.50 : moisture availability

0.50 : Bowen ratio

-99.9 : mixing height (m)

0.0 : cloud cover (%)

-99 : P-G stability class

2820.0 : averaging time for concentration (s)

4.57 : suggested receptor height (m)

3 : no. of distances downwind

1200.0 : distances downwind (m)

3.350E-02 : concentration (mg/m**3)

-9.990E-01 : cross-wind integrated conc. (mg/m**2)

-99.90 : sigma-y (m)

2400.0 : distances downwind (m)

5.310E-03 : concentration (mg/m**3)

-9.990E-01 : cross-wind integrated conc. (mg/m**2)

-99.90 : sigma-y (m)

4800.0 : distances downwind (m)

-9.990E-01 : concentration (mg/m**3)

-9.990E-01 : cross-wind integrated conc. (mg/m**2)

-99.90 : sigma-y (m)

0 : no. of lines-of-sight

12 : number of trials included in DOA

5 : time zone designation

28.40 : latitude (deg)

80.70 : longitude (deg)

ob41 : ob42 ob43

ob44

ob45

ob46

ob47

ob48

ob49

ob50

ob51

ob52

ob53

ob54

ob55

ob56

ob57

ob58

ob59

ob60

ob61

ob62

ob63

ob64

ob65

ob66

ob67

ob68

ob69

ob70

ob71

ob72

ob73

ob74

ob75

ob76

ob77

ob78

ob79

ob80

ob81

ob82

ob83

ob84

ob85

ob86

ob87

ob88

ob89

ob90

ob91

ob92

ob93

ob94

ob95

ob96

ob97

ob98

ob99

ob100

ob101

ob102

ob103

ob104

ob105

ob106

ob107

ob108

ob109

ob110

ob111

ob112

ob113

ob114

ob115

ob116

ob117

ob118

ob119

ob120

ob121

ob122

ob123

ob124

ob125

ob126

ob127

ob128

ob129

ob130

Ocean Breeze

12 : Number of trials included in DUA											
5 : time zone designation											
28.40 : latitude (deg)	31.40 : longitude (deg)	34.40 : trial ID	37.40 : trial ID	40.40 : trial ID	43.40 : trial ID	46.40 : trial ID	49.40 : trial ID	52.40 : trial ID	55.40 : trial ID	58.40 : trial ID	61.40 : trial ID
80.70 : latitude (deg)	83.70 : longitude (deg)	86.70 : trial ID	89.70 : trial ID	92.70 : trial ID	95.70 : trial ID	98.70 : trial ID	101.70 : trial ID	104.70 : trial ID	107.70 : trial ID	110.70 : trial ID	113.70 : trial ID
ob54	ob55	ob56	ob57	ob58	ob60	ob62	ob63	ob64	ob65	ob66	trial ID
3	3	3	3	3	3	3	3	3	3	3	3
10	13	13	14	14	16	16	17	17	20	22	month
162	162	162	162	162	162	162	162	162	162	162	day
15	15	16	13	15	15	17	13	14	15	15	hour
38	44	33	46	20	5	53	42	51	40	51	minute
1	1	1	1	1	1	1	1	1	1	1	no. of sources
0.0	0.0	0.0	0.0	0.0	0.0	0.0	0.0	0.0	0.0	0.0	x-coord. of source (m)
0.0	0.0	0.0	0.0	0.0	0.0	0.0	0.0	0.0	0.0	0.0	y-coord. of source (m)
2.50	2.50	2.50	2.50	2.50	2.50	2.50	2.50	2.50	2.50	2.50	source elevation (m)
1.661	1.661	1.661	1.661	1.661	1.661	1.661	1.661	1.661	1.661	1.661	emission rate (g/s)
1800.0	1800.0	1800.0	1800.0	1800.0	1800.0	1800.0	1800.0	1800.0	1800.0	1800.0	total mass emitted (kg)
-99.9	-99.9	-99.9	-99.9	-99.9	-99.9	-99.9	-99.9	-99.9	-99.9	-99.9	emission duration (s)
0.000	0.000	0.000	0.000	0.000	0.000	0.000	0.000	0.000	0.000	0.000	sigma-0 at the source (m)
0.000	0.000	0.000	0.000	0.000	0.000	0.000	0.000	0.000	0.000	0.000	sigma-0 at the source (m)
0.000	0.000	0.000	0.000	0.000	0.000	0.000	0.000	0.000	0.000	0.000	sigma-0 at the source (m)
-99.9	-99.9	-99.9	-99.9	-99.9	-99.9	-99.9	-99.9	-99.9	-99.9	-99.9	ambient pressure (atm)
-99.9	-99.9	-99.9	-99.9	-99.9	-99.9	-99.9	-99.9	-99.9	-99.9	-99.9	relative humidity (%)
294.65	294.65	294.65	294.65	294.65	294.65	294.65	294.65	294.65	294.65	294.65	temperature at level #1 (K)
1.80	1.80	1.80	1.80	1.80	1.80	1.80	1.80	1.80	1.80	1.80	measuring height for temperature #1 (m)
294.05	294.05	294.05	294.05	294.05	294.05	294.05	294.05	294.05	294.05	294.05	temperature at level #2 (K)
16.50	16.50	16.50	16.50	16.50	16.50	16.50	16.50	16.50	16.50	16.50	measuring height for temperature #2 (m)
3.20	3.20	3.20	3.20	3.20	3.20	3.20	3.20	3.20	3.20	3.20	wind speed (m/s) at a tower
3.20	3.20	3.20	3.20	3.20	3.20	3.20	3.20	3.20	3.20	3.20	measuring height for wind data (m)
3.20	3.20	3.20	3.20	3.20	3.20	3.20	3.20	3.20	3.20	3.20	domain-averaged wind speed (m/s)
24.0	24.0	24.0	24.0	24.0	24.0	24.0	24.0	24.0	24.0	24.0	domain-averaged wind direction (deg)
-99.90	-99.90	-99.90	-99.90	-99.90	-99.90	-99.90	-99.90	-99.90	-99.90	-99.90	domain-averaged sigma-u (m/s)
10.70	10.70	10.70	10.70	10.70	10.70	10.70	10.70	10.70	10.70	10.70	domain-averaged sigma-theta (deg)
-99.90	-99.90	-99.90	-99.90	-99.90	-99.90	-99.90	-99.90	-99.90	-99.90	-99.90	domain-averaged sigma-phi (deg)
3.70	3.70	3.70	3.70	3.70	3.70	3.70	3.70	3.70	3.70	3.70	measuring ht for domain-avg wind speed (m)
2820.0	2820.0	2820.0	2820.0	2820.0	2820.0	2820.0	2820.0	2820.0	2820.0	2820.0	averaging time for domain-avg wind speed (s)
-99.900	-99.900	-99.900	-99.900	-99.900	-99.900	-99.900	-99.900	-99.900	-99.900	-99.900	wind speed power law exponent
0.1000	0.1000	0.1000	0.1000	0.1000	0.1000	0.1000	0.1000	0.1000	0.1000	0.1000	surface roughness (m)
-99.900	-99.900	-99.900	-99.900	-99.900	-99.900	-99.900	-99.900	-99.900	-99.900	-99.900	friction velocity (m)
-99.9000	-99.9000	-99.9000	-99.9000	-99.9000	-99.9000	-99.9000	-99.9000	-99.9000	-99.9000	-99.9000	inverse Monin-Obukhov length (1/m)
0.18	0.18	0.18	0.18	0.18	0.18	0.18	0.18	0.18	0.18	0.18	albedo
0.50	0.50	0.50	0.50	0.50	0.50	0.50	0.50	0.50	0.50	0.50	moisture availability
0.50	0.50	0.50	0.50	0.50	0.50	0.50	0.50	0.50	0.50	0.50	Bowen ratio
-99.9	-99.9	-99.9	-99.9	-99.9	-99.9	-99.9	-99.9	-99.9	-99.9	-99.9	mixing height (m)
100.0	100.0	100.0	100.0	100.0	100.0	100.0	100.0	100.0	100.0	100.0	cloud cover (%)
-99	-99	-99	-99	-99	-99	-99	-99	-99	-99	-99	P-G stability class
2820.0	2820.0	2820.0	2820.0	2820.0	2820.0	2820.0	2820.0	2820.0	2820.0	2820.0	averaging time for concentration (s)
4.57	4.57	4.57	4.57	4.57	4.57	4.57	4.57	4.57	4.57	4.57	suggested receptor height (m)
3	3	3	3	3	3	3	3	3	3	3	no. of distances downwind
1200.0	1200.0	1200.0	1200.0	1200.0	1200.0	1200.0	1200.0	1200.0	1200.0	1200.0	distances downwind (m)
2.570E-02	2.570E-02	2.570E-02	2.570E-02	2.570E-02	2.570E-02	2.570E-02	2.570E-02	2.570E-02	2.570E-02	2.570E-02	concentration (mg/m**3)
-9.990E+01	-9.990E+01	-9.990E+01	-9.990E+01	-9.990E+01	-9.990E+01	-9.990E+01	-9.990E+01	-9.990E+01	-9.990E+01	-9.990E+01	cross-wind integrated conc. (mg/m**2)
-99.90	-99.90	-99.90	-99.90	-99.90	-99.90	-99.90	-99.90	-99.90	-99.90	-99.90	sigma-y (m)
2400.0	2400.0	2400.0	2400.0	2400.0	2400.0	2400.0	2400.0	2400.0	2400.0	2400.0	distances downwind (m)
7.950E-03	7.950E-03	7.950E-03	7.950E-03	7.950E-03	7.950E-03	7.950E-03	7.950E-03	7.950E-03	7.950E-03	7.950E-03	concentration (mg/m**3)
-9.990E+01	-9.990E+01	-9.990E+01	-9.990E+01	-9.990E+01	-9.990E+01	-9.990E+01	-9.990E+01	-9.990E+01	-9.990E+01	-9.990E+01	cross-wind integrated conc. (mg/m**2)
-99.90	-99.90	-99.90	-99.90	-99.90	-99.90	-99.90	-99.90	-99.90	-99.90	-99.90	sigma-y (m)
4800.0	4800.0	4800.0	4800.0	4800.0	4800.0	4800.0	4800.0	4800.0	4800.0	4800.0	distances downwind (m)
-9.990E+01	-9.990E+01	-9.990E+01	-9.990E+01	-9.990E+01	-9.990E+01	-9.990E+01	-9.990E+01	-9.990E+01	-9.990E+01	-9.990E+01	concentration (mg/m**3)
-9.990E+01	-9.990E+01	-9.990E+01	-9.990E+01	-9.990E+01	-9.990E+01	-9.990E+01	-9.990E+01	-9.990E+01	-9.990E+01	-9.990E+01	cross-wind integrated conc. (mg/m**2)
-99.90	-99.90	-99.90	-99.90	-99.90	-99.90	-99.90	-99.90	-99.90	-99.90	-99.90	sigma-y (m)
0	0	0	0	0	0	0	0	0	0	0	no. of lines-of-sight

Ocean breeze

5 : number of trials included in DDA
 24.10 : time zone designation
 80.10 : latitude (deg)
 80.10 : longitude (deg)

ob71	ob68	ob69	ob70	ob71	ob72	ob73	ob74	ob75	trial ID
3	3	3	3	3	3	3	3	3	3
24	24	27	27	28	28	28	30	30	month
1962	1962	1962	1962	1962	1962	1962	1962	1962	day
15	15	18	18	18	16	16	15	15	year
34	34	21	56	20	28	17	18	48	hour
1	1	1	1	1	1	1	1	1	minute
0.0	0.0	0.0	0.0	0.0	0.0	0.0	0.0	0.0	1 : no. of sources
0.0	0.0	0.0	0.0	0.0	0.0	0.0	0.0	0.0	0.0 : x-coord. of source (m)
0.0	0.0	0.0	0.0	0.0	0.0	0.0	0.0	0.0	0.0 : y-coord. of source (m)
2.50	2.50	2.50	2.50	2.50	2.50	2.50	2.50	2.50	2.50 : source elevation (m)
1.661	0.817	1.233	1.256	1.672	1.267	1.267	1.839	1.244	1.244 : emission rate (g/s)
1800.0	1800.0	1800.0	1800.0	1800.0	1800.0	1800.0	1800.0	1800.0	1800.0 : emission duration (s)
-99.9	-99.9	-99.9	-99.9	-99.9	-99.9	-99.9	-99.9	-99.9	-99.9 : total mass emitted (kg)
0.000	0.000	0.000	0.000	0.000	0.000	0.000	0.000	0.000	0.000 : sig0 at the source (m)
0.000	0.000	0.000	0.000	0.000	0.000	0.000	0.000	0.000	0.000 : sig90 at the source (m)
0.000	0.000	0.000	0.000	0.000	0.000	0.000	0.000	0.000	0.000 : sig0 at the source (m)
-99.9	-99.9	-99.9	-99.9	-99.9	-99.9	-99.9	-99.9	-99.9	-99.9 : ambient pressure (atm)
-99.9	-99.9	-99.9	-99.9	-99.9	-99.9	-99.9	-99.9	-99.9	-99.9 : relative humidity (%)
295.85	295.85	295.85	295.85	295.85	295.85	295.85	295.85	295.85	295.85 : temperature at level #1 (K)
1.80	1.80	1.80	1.80	1.80	1.80	1.80	1.80	1.80	1.80 : measuring height for temperature #1 (m)
296.15	296.15	296.15	296.15	296.15	296.15	296.15	296.15	296.15	296.15 : temperature at level #2 (K)
16.50	16.50	16.50	16.50	16.50	16.50	16.50	16.50	16.50	16.50 : measuring height for temperature #2 (m)
2.70	2.70	3.70	3.70	3.70	3.70	3.70	3.70	3.70	3.70 : wind speed (m/s) at a tower
3.70	3.70	3.70	3.70	3.70	3.70	3.70	3.70	3.70	3.70 : measuring height for wind data (m)
64.0	64.0	64.0	64.0	64.0	64.0	64.0	64.0	64.0	64.0 : domain-averaged wind speed (m/s)
-99.90	-99.90	-99.90	-99.90	-99.90	-99.90	-99.90	-99.90	-99.90	-99.90 : domain-averaged wind direction (deg)
16.60	16.60	16.60	16.60	16.60	16.60	16.60	16.60	16.60	16.60 : domain-averaged sigma-u (m/s)
-99.90	-99.90	-99.90	-99.90	-99.90	-99.90	-99.90	-99.90	-99.90	-99.90 : domain-averaged sigma-theta (deg)
3.70	3.70	3.70	3.70	3.70	3.70	3.70	3.70	3.70	3.70 : measuring ht for domain-avg wind speed (m)
2820.0	2820.0	2820.0	2820.0	2820.0	2820.0	2820.0	2820.0	2820.0	2820.0 : averaging time for domain-avg wind speed (s)
-99.900	-99.900	-99.900	-99.900	-99.900	-99.900	-99.900	-99.900	-99.900	-99.900 : wind speed power law exponent
0.1000	0.1000	0.1000	0.1000	0.1000	0.1000	0.1000	0.1000	0.1000	0.1000 : surface roughness (m)
-99.900	-99.900	-99.900	-99.900	-99.900	-99.900	-99.900	-99.900	-99.900	-99.900 : friction velocity (m)
-99.9000	-99.9000	-99.9000	-99.9000	-99.9000	-99.9000	-99.9000	-99.9000	-99.9000	-99.9000 : inverse Monin-Obukhov length (1/m)
0.18	0.18	0.18	0.18	0.18	0.18	0.18	0.18	0.18	0.18 : albedo
0.50	0.50	0.50	0.50	0.50	0.50	0.50	0.50	0.50	0.50 : moisture availability
0.50	0.50	0.50	0.50	0.50	0.50	0.50	0.50	0.50	0.50 : Bowen ratio
-99.9	-99.9	-99.9	-99.9	-99.9	-99.9	-99.9	-99.9	-99.9	-99.9 : mixing height (m)
37.5	37.5	37.5	37.5	37.5	37.5	37.5	37.5	37.5	37.5 : cloud cover (%)
-99	-99	-99	-99	-99	-99	-99	-99	-99	-99 : p-G stability class
2820.0	2820.0	2820.0	2820.0	2820.0	2820.0	2820.0	2820.0	2820.0	2820.0 : averaging time for concentration (s)
4.57	4.57	4.57	4.57	4.57	4.57	4.57	4.57	4.57	4.57 : suggested receptor height (m)
3	3	3	3	3	3	3	3	3	3 : no. of distances downwind
1200.0	1200.0	1200.0	1200.0	1200.0	1200.0	1200.0	1200.0	1200.0	1200.0 : distances downwind (m)
1.490E-02	1.390E-01	1.430E-02	1.450E-02	1.450E-02	1.450E-02	1.450E-02	1.450E-02	1.450E-02	1.450E-02 : concentration (mg/m**3)
-9.990E+01	-9.990E+01	-9.990E+01	-9.990E+01	-9.990E+01	-9.990E+01	-9.990E+01	-9.990E+01	-9.990E+01	-9.990E+01 : cross-wind integrated conc. (mg/m**2)
-99.90	-99.90	-99.90	-99.90	-99.90	-99.90	-99.90	-99.90	-99.90	-99.90 : sigma-y (m)
2400.0	2400.0	2400.0	2400.0	2400.0	2400.0	2400.0	2400.0	2400.0	2400.0 : distances downwind (m)
3.140E-03	3.140E-02	2.600E-03	2.600E-03	2.600E-03	2.600E-03	2.600E-03	2.600E-03	2.600E-03	2.600E-03 : concentration (mg/m**3)
-9.990E+01	-9.990E+01	-9.990E+01	-9.990E+01	-9.990E+01	-9.990E+01	-9.990E+01	-9.990E+01	-9.990E+01	-9.990E+01 : cross-wind integrated conc. (mg/m**2)
-99.90	-99.90	-99.90	-99.90	-99.90	-99.90	-99.90	-99.90	-99.90	-99.90 : sigma-y (m)
4800.0	4800.0	4800.0	4800.0	4800.0	4800.0	4800.0	4800.0	4800.0	4800.0 : distances downwind (m)
-9.990E+01	-9.990E+01	-9.990E+01	-9.990E+01	-9.990E+01	-9.990E+01	-9.990E+01	-9.990E+01	-9.990E+01	-9.990E+01 : concentration (mg/m**3)
-9.990E+01	-9.990E+01	-9.990E+01	-9.990E+01	-9.990E+01	-9.990E+01	-9.990E+01	-9.990E+01	-9.990E+01	-9.990E+01 : cross-wind integrated conc. (mg/m**2)
-99.90	-99.90	-99.90	-99.90	-99.90	-99.90	-99.90	-99.90	-99.90	-99.90 : sigma-y (m)
0	0	0	0	0	0	0	0	0	0 : no. of lines-of-sight

12 : number of trials included in DDA

8 : time zone designation

46.40 : latitude (deg)

119.23 : longitude (deg)

991	992	993	994	995	996	997	998	999	9910	9911	9912	9913	trial ID
6	6	6	6	6	6	6	6	6	6	6	6	6	7 : month
19	28	15	13	16	10	13	13	16	7	21	23	24	7 : day
1959	1959	1959	1959	1959	1959	1959	1959	1959	1959	1959	1959	1959	7 : year
21	21	21	22	23	22	22	22	23	22	22	0	22	30 : minute
28	49	20	17	24	0	0	0	24	0	0	15	30	1 : no. of sources
1	1	1	1	1	1	1	1	1	1	1	1	0.0	0.0 : x-coord. of source (m)
0.0	0.0	0.0	0.0	0.0	0.0	0.0	0.0	0.0	0.0	0.0	0.0	2.50	0.0 : y-coord. of source (m)
2.50	2.50	2.50	2.50	2.50	2.50	2.50	2.50	2.50	2.50	2.50	2.50	1800.0	2.50 : source elevation (m)
0.470	0.861	0.444	0.444	0.444	0.444	0.444	0.444	0.444	0.750	1.322	0.794	1.311	1.311 : emission rate (g/s)
1800.0	1800.0	1800.0	1800.0	1800.0	1800.0	1800.0	1800.0	1800.0	1800.0	1800.0	1800.0	1800.0	1800.0 : total mass emitted (kg)
-99.9	-99.9	-99.9	-99.9	-99.9	-99.9	-99.9	-99.9	-99.9	-99.9	-99.9	-99.9	-99.9	0.000 : signal at the source (m)
0.000	0.000	0.000	0.000	0.000	0.000	0.000	0.000	0.000	0.000	0.000	0.000	0.000	0.000 : signal at the source (m)
0.000	0.000	0.000	0.000	0.000	0.000	0.000	0.000	0.000	0.000	0.000	0.000	0.000	0.000 : ambient pressure (atm)
-99.9	-99.9	-99.9	-99.9	-99.9	-99.9	-99.9	-99.9	-99.9	-99.9	-99.9	-99.9	-99.9	-99.9 : relative humidity (%)
294.15	286.15	293.15	301.15	294.15	299.15	294.15	299.15	293.15	303.15	303.15	303.15	298.15	298.15 : temperature at level #1 (K)
0.90	0.90	0.90	0.90	0.90	0.90	0.90	0.90	0.90	0.90	0.90	0.90	0.90	0.90 : measuring height for temperature #1 (m)
298.95	297.05	296.45	301.95	297.05	300.45	297.05	300.45	296.45	303.35	303.35	303.35	298.65	298.65 : temperature at level #2 (K)
15.20	15.20	15.20	15.20	15.20	15.20	15.20	15.20	15.20	15.20	15.20	15.20	15.20	15.20 : measuring height for temperature #2 (m)
1.50	1.50	1.50	1.50	1.50	1.50	1.50	1.50	1.50	1.50	1.50	1.50	1.50	1.50 : wind speed (m/s) at a tower
3.00	3.00	3.00	3.00	3.00	3.00	3.00	3.00	3.00	3.00	3.00	3.00	3.00	3.00 : measuring height for wind data (m)
1.50	1.50	1.50	1.50	1.50	1.50	1.50	1.50	1.50	1.50	1.50	1.50	1.50	1.50 : domain-averaged wind speed (m/s)
219.0	314.0	304.0	304.0	304.0	304.0	304.0	304.0	319.0	316.0	315.0	329.0	296.0	296.0 : domain-averaged wind direction (deg)
-99.90	-99.90	-99.90	-99.90	-99.90	-99.90	-99.90	-99.90	-99.90	-99.90	-99.90	-99.90	-99.90	-99.90 : domain-averaged sigma-u (m/s)
-99.90	-99.90	-99.90	-99.90	-99.90	-99.90	-99.90	-99.90	-99.90	-99.90	-99.90	-99.90	-99.90	-99.90 : domain-averaged sigma-theta (deg)
-99.90	-99.90	-99.90	-99.90	-99.90	-99.90	-99.90	-99.90	-99.90	-99.90	-99.90	-99.90	-99.90	-99.90 : domain-averaged sigma-phi (deg)
3.00	3.00	3.00	3.00	3.00	3.00	3.00	3.00	3.00	3.00	3.00	3.00	3.00	3.00 : measuring ht for domain-avg wind speed (m)
-99.90	-99.90	-99.90	-99.90	-99.90	-99.90	-99.90	-99.90	-99.90	-99.90	-99.90	-99.90	-99.90	-99.90 : averaging time for domain-avg wind speed (s)
-99.90	-99.90	-99.90	-99.90	-99.90	-99.90	-99.90	-99.90	-99.90	-99.90	-99.90	-99.90	-99.90	-99.90 : wind speed power law exponent
-99.90	-99.90	-99.90	-99.90	-99.90	-99.90	-99.90	-99.90	-99.90	-99.90	-99.90	-99.90	-99.90	-99.90 : surface roughness (m)
-99.90	-99.90	-99.90	-99.90	-99.90	-99.90	-99.90	-99.90	-99.90	-99.90	-99.90	-99.90	-99.90	-99.90 : friction velocity (m)
-99.90	-99.90	-99.90	-99.90	-99.90	-99.90	-99.90	-99.90	-99.90	-99.90	-99.90	-99.90	-99.90	-99.90 : inverse Monin-Obukhov length (1/m)
0.30	0.30	0.30	0.30	0.30	0.30	0.30	0.30	0.30	0.30	0.30	0.30	0.30	0.30 : albedo
0.20	0.20	0.20	0.20	0.20	0.20	0.20	0.20	0.20	0.20	0.20	0.20	0.20	0.20 : moisture availability
5.00	5.00	5.00	5.00	5.00	5.00	5.00	5.00	5.00	5.00	5.00	5.00	5.00	5.00 : Bowen ratio
-99.9	-99.9	-99.9	-99.9	-99.9	-99.9	-99.9	-99.9	-99.9	-99.9	-99.9	-99.9	-99.9	-99.9 : mixing height (m)
75.0	75.0	75.0	75.0	75.0	75.0	75.0	75.0	75.0	75.0	75.0	75.0	75.0	75.0 : cloud cover (%)
-99.9	-99.9	-99.9	-99.9	-99.9	-99.9	-99.9	-99.9	-99.9	-99.9	-99.9	-99.9	-99.9	-99.9 : P-G stability class
-99.9	-99.9	-99.9	-99.9	-99.9	-99.9	-99.9	-99.9	-99.9	-99.9	-99.9	-99.9	-99.9	-99.9 : averaging time for concentration (s)
1.50	1.50	1.50	1.50	1.50	1.50	1.50	1.50	1.50	1.50	1.50	1.50	1.50	1.50 : suggested receptor height (m)
6	6	6	6	6	6	6	6	6	6	6	6	6	6 : no. of distances downwind
2.620E-01	6.120E-01	2.470E-01	2.470E-01	2.470E-01	2.470E-01	2.470E-01	2.470E-01	2.470E-01	2.470E-01	2.470E-01	2.470E-01	2.470E-01	2.470E-01 : distances downwind (m)
-9.990E-01	-9.990E-01	-9.990E-01	-9.990E-01	-9.990E-01	-9.990E-01	-9.990E-01	-9.990E-01	-9.990E-01	-9.990E-01	-9.990E-01	-9.990E-01	-9.990E-01	-9.990E-01 : concentration (mg/m**3)
-99.90	-99.90	-99.90	-99.90	-99.90	-99.90	-99.90	-99.90	-99.90	-99.90	-99.90	-99.90	-99.90	-99.90 : cross-wind integrated conc. (mg/m**2)
800.0	800.0	800.0	800.0	800.0	800.0	800.0	800.0	800.0	800.0	800.0	800.0	800.0	800.0 : sigma-y (m)
9.470E-02	9.110E-02	2.410E-02	2.410E-02	2.410E-02	2.410E-02	2.410E-02	2.410E-02	2.410E-02	2.410E-02	2.410E-02	2.410E-02	2.410E-02	2.410E-02 : distances downwind (m)
-9.990E-01	-9.990E-01	-9.990E-01	-9.990E-01	-9.990E-01	-9.990E-01	-9.990E-01	-9.990E-01	-9.990E-01	-9.990E-01	-9.990E-01	-9.990E-01	-9.990E-01	-9.990E-01 : concentration (mg/m**3)
-99.90	-99.90	-99.90	-99.90	-99.90	-99.90	-99.90	-99.90	-99.90	-99.90	-99.90	-99.90	-99.90	-99.90 : cross-wind integrated conc. (mg/m**2)
1600.0	1600.0	1600.0	1600.0	1600.0	1600.0	1600.0	1600.0	1600.0	1600.0	1600.0	1600.0	1600.0	1600.0 : sigma-y (m)
-9.990E-02	-9.990E-02	-9.990E-02	-9.990E-02	-9.990E-02	-9.990E-02	-9.990E-02	-9.990E-02	-9.990E-02	-9.990E-02	-9.990E-02	-9.990E-02	-9.990E-02	-9.990E-02 : distances downwind (m)
-9.990E-01	-9.990E-01	-9.990E-01	-9.990E-01	-9.990E-01	-9.990E-01	-9.990E-01	-9.990E-01	-9.990E-01	-9.990E-01	-9.990E-01	-9.990E-01	-9.990E-01	-9.990E-01 : concentration (mg/m**3)
-99.90	-99.90	-99.90	-99.90	-99.90	-99.90	-99.90	-99.90	-99.90	-99.90	-99.90	-99.90	-99.90	-99.90 : cross-wind integrated conc. (mg/m**2)
3200.0	3200.0	3200.0	3200.0	3200.0	3200.0	3200.0	3200.0	3200.0	3200.0	3200.0	3200.0	3200.0	3200.0 : sigma-y (m)
-9.990E-03	-9.990E-03	-9.990E-03	-9.990E-03	-9.990E-03	-9.990E-03	-9.990E-03	-9.990E-03	-9.990E-03	-9.990E-03	-9.990E-03	-9.990E-03	-9.990E-03	-9.990E-03 : distances downwind (m)
-9.990E-01	-9.990E-01	-9.990E-01	-9.990E-01	-9.990E-01	-9.990E-01	-9.990E-01	-9.990E-01	-9.990E-01	-9.990E-01	-9.990E-01	-9.990E-01	-9.990E-01	-9.990E-01 : concentration (mg/m**3)
-99.90	-99.90	-99.90	-99.90	-99.90	-99.90	-99.90	-99.90	-99.90	-99.90	-99.90	-99.90	-99.90	-99.90 : cross-wind integrated conc. (mg/m**2)
12800.0	12800.0	12800.0	12800.0	12800.0	12800.0	12800.0	12800.0	12800.0	12800.0	12800.0	12800.0	12800.0	12800.0 : sigma-y (m)
-9.990E-04	-9.990E-04	-9.990E-04	-9.990E-04	-9.990E-04	-9.990E-04	-9.990E-04	-9.990E-04	-9.990E-04	-9.990E-04	-9.990E-04	-9.990E-04	-9.990E-04	-9.990E-04 : distances downwind (m)
-9.990E-01	-9.990E-01	-9.990E-01	-9.990E-01	-9.990E-01	-9.990E-01	-9.990E-01	-9.990E-01	-9.990E-01	-9.990E-01	-9.990E-01	-9.990E-01	-9.990E-01	-9.990E-01 : concentration (mg/m**3)
-99.90	-99.90	-99.90	-99.90	-99.90	-99.90	-99.90	-99.90	-99.90	-99.90	-99.90	-99.90	-99.90	-99.90 : cross-wind integrated conc. (mg/m**2)
25600.0	25600.0	25600.0	25600.0	25600.0	25600.0	25600.0	25600.0	25600.0	25600.0	25600.0	25600.0	25600.0	25600.0 : sigma-y (m)
-9.990E-05	-9.990E-05	-9.990E-05	-9.990E-05	-9.990E-05	-9.990E-05	-9.990E-05	-9.990E-05	-9.990E-05	-9.990E-05	-9.990E-05	-9.990E-05	-9.990E-05	-9.990E-05 : distances downwind (m)
-9.990E-01	-9.990E-01	-9.990E-01	-9.990E-01	-9.990E-01	-9.990E-01	-9.990E-01	-9.990E-01	-9.990E-01	-9.990E-01	-9.990E-01	-9.990E-01	-9.990E-01	-9.990E-01 : concentration (mg/m**3)
-99.90	-99.90	-99.90	-99.90	-99.90	-99.90	-99.90	-99.90	-99.90	-99.90	-99.90	-99.90	-99.90	-99.90 : cross-wind integrated conc. (mg/m**2)
0.0	0.0	0.0	0.0	0.0	0.0	0.0	0.0	0.0	0.0	0.0	0.0	0.0	0.0 : no. of lines-of-sight

Profile Grass
12 : number of trials included in DDA
6 : time designation
42.30 : latitude (deg)
98.30 : longitude (deg)

pg7	pg8	pg9	pg10	pg13	pg15	pg16	pg17	pg18	pg19	pg20	pg21	trial ID
7	7	7	7	7	7	7	7	7	7	7	7	7 : trial ID
10	10	11	11	22	23	23	23	23	25	25	25	25 : day
1956	1956	1956	1956	1956	1956	1956	1956	1956	1956	1956	1956	1956 : year
14	17	16	12	20	8	10	20	22	11	14	14	22 : hour
15	0	0	0	0	0	0	0	0	0	0	0	0 : minute
1	1	1	1	1	1	1	1	1	1	1	1	1 : no. of sources
0.0	0.0	0.0	0.0	0.0	0.0	0.0	0.0	0.0	0.0	0.0	0.0	0.0 : x-coord. of source (m)
0.0	0.0	0.0	0.0	0.0	0.0	0.0	0.0	0.0	0.0	0.0	0.0	0.0 : y-coord. of source (m)
0.45	0.45	0.45	0.45	0.45	0.45	0.45	0.45	0.45	0.45	0.45	0.45	0.45 : source elevation (m)
89.900	91.100	92.000	92.100	95.500	95.500	93.000	56.500	57.600	101.800	101.200	50.900	50.900 : emission rate (g/s)
600.0	600.0	600.0	600.0	600.0	600.0	600.0	600.0	600.0	600.0	600.0	600.0	600.0 : emission duration (s)
-99.9	-99.9	-99.9	-99.9	-99.9	-99.9	-99.9	-99.9	-99.9	-99.9	-99.9	-99.9	-99.9 : total mass emitted (kg)
0.000	0.000	0.000	0.000	0.000	0.000	0.000	0.000	0.000	0.000	0.000	0.000	0.000 : sign0 at the source (m)
0.000	0.000	0.000	0.000	0.000	0.000	0.000	0.000	0.000	0.000	0.000	0.000	0.000 : sign0 at the source (m)
0.000	0.000	0.000	0.000	0.000	0.000	0.000	0.000	0.000	0.000	0.000	0.000	0.000 : sign0 at the source (m)
-99.9	-99.9	-99.9	-99.9	-99.9	-99.9	-99.9	-99.9	-99.9	-99.9	-99.9	-99.9	-99.9 : ambient pressure (atm)
-99.9	-99.9	-99.9	-99.9	-99.9	-99.9	-99.9	-99.9	-99.9	-99.9	-99.9	-99.9	-99.9 : relative humidity (%)
305.15	305.15	305.15	304.15	295.15	295.15	301.15	300.15	297.15	302.15	307.15	302.15	302.15 : temperature at level #1 (K)
2.00	2.00	2.00	2.00	2.00	2.00	2.00	2.00	2.00	2.00	2.00	2.00	2.00 : measuring height for temperature #1 (m)
303.55	303.55	299.55	302.15	295.05	294.05	300.15	300.65	298.75	300.85	304.85	302.45	302.45 : temperature at level #2 (K)
16.00	16.00	16.00	16.00	16.00	16.00	16.00	16.00	16.00	16.00	16.00	16.00	16.00 : measuring height for temperature #2 (m)
4.20	4.90	6.90	4.60	3.40	3.40	3.20	3.30	3.50	5.80	8.60	6.10	6.10 : wind speed (m/s) at a tower
2.00	2.00	2.00	2.00	2.00	2.00	2.00	2.00	2.00	2.00	2.00	2.00	2.00 : measuring height for wind data (m)
4.20	4.90	6.90	4.60	3.40	3.40	3.20	3.30	3.50	5.80	8.60	6.10	6.10 : domain-averaged wind speed (m/s)
186.0	184.0	204.0	225.0	190.0	209.0	192.0	184.0	187.0	166.0	178.0	181.0	181.0 : domain-averaged wind direction (deg)
-99.90	-99.90	-99.90	-99.90	-99.90	-99.90	-99.90	-99.90	-99.90	-99.90	-99.90	-99.90	-99.90 : domain-averaged sigma-u (deg)
25.60	10.20	10.20	15.80	3.20	12.80	18.50	5.60	5.30	11.50	8.20	8.60	8.60 : domain-averaged sigma-theta (deg)
-99.90	-99.90	-99.90	-99.90	-99.90	-99.90	-99.90	-99.90	-99.90	-99.90	-99.90	-99.90	-99.90 : domain-averaged sigma-phi (deg)
2.00	2.00	2.00	2.00	2.00	2.00	2.00	2.00	2.00	2.00	2.00	2.00	2.00 : measuring ht for domain-avg phi (deg)
600.0	600.0	600.0	600.0	600.0	600.0	600.0	600.0	600.0	600.0	600.0	600.0	600.0 : averaging time for domain-avg wind speed (m)
-99.900	-99.900	-99.900	-99.900	-99.900	-99.900	-99.900	-99.900	-99.900	-99.900	-99.900	-99.900	-99.900 : wind speed power law exponent
0.0060	0.0060	0.0060	0.0060	0.0060	0.0060	0.0060	0.0060	0.0060	0.0060	0.0060	0.0060	0.0060 : surface roughness (m)
0.310	0.310	0.460	0.320	0.090	0.230	0.240	0.210	0.200	0.390	0.600	0.380	0.380 : friction velocity (m)
-0.1020	-0.0556	-0.0323	-0.0909	0.2941	-0.1316	-0.1923	0.0208	0.0400	-0.0357	-0.0161	0.0058	0.0058 : inverse Monin-Obukhov length (1/m)
0.20	0.20	0.20	0.20	0.20	0.20	0.20	0.20	0.20	0.20	0.20	0.20	0.20 : albedo
0.50	0.50	0.50	0.50	0.50	0.50	0.50	0.50	0.50	0.50	0.50	0.50	0.50 : moisture availability
2.00	2.00	2.00	2.00	2.00	2.00	2.00	2.00	2.00	2.00	2.00	2.00	2.00 : Bowen ratio
1539.0	1580.0	626.0	1090.0	-99.9	86.0	1259.0	-99.9	-99.9	745.0	813.0	-99.9	-99.9 : mixing height (m)
0.0	0.0	30.0	30.0	20.0	0.0	0.0	70.0	10.0	30.0	20.0	100.0	100.0 : cloud cover (%)
2	3	3	2	6	1	1	4	5	3	4	4	4 : P-G stability class
600.0	600.0	600.0	600.0	600.0	600.0	600.0	600.0	600.0	600.0	600.0	600.0	600.0 : averaging time for concentration (s)
1.50	1.50	1.50	1.50	1.50	1.50	1.50	1.50	1.50	1.50	1.50	1.50	1.50 : suggested receptor height (m)
5	5	5	5	5	5	5	5	5	5	5	5	5 : no. of distances downwind
50.0	50.0	50.0	50.0	50.0	50.0	50.0	50.0	50.0	50.0	50.0	50.0	50.0 : distances downwind (m)
9.260E+01	3.963E+02	1.858E+02	1.704E+02	-9.990E+01	3.887E+02	1.748E+02	6.102E+02	6.048E+02	2.024E+02	1.569E+02	2.693E+02	2.693E+02 : concentration (mg/m**3)
4.001E+01	5.102E+03	3.698E+03	4.504E+03	-9.990E+01	7.096E+03	5.003E+03	5.933E+03	6.221E+03	4.500E+03	3.400E+03	2.952E+03	2.952E+03 : cross-wind integrated conc. (mg/m**2)
100.0	100.0	100.0	100.0	100.0	100.0	100.0	100.0	100.0	100.0	100.0	100.0	100.0 : sigma-y (m)
2.167E+01	1.066E+02	5.272E+01	4.052E+01	-9.990E+01	1.031E+02	3.301E+01	2.554E+02	2.494E+02	5.100E+01	4.858E+01	9.366E+01	9.366E+01 : distances downwind (m)
2.203E+03	2.596E+03	2.199E+03	1.796E+03	-9.990E+01	3.400E+03	1.795E+03	-9.990E+01	-9.990E+01	2.199E+03	1.801E+03	-9.990E+01	-9.990E+01 : concentration (mg/m**3)
200.0	200.0	200.0	200.0	200.0	200.0	200.0	200.0	200.0	200.0	200.0	200.0	200.0 : sigma-y (m)
4.225E+00	2.378E+01	1.306E+01	1.050E+01	-9.990E+01	2.063E+01	6.008E+00	8.023E+01	9.216E+01	1.222E+01	1.417E+01	2.784E+01	2.784E+01 : distances downwind (m)
9.975E+02	1.102E+03	1.003E+03	7.101E+02	-9.990E+01	1.347E+03	4.799E+02	1.921E+03	2.650E+03	8.602E+02	8.501E+02	9.162E+02	9.162E+02 : cross-wind integrated conc. (mg/m**2)
22.00	21.00	31.00	35.00	-99.90	26.00	49.00	-99.90	-99.90	32.00	27.00	-99.90	-99.90 : sigma-y (m)
400.0	400.0	400.0	400.0	400.0	400.0	400.0	400.0	400.0	400.0	400.0	400.0	400.0 : distances downwind (m)
6.841E-01	3.781E+00	2.696E+00	2.487E+00	1.248E+02	4.518E+00	5.924E-01	2.475E+01	3.010E+01	1.918E+00	3.008E+00	8.602E+00	8.602E+00 : concentration (mg/m**3)
4.001E+02	3.899E+02	4.103E+02	1.999E+02	-9.990E+01	3.698E+02	1.004E+02	-9.990E+01	-9.990E+01	2.698E+02	3.400E+02	-9.990E+01	-9.990E+01 : cross-wind integrated conc. (mg/m**2)
39.00	41.00	63.00	61.00	-99.90	45.00	72.00	-99.90	-99.90	55.00	49.00	-99.90	-99.90 : sigma-y (m)
800.0	800.0	800.0	800.0	800.0	800.0	800.0	800.0	800.0	800.0	800.0	800.0	800.0 : distances downwind (m)
7.363E-02	6.714E-01	4.839E-01	1.584E-01	-9.990E+01	5.186E-01	4.752E-02	9.040E+00	1.359E+01	3.370E-01	7.124E-01	3.034E+00	3.034E+00 : concentration (mg/m**3)
1.798E+02	1.403E+02	1.297E+02	3.223E+01	8.126E+03	1.098E+02	1.674E+01	6.215E+02	1.152E+03	5.803E+01	1.295E+02	3.054E+02	3.054E+02 : cross-wind integrated conc. (mg/m**2)
71.00	86.00	116.00	97.00	-99.90	92.00	116.00	-99.90	-99.90	85.00	90.00	-99.90	-99.90 : sigma-y (m)
0	0	0	0	0	0	0	0	0	0	0	0	0 : no. of lines-of-sight

Profile Grass

12 : number of trials included in DDA

16 : time zone designation

42.30 : latitude (deg)

98.30 : longitude (deg)

pg22 : pg23

pg24 : pg25

pg26 : pg27

pg28 : pg29

pg30 : pg31

pg32 : pg33

pg34 : pg35

pg36 : pg37

pg38 : pg39

pg40 : pg41

pg42 : pg43

pg44 : pg45

pg46 : pg47

pg48 : pg49

pg50 : pg51

pg52 : pg53

pg54 : pg55

pg56 : pg57

pg58 : pg59

pg60 : pg61

pg62 : pg63

pg64 : pg65

pg66 : pg67

pg68 : pg69

pg70 : pg71

pg72 : pg73

pg74 : pg75

pg76 : pg77

pg78 : pg79

pg80 : pg81

pg82 : pg83

pg84 : pg85

pg86 : pg87

pg88 : pg89

pg90 : pg91

pg92 : pg93

pg94 : pg95

pg96 : pg97

pg98 : pg99

pg100 : pg101

pg102 : pg103

pg104 : pg105

pg106 : pg107

pg108 : pg109

pg110 : pg111

pg112 : pg113

pg114 : pg115

pg116 : pg117

pg118 : pg119

pg120 : pg121

pg122 : pg123

pg124 : pg125

pg126 : pg127

pg128 : pg129

pg130 : pg131

pg132 : pg133

pg134 : pg135

pg136 : pg137

pg138 : pg139

pg140 : pg141

pg142 : pg143

pg144 : pg145

pg146 : pg147

pg148 : pg149

pg150 : pg151

pg152 : pg153

pg154 : pg155

pg156 : pg157

pg158 : pg159

pg160 : pg161

pg162 : pg163

pg164 : pg165

pg166 : pg167

pg168 : pg169

pg170 : pg171

pg172 : pg173

pg174 : pg175

pg176 : pg177

pg178 : pg179

pg180 : pg181

pg182 : pg183

pg184 : pg185

pg186 : pg187

pg188 : pg189

pg190 : pg191

Prairie Grass
 11 : number of trials included in DDA
 6 : time zone designation
 42.10 : latitude (deg)
 98.30 : longitude (deg)

pg41	pg42	pg43	pg44	pg45	pg46	pg49	pg50	pg51	pg53	pg54	trial ID
8	8	8	8	8	8	8	8	8	8	8	8
14	14	15	15	15	21	21	21	21	24	24	month
1956	1956	1956	1956	1956	1956	1956	1956	1956	1956	1956	year
3	3	12	14	17	9	10	14	15	20	22	hour
5	5	0	0	59	6	59	6	29	0	2	minute
1	1	1	1	1	1	1	1	1	1	1	no. of sources
0.0	0.0	0.0	0.0	0.0	0.0	0.0	0.0	0.0	0.0	0.0	x-coord. of source (m)
0.0	0.0	0.0	0.0	0.0	0.0	0.0	0.0	0.0	0.0	0.0	y-coord. of source (m)
0.45	0.45	0.45	0.45	0.45	0.45	0.45	0.45	0.45	0.45	0.45	source elevation (m)
39.900	56.400	98.600	100.700	100.800	104.100	102.000	102.800	102.400	45.200	43.400	emission rate (g/s)
600.0	600.0	600.0	600.0	600.0	600.0	600.0	600.0	600.0	600.0	600.0	emission duration (s)
-99.9	-99.9	-99.9	-99.9	-99.9	-99.9	-99.9	-99.9	-99.9	-99.9	-99.9	total mass emitted (kg)
0.000	0.000	0.000	0.000	0.000	0.000	0.000	0.000	0.000	0.000	0.000	sig0 at the source (m)
0.000	0.000	0.000	0.000	0.000	0.000	0.000	0.000	0.000	0.000	0.000	sig0 at the source (m)
0.000	0.000	0.000	0.000	0.000	0.000	0.000	0.000	0.000	0.000	0.000	sig0 at the source (m)
-99.9	-99.9	-99.9	-99.9	-99.9	-99.9	-99.9	-99.9	-99.9	-99.9	-99.9	ambient pressure (atm)
-99.9	-99.9	-99.9	-99.9	-99.9	-99.9	-99.9	-99.9	-99.9	-99.9	-99.9	relative humidity (%)
294.15	296.15	308.15	310.15	309.15	293.15	297.15	304.15	305.15	290.15	292.15	temperature at level #1 (K)
2.00	2.00	2.00	2.00	2.00	2.00	2.00	2.00	2.00	2.00	2.00	measuring height for temperature #1 (m)
293.55	295.55	306.55	308.55	308.75	291.95	295.35	302.55	303.75	294.05	293.05	temperature at level #2 (K)
16.00	16.00	16.00	16.00	16.00	16.00	16.00	16.00	16.00	16.00	16.00	measuring height for temperature #2 (m)
5.00	5.00	5.00	5.00	5.00	5.00	5.00	5.00	5.00	5.00	5.00	wind speed (m/s) at a tower
2.00	2.00	2.00	2.00	2.00	2.00	2.00	2.00	2.00	2.00	2.00	measuring height for wind data (m)
4.00	4.00	4.00	4.00	4.00	4.00	4.00	4.00	4.00	4.00	4.00	domain-averaged wind speed (m/s)
198.0	212.0	170.0	158.0	163.0	214.0	199.0	215.0	245.0	132.0	140.0	domain-averaged wind direction (deg)
-99.90	-99.90	-99.90	-99.90	-99.90	-99.90	-99.90	-99.90	-99.90	-99.90	-99.90	domain-averaged sigma-u (m/s)
5.00	6.60	12.20	12.70	6.90	8.10	11.90	10.90	10.80	3.90	5.90	domain-averaged sigma-theta (deg)
-99.90	-99.90	-99.90	-99.90	-99.90	-99.90	-99.90	-99.90	-99.90	-99.90	-99.90	domain-averaged sigma-phi (deg)
2.00	2.00	2.00	2.00	2.00	2.00	2.00	2.00	2.00	2.00	2.00	measuring ht for domain-avg wind speed (m)
600.0	600.0	600.0	600.0	600.0	600.0	600.0	600.0	600.0	600.0	600.0	averaging time for domain-avg data (s)
-99.900	-99.900	-99.900	-99.900	-99.900	-99.900	-99.900	-99.900	-99.900	-99.900	-99.900	wind speed power law exponent
0.0060	0.0060	0.0060	0.0060	0.0060	0.0060	0.0060	0.0060	0.0060	0.0060	0.0060	surface roughness (m)
0.370	0.370	0.350	0.400	0.390	0.510	0.450	0.400	0.450	0.170	0.240	friction velocity (m)
0.0286	0.0286	-0.0625	-0.0400	-0.0115	-0.0159	-0.0357	-0.0385	-0.0250	0.1000	0.0250	inverse Monin-Obukhov length (1/m)
0.20	0.20	0.20	0.20	0.20	0.20	0.20	0.20	0.20	0.20	0.20	albedo
0.50	0.50	0.50	0.50	0.50	0.50	0.50	0.50	0.50	0.50	0.50	moisture availability
2.00	2.00	2.00	2.00	2.00	2.00	2.00	2.00	2.00	2.00	2.00	Bowen ratio
-99.9	-99.9	683.0	1684.0	-99.9	-99.9	638.0	851.0	2136.0	-99.9	-99.9	mixing height (m)
0.0	0.0	100.0	80.0	90.0	10.0	10.0	10.0	10.0	0.0	0.0	cloud cover (%)
5	5	3	3	4	4	3	3	4	6	4	P-G stability class
600.0	600.0	600.0	600.0	600.0	600.0	600.0	600.0	600.0	600.0	600.0	averaging time for concentration (s)
1.50	1.50	1.50	1.50	1.50	1.50	1.50	1.50	1.50	1.50	1.50	suggested receptor height (m)
5	5	5	5	5	5	5	5	5	5	5	no. of distances downwind
4.349E+02	2.651E+02	2.269E+02	1.742E+02	3.326E+02	2.155E+02	2.030E+02	2.231E+02	2.560E+02	9.130E+02	4.136E+02	distances downwind (m)
3.152E+03	2.933E+03	4.999E+03	4.501E+03	5.242E+03	4.997E+03	4.304E+03	4.205E+03	4.700E+03	6.961E+03	3.515E+03	concentration (mg/m**3)
100.0	100.0	100.0	100.0	100.0	100.0	100.0	100.0	100.0	100.0	100.0	sigma-y (m)
1.831E+02	9.701E+01	5.236E+01	4.582E+01	1.048E+02	6.298E+01	6.344E+01	7.165E+01	6.748E+01	5.198E+02	1.641E+02	distances downwind (m)
-9.990E+01	-9.990E+01	2.395E+03	2.295E+03	-9.990E+01	-9.990E+01	2.397E+03	2.303E+03	2.397E+03	-9.990E+01	-9.990E+01	concentration (mg/m**3)
200.0	200.0	200.0	200.0	200.0	200.0	200.0	200.0	200.0	200.0	200.0	sigma-y (m)
6.504E+01	3.023E+01	1.469E+01	1.309E+01	3.539E+01	1.624E+01	1.754E+01	1.708E+01	1.710E+01	2.237E+02	5.946E+01	distances downwind (m)
1.277E+03	9.588E+02	1.083E+03	1.088E+03	1.714E+03	6.246E+02	1.163E+03	9.092E+02	1.000E+03	3.752E+03	1.302E+03	concentration (mg/m**3)
-99.90	-99.90	40.00	43.00	-99.90	-99.90	35.00	28.00	32.00	-99.90	-99.90	sigma-y (m)
400.0	400.0	400.0	400.0	400.0	400.0	400.0	400.0	400.0	400.0	400.0	distances downwind (m)
2.374E+01	7.588E+00	2.288E+00	2.648E+00	7.772E+00	4.497E+00	3.091E+00	3.526E+00	2.703E+00	8.181E+01	2.161E+01	concentration (mg/m**3)
-9.990E+01	-9.990E+01	3.698E+02	4.300E+02	-9.990E+01	-9.990E+01	4.498E+02	3.895E+02	3.799E+02	-9.990E+01	-9.990E+01	cross-wind integrated conc. (mg/m**2)
800.0	800.0	800.0	800.0	800.0	800.0	800.0	800.0	800.0	800.0	800.0	sigma-y (m)
9.516E+00	2.044E+00	4.693E-01	5.367E-01	2.591E+00	1.260E+00	5.355E-01	5.520E-01	4.055E-01	9.244E+00	9.244E+00	concentration (mg/m**3)
4.788E+02	2.820E+02	1.203E+02	1.400E+02	3.528E+02	-9.990E+01	1.499E+02	1.100E+02	8.397E+01	2.802E+03	4.774E+02	cross-wind integrated conc. (mg/m**2)
-99.90	-99.90	200.00	126.00	-99.90	-99.90	118.00	115.00	17.00	-99.90	-99.90	sigma-y (m)
0	0	0	0	0	0	0	0	0	0	0	no. of lines-of-sight

APPENDIX F-2

LISTINGS OF THE DUGWAY DATA ARCHIVES - SMOKE/OBSCURANT DATASETS

The Inventory Smoke Tests of MC Grenades (INMHC)

g : number of trials included in DMA

g : time zone designation

40.20 : latitude (deg)

113.00 : longitude (deg)

T3	T4	T25	T33
10 : month	10	10	10 : month
20 : day	20	20	20 : day
77 : year	77	77	77 : year
13 : hour	13	13	13 : hour
30 : minute	30	30	30 : minute
1 : no. of sources	1	1	1 : no. of sources
0.0 : x-coord. of source (m)	-85.2	-85.2	0.0 : x-coord. of source (m)
0.0 : y-coord. of source (m)	126.3	126.3	0.0 : y-coord. of source (m)
0.00 : source elevation (m)	-99.9	-99.9	0.00 : source elevation (m)
155.0 : emission rate (g/s)	130.0	130.0	155.0 : emission rate (g/s)
10.504 : total mass emitted (kg)	3.527	3.527	10.504 : total mass emitted (kg)
0.170 : sigx0 at the source (m)	0.350	0.350	0.170 : sigx0 at the source (m)
0.170 : sigy0 at the source (m)	0.350	0.350	0.170 : sigy0 at the source (m)
-99.9 : ambient pressure (atm)	-99.9	-99.9	-99.9 : ambient pressure (atm)
-99.9 : relative humidity (%)	-99.9	-99.9	-99.9 : relative humidity (%)
300.00 : temperature at level #1 (K)	300.00	300.00	300.00 : temperature at level #1 (K)
2.00 : measuring height for temperature #1 (m)	2.00	2.00	2.00 : measuring height for temperature #1 (m)
-99.90 : temperature at level #2 (K)	-99.90	-99.90	-99.90 : temperature at level #2 (K)
-99.90 : measuring height for temperature #2 (m)	-99.90	-99.90	-99.90 : measuring height for temperature #2 (m)
2.64 : wind speed (m/s) at a tower	3.14	3.14	2.64 : wind speed (m/s) at a tower
2.00 : measuring height for wind data (m)	2.00	2.00	2.00 : measuring height for wind data (m)
2.64 : domain-averaged wind speed (m/s)	3.14	3.14	2.64 : domain-averaged wind speed (m/s)
175.8 : domain-averaged wind direction (deg)	344.4	344.4	175.8 : domain-averaged wind direction (deg)
-99.90 : domain-averaged sigma-u (m/s)	-99.90	-99.90	-99.90 : domain-averaged sigma-u (m/s)
9.44 : domain-averaged sigma-theta (deg)	8.67	8.67	9.44 : domain-averaged sigma-theta (deg)
-99.90 : domain-averaged sigma-phi (deg)	-99.90	-99.90	-99.90 : domain-averaged sigma-phi (deg)
2.00 : measuring time for domain-avg wind speed (s)	2.00	2.00	2.00 : measuring time for domain-avg wind speed (s)
0.07 : surface roughness (m)	0.030	0.030	0.07 : surface roughness (m)
-99.900 : friction velocity (m)	-99.900	-99.900	-99.900 : friction velocity (m)
-99.9000 : inverse Monin-Obukhov length (1/m)	-99.9000	-99.9000	-99.9000 : inverse Monin-Obukhov length (1/m)
0.18 : albedo	0.18	0.18	0.18 : albedo
0.50 : moisture availability	0.50	0.50	0.50 : moisture availability
-99.9 : Bowen ratio	-99.9	-99.9	-99.9 : Bowen ratio
-99.9 : mixing height (m)	-99.9	-99.9	-99.9 : mixing height (m)
-99.9 : cloud cover (%)	-99.9	-99.9	-99.9 : cloud cover (%)
-99.9 : P-G stability class	-99.9	-99.9	-99.9 : P-G stability class
60.0 : averaging time for concentration (s)	60.0	60.0	60.0 : averaging time for concentration (s)
1.50 : suggested receptor height (m)	1.50	1.50	1.50 : suggested receptor height (m)
0 : no. of distances downwind	0	0	0 : no. of distances downwind
3 : no. of lines-of-sight	3	3	3 : no. of lines-of-sight
240.2 : x-coord. of 1st end-point for LOS1 (m)	240.2	240.2	240.2 : x-coord. of 1st end-point for LOS1 (m)
180.4 : y-coord. of 1st end-point for LOS1 (m)	180.4	180.4	180.4 : y-coord. of 1st end-point for LOS1 (m)
-257.2 : x-coord. of 2nd end-point for LOS1 (m)	-257.2	-257.2	-257.2 : x-coord. of 2nd end-point for LOS1 (m)
-155.1 : y-coord. of 2nd end-point for LOS1 (m)	-155.1	-155.1	-155.1 : y-coord. of 2nd end-point for LOS1 (m)
-99.9 : LOS integrated conc. (mg/m**2)	-99.9	-99.9	-99.9 : LOS integrated conc. (mg/m**2)
1.2572E+06 : LOS integrated dosage (mg-m**2)	1.633E+05	1.633E+05	1.2572E+06 : LOS integrated dosage (mg-m**2)
206.1 : x-coord. of 1st end-point for LOS1 (m)	206.1	206.1	206.1 : x-coord. of 1st end-point for LOS1 (m)
230.9 : y-coord. of 1st end-point for LOS1 (m)	230.9	230.9	230.9 : y-coord. of 1st end-point for LOS1 (m)
-291.3 : x-coord. of 2nd end-point for LOS1 (m)	-291.3	-291.3	-291.3 : x-coord. of 2nd end-point for LOS1 (m)
-104.6 : y-coord. of 2nd end-point for LOS1 (m)	-104.6	-104.6	-104.6 : y-coord. of 2nd end-point for LOS1 (m)
-99.9 : LOS integrated conc. (mg/m**2)	-99.9	-99.9	-99.9 : LOS integrated conc. (mg/m**2)
3.4962E+05 : LOS integrated dosage (mg-m**2)	1.634E+05	1.634E+05	3.4962E+05 : LOS integrated dosage (mg-m**2)
172.0 : x-coord. of 1st end-point for LOS1 (m)	172.0	172.0	172.0 : x-coord. of 1st end-point for LOS1 (m)
281.5 : y-coord. of 1st end-point for LOS1 (m)	281.5	281.5	281.5 : y-coord. of 1st end-point for LOS1 (m)
-325.4 : x-coord. of 2nd end-point for LOS1 (m)	-325.4	-325.4	-325.4 : x-coord. of 2nd end-point for LOS1 (m)
-54.0 : y-coord. of 2nd end-point for LOS1 (m)	-54.0	-54.0	-54.0 : y-coord. of 2nd end-point for LOS1 (m)
-99.9 : LOS integrated conc. (mg/m**2)	-99.9	-99.9	-99.9 : LOS integrated conc. (mg/m**2)
1.0032E+05 : LOS integrated dosage (mg-m**2)	4.984E+05	4.984E+05	1.0032E+05 : LOS integrated dosage (mg-m**2)
240.2 : x-coord. of 1st end-point for LOS1 (m)	240.2	240.2	240.2 : x-coord. of 1st end-point for LOS1 (m)
180.4 : y-coord. of 1st end-point for LOS1 (m)	180.4	180.4	180.4 : y-coord. of 1st end-point for LOS1 (m)
-257.2 : x-coord. of 2nd end-point for LOS1 (m)	-257.2	-257.2	-257.2 : x-coord. of 2nd end-point for LOS1 (m)
-155.1 : y-coord. of 2nd end-point for LOS1 (m)	-155.1	-155.1	-155.1 : y-coord. of 2nd end-point for LOS1 (m)
-99.9 : LOS integrated conc. (mg/m**2)	-99.9	-99.9	-99.9 : LOS integrated conc. (mg/m**2)
1.936E+05 : LOS integrated dosage (mg-m**2)	5.441E+05	5.441E+05	1.936E+05 : LOS integrated dosage (mg-m**2)
206.1 : x-coord. of 1st end-point for LOS1 (m)	206.1	206.1	206.1 : x-coord. of 1st end-point for LOS1 (m)
230.9 : y-coord. of 1st end-point for LOS1 (m)	230.9	230.9	230.9 : y-coord. of 1st end-point for LOS1 (m)
-291.3 : x-coord. of 2nd end-point for LOS1 (m)	-291.3	-291.3	-291.3 : x-coord. of 2nd end-point for LOS1 (m)
-104.6 : y-coord. of 2nd end-point for LOS1 (m)	-104.6	-104.6	-104.6 : y-coord. of 2nd end-point for LOS1 (m)
-99.9 : LOS integrated conc. (mg/m**2)	-99.9	-99.9	-99.9 : LOS integrated conc. (mg/m**2)
1.420E+05 : LOS integrated dosage (mg-m**2)	3.619E+05	3.619E+05	1.420E+05 : LOS integrated dosage (mg-m**2)
172.0 : x-coord. of 1st end-point for LOS1 (m)	172.0	172.0	172.0 : x-coord. of 1st end-point for LOS1 (m)
281.5 : y-coord. of 1st end-point for LOS1 (m)	281.5	281.5	281.5 : y-coord. of 1st end-point for LOS1 (m)
-325.4 : x-coord. of 2nd end-point for LOS1 (m)	-325.4	-325.4	-325.4 : x-coord. of 2nd end-point for LOS1 (m)
-54.0 : y-coord. of 2nd end-point for LOS1 (m)	-54.0	-54.0	-54.0 : y-coord. of 2nd end-point for LOS1 (m)
-99.9 : LOS integrated conc. (mg/m**2)	-99.9	-99.9	-99.9 : LOS integrated conc. (mg/m**2)
1.374E+05 : LOS integrated dosage (mg-m**2)	1.705E+05	1.705E+05	1.374E+05 : LOS integrated dosage (mg-m**2)
-9.990E+01 : LOS integrated dosage (mg-m**2)	-9.990E+01	-9.990E+01	-9.990E+01 : LOS integrated dosage (mg-m**2)

1) Number of trials included in DCH

2) Time zone designation

3) Latitude (deg)

4) Longitude (deg)

5) Time zone designation

6) Latitude (deg)

7) Longitude (deg)

8) Time zone designation

9) Latitude (deg)

10) Longitude (deg)

11) Time zone designation

12) Latitude (deg)

13) Longitude (deg)

14) Time zone designation

15) Latitude (deg)

16) Longitude (deg)

17) Time zone designation

18) Latitude (deg)

19) Longitude (deg)

20) Time zone designation

21) Latitude (deg)

22) Longitude (deg)

23) Time zone designation

24) Latitude (deg)

25) Longitude (deg)

26) Time zone designation

27) Latitude (deg)

28) Longitude (deg)

29) Time zone designation

30) Latitude (deg)

31) Longitude (deg)

32) Time zone designation

33) Latitude (deg)

34) Longitude (deg)

35) Time zone designation

36) Latitude (deg)

37) Longitude (deg)

38) Time zone designation

39) Latitude (deg)

40) Longitude (deg)

41) Time zone designation

42) Latitude (deg)

43) Longitude (deg)

44) Time zone designation

45) Latitude (deg)

46) Longitude (deg)

47) Time zone designation

48) Latitude (deg)

49) Longitude (deg)

50) Time zone designation

51) Latitude (deg)

52) Longitude (deg)

53) Time zone designation

54) Latitude (deg)

55) Longitude (deg)

56) Time zone designation

57) Latitude (deg)

58) Longitude (deg)

59) Time zone designation

60) Latitude (deg)

61) Longitude (deg)

62) Time zone designation

63) Latitude (deg)

64) Longitude (deg)

65) Time zone designation

66) Latitude (deg)

67) Longitude (deg)

68) Time zone designation

69) Latitude (deg)

70) Longitude (deg)

71) Time zone designation

72) Latitude (deg)

73) Longitude (deg)

74) Time zone designation

75) Latitude (deg)

76) Longitude (deg)

77) Time zone designation

78) Latitude (deg)

79) Longitude (deg)

80) Time zone designation

81) Latitude (deg)

82) Longitude (deg)

83) Time zone designation

84) Latitude (deg)

85) Longitude (deg)

86) Time zone designation

87) Latitude (deg)

88) Longitude (deg)

89) Time zone designation

90) Latitude (deg)

91) Longitude (deg)

14 : Number of trials included in data

6 : Time zone designation

40.20 : Latitude (deg)

113.00 : Longitude (deg)

G1A2 : G1A1

G1A2 : G1A1

G1A2 : G1A1

G1A2 : G1A1

G1A2 : G1A1

G1A2 : G1A1

G1A2 : G1A1

G1A2 : G1A1

G1A2 : G1A1

G1A2 : G1A1

G1A2 : G1A1

G1A2 : G1A1

G1A2 : G1A1

G1A2 : G1A1

G1A2 : G1A1

G1A2 : G1A1

G1A2 : G1A1

G1A2 : G1A1

G1A2 : G1A1

G1A2 : G1A1

G1A2 : G1A1

G1A2 : G1A1

G1A2 : G1A1

G1A2 : G1A1

G1A2 : G1A1

G1A2 : G1A1

G1A2 : G1A1

G1A2 : G1A1

G1A2 : G1A1

G1A2 : G1A1

G1A2 : G1A1

G1A2 : G1A1

G1A2 : G1A1

G1A2 : G1A1

G1A2 : G1A1

G1A2 : G1A1

G1A2 : G1A1

G1A2 : G1A1

G1A2 : G1A1

G1A2 : G1A1

G1A2 : G1A1

G1A2 : G1A1

G1A2 : G1A1

G1A2 : G1A1

G1A2 : G1A1

G1A2 : G1A1

G1A2 : G1A1

G1A2 : G1A1

G1A2 : G1A1

G1A2 : G1A1

G1A2 : G1A1

G1A2 : G1A1

G1A2 : G1A1

G1A2 : G1A1

G1A2 : G1A1

G1A2 : G1A1

G1A2 : G1A1

G1A2 : G1A1

G1A2 : G1A1

G1A2 : G1A1

G1A2 : G1A1

G1A2 : G1A1

G1A2 : G1A1

G1A2 : G1A1

G1A2 : G1A1

G1A2 : G1A1

G1A2 : G1A1

G1A2 : G1A1

G1A2 : G1A1

G1A2 : G1A1

G1A2 : G1A1

G1A2 : G1A1

G1A2 : G1A1

G1A2 : G1A1

G1A2 : G1A1

G1A2 : G1A1

G1A2 : G1A1

G1A2 : G1A1

F-34

F-35

F-37

The Development Test II of 155MM SMOKE GRENADES (M116A1, 2 projectiles, DT2M2)

4 : number of trials included in DOA	5 : time zone designation	6 : latitude (deg)	7 : longitude (deg)	HC4	HC5	HC6	HC7	HC8	HC9	trial ID
40.20	19	81	15	10	48	7	52.0	24.8	7.5	8 : x-coord. of source (m)
113.00	19	81	15	10	48	7	52.0	24.8	7.5	9 : y-coord. of source (m)
										10 : source elevation (m)
										11 : total mass emitted (kg)
										12 : sigx0 at the source (m)
										13 : sigy0 at the source (m)
										14 : sigz0 at the source (m)
										15 : x-coord. of source (m)
										16 : y-coord. of source (m)
										17 : source elevation (m)
										18 : emission rate (g/s)
										19 : emission duration (s)
										20 : total mass emitted (kg)
										21 : sigx0 at the source (m)
										22 : sigy0 at the source (m)
										23 : sigz0 at the source (m)
										24 : x-coord. of source (m)
										25 : y-coord. of source (m)
										26 : source elevation (m)
										27 : emission rate (g/s)
										28 : emission duration (s)
										29 : total mass emitted (kg)
										30 : sigx0 at the source (m)
										31 : sigy0 at the source (m)
										32 : sigz0 at the source (m)
										33 : x-coord. of source (m)
										34 : y-coord. of source (m)
										35 : source elevation (m)
										36 : emission rate (g/s)
										37 : emission duration (s)
										38 : total mass emitted (kg)
										39 : sigx0 at the source (m)
										40 : sigy0 at the source (m)
										41 : sigz0 at the source (m)
										42 : x-coord. of source (m)
										43 : y-coord. of source (m)
										44 : source elevation (m)
										45 : emission rate (g/s)
										46 : emission duration (s)
										47 : total mass emitted (kg)
										48 : sigx0 at the source (m)
										49 : sigy0 at the source (m)
										50 : sigz0 at the source (m)
										51 : x-coord. of source (m)
										52 : y-coord. of source (m)
										53 : source elevation (m)
										54 : emission rate (g/s)
										55 : emission duration (s)
										56 : total mass emitted (kg)
										57 : sigx0 at the source (m)
										58 : sigy0 at the source (m)
										59 : sigz0 at the source (m)
										60 : x-coord. of source (m)
										61 : y-coord. of source (m)
										62 : source elevation (m)
										63 : emission rate (g/s)
										64 : emission duration (s)
										65 : total mass emitted (kg)
										66 : sigx0 at the source (m)
										67 : sigy0 at the source (m)
										68 : sigz0 at the source (m)
										69 : x-coord. of source (m)
										70 : y-coord. of source (m)
										71 : source elevation (m)
										72 : emission rate (g/s)
										73 : emission duration (s)
										74 : total mass emitted (kg)
										75 : sigx0 at the source (m)
										76 : sigy0 at the source (m)
										77 : sigz0 at the source (m)
										78 : x-coord. of source (m)
										79 : y-coord. of source (m)
										80 : source elevation (m)
										81 : emission rate (g/s)
										82 : emission duration (s)
										83 : total mass emitted (kg)
										84 : sigx0 at the source (m)
										85 : sigy0 at the source (m)
										86 : sigz0 at the source (m)
										87 : x-coord. of source (m)
										88 : y-coord. of source (m)
										89 : source elevation (m)
										90 : emission rate (g/s)
										91 : emission duration (s)
										92 : total mass emitted (kg)
										93 : sigx0 at the source (m)
										94 : sigy0 at the source (m)
										95 : sigz0 at the source (m)
										96 : x-coord. of source (m)
										97 : y-coord. of source (m)
										98 : source elevation (m)
										99 : ambient pressure (atm)

The Development Test 3 of 8mm Smoke Cartridge (M4019, a projectile, DT111) is a number of trials included in DOA

13, number of trials included is 800

01/20/2019 09:00 AM

10-20 s latitude (deg)	10-20 s longitude (deg)	2024	2023	2022	2021	2020	2019	2018	2017	2016	2015	2014	2013	2012	2011	2010	2009	2008	2007	2006	2005	2004	2003	2002	2001	2000	1999	1998	1997	1996	1995	1994	1993	1992	1991	1990	1989	1988	1987	1986	1985	1984	1983	1982	1981	1980	1979	1978	1977	1976	1975	1974	1973	1972	1971	1970	1969	1968	1967	1966	1965	1964	1963	1962	1961	1960	1959	1958	1957	1956	1955	1954	1953	1952	1951	1950	1949	1948	1947	1946	1945	1944	1943	1942	1941	1940	1939	1938	1937	1936	1935	1934	1933	1932	1931	1930	1929	1928	1927	1926	1925	1924	1923	1922	1921	1920	1919	1918	1917	1916	1915	1914	1913	1912	1911	1910	1909	1908	1907	1906	1905	1904	1903	1902	1901	1900	1899	1898	1897	1896	1895	1894	1893	1892	1891	1890	1889	1888	1887	1886	1885	1884	1883	1882	1881	1880	1879	1878	1877	1876	1875	1874	1873	1872	1871	1870	1869	1868	1867	1866	1865	1864	1863	1862	1861	1860	1859	1858	1857	1856	1855	1854	1853	1852	1851	1850	1849	1848	1847	1846	1845	1844	1843	1842	1841	1840	1839	1838	1837	1836	1835	1834	1833	1832	1831	1830	1829	1828	1827	1826	1825	1824	1823	1822	1821	1820	1819	1818	1817	1816	1815	1814	1813	1812	1811	1810	1809	1808	1807	1806	1805	1804	1803	1802	1801	1800	1799	1798	1797	1796	1795	1794	1793	1792	1791	1790	1789	1788	1787	1786	1785	1784	1783	1782	1781	1780	1779	1778	1777	1776	1775	1774	1773	1772	1771	1770	1769	1768	1767	1766	1765	1764	1763	1762	1761	1760	1759	1758	1757	1756	1755	1754	1753	1752	1751	1750	1749	1748	1747	1746	1745	1744	1743	1742	1741	1740	1739	1738	1737	1736	1735	1734	1733	1732	1731	1730	1729	1728	1727	1726	1725	1724	1723	1722	1721	1720	1719	1718	1717	1716	1715	1714	1713	1712	1711	1710	1709	1708	1707	1706	1705	1704	1703	1702	1701	1700	1699	1698	1697	1696	1695	1694	1693	1692	1691	1690	1689	1688	1687	1686	1685	1684	1683	1682	1681	1680	1679	1678	1677	1676	1675	1674	1673	1672	1671	1670	1669	1668	1667	1666	1665	1664	1663	1662	1661	1660	1659	1658	1657	1656	1655	1654	1653	1652	1651	1650	1649	1648	1647	1646	1645	1644	1643	1642	1641	1640	1639	1638	1637	1636	1635	1634	1633	1632	1631	1630	1629	1628	1627	1626	1625	1624	1623	1622	1621	1620	1619	1618	1617	1616	1615	1614	1613	1612	1611	1610	1609	1608	1607	1606	1605	1604	1603	1602	1601	1600	1599	1598	1597	1596	1595	1594	1593	1592	1591	1590	1589	1588	1587	1586	1585	1584	1583	1582	1581	1580	1579	1578	1577	1576	1575	1574	1573	1572	1571	1570	1569	1568	1567	1566	1565	1564	1563	1562	1561	1560	1559	1558	1557	1556	1555	1554	1553	1552	1551	1550	1549	1548	1547	1546	1545	1544	1543	1542	1541	1540	1539	1538	1537	1536	1535	1534	1533	1532	1531	1530	1529	1528	1527	1526	1525	1524	1523	1522	1521	1520	1519	1518	1517	1516	1515	1514	1513	1512	1511	1510	1509	1508	1507	1506	1505	1504	1503	1502	1501	1500	1499	1498	1497	1496	1495	1494	1493	1492	1491	1490	1489	1488	1487	1486	1485	1484	1483	1482	1481	1480	1479	1478	1477	1476	1475	1474	1473	1472	1471	1470	1469	1468	1467	1466	1465	1464	1463	1462	1461	1460	1459	1458	1457	1456	1455	1454	1453	1452	1451	1450	1449	1448	1447	1446	1445	1444	1443	1442	1441	1440	1439	1438	1437	1436	1435	1434	1433	1432	1431	1430	1429	1428	1427	1426	1425	1424	1423	1422	1421	1420	1419	1418	1417	1416	1415	1414	1413	1412	1411	1410	1409	1408	1407	1406	1405	1404	1403	1402	1401	1400	1399	1398	1397	1396	1395	1394	1393	1392	1391	1390	1389	1388	1387	1386	1385	1384	1383	1382	1381	1380	1379	1378	1377	1376	1375	1374	1373	1372	1371	1370	1369	1368	1367	1366	1365	1364	1363	1362	1361	1360	1359	1358	1357	1356	1355	1354	1353	1352	1351	1350	1349	1348	1347	1346	1345	1344	1343	1342	1341	1340	1339	1338	1337	1336	1335	1334	1333	1332	1331	1330	1329	1328	1327	1326	1325	1324	1323	1322	1321	1320	1319	1318	1317	1316	1315	1314	1313	1312	1311	1310	1309	1308	1307	1306	1305	1304	1303	1302	1301	1300	1299	1298	1297	1296	1295	1294	1293	1292	1291	1290	1289	1288	1287	1286	1285	1284	1283	1282	1281	1280	1279	1278	1277	1276	1275	1274	1273	1272	1271	1270	1269	1268	1267	1266	1265	1264	1263	1262	1261	1260	1259	1258	1257	1256	1255	1254	1253	1252	1251	1250	1249	1248	1247	1246	1245	1244	1243	1242	1241	1240	1239	1238	1237	1236	1235	1234	1233	1232	1231	1230	1229	1228	1227	1226	1225	1224	1223	1222	1221	1220	1219	1218	1217	1216	1215	1214	1213	1212	1211	1210	1209	1208	1207	1206	1205	1204	1203	1202	1201	1200	1199	1198	1197	1196	1195	1194	1193	1192	1191	1190	1189	1188	1187	1186	1185	1184	1183	1182	1181	1180	1179	1178	1177	1176	1175	1174	1173	1172	1171	1170	1169	1168	1167	1166	1165	1164	1163	1162	1161	1160	1159	1158	1157	1156	1155	1154	1153	1152	1151	1150	1149	1148	1147	1146	1145	1144	1143	1142	1141	1140	1139	1138	1137	1136	1135	1134	1133	1132	1131	1130	1129	1128	1127	1126	1125	1124	1123	1122	1121	1120	1119	1118	1117	1116	1115	1114	1113	1112	1111	1110	1109	1108	1107	1106	1105	1104	1103	1102	1101	1100	1099	1098	1097	1096	1095	1094	1093	1092	1091	1090	1089	1088	1087	1086	1085	1084	1083	1082	1081	1080	1079	1078	1077	1076	1075	1074	1073	1072	1071	1070	1069	1068	1067	1066	1065	1064	1063	1062	1061	1060	1059	1058	1057	1056	1055	1054	1053	1052	1051	1050	1049	1048	1047	1046	1045	1044	1043	1042	1041	1040	1039	1038	1037	1036	1035	1034	1033	1032	1031	1030	1029	1028	1027	1026	1025	1024	1023	1022	1021	1020	1019	1018	1017	1016	1015	1014	1013	1012	1011	1010	1009	1008	1007	1006	1005	1004	1003	1002	1001	1000	999	998	997	996	995	994	993	992	991	990	989	988	987	986	985	984	983	982	981	980	979	978	977	976	975	974	973	972	971	970	969	968	967	966	965	964	963	962	961	960	959	958	957	956	955	954	953	952	951	950	949	948	947	946	945	944	943	942	941	940	939	938	937	936	935	934	933	932	931	930	929	928	927	926	925	924	923	922	921	920	919	918	917	916	915	914	913	912	911	910	909	908	907	906	905	904	903	902	901	900	899	898	897	896	895	894	893	892	891	890	889	888	887	886	885	884	883	882	881	880	879	878	877	876	875	874	873	872	871	870	869	868	867	866	865	864	863	862	861	860	859	858	857	856	855	854	853	852	851	850	849	848	847	846	845	844	843	842	841	840	839	838	837	836	835	834	833	832	831	830	829	828	827	826	825	824	823	822	821	820	819	818	817	816	815	814	813	812	811	810	809	808	807	806	805	804	803	802	801	800	799	798	797	796	795	794	793	792	791	790	789	788	787	786	785	784	783	782	781	780	779	778	777	776	775	774	773	772	771	770	769	768	767	766	765	764	763	762	761	760	759	758	757	756	755	754	753	752	751	750	749	748	747	746	745	744	743	742	741	740	739	738	737	736	735	734	733	732	731	730	729	728	727	726	725	724	723	722	721	720	719	718	717	716	715	714	713	712	711	710	709	708	707	706	705	704	703	702	701	700	699	698	697	696	695	694	693	692	691	690	689	688	687	686	685	684	683	682	681	680	679	678	677	676	675	674	673	672	671	670	669	668	667	666	665	664	663	662	661	660	659	658	657	656	655	654	653	652	651	650	649	648	647	646	645	644	643	642	641	640	639	638	637	636	635	634	633	632	631	630	629	628	627	626	625	624	623	622	621	620	619	618	617	616	615	614	613	612	611	610	609
------------------------	-------------------------	------	------	------	------	------	------	------	------	------	------	------	------	------	------	------	------	------	------	------	------	------	------	------	------	------	------	------	------	------	------	------	------	------	------	------	------	------	------	------	------	------	------	------	------	------	------	------	------	------	------	------	------	------	------	------	------	------	------	------	------	------	------	------	------	------	------	------	------	------	------	------	------	------	------	------	------	------	------	------	------	------	------	------	------	------	------	------	------	------	------	------	------	------	------	------	------	------	------	------	------	------	------	------	------	------	------	------	------	------	------	------	------	------	------	------	------	------	------	------	------	------	------	------	------	------	------	------	------	------	------	------	------	------	------	------	------	------	------	------	------	------	------	------	------	------	------	------	------	------	------	------	------	------	------	------	------	------	------	------	------	------	------	------	------	------	------	------	------	------	------	------	------	------	------	------	------	------	------	------	------	------	------	------	------	------	------	------	------	------	------	------	------	------	------	------	------	------	------	------	------	------	------	------	------	------	------	------	------	------	------	------	------	------	------	------	------	------	------	------	------	------	------	------	------	------	------	------	------	------	------	------	------	------	------	------	------	------	------	------	------	------	------	------	------	------	------	------	------	------	------	------	------	------	------	------	------	------	------	------	------	------	------	------	------	------	------	------	------	------	------	------	------	------	------	------	------	------	------	------	------	------	------	------	------	------	------	------	------	------	------	------	------	------	------	------	------	------	------	------	------	------	------	------	------	------	------	------	------	------	------	------	------	------	------	------	------	------	------	------	------	------	------	------	------	------	------	------	------	------	------	------	------	------	------	------	------	------	------	------	------	------	------	------	------	------	------	------	------	------	------	------	------	------	------	------	------	------	------	------	------	------	------	------	------	------	------	------	------	------	------	------	------	------	------	------	------	------	------	------	------	------	------	------	------	------	------	------	------	------	------	------	------	------	------	------	------	------	------	------	------	------	------	------	------	------	------	------	------	------	------	------	------	------	------	------	------	------	------	------	------	------	------	------	------	------	------	------	------	------	------	------	------	------	------	------	------	------	------	------	------	------	------	------	------	------	------	------	------	------	------	------	------	------	------	------	------	------	------	------	------	------	------	------	------	------	------	------	------	------	------	------	------	------	------	------	------	------	------	------	------	------	------	------	------	------	------	------	------	------	------	------	------	------	------	------	------	------	------	------	------	------	------	------	------	------	------	------	------	------	------	------	------	------	------	------	------	------	------	------	------	------	------	------	------	------	------	------	------	------	------	------	------	------	------	------	------	------	------	------	------	------	------	------	------	------	------	------	------	------	------	------	------	------	------	------	------	------	------	------	------	------	------	------	------	------	------	------	------	------	------	------	------	------	------	------	------	------	------	------	------	------	------	------	------	------	------	------	------	------	------	------	------	------	------	------	------	------	------	------	------	------	------	------	------	------	------	------	------	------	------	------	------	------	------	------	------	------	------	------	------	------	------	------	------	------	------	------	------	------	------	------	------	------	------	------	------	------	------	------	------	------	------	------	------	------	------	------	------	------	------	------	------	------	------	------	------	------	------	------	------	------	------	------	------	------	------	------	------	------	------	------	------	------	------	------	------	------	------	------	------	------	------	------	------	------	------	------	------	------	------	------	------	------	------	------	------	------	------	------	------	------	------	------	------	------	------	------	------	------	------	------	------	------	------	------	------	------	------	------	------	------	------	------	------	------	------	------	------	------	------	------	------	------	------	------	------	------	------	------	------	------	------	------	------	------	------	------	------	------	------	------	------	------	------	------	------	------	------	------	------	------	------	------	------	------	------	------	------	------	------	------	------	------	------	------	------	------	------	------	------	------	------	------	------	------	------	------	------	------	------	------	------	------	------	------	------	------	------	------	------	------	------	------	------	------	------	------	------	------	------	------	------	------	------	------	------	------	------	------	------	------	------	------	------	------	------	------	------	------	------	------	------	------	------	------	------	------	------	------	------	------	------	------	------	------	------	------	------	------	------	------	------	------	------	------	------	------	------	------	------	------	------	------	------	------	------	------	------	------	------	------	------	------	------	------	------	------	------	------	------	------	------	------	------	------	------	------	------	------	------	------	------	------	------	------	------	------	------	------	------	------	------	------	------	------	------	------	------	------	------	------	------	------	------	------	------	------	------	------	------	------	------	------	------	------	------	------	------	------	------	------	------	------	------	------	------	------	------	------	------	------	------	------	------	------	------	------	------	------	------	------	------	------	------	------	------	------	------	------	------	------	------	------	------	------	------	------	------	------	------	------	------	------	------	------	------	------	------	------	------	------	------	------	------	------	------	------	------	------	------	------	------	------	------	------	------	------	------	------	------	------	------	------	------	------	------	------	------	------	------	------	------	------	------	------	------	------	------	------	------	------	------	------	------	------	-----	-----	-----	-----	-----	-----	-----	-----	-----	-----	-----	-----	-----	-----	-----	-----	-----	-----	-----	-----	-----	-----	-----	-----	-----	-----	-----	-----	-----	-----	-----	-----	-----	-----	-----	-----	-----	-----	-----	-----	-----	-----	-----	-----	-----	-----	-----	-----	-----	-----	-----	-----	-----	-----	-----	-----	-----	-----	-----	-----	-----	-----	-----	-----	-----	-----	-----	-----	-----	-----	-----	-----	-----	-----	-----	-----	-----	-----	-----	-----	-----	-----	-----	-----	-----	-----	-----	-----	-----	-----	-----	-----	-----	-----	-----	-----	-----	-----	-----	-----	-----	-----	-----	-----	-----	-----	-----	-----	-----	-----	-----	-----	-----	-----	-----	-----	-----	-----	-----	-----	-----	-----	-----	-----	-----	-----	-----	-----	-----	-----	-----	-----	-----	-----	-----	-----	-----	-----	-----	-----	-----	-----	-----	-----	-----	-----	-----	-----	-----	-----	-----	-----	-----	-----	-----	-----	-----	-----	-----	-----	-----	-----	-----	-----	-----	-----	-----	-----	-----	-----	-----	-----	-----	-----	-----	-----	-----	-----	-----	-----	-----	-----	-----	-----	-----	-----	-----	-----	-----	-----	-----	-----	-----	-----	-----	-----	-----	-----	-----	-----	-----	-----	-----	-----	-----	-----	-----	-----	-----	-----	-----	-----	-----	-----	-----	-----	-----	-----	-----	-----	-----	-----	-----	-----	-----	-----	-----	-----	-----	-----	-----	-----	-----	-----	-----	-----	-----	-----	-----	-----	-----	-----	-----	-----	-----	-----	-----	-----	-----	-----	-----	-----	-----	-----	-----	-----	-----	-----	-----	-----	-----	-----	-----	-----	-----	-----	-----	-----	-----	-----	-----	-----	-----	-----	-----	-----	-----	-----	-----	-----	-----	-----	-----	-----	-----	-----	-----	-----	-----	-----	-----	-----	-----	-----	-----	-----	-----	-----	-----	-----	-----	-----	-----	-----	-----	-----	-----	-----	-----	-----	-----	-----	-----	-----	-----	-----	-----	-----	-----	-----	-----	-----	-----	-----	-----	-----	-----	-----	-----	-----	-----	-----	-----	-----	-----	-----	-----	-----	-----	-----	-----	-----	-----	-----	-----	-----	-----	-----	-----	-----	-----	-----	-----	-----	-----	-----	-----	-----	-----	-----	-----	-----	-----	-----	-----	-----	-----	-----	-----	-----	-----	-----	-----	-----	-----	-----	-----	-----	-----	-----	-----	-----	-----	-----	-----	-----	-----	-----	-----	-----	-----

The Development Test 1 of 81mm Smoke Cartridges (XM819, 3 projectiles, DT1X3)

7 : number of trials included in DOA

6 : time zone designation

40.20 : latitude (deg)

113.00 : longitude (deg)

602A : longitude (deg)

702A : longitude (deg)

801A : longitude (deg)

901A : longitude (deg)

1001A : longitude (deg)

1101A : longitude (deg)

1201A : longitude (deg)

1301A : longitude (deg)

1401A : longitude (deg)

1501A : longitude (deg)

1601A : longitude (deg)

1701A : longitude (deg)

1801A : longitude (deg)

1901A : longitude (deg)

2001A : longitude (deg)

2101A : longitude (deg)

2201A : longitude (deg)

2301A : longitude (deg)

2401A : longitude (deg)

2501A : longitude (deg)

2601A : longitude (deg)

2701A : longitude (deg)

2801A : longitude (deg)

2901A : longitude (deg)

3001A : longitude (deg)

3101A : longitude (deg)

3201A : longitude (deg)

3301A : longitude (deg)

3401A : longitude (deg)

3501A : longitude (deg)

3601A : longitude (deg)

3701A : longitude (deg)

3801A : longitude (deg)

3901A : longitude (deg)

4001A : longitude (deg)

4101A : longitude (deg)

4201A : longitude (deg)

4301A : longitude (deg)

4401A : longitude (deg)

4501A : longitude (deg)

4601A : longitude (deg)

4701A : longitude (deg)

4801A : longitude (deg)

4901A : longitude (deg)

5001A : longitude (deg)

5101A : longitude (deg)

5201A : longitude (deg)

5301A : longitude (deg)

5401A : longitude (deg)

5501A : longitude (deg)

5601A : longitude (deg)

5701A : longitude (deg)

5801A : longitude (deg)

5901A : longitude (deg)

6001A : longitude (deg)

6101A : longitude (deg)

6201A : longitude (deg)

6301A : longitude (deg)

6401A : longitude (deg)

6501A : longitude (deg)

6601A : longitude (deg)

6701A : longitude (deg)

6801A : longitude (deg)

6901A : longitude (deg)

7001A : longitude (deg)

7101A : longitude (deg)

7201A : longitude (deg)

7301A : longitude (deg)

7401A : longitude (deg)

7501A : longitude (deg)

7601A : longitude (deg)

7701A : longitude (deg)

7801A : longitude (deg)

7901A : longitude (deg)

8001A : longitude (deg)

8101A : longitude (deg)

8201A : longitude (deg)

8301A : longitude (deg)

8401A : longitude (deg)

8501A : longitude (deg)

8601A : longitude (deg)

8701A : longitude (deg)

8801A : longitude (deg)

8901A : longitude (deg)

9001A : longitude (deg)

-9.9902E+01	-9.9902E+01	-9.9902E+01	-9.9902E+01	-9.9902E+01	-9.9902E+01	1.0702E+05	9.0002E+04	LOS integrated dosage (mg-s/m ³ -2)	(m)
-21.7	-21.7	-21.7	-21.7	-21.7	-21.7	-21.7	-21.7	x-coord. of 1st end-point for LOS1	(m)
142.3	142.3	142.3	142.3	142.3	142.3	142.3	142.3	y-coord. of 1st end-point for LOS1	(m)
408.7	408.7	408.7	408.7	408.7	408.7	408.7	408.7	x-coord. of 2nd end-point for LOS1	(m)
-768.2	-768.2	-768.2	-768.2	-768.2	-768.2	-768.2	-768.2	y-coord. of 2nd end-point for LOS1	(m)
-99.9	-99.9	-99.9	-99.9	-99.9	-99.9	-99.9	-99.9	LOS integrated conc. (mg/m ³ -2)	(m)
-9.9902E+01	-9.9902E+01	-9.9902E+01	-9.9902E+01	-9.9902E+01	-9.9902E+01	-9.9902E+01	-9.9902E+01	LOS integrated dosage (mg-s/m ³ -2)	(m)
78.6	78.6	78.6	78.6	78.6	78.6	78.6	78.6	x-coord. of 1st end-point for LOS1	(m)
110.8	110.8	110.8	110.8	110.8	110.8	110.8	110.8	y-coord. of 1st end-point for LOS1	(m)
395.5	395.5	395.5	395.5	395.5	395.5	395.5	395.5	x-coord. of 2nd end-point for LOS1	(m)
-775.5	-775.5	-775.5	-775.5	-775.5	-775.5	-775.5	-775.5	y-coord. of 2nd end-point for LOS1	(m)
-99.9	-99.9	-99.9	-99.9	-99.9	-99.9	-99.9	-99.9	LOS integrated conc. (mg/m ³ -2)	(m)
-9.9902E+01	-9.9902E+01	-9.9902E+01	-9.9902E+01	-9.9902E+01	-9.9902E+01	-9.9902E+01	-9.9902E+01	LOS integrated dosage (mg-s/m ³ -2)	(m)

16. Number of trials included in ODA

10.10 : latitude (deg)

10.10 : longitude (deg)

10.10 : time zone designation

10.10 : trial ID

10.10 : trial ID

10.10 : trial ID

10.10 : trial ID

10.10 : trial ID

10.10 : trial ID

10.10 : trial ID

10.10 : trial ID

10.10 : trial ID

10.10 : trial ID

10.10 : trial ID

10.10 : trial ID

10.10 : trial ID

10.10 : trial ID

10.10 : trial ID

10.10 : trial ID

10.10 : trial ID

10.10 : trial ID

10.10 : trial ID

10.10 : trial ID

10.10 : trial ID

10.10 : trial ID

10.10 : trial ID

10.10 : trial ID

10.10 : trial ID

10.10 : trial ID

10.10 : trial ID

10.10 : trial ID

10.10 : trial ID

10.10 : trial ID

10.10 : trial ID

10.10 : trial ID

10.10 : trial ID

10.10 : trial ID

10.10 : trial ID

10.10 : trial ID

10.10 : trial ID

10.10 : trial ID

10.10 : trial ID

10.10 : trial ID

10.10 : trial ID

10.10 : trial ID

10.10 : trial ID

10.10 : trial ID

10.10 : trial ID

10.10 : trial ID

10.10 : trial ID

10.10 : trial ID

10.10 : trial ID

10.10 : trial ID

10.10 : trial ID

10.10 : trial ID

10.10 : trial ID

10.10 : trial ID

10.10 : trial ID

10.10 : trial ID

10.10 : trial ID

10.10 : trial ID

10.10 : trial ID

10.10 : trial ID

10.10 : trial ID

10.10 : trial ID

10.10 : trial ID

10.10 : trial ID

10.10 : trial ID

10.10 : trial ID

10.10 : trial ID

10.10 : trial ID

10.10 : trial ID

10.10 : trial ID

10.10 : trial ID

10.10 : trial ID

10.10 : trial ID

10.10 : trial ID

10.10 : trial ID

10.10 : trial ID

10.10 : trial ID

The Development Test I of Blame Smoke Cartridges (M375A2, 3 projectiles, DTIM3)

10 : number of trials included in DOA

6 : time zone designation

40.20 : latitude (deg)

113.00 : longitude (deg)

6018	6028	6038	7018	7028	8018	8028	11018	11028	trial ID
12	12	12	12	12	12	12	12	12	3 : month
17	22	23	23	23	23	23	23	23	9 : day
80	80	81	81	81	81	81	81	81	9 : year
15	15	15	15	15	15	15	15	15	14 : hour
37	34	34	34	34	34	34	34	34	45 : minute
3	3	3	3	3	3	3	3	3	3 : no. of sources
-48.8	-58.7	-58.7	-77.9	-46.1	-12.2	17.1	-88.0	-101.1	1 : x-coord. of source (m)
32.4	23.5	26.1	-94.6	-104.5	-114.2	-36.6	37.0	29.7	2 : y-coord. of source (m)
0.00	0.00	0.00	0.00	0.00	0.00	0.00	0.00	0.00	3 : source elevation (m)
-99.9	-99.9	-99.9	-99.9	-99.9	-99.9	-99.9	-99.9	-99.9	4 : emission rate (g/s)
120.0	120.0	120.0	120.0	120.0	120.0	120.0	120.0	120.0	5 : emission duration (s)
7.180	8.100	6.800	5.110	5.510	5.510	5.300	4.660	4.380	6 : total mass emitted (kg)
1.630	1.630	1.630	1.630	1.630	1.630	1.630	1.630	1.630	7 : sigm0 at the source (m)
0.930	0.930	0.930	0.930	0.930	0.930	0.930	0.930	0.930	8 : sigm0 at the source (m)
1.400	1.400	1.400	1.400	1.400	1.400	1.400	1.400	1.400	9 : sigm0 at the source (m)
-64.6	-47.2	-35.3	-35.3	-31.4	-16.3	-25.9	-58.6	-33.1	10 : x-coord. of source (m)
13.4	25.3	17.7	-101.6	-94.0	-89.3	-71.4	23.1	31.8	11 : y-coord. of source (m)
0.00	0.00	0.00	0.00	0.00	0.00	0.00	0.00	0.00	12 : source elevation (m)
-99.9	-99.9	-99.9	-99.9	-99.9	-99.9	-99.9	-99.9	-99.9	13 : emission rate (g/s)
120.0	120.0	120.0	120.0	120.0	120.0	120.0	120.0	120.0	14 : emission duration (s)
7.180	8.100	6.800	5.110	5.510	5.510	5.300	4.660	4.380	15 : total mass emitted (kg)
1.630	1.630	1.630	1.630	1.630	1.630	1.630	1.630	1.630	16 : sigm0 at the source (m)
0.930	0.930	0.930	0.930	0.930	0.930	0.930	0.930	0.930	17 : sigm0 at the source (m)
1.400	1.400	1.400	1.400	1.400	1.400	1.400	1.400	1.400	18 : sigm0 at the source (m)
-99.9	-99.9	-99.9	-99.9	-99.9	-99.9	-99.9	-99.9	-99.9	19 : ambient pressure (atm)
300.00	300.00	300.00	300.00	300.00	300.00	300.00	300.00	300.00	20 : relative humidity (%)
2.00	2.00	2.00	2.00	2.00	2.00	2.00	2.00	2.00	21 : temperature at level #1 (K)
-99.90	-99.90	-99.90	-99.90	-99.90	-99.90	-99.90	-99.90	-99.90	22 : temperature at level #2 (K)
-99.90	-99.90	-99.90	-99.90	-99.90	-99.90	-99.90	-99.90	-99.90	23 : measuring height for temperature #1 (m)
1.60	1.60	1.60	1.60	1.60	1.60	1.60	1.60	1.60	24 : measuring height for temperature #2 (m)
2.00	2.00	2.00	2.00	2.00	2.00	2.00	2.00	2.00	25 : wind speed (m/s) at a tower
1.40	1.40	1.40	1.40	1.40	1.40	1.40	1.40	1.40	26 : measuring height for wind data (m)
319.0	19.0	350.0	14.0	126.0	157.0	180.0	1.0	2.60	27 : domain-averaged wind speed (m/s)
-99.90	-99.90	-99.90	-99.90	-99.90	-99.90	-99.90	-99.90	-99.90	28 : domain-averaged wind direction (deg)
11.40	5.40	6.80	3.40	27.80	3.30	13.90	10.90	7.70	29 : domain-averaged sigma-u (deg)
-99.90	-99.90	-99.90	-99.90	-99.90	-99.90	-99.90	-99.90	-99.90	30 : domain-averaged sigma-phi (deg)
2.00	2.00	2.00	2.00	2.00	2.00	2.00	2.00	2.00	31 : measuring ht for domain-avg phi (deg)
308.0	123.0	145.0	296.0	172.0	165.0	181.0	134.0	164.0	32 : averaging time for domain-avg wind speed (m)
0.045	0.092	0.271	0.080	0.036	0.050	0.101	0.084	0.048	33 : wind speed power law exponent
0.0300	0.0300	0.0300	0.0300	0.0300	0.0300	0.0300	0.0300	0.0300	34 : surface roughness (m)
-99.9000	-99.9000	-99.9000	-99.9000	-99.9000	-99.9000	-99.9000	-99.9000	-99.9000	35 : friction velocity (m)
0.18	0.18	0.18	0.18	0.18	0.18	0.18	0.18	0.18	36 : inverse Monin-Obukhov length (1/m)
0.50	0.50	0.50	0.50	0.50	0.50	0.50	0.50	0.50	37 : albedo
0.50	0.50	0.50	0.50	0.50	0.50	0.50	0.50	0.50	38 : Bowen ratio
-99.9	-99.9	-99.9	-99.9	-99.9	-99.9	-99.9	-99.9	-99.9	39 : mixing height (m)
-99.9	-99.9	-99.9	-99.9	-99.9	-99.9	-99.9	-99.9	-99.9	40 : cloud cover (%)
120.0	120.0	120.0	120.0	120.0	120.0	120.0	120.0	120.0	41 : P-G stability class
1.50	1.50	1.50	1.50	1.50	1.50	1.50	1.50	1.50	42 : averaging time for concentration (s)
0	0	0	0	0	0	0	0	0	43 : suggested receptor height (m)
5	5	5	5	5	5	5	5	5	44 : no. of distances downwind
-247.7	-247.7	-247.7	-247.7	-247.7	-247.7	-247.7	-247.7	-247.7	45 : no. of lines-of-sight
-68.7	-68.7	-68.7	-68.7	-68.7	-68.7	-68.7	-68.7	-68.7	46 : x-coord. of 1st end-point for LOS1 (m)
1064.2	1064.2	1064.2	1064.2	1064.2	1064.2	1064.2	1064.2	1064.2	47 : y-coord. of 1st end-point for LOS1 (m)
658.5	658.5	658.5	658.5	658.5	658.5	658.5	658.5	658.5	48 : x-coord. of 2nd end-point for LOS1 (m)
-99.9	-99.9	-99.9	-99.9	-99.9	-99.9	-99.9	-99.9	-99.9	49 : y-coord. of 2nd end-point for LOS1 (m)
-9.9902E+01	-9.9902E+01	-9.9902E+01	-9.9902E+01	-9.9902E+01	-9.9902E+01	-9.9902E+01	-9.9902E+01	-9.9902E+01	50 : LOS integrated conc. (mg/m**2)
-189.6	-189.6	-189.6	-189.6	-189.6	-189.6	-189.6	-189.6	-189.6	51 : LOS integrated dosage (mg-m**2)
1122.4	1122.4	1122.4	1122.4	1122.4	1122.4	1122.4	1122.4	1122.4	52 : x-coord. of 1st end-point for LOS1 (m)
553.5	553.5	553.5	553.5	553.5	553.5	553.5	553.5	553.5	53 : y-coord. of 1st end-point for LOS1 (m)
9.5002E+04	9.5002E+04	9.5002E+04	9.5002E+04	9.5002E+04	9.5002E+04	9.5002E+04	9.5002E+04	9.5002E+04	54 : x-coord. of 2nd end-point for LOS1 (m)
-152.9	-152.9	-152.9	-152.9	-152.9	-152.9	-152.9	-152.9	-152.9	55 : y-coord. of 2nd end-point for LOS1 (m)
69.6	69.6	69.6	69.6	69.6	69.6	69.6	69.6	69.6	56 : LOS integrated dosage (mg-m**2)
421.8	421.8	421.8	421.8	421.8	421.8	421.8	421.8	421.8	57 : x-coord. of 1st end-point for LOS1 (m)
-760.9	-760.9	-760.9	-760.9	-760.9	-760.9	-760.9	-760.9	-760.9	58 : y-coord. of 1st end-point for LOS1 (m)
-99.9	-99.9	-99.9	-99.9	-99.9	-99.9	-99.9	-99.9	-99.9	59 : x-coord. of 2nd end-point for LOS1 (m)
-99.9	-99.9	-99.9	-99.9	-99.9	-99.9	-99.9	-99.9	-99.9	60 : y-coord. of 2nd end-point for LOS1 (m)

The Evaluation of the 18 Series Grenades (L81A1)

7 : number of trials included in DUA

6 : time zone designation

40.20 : latitude (deg)

113.00 : longitude (deg)

BB2	BB3	BB4	BB5	BB6	BB7	BB8	trial ID
6	6	6	6	6	6	6	6
10	10	10	10	10	15	15	17
81	81	81	81	81	81	81	81
11	11	12	13	14	11	11	11
51	51	59	51	29	22	22	18
1	1	1	1	1	1	1	1
-62.9	-24.4	-24.4	-24.4	-24.4	-45.4	-45.4	-24.4
68.0	89.4	89.4	89.4	89.4	77.7	77.7	89.4
0.00	0.00	0.00	0.00	0.00	0.00	0.00	0.00
-99.9	-99.9	-99.9	-99.9	-99.9	-99.9	-99.9	-99.9
251.0	251.0	251.0	251.0	251.0	251.0	251.0	251.0
0.859	0.859	0.840	0.840	0.840	0.878	0.878	0.859
9.387	4.224	6.857	8.154	0.491	11.425	11.425	2.407
13.758	16.112	15.180	14.524	16.649	12.120	12.120	16.482
0.120	0.120	0.120	0.120	0.120	0.120	0.120	0.120
-99.9	-99.9	-99.9	-99.9	-99.9	-99.9	-99.9	-99.9
-99.9	-99.9	-99.9	-99.9	-99.9	-99.9	-99.9	-99.9
300.00	300.00	300.00	300.00	300.00	300.00	300.00	300.00
2.00	2.00	2.00	2.00	2.00	2.00	2.00	2.00
-99.90	-99.90	-99.90	-99.90	-99.90	-99.90	-99.90	-99.90
-99.90	-99.90	-99.90	-99.90	-99.90	-99.90	-99.90	-99.90
3.10	3.80	2.80	3.60	3.20	2.20	2.20	5.60
2.00	2.00	2.00	2.00	2.00	2.00	2.00	2.00
3.10	3.80	2.80	3.60	3.20	2.20	2.20	5.60
35.0	24.0	34.0	34.0	11.0	326.0	326.0	1.0
-99.90	-99.90	-99.90	-99.90	-99.90	-99.90	-99.90	-99.90
13.70	10.70	28.80	28.10	16.40	24.30	24.30	10.10
-99.90	-99.90	-99.90	-99.90	-99.90	-99.90	-99.90	-99.90
2.00	2.00	2.00	2.00	2.00	2.00	2.00	2.00
261.0	232.0	245.0	255.0	281.0	600.0	600.0	211.0
0.048	0.047	0.079	0.073	0.106	0.019	0.019	0.042
0.0300	0.0300	0.0300	0.0300	0.0300	0.0300	0.0300	0.0300
-99.900	-99.900	-99.900	-99.900	-99.900	-99.900	-99.900	-99.900
-99.9000	-99.9000	-99.9000	-99.9000	-99.9000	-99.9000	-99.9000	-99.9000
0.18	0.18	0.18	0.18	0.18	0.18	0.18	0.18
0.50	0.50	0.50	0.50	0.50	0.50	0.50	0.50
0.50	0.50	0.50	0.50	0.50	0.50	0.50	0.50
-99.9	-99.9	-99.9	-99.9	-99.9	-99.9	-99.9	-99.9
-99.9	-99.9	-99.9	-99.9	-99.9	-99.9	-99.9	-99.9
-99.9	-99.9	-99.9	-99.9	-99.9	-99.9	-99.9	-99.9
251.0	251.0	251.0	251.0	251.0	251.0	251.0	251.0
1.00	1.00	1.00	1.00	1.00	1.00	1.00	1.00
2	2	2	2	2	2	2	2
-247.7	-247.7	-247.7	-247.7	-247.7	-247.7	-247.7	-247.7
-68.7	-68.7	-68.7	-68.7	-68.7	-68.7	-68.7	-68.7
189.6	189.6	189.6	189.6	189.6	189.6	189.6	189.6
173.7	173.7	173.7	173.7	173.7	173.7	173.7	173.7
-99.9	-99.9	-99.9	-99.9	-99.9	-99.9	-99.9	-99.9
2.510E+04	5.300E+04	2.840E+04	3.490E+04	5.140E+04	1.700E+04	5.070E+04	5.070E+04
-189.6	-189.6	-189.6	-189.6	-189.6	-189.6	-189.6	-189.6
-173.7	-173.7	-173.7	-173.7	-173.7	-173.7	-173.7	-173.7
247.7	247.7	247.7	247.7	247.7	247.7	247.7	247.7
68.7	68.7	68.7	68.7	68.7	68.7	68.7	68.7
-99.9	-99.9	-99.9	-99.9	-99.9	-99.9	-99.9	-99.9
6.500E+03	-9.990E+01	7.600E+03	-9.990E+01	-9.990E+01	6.400E+03	2.490E+04	2.490E+04

The Evaluation of the 18 Series Grenades (L8181)

6 : number of trials included in DWA

6 : time zone designation

40.20 : latitude (deg)

113.00 : longitude (deg)

8811	8812	8813	8814	8815	8816	8817	8818	8819	8820	8821	8822	8823	8824	8825	8826	8827	8828	8829	8830	8831	8832	8833	8834	8835	8836	8837	8838	8839	8840	8841	8842	8843	8844	8845	8846	8847	8848	8849	8850	8851	8852	8853	8854	8855	8856	8857	8858	8859	8860	8861	8862	8863	8864	8865	8866	8867	8868	8869	8870	8871	8872	8873	8874	8875	8876	8877	8878	8879	8880	8881	8882	8883	8884	8885	8886	8887	8888	8889	8890	8891	8892	8893	8894	8895	8896	8897	8898	8899	8900	8901	8902	8903	8904	8905	8906	8907	8908	8909	8910	8911	8912	8913	8914	8915	8916	8917	8918	8919	8920	8921	8922	8923	8924	8925	8926	8927	8928	8929	8930	8931	8932	8933	8934	8935	8936	8937	8938	8939	8940	8941	8942	8943	8944	8945	8946	8947	8948	8949	8950	8951	8952	8953	8954	8955	8956	8957	8958	8959	8960	8961	8962	8963	8964	8965	8966	8967	8968	8969	8970	8971	8972	8973	8974	8975	8976	8977	8978	8979	8980	8981	8982	8983	8984	8985	8986	8987	8988	8989	8990	8991	8992	8993	8994	8995	8996	8997	8998	8999	9000	9001	9002	9003	9004	9005	9006	9007	9008	9009	9010	9011	9012	9013	9014	9015	9016	9017	9018	9019	9020	9021	9022	9023	9024	9025	9026	9027	9028	9029	9030	9031	9032	9033	9034	9035	9036	9037	9038	9039	9040	9041	9042	9043	9044	9045	9046	9047	9048	9049	9050	9051	9052	9053	9054	9055	9056	9057	9058	9059	9060	9061	9062	9063	9064	9065	9066	9067	9068	9069	9070	9071	9072	9073	9074	9075	9076	9077	9078	9079	9080	9081	9082	9083	9084	9085	9086	9087	9088	9089	9090	9091	9092	9093	9094	9095	9096	9097	9098	9099	9100	9101	9102	9103	9104	9105	9106	9107	9108	9109	9110	9111	9112	9113	9114	9115	9116	9117	9118	9119	9120	9121	9122	9123	9124	9125	9126	9127	9128	9129	9130	9131	9132	9133	9134	9135	9136	9137	9138	9139	9140	9141	9142	9143	9144	9145	9146	9147	9148	9149	9150	9151	9152	9153	9154	9155	9156	9157	9158	9159	9160	9161	9162	9163	9164	9165	9166	9167	9168	9169	9170	9171	9172	9173	9174	9175	9176	9177	9178	9179	9180	9181	9182	9183	9184	9185	9186	9187	9188	9189	9190	9191	9192	9193	9194	9195	9196	9197	9198	9199	9200	9201	9202	9203	9204	9205	9206	9207	9208	9209	9210	9211	9212	9213	9214	9215	9216	9217	9218	9219	9220	9221	9222	9223	9224	9225	9226	9227	9228	9229	9230	9231	9232	9233	9234	9235	9236	9237	9238	9239	9240	9241	9242	9243	9244	9245	9246	9247	9248	9249	9250	9251	9252	9253	9254	9255	9256	9257	9258	9259	9260	9261	9262	9263	9264	9265	9266	9267	9268	9269	9270	9271	9272	9273	9274	9275	9276	9277	9278	9279	9280	9281	9282	9283	9284	9285	9286	9287	9288	9289	9290	9291	9292	9293	9294	9295	9296	9297	9298	9299	9300	9301	9302	9303	9304	9305	9306	9307	9308	9309	9310	9311	9312	9313	9314	9315	9316	9317	9318	9319	9320	9321	9322	9323	9324	9325	9326	9327	9328	9329	9330	9331	9332	9333	9334	9335	9336	9337	9338	9339	9340	9341	9342	9343	9344	9345	9346	9347	9348	9349	9350	9351	9352	9353	9354	9355	9356	9357	9358	9359	9360	9361	9362	9363	9364	9365	9366	9367	9368	9369	9370	9371	9372	9373	9374	9375	9376	9377	9378	9379	9380	9381	9382	9383	9384	9385	9386	9387	9388	9389	9390	9391	9392	9393	9394	9395	9396	9397	9398	9399	9400	9401	9402	9403	9404	9405	9406	9407	9408	9409	9410	9411	9412	9413	9414	9415	9416	9417	9418	9419	9420	9421	9422	9423	9424	9425	9426	9427	9428	9429	9430	9431	9432	9433	9434	9435	9436	9437	9438	9439	9440	9441	9442	9443	9444	9445	9446	9447	9448	9449	9450	9451	9452	9453	9454	9455	9456	9457	9458	9459	9460	9461	9462	9463	9464	9465	9466	9467	9468	9469	9470	9471	9472	9473	9474	9475	9476	9477	9478	9479	9480	9481	9482	9483	9484	9485	9486	9487	9488	9489	9490	9491	9492	9493	9494	9495	9496	9497	9498	9499	9500	9501	9502	9503	9504	9505	9506	9507	9508	9509	9510	9511	9512	9513	9514	9515	9516	9517	9518	9519	9520	9521	9522	9523	9524	9525	9526	9527	9528	9529	9530	9531	9532	9533	9534	9535	9536	9537	9538	9539	9540	9541	9542	9543	9544	9545	9546	9547	9548	9549	9550	9551	9552	9553	9554	9555	9556	9557	9558	9559	9560	9561	9562	9563	9564	9565	9566	9567	9568	9569	9570	9571	9572	9573	9574	9575	9576	9577	9578	9579	9580	9581	9582	9583	9584	9585	9586	9587	9588	9589	9590	9591	9592	9593	9594	9595	9596	9597	9598	9599	9600	9601	9602	9603	9604	9605	9606	9607	9608	9609	9610	9611	9612	9613	9614	9615	9616	9617	9618	9619	9620	9621	9622	9623	9624	9625	9626	9627	9628	9629	9630	9631	9632	9633	9634	9635	9636	9637	9638	9639	9640	9641	9642	9643	9644	9645	9646	9647	9648	9649	9650	9651	9652	9653	9654	9655	9656	9657	9658	9659	9660	9661	9662	9663	9664	9665	9666	9667	9668	9669	9670	9671	9672	9673	9674	9675	9676	9677	9678	9679	9680	9681	9682	9683	9684	9685	9686	9687	9688	9689	9690	9691	9692	9693	9694	9695	9696	9697	9698	9699	9700	9701	9702	9703	9704	9705	9706	9707	9708	9709	9710	9711	9712	9713	9714	9715	9716	9717	9718	9719	9720	9721	9722	9723	9724	9725	9726	9727	9728	9729	9730	9731	9732	9733	9734	9735	9736	9737	9738	9739	9740	9741	9742	9743	9744	9745	9746	9747	9748	9749	9750	9751	9752	9753	9754	9755	9756	9757	9758	9759	9760	9761	9762	9763	9764	9765	9766	9767	9768	9769	9770	9771	9772	9773	9774	9775	9776	9777	9778	9779	9780	9781	9782	9783	9784	9785	9786	9787	9788	9789	9790	9791	9792	9793	9794	9795	9796	9797	9798	9799	9800	9801	9802	9803	9804	9805	9806	9807	9808	9809	9810	9811	9812	9813	9814	9815	9816	9817	9818	9819	9820	9821	9822	9823	9824	9825	9826	9827	9828	9829	9830	9831	9832	9833	9834	9835	9836	9837	9838	9839	9840	9841	9842	9843	9844	9845	9846	9847	9848	9849	9850	9851	9852	9853	9854	9855	9856	9857	9858	9859	9860	9861	9862	9863	9864	9865	9866	9867	9868	9869	9870	9871	9872	9873	9874	9875	9876	9877	9878	9879	9880	9881	9882	9883	9884	9885	9886	9887	9888	9889	9890	9891	9892	9893	9894	9895	9896	9897	9898	9899	9900	9901	9902	9903	9904	9905	9906	9907	9908	9909	9910	9911	9912	9913	9914	9915	9916	9917	9918	9919	9920	9921	9922	9923	9924	9925	9926	9927	9928	9929	9930	9931	9932	9933	9934	9935	9936	9937	9938	9939	9940	9941	9942	9943	9944	9945	9946	9947	9948	9949	9950	9951	9952	9953	9954	9955	9956	9957	9958	9959	9960	9961	9962	9963	9964	9965	9966	9967	9968	9969	9970	9971	9972	9973	9974	9975	9976	9977	9978	9979	9980	9981	9982	9983	9984	9985	9986	9987	9988	9989	9990	9991	9992	9993	9994	9995	9996	9997	9998	9999	10000
------	------	------	------	------	------	------	------	------	------	------	------	------	------	------	------	------	------	------	------	------	------	------	------	------	------	------	------	------	------	------	------	------	------	------	------	------	------	------	------	------	------	------	------	------	------	------	------	------	------	------	------	------	------	------	------	------	------	------	------	------	------	------	------	------	------	------	------	------	------	------	------	------	------	------	------	------	------	------	------	------	------	------	------	------	------	------	------	------	------	------	------	------	------	------	------	------	------	------	------	------	------	------	------	------	------	------	------	------	------	------	------	------	------	------	------	------	------	------	------	------	------	------	------	------	------	------	------	------	------	------	------	------	------	------	------	------	------	------	------	------	------	------	------	------	------	------	------	------	------	------	------	------	------	------	------	------	------	------	------	------	------	------	------	------	------	------	------	------	------	------	------	------	------	------	------	------	------	------	------	------	------	------	------	------	------	------	------	------	------	------	------	------	------	------	------	------	------	------	------	------	------	------	------	------	------	------	------	------	------	------	------	------	------	------	------	------	------	------	------	------	------	------	------	------	------	------	------	------	------	------	------	------	------	------	------	------	------	------	------	------	------	------	------	------	------	------	------	------	------	------	------	------	------	------	------	------	------	------	------	------	------	------	------	------	------	------	------	------	------	------	------	------	------	------	------	------	------	------	------	------	------	------	------	------	------	------	------	------	------	------	------	------	------	------	------	------	------	------	------	------	------	------	------	------	------	------	------	------	------	------	------	------	------	------	------	------	------	------	------	------	------	------	------	------	------	------	------	------	------	------	------	------	------	------	------	------	------	------	------	------	------	------	------	------	------	------	------	------	------	------	------	------	------	------	------	------	------	------	------	------	------	------	------	------	------	------	------	------	------	------	------	------	------	------	------	------	------	------	------	------	------	------	------	------	------	------	------	------	------	------	------	------	------	------	------	------	------	------	------	------	------	------	------	------	------	------	------	------	------	------	------	------	------	------	------	------	------	------	------	------	------	------	------	------	------	------	------	------	------	------	------	------	------	------	------	------	------	------	------	------	------	------	------	------	------	------	------	------	------	------	------	------	------	------	------	------	------	------	------	------	------	------	------	------	------	------	------	------	------	------	------	------	------	------	------	------	------	------	------	------	------	------	------	------	------	------	------	------	------	------	------	------	------	------	------	------	------	------	------	------	------	------	------	------	------	------	------	------	------	------	------	------	------	------	------	------	------	------	------	------	------	------	------	------	------	------	------	------	------	------	------	------	------	------	------	------	------	------	------	------	------	------	------	------	------	------	------	------	------	------	------	------	------	------	------	------	------	------	------	------	------	------	------	------	------	------	------	------	------	------	------	------	------	------	------	------	------	------	------	------	------	------	------	------	------	------	------	------	------	------	------	------	------	------	------	------	------	------	------	------	------	------	------	------	------	------	------	------	------	------	------	------	------	------	------	------	------	------	------	------	------	------	------	------	------	------	------	------	------	------	------	------	------	------	------	------	------	------	------	------	------	------	------	------	------	------	------	------	------	------	------	------	------	------	------	------	------	------	------	------	------	------	------	------	------	------	------	------	------	------	------	------	------	------	------	------	------	------	------	------	------	------	------	------	------	------	------	------	------	------	------	------	------	------	------	------	------	------	------	------	------	------	------	------	------	------	------	------	------	------	------	------	------	------	------	------	------	------	------	------	------	------	------	------	------	------	------	------	------	------	------	------	------	------	------	------	------	------	------	------	------	------	------	------	------	------	------	------	------	------	------	------	------	------	------	------	------	------	------	------	------	------	------	------	------	------	------	------	------	------	------	------	------	------	------	------	------	------	------	------	------	------	------	------	------	------	------	------	------	------	------	------	------	------	------	------	------	------	------	------	------	------	------	------	------	------	------	------	------	------	------	------	------	------	------	------	------	------	------	------	------	------	------	------	------	------	------	------	------	------	------	------	------	------	------	------	------	------	------	------	------	------	------	------	------	------	------	------	------	------	------	------	------	------	------	------	------	------	------	------	------	------	------	------	------	------	------	------	------	------	------	------	------	------	------	------	------	------	------	------	------	------	------	------	------	------	------	------	------	------	------	------	------	------	------	------	------	------	------	------	------	------	------	------	------	------	------	------	------	------	------	------	------	------	------	------	------	------	------	------	------	------	------	------	------	------	------	------	------	------	------	------	------	------	------	------	------	------	------	------	------	------	------	------	------	------	------	------	------	------	------	------	------	------	------	------	------	------	------	------	------	------	------	------	------	------	------	------	------	------	------	------	------	------	------	------	------	------	------	------	------	------	------	------	------	------	------	------	------	------	------	------	------	------	------	------	------	------	------	------	------	------	------	------	------	------	------	------	------	------	------	------	------	------	------	------	------	------	------	------	------	------	------	------	------	------	------	------	------	------	------	------	------	------	------	------	------	------	------	------	------	------	------	------	------	------	------	------	------	------	------	------	------	------	------	------	------	------	------	------	------	------	------	------	------	------	------	------	------	------	------	------	------	------	------	------	------	------	------	------	------	------	------	------	------	------	------	------	------	------	------	------	------	------	------	------	------	------	------	------	------	------	------	------	------	------	------	------	------	------	------	------	------	------	------	------	------	------	------	------	------	------	------	------	------	------	------	------	------	------	------	------	------	------	------	------	------	------	------	------	------	------	------	------	------	------	------	------	------	------	------	------	------	------	------	------	------	------	------	------	------	------	------	------	------	------	------	------	------	------	------	------	------	------	------	------	------	------	------	------	------	------	------	------	------	------	------	------	-------

The Evaluation of the 18 Series Grenades (18IC1)

6 : number of trials included in DUA

6 : time zone designation

40.20 : latitude (deg)

113.00 : longitude (deg)

8821	8822	8825	8826	8828	8830 : trial ID
6	6	6	6	6	17 : month
8	10	10	10	16	17 : day
81	81	81	81	81	81 : year
13	10	13	14	11	12 : hour
25	6	37	56	22	5 : minute
1	1	1	1	1	1 : no. of sources
34.0	-25.3	-25.3	-25.3	34.0	-20.9 : x-coord. of source (m)
-84.0	88.9	88.9	88.9	-84.0	91.3 : y-coord. of source (m)
0.00	0.00	0.00	0.00	0.00	0.00 : source elevation (m)
-99.9	-99.9	-99.9	-99.9	-99.9	-99.9 : emission rate (g/s)
126.0	126.0	126.0	126.0	126.0	126.0 : emission duration (s)
0.820	0.897	0.840	0.859	0.763	0.859 : total mass emitted (kg)
4.144	5.326	7.128	5.557	7.769	4.384 : sign0 at the source (m)
13.734	13.320	12.449	13.225	12.059	13.859 : sign0 at the source (m)
0.120	0.120	0.120	0.120	0.120	0.120 : sign0 at the source (m)
-99.9	-99.9	-99.9	-99.9	-99.9	-99.9 : ambient pressure (atm)
-99.9	-99.9	-99.9	-99.9	-99.9	-99.9 : relative humidity (%)
300.00	300.00	300.00	300.00	300.00	300.00 : temperature at level #1 (K)
2.00	2.00	2.00	2.00	2.00	2.00 : measuring height for temperature #1 (m)
-99.90	-99.90	-99.90	-99.90	-99.90	-99.90 : temperature at level #2 (K)
-99.90	-99.90	-99.90	-99.90	-99.90	-99.90 : measuring height for temperature #2 (m)
3.90	3.60	4.00	5.10	7.30	3.30 : wind speed (m/s) at a tower
2.00	2.00	2.00	2.00	2.00	2.00 : measuring height for wind data (m)
3.90	3.60	4.00	5.10	7.30	3.30 : domain-averaged wind speed (m/s)
175.0	350.0	342.0	349.0	159.0	354.0 : domain-averaged wind direction (deg)
-99.90	-99.90	-99.90	-99.90	-99.90	-99.90 : domain-averaged sigma-u (m/s)
16.00	17.90	11.50	6.50	6.70	20.40 : domain-averaged sigma-theta (deg)
-99.90	-99.90	-99.90	-99.90	-99.90	-99.90 : domain-averaged sigma-phi (deg)
2.00	2.00	2.00	2.00	2.00	2.00 : measuring ht for domain-avg wind speed (m)
236.0	600.0	221.0	223.0	165.0	230.0 : averaging time for domain-avg wind speed (s)
0.080	0.020	0.067	0.075	0.083	0.116 : wind speed power law exponent
0.0300	0.0300	0.0300	0.0300	0.0300	0.0300 : surface roughness (m)
-99.9000	-99.9000	-99.9000	-99.9000	-99.9000	-99.9000 : friction velocity (m)
-99.9000	-99.9000	-99.9000	-99.9000	-99.9000	-99.9000 : Inverse Monin-Obukhov length (1/m)
0.18	0.18	0.18	0.18	0.18	0.18 : albedo
0.50	0.50	0.50	0.50	0.50	0.50 : moisture availability
0.50	0.50	0.50	0.50	0.50	0.50 : Bowen ratio
-99.9	-99.9	-99.9	-99.9	-99.9	-99.9 : mixing height (m)
-99.9	-99.9	-99.9	-99.9	-99.9	-99.9 : cloud cover (%)
-99	-99	-99	-99	-99	-99 : P-G stability class
126.0	126.0	126.0	126.0	126.0	126.0 : averaging time for concentration (s)
1.00	1.00	1.00	1.00	1.00	1.00 : suggested receptor height (m)
0	0	0	0	0	0 : no. of distances downwind
2	2	2	2	2	2 : no. of lines-of-sight
-247.7	-247.7	-247.7	-247.7	-247.7	-247.7 : x-coord. of 1st end-point for LOS1 (m)
-68.7	-68.7	-68.7	-68.7	-68.7	-68.7 : y-coord. of 1st end-point for LOS1 (m)
189.6	189.6	189.6	189.6	189.6	189.6 : x-coord. of 2nd end-point for LOS1 (m)
173.7	173.7	173.7	173.7	173.7	173.7 : y-coord. of 2nd end-point for LOS1 (m)
-99.9	-99.9	-99.9	-99.9	-99.9	-99.9 : LOS integrated conc. (mg/m**2)
3.670E+04	3.670E+04	3.670E+04	3.670E+04	3.670E+04	3.670E+04 : LOS integrated dosage (mg-s/m**2)
-189.6	-189.6	-189.6	-189.6	-189.6	-189.6 : x-coord. of 1st end-point for LOS1 (m)
-173.7	-173.7	-173.7	-173.7	-173.7	-173.7 : y-coord. of 1st end-point for LOS1 (m)
247.7	247.7	247.7	247.7	247.7	247.7 : x-coord. of 2nd end-point for LOS1 (m)
68.7	68.7	68.7	68.7	68.7	68.7 : y-coord. of 2nd end-point for LOS1 (m)
-99.9	-99.9	-99.9	-99.9	-99.9	-99.9 : LOS integrated conc. (mg/m**2)
1.870E+04	1.870E+04	1.870E+04	1.870E+04	1.870E+04	1.870E+04 : LOS integrated dosage (mg-s/m**2)

The Evaluation of the LA Series Grenades (L8101)

2 : number of trials included in DUA

6 : time zone designation

40.20 : latitude (deg)

113.00 : longitude (deg)

BB32 : latitude (deg)

BB33 : longitude (deg)

BB34 : latitude (deg)

BB35 : longitude (deg)

BB36 : latitude (deg)

BB37 : longitude (deg)

BB38 : latitude (deg)

BB39 : longitude (deg)

BB40 : latitude (deg)

BB41 : longitude (deg)

BB42 : latitude (deg)

BB43 : longitude (deg)

BB44 : latitude (deg)

BB45 : longitude (deg)

BB46 : latitude (deg)

BB47 : longitude (deg)

BB48 : latitude (deg)

BB49 : longitude (deg)

BB50 : latitude (deg)

BB51 : longitude (deg)

BB52 : latitude (deg)

BB53 : longitude (deg)

BB54 : latitude (deg)

BB55 : longitude (deg)

BB56 : latitude (deg)

BB57 : longitude (deg)

BB58 : latitude (deg)

BB59 : longitude (deg)

BB60 : latitude (deg)

BB61 : longitude (deg)

BB62 : latitude (deg)

BB63 : longitude (deg)

BB64 : latitude (deg)

BB65 : longitude (deg)

BB66 : latitude (deg)

BB67 : longitude (deg)

BB68 : latitude (deg)

BB69 : longitude (deg)

BB70 : latitude (deg)

BB71 : longitude (deg)

BB72 : latitude (deg)

BB73 : longitude (deg)

BB74 : latitude (deg)

BB75 : longitude (deg)

BB76 : latitude (deg)

BB77 : longitude (deg)

BB78 : latitude (deg)

BB79 : longitude (deg)

BB80 : latitude (deg)

BB81 : longitude (deg)

BB82 : latitude (deg)

BB83 : longitude (deg)

BB84 : latitude (deg)

BB85 : longitude (deg)

BB86 : latitude (deg)

BB87 : longitude (deg)

BB88 : latitude (deg)

BB89 : longitude (deg)

BB90 : latitude (deg)

BB91 : longitude (deg)

BB92 : latitude (deg)

BB93 : longitude (deg)

BB94 : latitude (deg)

BB95 : longitude (deg)

BB96 : latitude (deg)

BB97 : longitude (deg)

BB98 : latitude (deg)

BB99 : longitude (deg)

BB100 : latitude (deg)

BB101 : longitude (deg)

BB102 : latitude (deg)

BB103 : longitude (deg)

BB104 : latitude (deg)

BB105 : longitude (deg)

BB106 : latitude (deg)

BB107 : longitude (deg)

BB108 : latitude (deg)

BB109 : longitude (deg)

BB110 : latitude (deg)

BB111 : longitude (deg)

BB112 : latitude (deg)

BB113 : longitude (deg)

BB114 : latitude (deg)

BB115 : longitude (deg)

BB116 : latitude (deg)

BB117 : longitude (deg)

The Evaluation of the 18 Series Grenada (L112)

6 : number of trials included in DUA

6 : time zone designation

40.20 : latitude (deg)

113.00 : longitude (deg)

8841	8842	8843	8844	8845	8846	trial ID
16	16	16	16	16	16	6 : month
81	81	81	81	81	81	16 : day
8	8	8	8	8	8	81 : year
4	4	4	4	4	4	9 : hour
12	12	12	12	12	12	10 : minute
67.7	64.2	57.3	70.2	62.4	62.4	12 : no. of sources
-118.0	-119.9	-123.7	-116.6	-120.9	-120.9	62.4 : x-coord. of source (m)
0.00	0.00	0.00	0.00	0.00	0.00	-120.9 : y-coord. of source (m)
-99.9	-99.9	-99.9	-99.9	-99.9	-99.9	0.00 : source elevation (m)
251.0	251.0	199.0	199.0	126.0	126.0	-99.9 : emission rate (g/s)
6.053	3.942	3.468	3.468	3.420	3.420	0.781 : total mass emitted (kg)
15.518	16.183	19.992	19.992	13.932	13.932	1.397 : sigx0 at the source (m)
97.6	34.2	90.8	38.7	92.9	92.9	13.432 : sigy0 at the source (m)
-144.0	-144.0	-152.9	-87.4	-147.4	-147.4	0.120 : sigz0 at the source (m)
0.00	0.00	0.00	0.00	0.00	0.00	92.9 : x-coord. of source (m)
-99.9	-99.9	-99.9	-99.9	-99.9	-99.9	-147.4 : y-coord. of source (m)
251.0	251.0	199.0	199.0	126.0	126.0	0.00 : source elevation (m)
0.820	0.801	0.820	0.801	0.813	0.813	-99.9 : emission rate (g/s)
0.381	9.239	3.579	3.579	1.551	1.551	0.781 : total mass emitted (kg)
16.652	13.859	19.972	19.972	14.251	14.251	1.397 : sigx0 at the source (m)
0.120	0.120	0.120	0.120	0.120	0.120	3.282 : sigy0 at the source (m)
-126.4	-113.1	-103.1	-103.1	-129.4	-129.4	13.100 : sigz0 at the source (m)
0.00	0.00	0.00	0.00	0.00	0.00	0.120 : sigx0 at the source (m)
-99.9	-99.9	-99.9	-99.9	-99.9	-99.9	0.120 : sigy0 at the source (m)
251.0	251.0	199.0	199.0	126.0	126.0	68.2 : x-coord. of source (m)
0.820	0.801	0.820	0.801	0.813	0.813	-129.4 : y-coord. of source (m)
0.656	8.656	3.579	3.579	1.551	1.551	0.00 : source elevation (m)
14.231	16.622	19.086	19.086	13.126	13.126	-99.9 : emission rate (g/s)
0.120	0.120	0.120	0.120	0.120	0.120	0.781 : total mass emitted (kg)
107.3	24.5	101.7	25.8	102.8	102.8	1.397 : sigx0 at the source (m)
-146.8	-146.8	-156.0	-84.3	-150.2	-150.2	12.586 : sigy0 at the source (m)
0.00	0.00	0.00	0.00	0.00	0.00	0.120 : sigz0 at the source (m)
-99.9	-99.9	-99.9	-99.9	-99.9	-99.9	102.8 : x-coord. of source (m)
251.0	251.0	199.0	199.0	126.0	126.0	-150.2 : y-coord. of source (m)
0.820	0.801	0.820	0.801	0.813	0.813	0.00 : source elevation (m)
2.517	11.506	6.993	6.993	4.004	4.004	-99.9 : emission rate (g/s)
16.465	12.044	19.047	19.047	13.775	13.775	0.781 : total mass emitted (kg)
0.120	0.120	0.120	0.120	0.120	0.120	1.397 : sigx0 at the source (m)
88.5	43.3	80.6	48.9	83.7	83.7	12.331 : sigy0 at the source (m)
-139.6	-139.6	-147.9	-92.4	-142.9	-142.9	0.120 : sigz0 at the source (m)
0.00	0.00	0.00	0.00	0.00	0.00	83.7 : x-coord. of source (m)
-99.9	-99.9	-99.9	-99.9	-99.9	-99.9	-142.9 : y-coord. of source (m)
251.0	251.0	199.0	199.0	126.0	126.0	0.00 : source elevation (m)
0.820	0.801	0.820	0.801	0.813	0.813	-99.9 : emission rate (g/s)
3.267	6.692	3.267	3.267	0.957	0.957	0.781 : total mass emitted (kg)
16.333	15.253	20.290	20.290	14.314	14.314	1.397 : sigx0 at the source (m)
0.120	0.120	0.120	0.120	0.120	0.120	13.471 : sigy0 at the source (m)
64.7	64.7	57.3	70.2	62.4	62.4	0.120 : sigz0 at the source (m)
-118.0	-119.9	-123.7	-116.6	-120.9	-120.9	62.4 : x-coord. of source (m)
0.00	0.00	0.00	0.00	0.00	0.00	-120.9 : y-coord. of source (m)
-99.9	-99.9	-99.9	-99.9	-99.9	-99.9	0.00 : source elevation (m)
251.0	251.0	199.0	199.0	126.0	126.0	-99.9 : emission rate (g/s)
0.820	0.801	0.820	0.801	0.813	0.813	0.781 : total mass emitted (kg)
10.995	1.831	10.096	10.096	7.939	7.939	1.397 : sigx0 at the source (m)
12.511	16.556	17.600	17.600	11.922	11.922	12.145 : sigy0 at the source (m)
61.1	70.7	49.9	77.6	55.8	55.8	0.120 : sigz0 at the source (m)
-98.9	-98.9	-102.4	-137.9	-101.5	-101.5	55.8 : x-coord. of source (m)
0.00	0.00	0.00	0.00	0.00	0.00	-101.5 : y-coord. of source (m)
-99.9	-99.9	-99.9	-99.9	-99.9	-99.9	0.00 : source elevation (m)
251.0	251.0	199.0	199.0	126.0	126.0	-99.9 : emission rate (g/s)
0.820	0.801	0.820	0.801	0.813	0.813	0.781 : total mass emitted (kg)
14.612	7.383	15.507	15.507	11.575	11.575	1.397 : sigx0 at the source (m)
7.996	14.931	13.085	13.085	8.474	8.474	9.704 : sigy0 at the source (m)
0.120	0.120	0.120	0.120	0.120	0.120	9.392 : sigz0 at the source (m)
61.5	70.4	50.3	77.2	56.1	56.1	56.1 : x-coord. of source (m)

-78.8	-159.1	-79.9	-160.4	-81.0	-81.0 : y-coord. of source (m)
0.00	0.00	0.00	0.00	0.00	0.00 : source elevation (m)
-99.9	-99.9	-99.9	-99.9	-99.9	-99.9 : emission rate (g/s)
251.0	251.0	199.0	-199.0	115.0	115.0 : emission duration (s)
0.801	0.801	0.820	0.801	0.781	0.781 : total mass emitted (kg)
16.465	12.044	19.047	19.047	12.331	12.331 : sigx0 at the source (m)
2.517	11.506	6.993	6.993	5.507	5.507 : sigy0 at the source (m)
0.120	0.120	0.120	0.120	0.120	0.120 : sigz0 at the source (m)
-108.7	-123.2	-113.4	-126.9	-111.5	-111.5 : x-coord. of source (m)
0.00	0.00	0.00	0.00	0.00	0.00 : y-coord. of source (m)
-99.9	-99.9	-99.9	-99.9	-99.9	-99.9 : emission rate (g/s)
251.0	251.0	199.0	-199.0	115.0	115.0 : emission duration (s)
0.820	0.801	0.820	0.801	0.781	0.781 : total mass emitted (kg)
13.001	4.678	12.999	12.999	7.926	7.926 : sigx0 at the source (m)
10.412	15.986	15.579	15.579	10.934	10.934 : sigy0 at the source (m)
0.120	0.120	0.120	0.120	0.120	0.120 : sigz0 at the source (m)
64.3	67.6	53.4	74.0	59.0	59.0 : x-coord. of source (m)
-168.8	-168.8	-69.0	-171.3	-71.1	-71.1 : y-coord. of source (m)
0.00	0.00	0.00	0.00	0.00	0.00 : source elevation (m)
-99.9	-99.9	-99.9	-99.9	-99.9	-99.9 : emission rate (g/s)
251.0	251.0	199.0	-199.0	115.0	115.0 : emission duration (s)
0.820	0.801	0.820	0.801	0.781	0.781 : total mass emitted (kg)
16.552	13.859	19.972	19.972	13.100	13.100 : sigx0 at the source (m)
0.381	9.239	3.578	3.578	3.292	3.292 : sigy0 at the source (m)
0.120	0.120	0.120	0.120	0.120	0.120 : sigz0 at the source (m)
60.4	71.4	49.1	78.3	55.0	55.0 : x-coord. of source (m)
-88.8	-149.0	-91.2	-149.2	-91.3	-91.3 : y-coord. of source (m)
0.00	0.00	0.00	0.00	0.00	0.00 : source elevation (m)
-99.9	-99.9	-99.9	-99.9	-99.9	-99.9 : emission rate (g/s)
251.0	251.0	199.0	-199.0	115.0	115.0 : emission duration (s)
0.820	0.801	0.820	0.801	0.781	0.781 : total mass emitted (kg)
15.778	9.863	17.544	17.544	11.187	11.187 : sigx0 at the source (m)
5.338	13.422	10.194	10.194	7.564	7.564 : sigy0 at the source (m)
0.120	0.120	0.120	0.120	0.120	0.120 : sigz0 at the source (m)
-99.9	-99.9	-99.9	-99.9	-99.9	-99.9 : ambient pressure (atm)
-99.9	-99.9	-99.9	-99.9	-99.9	-99.9 : relative humidity (%)
300.00	300.00	300.00	300.00	300.00	300.00 : temperature at level #1 (K)
2.00	2.00	2.00	2.00	2.00	2.00 : measuring height for temperature #1 (m)
-99.90	-99.90	-99.90	-99.90	-99.90	-99.90 : temperature at level #2 (K)
6.40	4.30	5.50	5.80	5.60	5.60 : wind speed (m/s) at a tower
2.00	2.00	2.00	2.00	2.00	2.00 : measuring height for wind data (m)
6.40	4.30	5.50	5.80	5.60	5.60 : domain-averaged wind speed (m/s)
148.0	148.0	163.0	163.0	163.0	163.0 : domain-averaged wind direction (deg)
-99.90	-99.90	-99.90	-99.90	-99.90	-99.90 : domain-averaged sigma-u (m/s)
6.80	12.50	10.80	9.10	8.10	8.10 : domain-averaged sigma-theta (deg)
-99.90	-99.90	-99.90	-99.90	-99.90	-99.90 : domain-averaged sigma-phi (deg)
2.00	2.00	2.00	2.00	2.00	2.00 : measuring ht for domain-avg wind speed (m)
391.0	391.0	386.0	351.0	192.0	192.0 : averaging time for domain-avg data (s)
0.087	0.070	0.072	0.075	0.073	0.073 : wind speed power law exponent
0.0300	0.0300	0.0300	0.0300	0.0300	0.0300 : surface roughness (m)
-99.900	-99.900	-99.900	-99.900	-99.900	-99.900 : friction velocity (m)
-99.9000	-99.9000	-99.9000	-99.9000	-99.9000	-99.9000 : inverse Monin-Obukhov length (1/m)
0.18	0.18	0.18	0.18	0.18	0.18 : albedo
0.50	0.50	0.50	0.50	0.50	0.50 : moisture availability
0.50	0.50	0.50	0.50	0.50	0.50 : Bowen ratio
-99.9	-99.9	-99.9	-99.9	-99.9	-99.9 : mixing height (m)
-99.9	-99.9	-99.9	-99.9	-99.9	-99.9 : cloud cover (%)
-99.9	-99.9	-99.9	-99.9	-99.9	-99.9 : P-G stability class
251.0	251.0	199.0	199.0	115.0	115.0 : suggested time for concentration (s)
1.00	1.00	1.00	1.00	1.00	1.00 : suggested receptor height (m)
0	0	0	0	0	0 : no. of distances downwind
2	2	2	2	2	2 : no. of lines-of-sight
-247.7	-247.7	-247.7	-247.7	-247.7	-247.7 : x-coord. of 1st end-point for LOS1 (m)
-68.7	-68.7	-68.7	-68.7	-68.7	-68.7 : y-coord. of 1st end-point for LOS1 (m)
189.6	189.6	189.6	189.6	189.6	189.6 : x-coord. of 2nd end-point for LOS1 (m)
173.7	173.7	173.7	173.7	173.7	173.7 : y-coord. of 2nd end-point for LOS1 (m)
-99.9	-99.9	-99.9	-99.9	-99.9	-99.9 : LOS integrated conc. (mg/m**2)
1.934E+05	9.990E+01	1.838E+05	1.506E+05	1.658E+05	1.232E+05 : LOS integrated dosage (mg-s/m**2)
-189.6	-189.6	-189.6	-189.6	-189.6	-189.6 : x-coord. of 1st end-point for LOS1 (m)
-173.7	-173.7	-173.7	-173.7	-173.7	-173.7 : y-coord. of 1st end-point for LOS1 (m)
247.7	247.7	247.7	247.7	247.7	247.7 : x-coord. of 2nd end-point for LOS1 (m)
68.7	68.7	68.7	68.7	68.7	68.7 : y-coord. of 2nd end-point for LOS1 (m)
-99.9	-99.9	-99.9	-99.9	-99.9	-99.9 : LOS integrated conc. (mg/m**2)
2.978E+05	2.086E+05	3.166E+05	2.660E+05	4.909E+05	2.118E+05 : LOS integrated dosage (mg-s/m**2)

F-53

The Evaluation of the 18 Series Grenades (18A), 8 grenades, 18128)

6 : number of trials included in DDA		6 : trial ID	
6 : time zone designation		6 : month	
40.20 : latitude (deg)		7 : day	
113.00 : longitude (deg)		82 : year	
87b		21 : hour	
88b		51 : minute	
89b		8 : no. of sources	
90b		62.6 : x-coord. of source (m)	
91b		-73.5 : y-coord. of source (m)	
92b		0.00 : source elevation (m)	
93b		-99.9 : emission rate (g/s)	
94b		101.0 : emission duration (s)	
95b		0.763 : total mass emitted (kg)	
96b		1.848 : sigx0 at the source (m)	
97b		16.853 : sigy0 at the source (m)	
98b		0.120 : sigz0 at the source (m)	
99b		51.4 : x-coord. of source (m)	
100b		-60.4 : y-coord. of source (m)	
101b		0.00 : source elevation (m)	
102b		-99.9 : emission rate (g/s)	
103b		101.0 : emission duration (s)	
104b		0.763 : total mass emitted (kg)	
105b		2.579 : sigx0 at the source (m)	
106b		16.767 : sigy0 at the source (m)	
107b		0.120 : sigz0 at the source (m)	
108b		37.2 : x-coord. of source (m)	
109b		-50.6 : y-coord. of source (m)	
110b		0.00 : source elevation (m)	
111b		-99.9 : emission rate (g/s)	
112b		101.0 : emission duration (s)	
113b		0.763 : total mass emitted (kg)	
114b		8.831 : sigx0 at the source (m)	
115b		15.528 : sigy0 at the source (m)	
116b		0.120 : sigz0 at the source (m)	
117b		20.9 : x-coord. of source (m)	
118b		-44.9 : y-coord. of source (m)	
119b		0.00 : source elevation (m)	
120b		-99.9 : emission rate (g/s)	
121b		101.0 : emission duration (s)	
122b		0.763 : total mass emitted (kg)	
123b		10.617 : sigx0 at the source (m)	
124b		13.231 : sigy0 at the source (m)	
125b		0.120 : sigz0 at the source (m)	
126b		68.0 : x-coord. of source (m)	
127b		-83.6 : y-coord. of source (m)	
128b		0.00 : source elevation (m)	
129b		-99.9 : emission rate (g/s)	
130b		101.0 : emission duration (s)	
131b		0.763 : total mass emitted (kg)	
132b		4.748 : sigx0 at the source (m)	
133b		16.286 : sigy0 at the source (m)	
134b		0.120 : sigz0 at the source (m)	
135b		72.6 : x-coord. of source (m)	
136b		-100.2 : y-coord. of source (m)	
137b		0.00 : source elevation (m)	
138b		-99.9 : emission rate (g/s)	
139b		101.0 : emission duration (s)	
140b		0.763 : total mass emitted (kg)	
141b		8.402 : sigx0 at the source (m)	
142b		14.502 : sigy0 at the source (m)	
143b		0.120 : sigz0 at the source (m)	
144b		72.6 : x-coord. of source (m)	
145b		-117.5 : y-coord. of source (m)	
146b		0.00 : source elevation (m)	
147b		-99.9 : emission rate (g/s)	
148b		101.0 : emission duration (s)	
149b		0.763 : total mass emitted (kg)	
150b		12.255 : sigx0 at the source (m)	
151b		11.730 : sigy0 at the source (m)	
152b		0.120 : sigz0 at the source (m)	
153b		68.4 : x-coord. of source (m)	
154b		-134.1 : y-coord. of source (m)	
155b		0.00 : source elevation (m)	
156b		-99.9 : emission rate (g/s)	
157b		101.0 : emission duration (s)	
158b		0.763 : total mass emitted (kg)	
159b		14.873 : sigx0 at the source (m)	
160b		8.158 : sigy0 at the source (m)	
161b		0.120 : sigz0 at the source (m)	
162b		-99.9 : ambient pressure (atm)	

[illegible]

The Evaluation of the 18 Series Grenades (18A), low condition temp., (81EL)

5 : number of trials included in DDA

6 : time zone designation

40.20 : latitude (deg)

113.00 : longitude (deg)

82a	87a	88a	81ja	81da	trial ID
5	6	7	5	5	month
25	7	25	26	26	day
82	82	82	82	82	year
16	16	16	13	13	hour
52	5	5	29	29	minute
15	7	8	12	12	no. of sources
62.6	62.6	62.6	62.6	62.6	x-coord. of source (m)
73.5	73.5	73.5	73.5	73.5	y-coord. of source (m)
0.00	0.00	0.00	0.00	0.00	source elevation (m)
0.00	0.00	0.00	0.00	0.00	emission rate (g/s)
0.859	0.859	0.859	0.859	0.859	total mass emitted (kg)
0.859	0.859	0.859	0.859	0.859	sigx0 at the source (m)
11.624	11.624	11.624	11.624	11.624	sigy0 at the source (m)
15.586	15.586	15.586	15.586	15.586	sigz0 at the source (m)
0.120	0.120	0.120	0.120	0.120	x-coord. of source (m)
51.4	51.4	51.4	51.4	51.4	y-coord. of source (m)
60.4	60.4	60.4	60.4	60.4	source elevation (m)
0.00	0.00	0.00	0.00	0.00	emission rate (g/s)
0.859	0.859	0.859	0.859	0.859	total mass emitted (kg)
0.859	0.859	0.859	0.859	0.859	sigx0 at the source (m)
0.963	0.963	0.963	0.963	0.963	sigy0 at the source (m)
16.937	16.937	16.937	16.937	16.937	sigz0 at the source (m)
0.120	0.120	0.120	0.120	0.120	x-coord. of source (m)
43.1	43.1	43.1	43.1	43.1	y-coord. of source (m)
130.3	130.3	130.3	130.3	130.3	source elevation (m)
0.00	0.00	0.00	0.00	0.00	emission rate (g/s)
0.859	0.859	0.859	0.859	0.859	total mass emitted (kg)
0.859	0.859	0.859	0.859	0.859	sigx0 at the source (m)
7.634	7.634	7.634	7.634	7.634	sigy0 at the source (m)
15.149	15.149	15.149	15.149	15.149	sigz0 at the source (m)
0.120	0.120	0.120	0.120	0.120	x-coord. of source (m)
28.0	28.0	28.0	28.0	28.0	y-coord. of source (m)
45.5	45.5	45.5	45.5	45.5	source elevation (m)
0.00	0.00	0.00	0.00	0.00	emission rate (g/s)
0.859	0.859	0.859	0.859	0.859	total mass emitted (kg)
0.859	0.859	0.859	0.859	0.859	sigx0 at the source (m)
16.245	16.245	16.245	16.245	16.245	sigy0 at the source (m)
4.888	4.888	4.888	4.888	4.888	sigz0 at the source (m)
0.120	0.120	0.120	0.120	0.120	x-coord. of source (m)
25.8	25.8	25.8	25.8	25.8	y-coord. of source (m)
79.7	79.7	79.7	79.7	79.7	source elevation (m)
0.00	0.00	0.00	0.00	0.00	emission rate (g/s)
0.859	0.859	0.859	0.859	0.859	total mass emitted (kg)
0.859	0.859	0.859	0.859	0.859	sigx0 at the source (m)
11.624	11.624	11.624	11.624	11.624	sigy0 at the source (m)
12.355	12.355	12.355	12.355	12.355	sigz0 at the source (m)
0.120	0.120	0.120	0.120	0.120	x-coord. of source (m)
25.6	25.6	25.6	25.6	25.6	y-coord. of source (m)
56.8	56.8	56.8	56.8	56.8	source elevation (m)
0.00	0.00	0.00	0.00	0.00	emission rate (g/s)
0.859	0.859	0.859	0.859	0.859	total mass emitted (kg)
0.859	0.859	0.859	0.859	0.859	sigx0 at the source (m)
15.014	15.014	15.014	15.014	15.014	sigy0 at the source (m)
0.120	0.120	0.120	0.120	0.120	sigz0 at the source (m)
37.2	37.2	37.2	37.2	37.2	x-coord. of source (m)
50.6	50.6	50.6	50.6	50.6	y-coord. of source (m)
0.00	0.00	0.00	0.00	0.00	source elevation (m)
0.859	0.859	0.859	0.859	0.859	total mass emitted (kg)
0.859	0.859	0.859	0.859	0.859	sigx0 at the source (m)
2.286	2.286	2.286	2.286	2.286	sigy0 at the source (m)
16.809	16.809	16.809	16.809	16.809	sigz0 at the source (m)
0.120	0.120	0.120	0.120	0.120	x-coord. of source (m)
68.0	68.0	68.0	68.0	68.0	y-coord. of source (m)
83.6	83.6	83.6	83.6	83.6	source elevation (m)
0.00	0.00	0.00	0.00	0.00	emission rate (g/s)
0.859	0.859	0.859	0.859	0.859	total mass emitted (kg)
0.859	0.859	0.859	0.859	0.859	sigx0 at the source (m)
14.346	14.346	14.346	14.346	14.346	sigy0 at the source (m)
0.120	0.120	0.120	0.120	0.120	sigz0 at the source (m)
73.1	73.1	73.1	73.1	73.1	x-coord. of source (m)
106.0	106.0	106.0	106.0	106.0	y-coord. of source (m)
0.00	0.00	0.00	0.00	0.00	source elevation (m)
0.859	0.859	0.859	0.859	0.859	total mass emitted (kg)
0.859	0.859	0.859	0.859	0.859	sigx0 at the source (m)
13.414	13.414	13.414	13.414	13.414	sigy0 at the source (m)
10.385	10.385	10.385	10.385	10.385	sigz0 at the source (m)
0.120	0.120	0.120	0.120	0.120	x-coord. of source (m)
70.3	70.3	70.3	70.3	70.3	y-coord. of source (m)
0.00	0.00	0.00	0.00	0.00	source elevation (m)

[illegible]

The Evaluation of the 18 Series Grenades (L8A1, medium condition temp., 1812M)

6 : number of trials included in QDA

6 : time zone designation

40.20 : latitude (deg)

113.00 : longitude (deg)

834 : B4

834 : B4

834 : B4

834 : B4

834 : B4

834 : B4

834 : B4

834 : B4

834 : B4

834 : B4

834 : B4

834 : B4

834 : B4

834 : B4

834 : B4

834 : B4

834 : B4

834 : B4

834 : B4

834 : B4

834 : B4

834 : B4

834 : B4

834 : B4

834 : B4

834 : B4

834 : B4

834 : B4

834 : B4

834 : B4

834 : B4

834 : B4

834 : B4

834 : B4

834 : B4

834 : B4

834 : B4

834 : B4

834 : B4

834 : B4

834 : B4

834 : B4

834 : B4

834 : B4

834 : B4

834 : B4

834 : B4

834 : B4

834 : B4

834 : B4

834 : B4

834 : B4

834 : B4

834 : B4

834 : B4

834 : B4

834 : B4

834 : B4

834 : B4

834 : B4

834 : B4

834 : B4

834 : B4

834 : B4

834 : B4

834 : B4

834 : B4

834 : B4

834 : B4

834 : B4

834 : B4

834 : B4

834 : B4

834 : B4

834 : B4

834 : B4

834 : B4

834 : B4

834 : B4

834 : B4

834 : B4

834 : B4

834 : B4

834 : B4

834 : B4

834 : B4

834 : B4

[illegible]

[illegible]

The Evaluation of the 18 Series Grenades (Reworked 18A1, 6 grenades, 181K6)

6 : number of trials included in DOA

6 : time zone designation

40.20 : latitude (deg)

113.00 : longitude (deg)

819b : B22b

819b : B22b

819b : B22b

819b : B22b

819b : B22b

819b : B22b

819b : B22b

819b : B22b

819b : B22b

819b : B22b

819b : B22b

819b : B22b

819b : B22b

819b : B22b

819b : B22b

819b : B22b

819b : B22b

819b : B22b

819b : B22b

819b : B22b

819b : B22b

819b : B22b

819b : B22b

819b : B22b

819b : B22b

819b : B22b

819b : B22b

819b : B22b

819b : B22b

819b : B22b

819b : B22b

819b : B22b

819b : B22b

819b : B22b

819b : B22b

819b : B22b

819b : B22b

819b : B22b

819b : B22b

819b : B22b

819b : B22b

819b : B22b

819b : B22b

819b : B22b

819b : B22b

819b : B22b

819b : B22b

819b : B22b

819b : B22b

819b : B22b

819b : B22b

819b : B22b

819b : B22b

819b : B22b

819b : B22b

819b : B22b

819b : B22b

819b : B22b

819b : B22b

819b : B22b

819b : B22b

819b : B22b

819b : B22b

819b : B22b

819b : B22b

819b : B22b

819b : B22b

819b : B22b

819b : B22b

819b : B22b

819b : B22b

819b : B22b

819b : B22b

819b : B22b

819b : B22b

819b : B22b

819b : B22b

819b : B22b

819b : B22b

819b : B22b

819b : B22b

819b : B22b

819b : B22b

819b : B22b

819b : B22b

819b : B22b

819b : B22b

The Evaluation of the 18 Series Grenades (Neworked LBA1, 8 grenades, LBA187)

6 : number of trials included in DUA

6 : time zone designation

40.20 : latitude (deg)

113.00 : longitude (deg)

B25b : latitude (deg)

B25b : longitude (deg)

B25b : latitude (deg)

B25b : longitude (deg)

B25b : latitude (deg)

B25b : longitude (deg)

B25b : latitude (deg)

B25b : longitude (deg)

B25b : latitude (deg)

B25b : longitude (deg)

B25b : latitude (deg)

B25b : longitude (deg)

B25b : latitude (deg)

B25b : longitude (deg)

B25b : latitude (deg)

B25b : longitude (deg)

B25b : latitude (deg)

B25b : longitude (deg)

B25b : latitude (deg)

B25b : longitude (deg)

B25b : latitude (deg)

B25b : longitude (deg)

B25b : latitude (deg)

B25b : longitude (deg)

B25b : latitude (deg)

B25b : longitude (deg)

B25b : latitude (deg)

B25b : longitude (deg)

B25b : latitude (deg)

B25b : longitude (deg)

B25b : latitude (deg)

B25b : longitude (deg)

B25b : latitude (deg)

B25b : longitude (deg)

B25b : latitude (deg)

B25b : longitude (deg)

B25b : latitude (deg)

B25b : longitude (deg)

B25b : latitude (deg)

B25b : longitude (deg)

B25b : latitude (deg)

B25b : longitude (deg)

B25b : latitude (deg)

B25b : longitude (deg)

B25b : latitude (deg)

B25b : longitude (deg)

B25b : latitude (deg)

B25b : longitude (deg)

B25b : latitude (deg)

B25b : longitude (deg)

B25b : latitude (deg)

B25b : longitude (deg)

B25b : latitude (deg)

B25b : longitude (deg)

B25b : latitude (deg)

B25b : longitude (deg)

B25b : latitude (deg)

B25b : longitude (deg)

B25b : latitude (deg)

B25b : longitude (deg)

B25b : latitude (deg)

B25b : longitude (deg)

B25b : latitude (deg)

B25b : longitude (deg)

B25b : latitude (deg)

B25b : longitude (deg)

B25b : latitude (deg)

B25b : longitude (deg)

B25b : latitude (deg)

B25b : longitude (deg)

B25b : latitude (deg)

B25b : longitude (deg)

B25b : latitude (deg)

B25b : longitude (deg)

B25b : latitude (deg)

B25b : longitude (deg)

B25b : latitude (deg)

B25b : longitude (deg)

B25b : latitude (deg)

B25b : longitude (deg)

B25b : latitude (deg)

B25b : longitude (deg)

B25b : latitude (deg)

B25b : longitude (deg)

B25b : latitude (deg)

B25b : longitude (deg)

F-71

The Evaluation of the 18 Series Grenades (Reworked L8A1, 12 grenades, L81R2)

6 : number of trials included in DOA

6 : time zone designation

40.20 : latitude (deg)

113.60 : longitude (deg)

831b : longitude (deg)

832b : longitude (deg)

833b : longitude (deg)

834b : longitude (deg)

835b : longitude (deg)

836b : longitude (deg)

837b : longitude (deg)

838b : longitude (deg)

839b : longitude (deg)

840b : longitude (deg)

841b : longitude (deg)

842b : longitude (deg)

843b : longitude (deg)

844b : longitude (deg)

845b : longitude (deg)

846b : longitude (deg)

847b : longitude (deg)

848b : longitude (deg)

849b : longitude (deg)

850b : longitude (deg)

851b : longitude (deg)

852b : longitude (deg)

853b : longitude (deg)

854b : longitude (deg)

855b : longitude (deg)

856b : longitude (deg)

857b : longitude (deg)

858b : longitude (deg)

859b : longitude (deg)

860b : longitude (deg)

861b : longitude (deg)

862b : longitude (deg)

863b : longitude (deg)

864b : longitude (deg)

865b : longitude (deg)

866b : longitude (deg)

867b : longitude (deg)

868b : longitude (deg)

869b : longitude (deg)

870b : longitude (deg)

871b : longitude (deg)

872b : longitude (deg)

873b : longitude (deg)

874b : longitude (deg)

875b : longitude (deg)

876b : longitude (deg)

877b : longitude (deg)

878b : longitude (deg)

879b : longitude (deg)

880b : longitude (deg)

881b : longitude (deg)

882b : longitude (deg)

883b : longitude (deg)

884b : longitude (deg)

885b : longitude (deg)

886b : longitude (deg)

887b : longitude (deg)

888b : longitude (deg)

889b : longitude (deg)

890b : longitude (deg)

891b : longitude (deg)

892b : longitude (deg)

893b : longitude (deg)

894b : longitude (deg)

895b : longitude (deg)

896b : longitude (deg)

897b : longitude (deg)

898b : longitude (deg)

899b : longitude (deg)

900b : longitude (deg)

901b : longitude (deg)

902b : longitude (deg)

903b : longitude (deg)

904b : longitude (deg)

905b : longitude (deg)

906b : longitude (deg)

907b : longitude (deg)

908b : longitude (deg)

909b : longitude (deg)

910b : longitude (deg)

[illegible]

The Evaluation of the L8 Series Grenades (Numbered L8A1, low condition temp., L018L)

6 : number of trials included in DOA	6 : time zone designation	6 : latitude (deg)	6 : longitude (deg)	B25a	B26a	B31a	B32a : trial ID
40.20 : latitude (deg)	25	25	25	6	6	25	5 : month
113.00 : longitude (deg)	82	82	82	7	7	82	26 : day
819a	15	15	15	18	18	17	82 : year
B20a	28	28	28	30	30	37	14 : hour
	4	4	4	7	7	12	17 : minute
-37.4	-37.4	60.9	60.9	-37.4	-37.4	11 : no. of sources	11 : no. of sources
99.7	99.7	-74.6	-74.6	99.7	99.7	60.9 : x-coord. of source (m)	60.9 : x-coord. of source (m)
0.00	0.00	0.00	0.00	0.00	0.00	-74.6 : y-coord. of source (m)	-74.6 : y-coord. of source (m)
-99.9	-99.9	-99.9	-99.9	-99.9	-99.9	0.00 : source elevation (m)	0.00 : source elevation (m)
118.0	118.0	118.0	118.0	118.0	118.0	-99.9 : emission rate (g/s)	-99.9 : emission rate (g/s)
0.916	0.916	0.859	0.859	0.801	0.763	118.0 : emission duration (s)	118.0 : emission duration (s)
2.576	1.251	11.003	9.136	0.840	0.840	0.840 : total mass emitted (kg)	0.840 : total mass emitted (kg)
18.137	18.276	14.647	15.878	16.975	16.975	1.624 : sigx0 at the source (m)	1.624 : sigx0 at the source (m)
0.120	0.120	0.120	0.120	0.120	0.120	18.247 : sigy0 at the source (m)	18.247 : sigy0 at the source (m)
-83.3	-83.3	36.3	20.5	-72.4	-72.4	0.120 : sigz0 at the source (m)	0.120 : sigz0 at the source (m)
128.3	128.3	-52.4	-46.8	126.0	126.0	25.9 : x-coord. of source (m)	25.9 : x-coord. of source (m)
0.00	0.00	0.00	0.00	0.00	0.00	-48.2 : y-coord. of source (m)	-48.2 : y-coord. of source (m)
118.0	118.0	118.0	118.0	118.0	118.0	0.00 : source elevation (m)	0.00 : source elevation (m)
0.916	0.859	0.801	0.763	0.840	0.840	-99.9 : emission rate (g/s)	-99.9 : emission rate (g/s)
6.837	10.221	14.419	12.934	0.666	0.666	118.0 : emission duration (s)	118.0 : emission duration (s)
16.935	15.202	11.300	12.934	18.307	18.307	0.840 : total mass emitted (kg)	0.840 : total mass emitted (kg)
0.120	0.120	0.120	0.120	0.120	0.120	4.715 : sigx0 at the source (m)	4.715 : sigx0 at the source (m)
-28.7	-28.7	20.5	46.1	-44.3	-44.3	17.702 : sigy0 at the source (m)	17.702 : sigy0 at the source (m)
79.2	79.2	-46.8	-84.4	108.5	108.5	0.120 : sigz0 at the source (m)	0.120 : sigz0 at the source (m)
0.00	0.00	0.00	0.00	0.00	0.00	54.0 : x-coord. of source (m)	54.0 : x-coord. of source (m)
-99.9	-99.9	-99.9	-99.9	-99.9	-99.9	-85.8 : y-coord. of source (m)	-85.8 : y-coord. of source (m)
118.0	118.0	118.0	118.0	118.0	118.0	0.00 : source elevation (m)	0.00 : source elevation (m)
0.916	0.859	0.801	0.763	0.840	0.840	-99.9 : emission rate (g/s)	-99.9 : emission rate (g/s)
13.632	16.746	16.852	3.208	9.731	9.731	118.0 : emission duration (s)	118.0 : emission duration (s)
12.238	7.426	7.183	18.036	15.521	15.521	0.840 : total mass emitted (kg)	0.840 : total mass emitted (kg)
-99.9	-99.9	66.1	70.6	-83.3	-83.3	4.768 : sigx0 at the source (m)	4.768 : sigx0 at the source (m)
0.00	0.00	0.00	0.00	0.00	0.00	17.688 : sigy0 at the source (m)	17.688 : sigy0 at the source (m)
-99.9	-99.9	79.2	-84.4	-100.5	-100.5	0.120 : sigz0 at the source (m)	0.120 : sigz0 at the source (m)
118.0	118.0	118.0	118.0	118.0	118.0	15.0 : x-coord. of source (m)	15.0 : x-coord. of source (m)
0.916	0.859	0.801	0.763	0.840	0.840	-45.9 : y-coord. of source (m)	-45.9 : y-coord. of source (m)
-99.900	10.790	3.782	7.767	2.523	2.523	0.00 : source elevation (m)	0.00 : source elevation (m)
-99.900	14.804	17.524	16.591	18.145	18.145	-99.9 : emission rate (g/s)	-99.9 : emission rate (g/s)
0.120	0.120	0.120	0.120	0.120	0.120	118.0 : emission duration (s)	118.0 : emission duration (s)
-99.9	-99.9	57.0	-27.6	-117.2	-117.2	0.840 : total mass emitted (kg)	0.840 : total mass emitted (kg)
0.00	0.00	0.00	0.00	0.00	0.00	1.570 : sigx0 at the source (m)	1.570 : sigx0 at the source (m)
-99.9	-99.9	-99.9	-99.9	-99.9	-99.9	18.252 : sigy0 at the source (m)	18.252 : sigy0 at the source (m)
118.0	118.0	118.0	118.0	118.0	118.0	0.120 : sigz0 at the source (m)	0.120 : sigz0 at the source (m)
0.916	0.859	0.801	0.763	0.840	0.840	-32.4 : y-coord. of source (m)	-32.4 : y-coord. of source (m)
-99.900	15.202	0.986	11.796	3.835	3.835	0.00 : source elevation (m)	0.00 : source elevation (m)
-99.900	10.221	18.292	14.016	17.913	17.913	-99.9 : emission rate (g/s)	-99.9 : emission rate (g/s)
0.120	0.120	0.120	0.120	0.120	0.120	118.0 : emission duration (s)	118.0 : emission duration (s)
-99.9	-99.9	66.6	70.6	-83.3	-83.3	0.840 : total mass emitted (kg)	0.840 : total mass emitted (kg)
-99.9	-99.9	-133.4	-133.4	-99.9	-99.9	1.570 : sigx0 at the source (m)	1.570 : sigx0 at the source (m)
0.00	0.00	0.00	0.00	0.00	0.00	18.252 : sigy0 at the source (m)	18.252 : sigy0 at the source (m)
-99.9	-99.9	-99.9	-99.9	-99.9	-99.9	0.120 : sigz0 at the source (m)	0.120 : sigz0 at the source (m)
118.0	118.0	118.0	118.0	118.0	118.0	-128.1 : y-coord. of source (m)	-128.1 : y-coord. of source (m)
0.916	0.859	0.801	0.763	0.840	0.840	0.00 : source elevation (m)	0.00 : source elevation (m)
-99.900	10.000	10.000	10.000	17.411	17.411	-99.9 : emission rate (g/s)	-99.9 : emission rate (g/s)
-99.900	15.349	15.349	15.349	0.635	0.635	118.0 : emission duration (s)	118.0 : emission duration (s)
-99.9	-99.9	0.120	0.120	0.120	0.120	0.840 : total mass emitted (kg)	0.840 : total mass emitted (kg)
-99.9	-99.9	-99.9	-99.9	-99.9	-99.9	17.702 : sigx0 at the source (m)	17.702 : sigx0 at the source (m)
0.00	0.00	0.00	0.00	0.00	0.00	4.715 : sigy0 at the source (m)	4.715 : sigy0 at the source (m)
-99.9	-99.9	-99.9	-99.9	-99.9	-99.9	0.120 : sigz0 at the source (m)	0.120 : sigz0 at the source (m)
-99.9	-99.9	-99.9	-99.9	-99.9	-99.9	69.6 : x-coord. of source (m)	69.6 : x-coord. of source (m)

F-77

F-78

208.5 208.5 208.5 208.5 208.5 : Y-coord. of 2nd end-point for LOS1 (m)
 -99.9 -99.9 -99.9 -99.9 -99.9 : LOS integrated conc. (mg/m³·2)
 -9.990E+01 -9.990E+01 1.380E+03 1.290E+05 -9.990E+01 -9.990E+01 : LOS integrated dosage (mg·s/m³·2)

```

6 : number of trials included
6 : time zone designation
40.20 : latitude (deg)
113.00 : longitude (deg)

```

113.00 : longitude (deg)	B23a	B24a	B29a	B30a	B35a	B36a	trial ID
	6	6	7	6	6	6	month
	8	8	7	7	8	8	day
	8	8	82	82	82	82	year
	16	20	20	21	19	17	hour
	57	55	13	38	12	29	minute
	6	5	8	7	15	12	no. of sources
-37.4	-37.4	60.9	60.9	60.9	-37.4	-37.4	x-coord. of source (m)
99.7	99.7	-74.6	-74.6	-74.6	99.7	99.7	y-coord. of source (m)
0.00	0.00	0.00	0.00	0.00	0.00	0.00	source elevation (m)
-99.9	-99.9	-99.9	-99.9	-99.9	-99.9	-99.9	emission rate (g/s)
118.0	118.0	118.0	118.0	118.0	118.0	118.0	total mass emitted (kg)
0.859	0.820	0.763	0.744	0.820	0.859	0.859	total mass emitted (kg)
0.859	0.820	0.763	0.744	0.820	0.859	0.859	total mass emitted (kg)
5.330	1.231	7.426	7.426	7.426	8.905	8.905	sig0 at the source (m)
17.414	16.276	16.742	16.742	16.742	16.009	16.009	sig0 at the source (m)
0.120	0.120	0.120	0.120	0.120	0.120	0.120	sig0 at the source (m)
-52.6	-52.6	50.0	50.0	50.0	-52.6	-52.6	x-coord. of source (m)
115.9	115.9	-61.9	-61.9	-61.9	115.9	115.9	y-coord. of source (m)
0.00	0.00	0.00	0.00	0.00	0.00	0.00	source elevation (m)
-99.9	-99.9	-99.9	-99.9	-99.9	-99.9	-99.9	emission rate (g/s)
118.0	118.0	118.0	118.0	118.0	118.0	118.0	total mass emitted (kg)
0.859	0.820	0.763	0.744	0.820	0.859	0.859	total mass emitted (kg)
0.859	0.820	0.763	0.744	0.820	0.859	0.859	total mass emitted (kg)
18.309	17.852	17.330	17.330	17.330	18.089	18.089	sig0 at the source (m)
0.120	0.120	0.120	0.120	0.120	0.120	0.120	sig0 at the source (m)
-83.3	-83.3	36.3	36.3	36.3	-72.4	-72.4	x-coord. of source (m)
128.3	128.3	-52.4	-52.4	-52.4	128.0	128.0	y-coord. of source (m)
0.00	0.00	0.00	0.00	0.00	0.00	0.00	source elevation (m)
-99.9	-99.9	-99.9	-99.9	-99.9	-99.9	-99.9	emission rate (g/s)
118.0	118.0	118.0	118.0	118.0	118.0	118.0	total mass emitted (kg)
0.859	0.820	0.763	0.744	0.820	0.859	0.859	total mass emitted (kg)
0.859	0.820	0.763	0.744	0.820	0.859	0.859	total mass emitted (kg)
16.937	16.937	16.937	16.937	16.937	17.988	17.988	sig0 at the source (m)
0.120	0.120	0.120	0.120	0.120	0.120	0.120	sig0 at the source (m)
-29.9	-29.9	20.5	20.5	20.5	-44.3	-44.3	x-coord. of source (m)
46.1	46.1	-46.8	-46.8	-46.8	108.5	108.5	y-coord. of source (m)
0.00	0.00	0.00	0.00	0.00	0.00	0.00	source elevation (m)
-99.9	-99.9	-99.9	-99.9	-99.9	-99.9	-99.9	emission rate (g/s)
118.0	118.0	118.0	118.0	118.0	118.0	118.0	total mass emitted (kg)
0.859	0.820	0.763	0.744	0.820	0.859	0.859	total mass emitted (kg)
0.859	0.820	0.763	0.744	0.820	0.859	0.859	total mass emitted (kg)
16.937	16.937	16.937	16.937	16.937	17.988	17.988	sig0 at the source (m)
0.120	0.120	0.120	0.120	0.120	0.120	0.120	sig0 at the source (m)
-28.7	-28.7	66.1	66.1	66.1	-83.3	-83.3	x-coord. of source (m)
75.2	75.2	-84.4	-84.4	-84.4	128.3	128.3	y-coord. of source (m)
0.00	0.00	0.00	0.00	0.00	0.00	0.00	source elevation (m)
-99.9	-99.9	-99.9	-99.9	-99.9	-99.9	-99.9	emission rate (g/s)
118.0	118.0	118.0	118.0	118.0	118.0	118.0	total mass emitted (kg)
0.859	0.820	0.763	0.744	0.820	0.859	0.859	total mass emitted (kg)
0.859	0.820	0.763					

F-85

The Evaluation of the 18 Series Grenades (LBA3, 8 Grenades, 1838)

4 : number of trials included in DDA

6 : time zone designation

40.20 : latitude (deg)

113.00 : longitude (deg)

844b : trial ID

6 : month

7 : day

22 : year

21 : hour

22 : minute

8 : no. of sources

51.7 : x-coord. of source (m)

-80.6 : y-coord. of source (m)

0.00 : source elevation (m)

-99.9 : emission rate (g/s)

105.0 : emission duration (s)

0.744 : total mass emitted (kg)

7.722 : sigx0 at the source (m)

11.683 : sigy0 at the source (m)

0.120 : sigz0 at the source (m)

31.3 : x-coord. of source (m)

-62.2 : y-coord. of source (m)

0.00 : source elevation (m)

-99.9 : emission rate (g/s)

105.0 : emission duration (s)

0.744 : total mass emitted (kg)

7.722 : sigx0 at the source (m)

11.683 : sigy0 at the source (m)

0.120 : sigz0 at the source (m)

31.3 : x-coord. of source (m)

-62.2 : y-coord. of source (m)

0.00 : source elevation (m)

-99.9 : emission rate (g/s)

105.0 : emission duration (s)

0.744 : total mass emitted (kg)

7.722 : sigx0 at the source (m)

11.683 : sigy0 at the source (m)

0.120 : sigz0 at the source (m)

31.3 : x-coord. of source (m)

-62.2 : y-coord. of source (m)

0.00 : source elevation (m)

-99.9 : emission rate (g/s)

105.0 : emission duration (s)

0.744 : total mass emitted (kg)

7.722 : sigx0 at the source (m)

11.683 : sigy0 at the source (m)

0.120 : sigz0 at the source (m)

31.3 : x-coord. of source (m)

-62.2 : y-coord. of source (m)

0.00 : source elevation (m)

-99.9 : emission rate (g/s)

105.0 : emission duration (s)

0.744 : total mass emitted (kg)

7.722 : sigx0 at the source (m)

11.683 : sigy0 at the source (m)

0.120 : sigz0 at the source (m)

31.3 : x-coord. of source (m)

-62.2 : y-coord. of source (m)

0.00 : source elevation (m)

-99.9 : emission rate (g/s)

105.0 : emission duration (s)

0.744 : total mass emitted (kg)

7.722 : sigx0 at the source (m)

11.683 : sigy0 at the source (m)

0.120 : sigz0 at the source (m)

31.3 : x-coord. of source (m)

-62.2 : y-coord. of source (m)

0.00 : source elevation (m)

-99.9 : emission rate (g/s)

105.0 : emission duration (s)

0.744 : total mass emitted (kg)

7.722 : sigx0 at the source (m)

11.683 : sigy0 at the source (m)

0.120 : sigz0 at the source (m)

31.3 : x-coord. of source (m)

-62.2 : y-coord. of source (m)

0.00 : source elevation (m)

-99.9 : emission rate (g/s)

105.0 : emission duration (s)

0.744 : total mass emitted (kg)

7.722 : sigx0 at the source (m)

11.683 : sigy0 at the source (m)

0.120 : sigz0 at the source (m)

31.3 : x-coord. of source (m)

-62.2 : y-coord. of source (m)

0.00 : source elevation (m)

-99.9 : emission rate (g/s)

105.0 : emission duration (s)

0.744 : total mass emitted (kg)

7.722 : sigx0 at the source (m)

11.683 : sigy0 at the source (m)

0.120 : sigz0 at the source (m)

-99.9 : relative humidity (%)
 300.00 : temperature at level #1 (K)
 2.00 : measuring height for temperature #1 (m)
 -99.90 : temperature at level #2 (K)
 -99.90 : measuring height for temperature #2 (m)
 -99.90 : wind speed (m/s) at a tower
 3.10 : measuring height for wind data (m)
 3.10 : domain-averaged wind speed (m/s)
 201.0 : domain-averaged wind direction (deg)
 -99.90 : domain-averaged sigma-u (m/s)
 9.10 : domain-averaged sigma-theta (deg)
 3.80 : domain-averaged sigma-phi (deg)
 2.00 : measuring ht for domain-avg wind speed (m)
 300.0 : averaging time for domain-avg data (s)
 0.108 : wind speed power law exponent
 0.0300 : surface roughness (m)
 -99.900 : friction velocity (m)
 -99.9000 : inverse Monin-Obukhov length (1/m)
 0.18 : albedo
 0.50 : moisture availability
 0.50 : Bowen ratio
 -99.9 : mixing height (m)
 -99.9 : cloud cover (%)
 -99.9 : P-G stability class
 300.0 : averaging time for concentration (s)
 2.00 : suggested receptor height (m)
 0 : no. of distances downwind
 3 : no. of lines-of-sight
 -220.7 : x-coord. of 1st end-point for LOS1 (m)
 -117.4 : y-coord. of 1st end-point for LOS1 (m)
 309.0 : x-coord. of 2nd end-point for LOS1 (m)
 164.3 : y-coord. of 2nd end-point for LOS1 (m)
 -99.9 : LOS integrated conc. (mg/m**2)
 1.320E+05 : LOS integrated dosage (mg-s/m**2)
 -244.2 : x-coord. of 1st end-point for LOS1 (m)
 -73.2 : y-coord. of 1st end-point for LOS1 (m)
 285.6 : x-coord. of 2nd end-point for LOS1 (m)
 208.5 : y-coord. of 2nd end-point for LOS1 (m)
 -99.9 : LOS integrated conc. (mg/m**2)
 8.300E+04 : LOS integrated dosage (mg-s/m**2)
 -257.7 : x-coord. of 1st end-point for LOS1 (m)
 -29.1 : y-coord. of 1st end-point for LOS1 (m)
 282.1 : x-coord. of 2nd end-point for LOS1 (m)
 252.6 : y-coord. of 2nd end-point for LOS1 (m)
 -99.9 : LOS integrated conc. (mg/m**2)
 -9.990E+01 : LOS integrated dosage (mg-s/m**2)

The Evaluation of the L8 Series Grenades (L8A3, L2 Grenades, L832)

6 : number of trials included in DOA

6 : time zone designation

40.20 : latitude (deg)

113.00 : longitude (deg)

B49b	B50b	B51b	B52b	B53b	B54b	trial ID
5	5	6	6	6	6	6 : month
25	26	1	1	8	8	8 : day
25	82	82	82	82	82	82 : year
18	18	18	18	18	18	18 : hour
10	44	44	44	44	44	0 : minute
12	12	12	12	12	12	11 : no. of sources
-46.6	51.7	-46.6	51.7	-46.6	51.7	-46.6 : x-coord. of source (m)
93.7	93.7	-80.6	-80.6	93.7	93.7	93.7 : y-coord. of source (m)
0.00	0.00	0.00	0.00	0.00	0.00	0.00 : source elevation (m)
-99.9	-99.9	-99.9	-99.9	-99.9	-99.9	-99.9 : emission rate (g/s)
105.0	105.0	105.0	105.0	105.0	105.0	105.0 : emission duration (s)
0.840	0.840	0.840	0.840	0.840	0.840	0.840 : total mass emitted (kg)
5.368	6.257	2.801	0.164	2.061	0.810	0.810 : total mass emitted (kg)
12.934	12.934	13.721	9.633	13.851	12.436	12.436 : sigm0 at the source (m)
0.120	0.120	0.120	0.120	0.120	0.120	0.120 : sigm0 at the source (m)
-59.2	39.1	-59.2	39.1	-59.2	39.1	-59.2 : x-coord. of source (m)
107.1	107.1	-67.1	-67.1	107.1	107.1	107.1 : y-coord. of source (m)
0.00	0.00	0.00	0.00	0.00	0.00	0.00 : source elevation (m)
-99.9	-99.9	-99.9	-99.9	-99.9	-99.9	-99.9 : emission rate (g/s)
105.0	105.0	105.0	105.0	105.0	105.0	105.0 : emission duration (s)
0.840	0.840	0.840	0.840	0.840	0.840	0.840 : total mass emitted (kg)
0.420	1.594	2.061	6.257	6.674	1.351	1.351 : sigm0 at the source (m)
13.930	13.930	13.851	12.528	12.311	13.938	13.938 : sigm0 at the source (m)
0.120	0.120	0.120	0.120	0.120	0.120	0.120 : sigm0 at the source (m)
-75.6	22.7	-75.6	22.7	-75.6	22.7	-75.6 : x-coord. of source (m)
115.5	115.5	-88.7	-88.7	115.5	115.5	115.5 : y-coord. of source (m)
0.00	0.00	0.00	0.00	0.00	0.00	0.00 : source elevation (m)
-99.9	-99.9	-99.9	-99.9	-99.9	-99.9	-99.9 : emission rate (g/s)
105.0	105.0	105.0	105.0	105.0	105.0	105.0 : emission duration (s)
0.840	0.840	0.840	0.840	0.840	0.840	0.840 : total mass emitted (kg)
4.202	3.260	6.674	1.594	10.482	3.497	3.497 : sigm0 at the source (m)
13.358	13.358	13.619	13.913	13.913	13.560	13.560 : sigm0 at the source (m)
0.120	0.120	0.120	0.120	0.120	0.120	0.120 : sigm0 at the source (m)
-52.3	46.0	-52.3	46.0	-52.3	46.0	-52.3 : x-coord. of source (m)
101.0	101.0	-73.3	-73.3	101.0	101.0	101.0 : y-coord. of source (m)
0.00	0.00	0.00	0.00	0.00	0.00	0.00 : source elevation (m)
-99.9	-99.9	-99.9	-99.9	-99.9	-99.9	-99.9 : emission rate (g/s)
105.0	105.0	105.0	105.0	105.0	105.0	105.0 : emission duration (s)
0.840	0.840	0.840	0.840	0.840	0.840	0.840 : total mass emitted (kg)
3.040	3.986	0.376	8.337	4.435	3.751	3.751 : sigm0 at the source (m)
13.670	13.670	13.499	11.252	13.283	13.492	13.492 : sigm0 at the source (m)
0.120	0.120	0.120	0.120	0.120	0.120	0.120 : sigm0 at the source (m)
-84.6	13.7	-84.6	13.7	-84.6	13.7	-84.6 : x-coord. of source (m)
117.4	117.4	-56.8	-56.8	117.4	117.4	117.4 : y-coord. of source (m)
0.00	0.00	0.00	0.00	0.00	0.00	0.00 : source elevation (m)
-99.9	-99.9	-99.9	-99.9	-99.9	-99.9	-99.9 : emission rate (g/s)
105.0	105.0	105.0	105.0	105.0	105.0	105.0 : emission duration (s)
0.840	0.840	0.840	0.840	0.840	0.840	0.840 : total mass emitted (kg)
6.458	5.576	8.710	0.846	11.935	5.799	5.799 : sigm0 at the source (m)
12.426	12.426	10.965	13.978	7.325	12.747	12.747 : sigm0 at the source (m)
0.120	0.120	0.120	0.120	0.120	0.120	0.120 : sigm0 at the source (m)
-67.0	31.3	-67.0	31.3	-67.0	31.3	-67.0 : x-coord. of source (m)
112.0	112.0	-62.2	-62.2	112.0	112.0	112.0 : y-coord. of source (m)
0.00	0.00	0.00	0.00	0.00	0.00	0.00 : source elevation (m)
-99.9	-99.9	-99.9	-99.9	-99.9	-99.9	-99.9 : emission rate (g/s)
105.0	105.0	105.0	105.0	105.0	105.0	105.0 : emission duration (s)
0.840	0.840	0.840	0.840	0.840	0.840	0.840 : total mass emitted (kg)
1.819	0.846	4.435	3.986	8.710	1.090	1.090 : sigm0 at the source (m)
13.885	13.885	13.283	13.424	10.965	13.961	13.961 : sigm0 at the source (m)
0.120	0.120	0.120	0.120	0.120	0.120	0.120 : sigm0 at the source (m)
-42.3	56.0	-42.3	56.0	-42.3	56.0	-42.3 : x-coord. of source (m)
85.5	85.5	-88.7	-88.7	85.5	85.5	85.5 : y-coord. of source (m)
0.00	0.00	0.00	0.00	0.00	0.00	0.00 : source elevation (m)
-99.9	-99.9	-99.9	-99.9	-99.9	-99.9	-99.9 : emission rate (g/s)
105.0	105.0	105.0	105.0	105.0	105.0	105.0 : emission duration (s)
0.840	0.840	0.840	0.840	0.840	0.840	0.840 : total mass emitted (kg)
7.532	8.337	5.141	11.683	0.916	8.140	8.140 : sigm0 at the source (m)
11.806	11.806	13.026	13.999	13.722	11.395	11.395 : sigm0 at the source (m)
0.120	0.120	0.120	0.120	0.120	0.120	0.120 : sigm0 at the source (m)
-38.2	60.1	-38.2	60.1	-38.2	60.1	-38.2 : x-coord. of source (m)
67.6	67.6	-106.6	-106.6	67.6	67.6	67.6 : y-coord. of source (m)
0.00	0.00	0.00	0.00	0.00	0.00	0.00 : source elevation (m)
-99.9	-99.9	-99.9	-99.9	-99.9	-99.9	-99.9 : emission rate (g/s)
105.0	105.0	105.0	105.0	105.0	105.0	105.0 : emission duration (s)
0.840	0.840	0.840	0.840	0.840	0.840	0.840 : total mass emitted (kg)
11.116	11.116	1.683	3.286	13.619	11.546	11.546 : sigm0 at the source (m)
8.518	8.518	7.722	10.482	13.026	7.324	7.324 : sigm0 at the source (m)
0.120	0.120	0.120	0.120	0.120	0.120	0.120 : sigm0 at the source (m)
-40.4	57.9	-40.4	57.9	-40.4	57.9	-40.4 : x-coord. of source (m)

F-90

6 : number of trials included in ODA

6 : time zone designation

40.20 : latitude (deg)

113.00 : longitude (deg)

8394	8404	8454	8464	8514	8524	trial ID
6	6	6	6	6	6	6
1	1	7	7	1	1	month
2	2	82	82	82	82	day
17	17	22	22	19	21	year
51	51	35	35	54	49	hour
12	12	8	8	12	12	minute
-46.6	-46.6	51.7	51.7	-46.6	51.7	no. of sources
93.7	93.7	-80.6	-80.6	93.7	-80.6	x-coord. of source (m)
0.00	0.00	0.00	0.00	0.00	0.00	y-coord. of source (m)
-99.9	-99.9	-99.9	-99.9	-99.9	-99.9	source elevation (m)
0.992	0.992	105.0	105.0	105.0	105.0	emission rate (g/s)
0.992	0.992	0.763	0.763	0.897	0.916	total mass emitted (kg)
13.915	13.915	6.674	6.674	2.061	6.257	sigm0 at the source (m)
0.120	0.120	13.430	13.430	13.951	12.528	sigm0 at the source (m)
-84.6	-84.6	0.120	0.120	0.120	0.120	sigm0 at the source (m)
117.4	117.4	31.3	31.3	-75.6	22.7	x-coord. of source (m)
0.00	0.00	-62.2	-62.2	115.5	-58.7	y-coord. of source (m)
-99.9	-99.9	0.00	0.00	0.00	0.00	source elevation (m)
105.0	105.0	-99.9	-99.9	-99.9	-99.9	emission rate (g/s)
0.992	0.992	105.0	105.0	105.0	105.0	total mass emitted (kg)
8.332	8.332	9.434	9.434	6.674	1.594	sigm0 at the source (m)
11.263	11.263	10.164	11.945	12.311	13.913	sigm0 at the source (m)
0.120	0.120	0.120	0.120	0.120	0.120	sigm0 at the source (m)
-40.4	-40.4	18.2	18.2	-52.3	46.0	x-coord. of source (m)
0.00	0.00	-57.6	-57.6	101.0	-71.3	y-coord. of source (m)
-99.9	-99.9	0.00	0.00	0.00	0.00	source elevation (m)
105.0	105.0	-99.9	-99.9	-99.9	-99.9	emission rate (g/s)
0.992	0.992	105.0	105.0	105.0	105.0	total mass emitted (kg)
12.537	12.537	11.935	10.152	0.897	8.337	sigm0 at the source (m)
6.240	6.240	7.325	9.646	13.999	11.252	sigm0 at the source (m)
-39.5	-39.5	56.0	0.120	-84.6	0.120	sigm0 at the source (m)
76.7	76.7	-88.7	-88.7	117.4	13.7	x-coord. of source (m)
0.00	0.00	0.00	0.00	0.00	0.00	source elevation (m)
-99.9	-99.9	-99.9	-99.9	-99.9	-99.9	emission rate (g/s)
105.0	105.0	105.0	105.0	105.0	105.0	total mass emitted (kg)
0.992	0.992	0.763	0.763	0.897	0.916	sigm0 at the source (m)
7.717	7.717	6.414	2.079	8.710	0.846	sigm0 at the source (m)
11.612	11.612	13.978	13.849	10.965	13.978	sigm0 at the source (m)
0.120	0.120	0.120	0.120	0.120	0.120	sigm0 at the source (m)
-38.5	-38.5	59.7	59.7	-67.0	31.3	x-coord. of source (m)
58.4	58.4	-102.0	-102.0	112.0	-62.2	y-coord. of source (m)
0.00	0.00	0.00	0.00	0.00	0.00	source elevation (m)
-99.9	-99.9	-99.9	-99.9	-99.9	-99.9	emission rate (g/s)
105.0	105.0	105.0	105.0	105.0	105.0	total mass emitted (kg)
0.992	0.992	0.763	0.763	0.897	0.916	sigm0 at the source (m)
11.263	11.263	2.801	5.592	4.435	3.986	sigm0 at the source (m)
8.332	8.332	13.721	12.839	13.283	13.424	sigm0 at the source (m)
-99.9	-99.9	0.120	0.120	0.120	0.120	sigm0 at the source (m)
-99.9	-99.9	59.8	59.8	-42.3	56.0	x-coord. of source (m)
-99.9	-99.9	-115.9	-115.9	85.5	-88.7	y-coord. of source (m)
0.00	0.00	0.00	0.00	0.00	0.00	source elevation (m)
-99.9	-99.9	-99.9	-99.9	-99.9	-99.9	emission rate (g/s)
105.0	105.0	105.0	105.0	105.0	105.0	total mass emitted (kg)
0.992	0.992	0.763	0.763	0.897	0.916	sigm0 at the source (m)
-99.900	-99.900	6.257	8.725	5.141	11.683	sigm0 at the source (m)
-99.900	-99.900	12.528	10.954	13.026	7.722	sigm0 at the source (m)
0.120	0.120	0.120	0.120	0.120	0.120	sigm0 at the source (m)
-99.9	-99.9	56.4	56.4	-38.2	60.1	x-coord. of source (m)
-99.9	-99.9	-129.3	-129.3	67.6	-106.6	y-coord. of source (m)
0.00	0.00	0.00	0.00	0.00	0.00	source elevation (m)
-99.9	-99.9	-99.9	-99.9	-99.9	-99.9	emission rate (g/s)
105.0	105.0	105.0	105.0	105.0	105.0	total mass emitted (kg)
0.992	0.992	0.763	0.763	0.897	0.916	sigm0 at the source (m)
-99.900	-99.900	9.286	11.263	9.286	13.619	sigm0 at the source (m)
-99.900	-99.900	10.482	8.322	10.482	3.260	sigm0 at the source (m)
0.120	0.120	0.120	0.120	0.120	0.120	sigm0 at the source (m)
-99.9	-99.9	-99.9	-99.9	-99.9	57.9	x-coord. of source (m)

F-96

The Evaluation of the L8 Series Grenades (L8A3, high condition temp., L83M)

5 : number of trials included in DUA

6 : time zone designation

40.20 : latitude (deg)

113.00 : longitude (deg)

8412 : latitude (deg)

8412 : longitude (deg)

8412 : latitude (deg)

8412 : longitude (deg)

8412 : latitude (deg)

8412 : longitude (deg)

8412 : latitude (deg)

8412 : longitude (deg)

8412 : latitude (deg)

8412 : longitude (deg)

8412 : latitude (deg)

8412 : longitude (deg)

8412 : latitude (deg)

8412 : longitude (deg)

8412 : latitude (deg)

8412 : longitude (deg)

8412 : latitude (deg)

8412 : longitude (deg)

8412 : latitude (deg)

8412 : longitude (deg)

8412 : latitude (deg)

8412 : longitude (deg)

8412 : latitude (deg)

8412 : longitude (deg)

8412 : latitude (deg)

8412 : longitude (deg)

8412 : latitude (deg)

8412 : longitude (deg)

8412 : latitude (deg)

8412 : longitude (deg)

8412 : latitude (deg)

8412 : longitude (deg)

8412 : latitude (deg)

8412 : longitude (deg)

8412 : latitude (deg)

8412 : longitude (deg)

8412 : latitude (deg)

8412 : longitude (deg)

8412 : latitude (deg)

8412 : longitude (deg)

8412 : latitude (deg)

8412 : longitude (deg)

8412 : latitude (deg)

8412 : longitude (deg)

8412 : latitude (deg)

8412 : longitude (deg)

8412 : latitude (deg)

8412 : longitude (deg)

8412 : latitude (deg)

8412 : longitude (deg)

8412 : latitude (deg)

8412 : longitude (deg)

8412 : latitude (deg)

8412 : longitude (deg)

8412 : latitude (deg)

8412 : longitude (deg)

8412 : latitude (deg)

8412 : longitude (deg)

8412 : latitude (deg)

8412 : longitude (deg)

8412 : latitude (deg)

8412 : longitude (deg)

8412 : latitude (deg)

8412 : longitude (deg)

8412 : latitude (deg)

8412 : longitude (deg)

8412 : latitude (deg)

8412 : longitude (deg)

8412 : latitude (deg)

8412 : longitude (deg)

8412 : latitude (deg)

8412 : longitude (deg)

8412 : latitude (deg)

8412 : longitude (deg)

8412 : latitude (deg)

8412 : longitude (deg)

8412 : latitude (deg)

8412 : longitude (deg)

8412 : latitude (deg)

8412 : longitude (deg)

8412 : latitude (deg)

8412 : longitude (deg)

8412 : latitude (deg)

8412 : longitude (deg)

8412 : latitude (deg)

8412 : longitude (deg)

8412 : latitude (deg)

8412 : longitude (deg)

8412 : latitude (deg)

8412 : longitude (deg)

[illegible]

The Tests of Foreign Smoke Pots/Generators (Japanese 3-00, INTJA)

7 : number of trials included in DOA

6 : time zone designation

4 : latitude (deg)

113.00 : longitude (deg)

3602 : longitude (deg)

3604 : longitude (deg)

3606 : longitude (deg)

3608 : longitude (deg)

3610 : longitude (deg)

3612 : longitude (deg)

3614 : longitude (deg)

3616 : longitude (deg)

3618 : longitude (deg)

3620 : longitude (deg)

3622 : longitude (deg)

3624 : longitude (deg)

3626 : longitude (deg)

3628 : longitude (deg)

3630 : longitude (deg)

3632 : longitude (deg)

3634 : longitude (deg)

3636 : longitude (deg)

3638 : longitude (deg)

3640 : longitude (deg)

3642 : longitude (deg)

3644 : longitude (deg)

3646 : longitude (deg)

3648 : longitude (deg)

3650 : longitude (deg)

3652 : longitude (deg)

3654 : longitude (deg)

3656 : longitude (deg)

3658 : longitude (deg)

3660 : longitude (deg)

3662 : longitude (deg)

3664 : longitude (deg)

3666 : longitude (deg)

3668 : longitude (deg)

3670 : longitude (deg)

3672 : longitude (deg)

3674 : longitude (deg)

3676 : longitude (deg)

3678 : longitude (deg)

3680 : longitude (deg)

3682 : longitude (deg)

3684 : longitude (deg)

3686 : longitude (deg)

3688 : longitude (deg)

3690 : longitude (deg)

3692 : longitude (deg)

3694 : longitude (deg)

3696 : longitude (deg)

3698 : longitude (deg)

3700 : longitude (deg)

3702 : longitude (deg)

3704 : longitude (deg)

3706 : longitude (deg)

3708 : longitude (deg)

3710 : longitude (deg)

3712 : longitude (deg)

3714 : longitude (deg)

3716 : longitude (deg)

3718 : longitude (deg)

3720 : longitude (deg)

3722 : longitude (deg)

3724 : longitude (deg)

3726 : longitude (deg)

3728 : longitude (deg)

3730 : longitude (deg)

3732 : longitude (deg)

3734 : longitude (deg)

17 : number of trials included in DQA

6 : time zone designation

40-20 : latitude (deg)

112-00 : longitude (deg)

C601 : C604

C605 : C608

C609 : C612

C613 : C616

C617 : C620

C621 : C624

C625 : C628

C629 : C632

C633 : C636

C637 : C640

C641 : C644

C645 : C648

C649 : C652

C653 : C656

C657 : C660

C661 : C664

C665 : C668

C669 : C672

C673 : C676

C677 : C680

C681 : C684

C685 : C688

C689 : C692

C693 : C696

C697 : C700

C701 : C704

C705 : C708

C709 : C712

C713 : C716

C717 : C720

C721 : C724

C725 : C728

C729 : C732

C733 : C736

C737 : C740

C741 : C744

C745 : C748

C749 : C752

C753 : C756

C757 : C760

C761 : C764

C765 : C768

C769 : C772

C773 : C776

C777 : C780

C781 : C784

C785 : C788

C789 : C792

C793 : C796

C797 : C800

C801 : C804

C805 : C808

C809 : C812

C813 : C816

C817 : C820

C821 : C824

C825 : C828

C829 : C832

C833 : C836

C837 : C840

C841 : C844

C845 : C848

C849 : C852

C853 : C856

C857 : C860

C861 : C864

C865 : C868

C869 : C872

C873 : C876

C877 : C880

C881 : C884

C885 : C888

C889 : C892

C893 : C896

C897 : C900

C901 : C904

C905 : C908

C909 : C912

C913 : C916

C917 : C920

C921 : C924

C925 : C928

C929 : C932

C933 : C936

C937 : C940

C941 : C944

C945 : C948

C949 : C952

C953 : C956

C957 : C960

C961 : C964

C965 : C968

C969 : C972

C973 : C976

C977 : C980

C981 : C984

C985 : C988

C989 : C992

C993 : C996

C997 : C1000

C1001 : C1004

C1005 : C1008

C1009 : C1012

C1013 : C1016

C1017 : C1020

C1021 : C1024

C1025 : C1028

C1029 : C1032

C1033 : C1036

C1037 : C1040

C1041 : C1044

C1045 : C1048

C1049 : C1052

C1053 : C1056

C1057 : C1060

C1061 : C1064

C1065 : C1068

C1069 : C1072

C1073 : C1076

C1077 : C1080

C1081 : C1084

C1085 : C1088

C1089 : C1092

C1093 : C1096

C1097 : C1100

C1101 : C1104

C1105 : C1108

C1109 : C1112

C1113 : C1116

C1117 : C1120

C1121 : C1124

C1125 : C1128

C1129 : C1132

C1133 : C1136

C1137 : C1140

C1141 : C1144

C1145 : C1148

C1149 : C1152

C1153 : C1156

C1157 : C1160

C1161 : C1164

C1165 : C1168

C1169 : C1172

C1173 : C1176

C1177 : C1180

C1181 : C1184

C1185 : C1188

C1189 : C1192

C1193 : C1196

C1197 : C1200

C1201 : C1204

C1205 : C1208

C1209 : C1212

C1213 : C1216

C1217 : C1220

C1221 : C1224

C1225 : C1228

C1229 : C1232

C1233 : C1236

C1237 : C1240

C1241 : C1244

C1245 : C1248

C1249 : C1252

C1253 : C1256

C1257 : C1260

C1261 : C1264

C1265 : C1268

C1269 : C1272

C1273 : C1276

C1277 : C1280

C1281 : C1284

C1285 : C1288

C1289 : C1292

C1293 : C1296

C1297 : C1300

C1301 : C1304

C1305 : C1308

C1309 : C1312

C1313 : C1316

C1317 : C1320

C1321 : C1324

C1325 : C1328

C1329 : C1332

C1333 : C1336

C1337 : C1340

C1341 : C1344

C1345 : C1348

C1349 : C1352

C1353 : C1356

C1357 : C1360

C1361 : C1364

C1365 : C1368

C1369 : C1372

C1373 : C1376

C1377 : C1380

C1381 : C1384

C1385 : C1388

C1389 : C1392

C1393 : C1396

C1397 : C1400

C1401 : C1404

C1405 : C1408

C1409 : C1412

C1413 : C1416

C1417 : C1420

C1421 : C1424

C1425 : C1428

C1429 : C1432

C1433 : C1436

C1437 : C1440

C1441 : C1444

C1445 : C1448

C1449 : C1452

C1453 : C1456

C1457 : C1460

C1461 : C1464

C1465 : C1468

C1469 : C1472

C1473 : C1476

C1477 : C1480

C1481 : C1484

C1485 : C1488

C1489 : C1492

C1493 : C1496

C1497 : C1500

C1501 : C1504

C1505 : C1508

C1509 : C1512

C1513 : C1516

C1517 : C1520

C1521 : C1524

C1525 : C1528

C1529 : C1532

C1533 : C1536

C1537 : C1540

C1541 : C1544

C1545 : C1548

C1549 : C1552

C1553 : C1556

C1557 : C1560

C1561 : C1564

C1565 : C1568

C1569 : C1572

C1573 : C1576

C1577 : C1580

C1581 : C1584

C1585 : C1588

C1589 : C1592

C1593 : C1596

C1597 : C1600

C1601 : C1604

C1605 : C1608

C1609 : C1612

C1613 : C1616

C1617 : C1620

C1621 : C1624

C1625 : C1628

C1629 : C1632

C1633 : C1636

C1637 : C1640

C1641 : C1644

C1645 : C1648

C1649 : C1652

C1653 : C1656

C1657 : C1660

C1661 : C1664

C1665 : C1668

C1669 : C1672

C1673 : C1676

C1677 : C1680

C1681 : C1684

C1685 : C1688

C1689 : C1692

C1693 : C1696

C1697 : C1700

C1701 : C1704

C1705 : C1708

C1709 : C1712

C1713 : C1716

C1717 : C1720

C1721 : C1724

C1725 : C1728

C1729 : C1732

C1733 : C1736

C1737 : C1740

C1741 : C1744

C1745 : C1748

C1749 : C1752

C1753 : C1756

C1757 : C1760

C1761 : C1764

C1765 : C1768

C1769 : C1772

C1773 : C1776

C1777 : C1780

C1781 : C1784

C1785 : C1788

C1789 : C1792

C1793 : C1796

C1797 : C1800

C1801 : C1804

C1805 : C1808

C1809 : C1812

C1813 : C1816

C1817 : C1820

C1821 : C1824

C1825 : C1828

C1829 : C1832

C1833 : C1836

C1837 : C1840

C1841 : C1844

C1845 : C1848

C1849 : C1852

C1853 : C1856

C1857 : C1860

C1861 : C1864

C1865 : C1868

C1

Development Test 1 of the Man-Portable Smoke Generators (XM49, fog oil only, FOXF)

12 : number of trials included in DDA											
6 : time zone designation											
40.20 : latitude (deg)											
113.00 : longitude (deg)											
FO01	FO03	FO04	FO05	FO08	FO10	FO12	FO13	FO15	FO16	FO17	FO18 : trial ID
4	4	4	4	4	4	4	4	4	4	4	4 : month
8	9	13	13	13	13	14	14	22	22	22	22 : day
81	81	81	81	81	81	81	81	81	81	81	81 : year
22	18	17	18	21	22	21	22	20	21	21	22 : hour
58	38	48	38	22	44	22	58	25	9	50	17 : minute
1	1	1	1	1	1	1	1	1	1	1	1 : no. of sources
-192.7	-280.1	-323.5	-308.4	-323.5	-323.5	-352.6	-352.6	-294.4	-308.9	-294.4	-294.4 : x-coord. of source (m)
-364.0	-412.5	-24.9	-51.2	-24.9	-24.9	-75.4	-75.4	-77.4	-51.2	-77.4	-77.4 : y-coord. of source (m)
0.38	0.38	0.38	0.38	0.38	0.38	0.38	0.38	0.38	0.38	0.38	0.38 : source elevation (m)
-99.9	-99.9	-99.9	-99.9	-99.9	-99.9	-99.9	-99.9	-99.9	-99.9	-99.9	-99.9 : emission rate (g/s)
300.0	300.0	300.0	300.0	300.0	300.0	300.0	300.0	300.0	300.0	300.0	300.0 : emission duration (s)
18.614	16.870	18.170	18.137	16.087	17.799	16.134	16.134	18.178	17.829	16.803	17.391 : total mass emitted (kg)
0.230	0.230	0.230	0.230	0.230	0.230	0.230	0.230	0.230	0.230	0.230	0.230 : sigma0 at the source (m)
0.230	0.230	0.230	0.230	0.230	0.230	0.230	0.230	0.230	0.230	0.230	0.230 : sigma0 at the source (m)
0.230	0.230	0.230	0.230	0.230	0.230	0.230	0.230	0.230	0.230	0.230	0.230 : sigma0 at the source (m)
-99.9	-99.9	-99.9	-99.9	-99.9	-99.9	-99.9	-99.9	-99.9	-99.9	-99.9	-99.9 : ambient pressure (atm)
-99.9	-99.9	-99.9	-99.9	-99.9	-99.9	-99.9	-99.9	-99.9	-99.9	-99.9	-99.9 : relative humidity (%)
300.0	300.0	300.0	300.0	300.0	300.0	300.0	300.0	300.0	300.0	300.0	300.0 : temperature at level #1 (K)
2.00	2.00	2.00	2.00	2.00	2.00	2.00	2.00	2.00	2.00	2.00	2.00 : measuring height for temperature #1 (m)
-99.90	-99.90	-99.90	-99.90	-99.90	-99.90	-99.90	-99.90	-99.90	-99.90	-99.90	-99.90 : temperature at level #2 (K)
-99.90	-99.90	-99.90	-99.90	-99.90	-99.90	-99.90	-99.90	-99.90	-99.90	-99.90	-99.90 : measuring height for temperature #2 (m)
4.00	3.70	4.70	5.40	5.80	5.10	2.80	2.80	5.00	4.40	5.00	5.30 : wind speed (m/s) at a tower
2.00	2.00	2.00	2.00	2.00	2.00	2.00	2.00	2.00	2.00	2.00	2.00 : measuring height for wind data (m)
4.00	3.70	4.70	5.40	5.80	6.10	2.80	2.80	6.00	4.40	5.00	6.30 : domain-averaged wind speed (m/s)
130.0	130.0	130.0	130.0	130.0	130.0	355.0	355.0	345.0	352.0	350.0	357.0 : domain-averaged wind direction (deg)
-99.90	-99.90	-99.90	-99.90	-99.90	-99.90	-99.90	-99.90	-99.90	-99.90	-99.90	-99.90 : domain-averaged sigma-u (m/s)
9.40	11.90	11.30	11.00	14.30	5.00	18.20	18.20	12.80	19.30	16.20	10.20 : domain-averaged sigma-theta (deg)
-99.90	-99.90	-99.90	-99.90	-99.90	-99.90	-99.90	-99.90	-99.90	-99.90	-99.90	-99.90 : domain-averaged sigma-phi (deg)
2.00	2.00	2.00	2.00	2.00	2.00	2.00	2.00	2.00	2.00	2.00	2.00 : measuring ht for domain-avg wind speed (m)
439.0	480.0	450.0	435.0	450.0	365.0	495.0	495.0	422.0	430.0	428.0	430.0 : averaging time for domain-avg data (s)
0.090	0.061	0.068	0.076	0.081	0.064	0.040	0.040	0.080	0.074	0.066	0.088 : wind speed power law exponent
0.0300	0.0300	0.0300	0.0300	0.0300	0.0300	0.0300	0.0300	0.0300	0.0300	0.0300	0.0300 : surface roughness (m)
-99.900	-99.900	-99.900	-99.900	-99.900	-99.900	-99.900	-99.900	-99.900	-99.900	-99.900	-99.900 : friction velocity (m)
-99.9000	-99.9000	-99.9000	-99.9000	-99.9000	-99.9000	-99.9000	-99.9000	-99.9000	-99.9000	-99.9000	-99.9000 : inverse Monin-Obukhov length (1/m)
0.18	0.18	0.18	0.18	0.18	0.18	0.18	0.18	0.18	0.18	0.18	0.18 : albedo
0.50	0.50	0.50	0.50	0.50	0.50	0.50	0.50	0.50	0.50	0.50	0.50 : moisture availability
0.50	0.50	0.50	0.50	0.50	0.50	0.50	0.50	0.50	0.50	0.50	0.50 : Bowen ratio
-99.9	-99.9	-99.9	-99.9	-99.9	-99.9	-99.9	-99.9	-99.9	-99.9	-99.9	-99.9 : mixing height (m)
-99.9	-99.9	-99.9	-99.9	-99.9	-99.9	-99.9	-99.9	-99.9	-99.9	-99.9	-99.9 : cloud cover (%)
-99.9	-99.9	-99.9	-99.9	-99.9	-99.9	-99.9	-99.9	-99.9	-99.9	-99.9	-99.9 : P-G stability class
300.0	300.0	300.0	300.0	300.0	300.0	300.0	300.0	300.0	300.0	300.0	300.0 : averaging time for concentration (s)
2.44	2.44	2.44	2.44	2.44	2.44	2.44	2.44	2.44	2.44	2.44	2.44 : suggested receptor height (m)
0	0	0	0	0	0	0	0	0	0	0	0 : no. of distances downwind
3	3	3	3	3	3	3	3	3	3	3	3 : no. of lines-of-sight
-779.9	-779.9	-779.9	-779.9	-779.9	-779.9	-779.9	-779.9	-779.9	-779.9	-779.9	-779.9 : x-coord. of 1st end-point for LOS1 (m)
-449.4	-449.4	-449.4	-449.4	-449.4	-449.4	-449.4	-449.4	-449.4	-449.4	-449.4	-449.4 : y-coord. of 1st end-point for LOS1 (m)
532.0	532.0	532.0	532.0	532.0	532.0	532.0	532.0	532.0	532.0	532.0	532.0 : x-coord. of 2nd end-point for LOS1 (m)
277.8	277.8	277.8	277.8	277.8	277.8	277.8	277.8	277.8	277.8	277.8	277.8 : y-coord. of 2nd end-point for LOS1 (m)
-99.9	-99.9	-99.9	-99.9	-99.9	-99.9	-99.9	-99.9	-99.9	-99.9	-99.9	-99.9 : LOS integrated conc. (mg/m**2)
1.560E+05	9.900E+04	2.110E+05	2.102E+05	2.120E+05	2.300E+05	1.070E+05	1.860E+05	1.540E+05	2.160E+05	1.580E+05	2.710E+05 : LOS integrated dosage (mg/m**2)
-750.8	-750.8	-750.8	-750.8	-750.8	-750.8	-750.8	-750.8	-750.8	-750.8	-750.8	-750.8 : x-coord. of 1st end-point for LOS1 (m)
-501.9	-501.9	-501.9	-501.9	-501.9	-501.9	-501.9	-501.9	-501.9	-501.9	-501.9	-501.9 : y-coord. of 1st end-point for LOS1 (m)
561.1	561.1	561.1	561.1	561.1	561.1	561.1	561.1	561.1	561.1	561.1	561.1 : x-coord. of 2nd end-point for LOS1 (m)
225.3	225.3	225.3	225.3	225.3	225.3	225.3	225.3	225.3	225.3	225.3	225.3 : y-coord. of 2nd end-point for LOS1 (m)
-99.9	-99.9	-99.9	-99.9	-99.9	-99.9	-99.9	-99.9	-99.9	-99.9	-99.9	-99.9 : LOS integrated conc. (mg/m**2)
2.250E+05	1.820E+05	1.190E+05	1.500E+05	1.360E+05	1.630E+05	8.900E+04	1.180E+05	8.200E+04	1.220E+05	7.400E+04	1.550E+05 : LOS integrated dosage (mg/m**2)
-721.7	-721.7	-721.7	-721.7	-721.7	-721.7	-721.7	-721.7	-721.7	-721.7	-721.7	-721.7 : x-coord. of 1st end-point for LOS1 (m)
-554.4	-554.4	-554.4	-554.4	-554.4	-554.4	-554.4	-554.4	-554.4	-554.4	-554.4	-554.4 : y-coord. of 1st end-point for LOS1 (m)
590.2	590.2	590.2	590.2	590.2	590.2	590.2	590.2	590.2	590.2	590.2	590.2 : x-coord. of 2nd end-point for LOS1 (m)
172.8	172.8	172.8	172.8	172.8	172.8	172.8	172.8	172.8	172.8	172.8	172.8 : y-coord. of 2nd end-point for LOS1 (m)
-99.9	-99.9	-99.9	-99.9	-99.9	-99.9	-99.9	-99.9	-99.9	-99.9	-99.9	-99.9 : LOS integrated conc. (mg/m**2)
3.260E+05	3.120E+05	8.100E+04	9.800E+04	1.110E+05	1.190E+05	4.100E+04	8.400E+04	5.100E+04	7.700E+04	5.200E+04	1.130E+05 : LOS integrated dosage (mg/m**2)

Development Test 1 of the Man-Portable Smoke Generators (MJA3, fog oil only, POME)

6 : number of trials included in DDA

7 : time zone designation

8 : latitude (deg)

9 : longitude (deg)

FOO2 : longitude (deg)

FOO3 : longitude (deg)

FOO4 : longitude (deg)

FOO5 : longitude (deg)

FOO6 : longitude (deg)

FOO7 : longitude (deg)

FOO8 : longitude (deg)

FOO9 : longitude (deg)

FOO10 : longitude (deg)

FOO11 : longitude (deg)

FOO12 : longitude (deg)

FOO13 : longitude (deg)

FOO14 : longitude (deg)

FOO15 : longitude (deg)

FOO16 : longitude (deg)

FOO17 : longitude (deg)

FOO18 : longitude (deg)

FOO19 : longitude (deg)

FOO20 : longitude (deg)

FOO21 : longitude (deg)

FOO22 : longitude (deg)

FOO23 : longitude (deg)

FOO24 : longitude (deg)

FOO25 : longitude (deg)

FOO26 : longitude (deg)

FOO27 : longitude (deg)

FOO28 : longitude (deg)

FOO29 : longitude (deg)

FOO30 : longitude (deg)

FOO31 : longitude (deg)

FOO32 : longitude (deg)

FOO33 : longitude (deg)

FOO34 : longitude (deg)

FOO35 : longitude (deg)

FOO36 : longitude (deg)

FOO37 : longitude (deg)

FOO38 : longitude (deg)

FOO39 : longitude (deg)

FOO40 : longitude (deg)

FOO41 : longitude (deg)

FOO42 : longitude (deg)

FOO43 : longitude (deg)

FOO44 : longitude (deg)

FOO45 : longitude (deg)

FOO46 : longitude (deg)

FOO47 : longitude (deg)

FOO48 : longitude (deg)

FOO49 : longitude (deg)

FOO50 : longitude (deg)

FOO51 : longitude (deg)

FOO52 : longitude (deg)

FOO53 : longitude (deg)

FOO54 : longitude (deg)

FOO55 : longitude (deg)

FOO56 : longitude (deg)

FOO57 : longitude (deg)

FOO58 : longitude (deg)

FOO59 : longitude (deg)

FOO60 : longitude (deg)

FOO61 : longitude (deg)

FOO62 : longitude (deg)

FOO63 : longitude (deg)

FOO64 : longitude (deg)

FOO65 : longitude (deg)

FOO66 : longitude (deg)

FOO67 : longitude (deg)

FOO68 : longitude (deg)

FOO69 : longitude (deg)

FOO70 : longitude (deg)

FOO71 : longitude (deg)

FOO72 : longitude (deg)

FOO73 : longitude (deg)

FOO74 : longitude (deg)

FOO75 : longitude (deg)

FOO76 : longitude (deg)

FOO77 : longitude (deg)

FOO78 : longitude (deg)

FOO79 : longitude (deg)

FOO80 : longitude (deg)

Development Test I of the Man-Portable Smoke Generators (KM49, diesel only and diesel part of diesel+1B, FOXD)

6 : number of trials included in DDA

6 : time zone designation

40.20 : latitude (deg)

113.00 : longitude (deg)

DO20 : DO21

DO20 : DO21

DO20 : DO21

DO20 : DO21

DO20 : DO21

DO20 : DO21

DO20 : DO21

DO20 : DO21

DO20 : DO21

DO20 : DO21

DO20 : DO21

DO20 : DO21

DO20 : DO21

DO20 : DO21

DO20 : DO21

DO20 : DO21

DO20 : DO21

DO20 : DO21

DO20 : DO21

DO20 : DO21

DO20 : DO21

DO20 : DO21

DO20 : DO21

DO20 : DO21

DO20 : DO21

DO20 : DO21

DO20 : DO21

DO20 : DO21

DO20 : DO21

DO20 : DO21

DO20 : DO21

DO20 : DO21

DO20 : DO21

DO20 : DO21

DO20 : DO21

DO20 : DO21

DO20 : DO21

DO20 : DO21

DO20 : DO21

DO20 : DO21

DO20 : DO21

DO20 : DO21

DO20 : DO21

DO20 : DO21

DO20 : DO21

DO20 : DO21

DO20 : DO21

DO20 : DO21

DO20 : DO21

DO20 : DO21

DO20 : DO21

DO20 : DO21

DO20 : DO21

DO20 : DO21

DO20 : DO21

DO20 : DO21

DO20 : DO21

DO20 : DO21

DO20 : DO21

DO20 : DO21

DO20 : DO21

DO20 : DO21

DO20 : DO21

DO20 : DO21

DO20 : DO21

DO20 : DO21

DO20 : DO21

DO20 : DO21

DO20 : DO21

DO20 : DO21

DO20 : DO21

DO20 : DO21

DO20 : DO21

DO20 : DO21

DO20 : DO21

DO20 : DO21

DO20 : DO21

DO20 : DO21

DO20 : DO21

DO20 : DO21

DO20 : DO21

DO20 : DO21

DO20 : DO21

DO20 : DO21

DO20 : DO21

Development Test 1 of the Man-Portable Smoke Generators (XM49, 1K only and 1A part of diesel 1K, FOX1)

6 : number of trials included in DDA

6 : time zone designation

40.20 : latitude (deg)

113.00 : longitude (deg)

EA22

EA23

EA24

EA25

EA26

EA27

EA28

EA29

EA30

EA31

EA32

EA33

EA34

EA35

EA36

EA37

EA38

EA39

EA40

EA41

EA42

EA43

EA44

EA45

EA46

EA47

EA48

EA49

EA50

EA51

EA52

EA53

EA54

EA55

EA56

EA57

EA58

EA59

EA60

EA61

EA62

EA63

EA64

EA65

EA66

EA67

EA68

EA69

EA70

EA71

EA72

EA73

EA74

EA75

EA76

EA77

EA78

EA79

EA80

EA81

EA82

EA83

EA84

EA85

EA86

EA87

EA88

EA89

EA90

EA91

EA92

EA93

DE36D

DE36E

DE36F

DE36G

DE36H

DE36I

DE36J

DE36K

DE36L

DE36M

DE36N

DE36O

DE36P

DE36Q

DE36R

DE36S

DE36T

DE36U

DE36V

DE36W

DE36X

DE36Y

DE36Z

DE36A

DE36B

DE36C

DE36D

DE36E

DE36F

DE36G

DE36H

DE36I

DE36J

DE36K

DE36L

DE36M

DE36N

DE36O

DE36P

DE36Q

DE36R

DE36S

DE36T

DE36U

DE36V

DE36W

DE36X

DE36Y

DE36Z

DE36A

DE36B

DE36C

DE36D

DE36E

DE36F

DE36G

DE36H

DE36I

DE36J

DE36K

DE36L

DE36M

DE36N

DE36O

DE36P

DE36Q

DE36R

DE36S

DE36T

DE36U

DE36V

DE36W

DE36X

DE36D

DE36E

DE36F

DE36G

DE36H

DE36I

DE36J

DE36K

DE36L

DE36M

DE36N

DE36O

DE36P

DE36Q

DE36R

DE36S

DE36T

DE36U

DE36V

DE36W

DE36X

DE36Y

DE36Z

DE36A

DE36B

DE36C

DE36D

DE36E

DE36F

DE36G

DE36H

DE36I

DE36J

DE36K

DE36L

DE36M

DE36N

DE36O

DE36P

DE36Q

DE36R

DE36S

DE36T

DE36U

DE36V

DE36W

DE36X

DE36Y

DE36Z

DE36A

DE36B

DE36C

DE36D

DE36E

DE36F

DE36G

DE36H

DE36I

DE36J

DE36K

DE36L

DE36M

DE36N

DE36O

DE36P

DE36Q

DE36R

DE36S

DE36T

DE36U

DE36V

DE36W

DE36X

Development Test 1 of the Man-Portable Smoke Generators (MX49, Fogall part of fogall-IR, FORFC)

ID : number of trials included in DDA

6 : time zone designation

40.20 : latitude (deg)

113.00 : longitude (deg)

FE26a : FE27a

FE26a : FE27a

FE26a : FE27a

FE26a : FE27a

FE26a : FE27a

FE26a : FE27a

FE26a : FE27a

FE26a : FE27a

FE26a : FE27a

FE26a : FE27a

FE26a : FE27a

FE26a : FE27a

FE26a : FE27a

FE26a : FE27a

FE26a : FE27a

FE26a : FE27a

FE26a : FE27a

FE26a : FE27a

FE26a : FE27a

FE26a : FE27a

FE26a : FE27a

FE26a : FE27a

FE26a : FE27a

FE26a : FE27a

FE26a : FE27a

FE26a : FE27a

FE26a : FE27a

FE26a : FE27a

FE26a : FE27a

FE26a : FE27a

FE26a : FE27a

FE26a : FE27a

FE26a : FE27a

FE26a : FE27a

FE26a : FE27a

FE26a : FE27a

FE26a : FE27a

FE26a : FE27a

FE26a : FE27a

FE26a : FE27a

FE26a : FE27a

FE26a : FE27a

FE26a : FE27a

FE26a : FE27a

FE26a : FE27a

FE26a : FE27a

FE26a : FE27a

FE26a : FE27a

FE26a : FE27a

FE26a : FE27a

FE26a : FE27a

FE26a : FE27a

FE26a : FE27a

FE26a : FE27a

FE26a : FE27a

FE26a : FE27a

FE26a : FE27a

FE26a : FE27a

FE26a : FE27a

FE26a : FE27a

FE26a : FE27a

FE26a : FE27a

FE26a : FE27a

FE26a : FE27a

FE26a : FE27a

FE26a : FE27a

FE26a : FE27a

FE26a : FE27a

FE26a : FE27a

FE26a : FE27a

FE26a : FE27a

FE26a : FE27a

FE26a : FE27a

FE26a : FE27a

FE26a : FE27a

FE26a : FE27a

FE26a : FE27a

FE26a : FE27a

FE26a : FE27a

FE26a : FE27a

FE26a : FE27a

FE26a : FE27a

FE26a : FE27a

FE26a : FE27a

FE26a : FE27a

FE26a : FE27a

FE26a : FE27a

FE26a : FE27a

Atterbury-07

F-110